

Table of Contents

| | |
|-----------|---|
| 6.0 | Engineered Safety Features |
| 6.1 | Engineered Safety Feature Materials |
| 6.1.1 | Metallic Materials |
| 6.1.1.1 | Materials Selection and Fabrication |
| 6.1.1.2 | Composition, Compatibility, and Stability of Containment and Core Spray Coolants |
| 6.1.1.2.1 | Post Accident Chemistry |
| 6.1.1.2.2 | Final Post Accident Chemistry |
| 6.1.2 | Organic Materials |
| 6.1.2.1 | Coatings and Paint in Westinghouse Scope |
| 6.1.2.2 | Coatings and Paint in Duke Scope |
| 6.1.2.3 | Quantities of Organic Materials Inside Containment |
| 6.1.3 | Polyethylene Material |
| 6.1.3.1 | High Density Polyethylene (HDPE) |
| 6.1.4 | References |
| 6.2 | Containment Systems |
| 6.2.1 | Containment Functional Design |
| 6.2.1.1 | Containment Structure |
| 6.2.1.1.1 | Design Bases |
| 6.2.1.1.2 | Design Features |
| 6.2.1.1.3 | Design Evaluation |
| 6.2.1.2 | Containment Subcompartments |
| 6.2.1.2.1 | Design Basis |
| 6.2.1.2.2 | Design Features |
| 6.2.1.2.3 | Design Evaluation |
| 6.2.1.3 | Mass and Energy Release Analysis for Postulated Loss-of-Coolant Accidents |
| 6.2.1.3.1 | Short Term Mass and Energy Release Data |
| 6.2.1.3.2 | Long Term Mass and Energy Release Data |
| 6.2.1.4 | Mass and Energy Release Analysis for Postulated Secondary System Pipe Ruptures Inside Containment |
| 6.2.1.4.1 | Pipe Break Blowdowns Spectra and Assumptions |
| 6.2.1.4.2 | Break Flow Calculations |
| 6.2.1.4.3 | Single Failure Effects |
| 6.2.1.5 | Minimum Containment Pressure Analysis for Performance Capability Studies of Emergency Core Cooling System |
| 6.2.1.5.1 | Mass and Energy Release Data |
| 6.2.1.5.2 | Initial Containment Internal Conditions |
| 6.2.1.5.3 | Containment Volume |
| 6.2.1.5.4 | Active Heat Sinks |
| 6.2.1.5.5 | Steam-Water Mixing |
| 6.2.1.5.6 | Passive Heat Sinks |
| 6.2.1.5.7 | Heat Transfer to Passive Sinks |
| 6.2.1.5.8 | Other Parameters |
| 6.2.1.6 | Testing and Inspection |
| 6.2.1.6.1 | Preoperational Testing |
| 6.2.1.6.2 | Periodic Inservice Surveillance |
| 6.2.1.7 | Instrumentation Requirements |
| 6.2.2 | Containment Heat Removal Systems |
| 6.2.2.1 | Design Bases |
| 6.2.2.2 | System Design |
| 6.2.2.3 | Design Evaluation |

- 6.2.2.4 Testing and Inspections
- 6.2.2.5 Instrumentation Requirements
- 6.2.2.6 Materials
- 6.2.3 Secondary Containment Functional Design
 - 6.2.3.1 Design Bases
 - 6.2.3.2 System Design
 - 6.2.3.3 Design Evaluation
 - 6.2.3.4 Tests and Inspections
 - 6.2.3.5 Instrumentation Application
- 6.2.4 Containment Isolation System
 - 6.2.4.1 Design Bases
 - 6.2.4.2 System Design
 - 6.2.4.2.1 Containment Isolation Systems
 - 6.2.4.2.2 Containment Valve Injection Water System
 - 6.2.4.3 Design Evaluation
 - 6.2.4.4 Testing and Inspection
 - 6.2.5 Combustible Gas Control in Containment
 - 6.2.5.1 Design Bases
 - 6.2.5.1.1 Electric Hydrogen Recombiners
 - 6.2.5.1.2 Containment Hydrogen Purge System
 - 6.2.5.2 System Design
 - 6.2.5.2.1 Electric Hydrogen Recombiners
 - 6.2.5.2.2 Containment Hydrogen Purge System
 - 6.2.5.3 Design Evaluation
 - 6.2.5.3.1 Deleted Per 2006 Update
 - 6.2.5.3.2 Containment Hydrogen Sample and Purge System
 - 6.2.5.3.3 Deleted Per 2006 Update
 - 6.2.5.4 Tests and Inspections
 - 6.2.5.4.1 Electric Hydrogen Recombiners
 - 6.2.5.4.2 Containment Hydrogen and Purge System
 - 6.2.5.5 Instrumentation Requirements
 - 6.2.5.6 Materials
 - 6.2.5.6.1 Electric Recombiner
 - 6.2.5.6.2 Containment Hydrogen Sample and Purge System
 - 6.2.5.7 Supplemental Hydrogen Control System/Hydrogen Mitigation System/Hydrogen Ignition System
 - 6.2.6 Containment Leakage Testing
 - 6.2.6.1 Containment Integrated Leak Rate Test
 - 6.2.6.2 Containment Penetration Leakage Rate Test
 - 6.2.6.3 Containment Isolation Valve Leakage Rate Test
 - 6.2.6.4 Scheduling and Reporting of Periodic Tests
 - 6.2.6.5 Special Testing Requirements
 - 6.2.7 References
 - 6.3 Emergency Core Cooling System
 - 6.3.1 Design Bases
 - 6.3.2 System Design
 - 6.3.2.1 Schematic Piping and Instrumentation Diagrams
 - 6.3.2.2 Equipment and Component Descriptions
 - 6.3.2.3 Applicable Codes and Classifications
 - 6.3.2.4 Material Specifications and Compatibility
 - 6.3.2.5 System Reliability
 - 6.3.2.6 Protection Provisions
 - 6.3.2.7 Provisions For Performance Testing
 - 6.3.2.8 Manual Actions
 - 6.3.2.9 Generic Letter 2004-02

- 6.3.3 Performance Evaluation
- 6.3.4 Tests and Inspections
 - 6.3.4.1 ECCS Performance Tests
 - 6.3.4.2 Reliability Tests and Inspections
 - 6.3.4.2.1 Description of Tests
- 6.3.5 Instrumentation Requirements
 - 6.3.5.1 Temperature Indication
 - 6.3.5.2 Pressure Indication
 - 6.3.5.3 Flow Indication
 - 6.3.5.4 Level Indication
 - 6.3.5.5 Valve Position Indication
- 6.3.6 References

- 6.4 Habitability Systems
 - 6.4.1 Design Bases
 - 6.4.2 System Design
 - 6.4.2.1 Definition of Control Room Envelope
 - 6.4.2.2 Ventilation Systems
 - 6.4.2.3 Leak Tightness
 - 6.4.2.4 Interaction With Other Zones and Pressure-Containing Equipment
 - 6.4.2.5 Shielding Design
 - 6.4.3 System Operational Procedures
 - 6.4.4 Design Evaluation
 - 6.4.4.1 Radiological Protection
 - 6.4.4.2 Toxic Gas Protection
 - 6.4.5 Testing and Inspection
 - 6.4.6 Instrumentation Requirements

- 6.5 Fission Product Removal and Control Systems
 - 6.5.1 Engineered Safety Feature (ESF) Filter Systems
 - 6.5.1.1 Design Bases
 - 6.5.1.2 System Design
 - 6.5.1.3 Design Evaluation
 - 6.5.1.4 Tests and Inspections
 - 6.5.1.5 Instrumentation Requirements
 - 6.5.1.6 Materials
 - 6.5.2 Containment Spray Systems
 - 6.5.3 Fission Product Control Systems
 - 6.5.3.1 Primary Containment
 - 6.5.3.2 Secondary Containment
 - 6.5.4 Ice Condenser as a Fission Product Cleanup System
 - 6.5.4.1 Ice Condenser Design Basis (Fission Product Cleanup Function)
 - 6.5.4.2 Ice Condenser System Design
 - 6.5.4.2.1 Component Description
 - 6.5.4.2.2 System Operation
 - 6.5.4.3 Ice Condenser System Design Evaluation (Fission Product Cleanup Function)
 - 6.5.4.4 Ice Condenser System Tests and Inspection
 - 6.5.4.4.1 Ice Condenser System Instrumentation
 - 6.5.4.5 Ice Condenser Materials

- 6.6 Inservice Inspection of Class 2 and 3 Components
 - 6.6.1 Components Subject to Examination
 - 6.6.2 Accessibility
 - 6.6.3 Examination Techniques and Procedures
 - 6.6.4 Inspection Schedule
 - 6.6.5 Examination Categories and Requirements

- 6.6.6 Evaluation of Examination Results
- 6.6.7 System Leakage and Hydrostatic Pressure Test
- 6.6.8 Augmented Inservice Inspection to Protect Against Postulated Piping Failures

- 6.7 Ice Condenser System
 - 6.7.1 Floor Structure and Cooling System
 - 6.7.1.1 Design Bases
 - 6.7.1.2 System Design
 - 6.7.1.3 Design Evaluation
 - 6.7.2 Wall Panels
 - 6.7.2.1 Design Bases
 - 6.7.2.2 System Design
 - 6.7.2.3 Design Evaluation
 - 6.7.3 Lattice Frames and Support Columns
 - 6.7.3.1 Design Bases
 - 6.7.3.2 System Design
 - 6.7.3.3 Design Evaluation
 - 6.7.4 Ice Baskets
 - 6.7.4.1 Design Bases
 - 6.7.4.2 System Design
 - 6.7.4.3 Design Evaluation
 - 6.7.5 Crane and Rail Assembly
 - 6.7.5.1 Design Bases
 - 6.7.5.2 System Design
 - 6.7.5.3 Design Evaluation
 - 6.7.6 Refrigeration System
 - 6.7.6.1 Design Bases
 - 6.7.6.2 System Design
 - 6.7.6.3 Design Evaluation
 - 6.7.7 Air Handling Units
 - 6.7.7.1 Design Bases
 - 6.7.7.2 System Design
 - 6.7.7.3 Design Evaluation
 - 6.7.8 Lower Inlet Doors
 - 6.7.8.1 Design Bases
 - 6.7.8.2 System Design
 - 6.7.8.3 Design Evaluation
 - 6.7.9 Lower Support Structure
 - 6.7.9.1 Design Bases
 - 6.7.9.2 System Design
 - 6.7.9.3 Design Evaluation
 - 6.7.10 Top Deck and Doors
 - 6.7.10.1 Design Bases
 - 6.7.10.2 System Design
 - 6.7.11 Intermediate Deck and Doors
 - 6.7.11.1 Design Bases
 - 6.7.11.2 System Design
 - 6.7.11.3 Design Evaluation
 - 6.7.12 Air Distribution Ducts
 - 6.7.12.1 Design Bases
 - 6.7.12.2 System Design
 - 6.7.12.3 Design Evaluation
 - 6.7.13 Equipment Access Door
 - 6.7.13.1 Design Bases
 - 6.7.13.2 System Design
 - 6.7.13.3 Design Evaluation

- 6.7.14 Ice Technology, Ice Performance, and Ice Chemistry
 - 6.7.14.1 Design Bases
 - 6.7.14.2 System Design
 - 6.7.14.3 Design Evaluation
- 6.7.15 Ice Condenser Instrumentation
 - 6.7.15.1 Design Bases
 - 6.7.15.2 Design Description
 - 6.7.15.3 Design Evaluation
- 6.7.16 Ice Condenser Structural Design
 - 6.7.16.1 Applicable Codes, Standards, and Specifications
 - 6.7.16.2 Loads and Loading Combinations
 - 6.7.16.3 Design and Analytical Procedures
 - 6.7.16.4 Structural Acceptance Criteria
- 6.7.17 Seismic Analysis
 - 6.7.17.1 Seismic Analysis Methods
 - 6.7.17.2 Seismic Load Development
 - 6.7.17.3 Vertical Seismic Response
- 6.7.18 Materials
 - 6.7.18.1 Design Criteria
 - 6.7.18.2 Environmental Effects
 - 6.7.18.3 Compliance With 10CFR50, Appendix B
 - 6.7.18.4 Materials Specifications
- 6.7.19 Tests and Inspections
- 6.7.20 References

List of Tables

Table 6-1. Engineered Safety Feature Materials

Table 6-2. Parameters of Final Post-Accident Chemistry

Table 6-3. Protective Coatings on Westinghouse-supplied Equipment Inside Containment

Table 6-4. Organic Materials Inside Containment

Table 6-5. Potential Water Traps Inside Containment

Table 6-6. Catawba Ice Condenser Design Parameters

Table 6-7. Catawba Nuclear Station ECCS Flow Rates

Table 6-8. Structural Heat Sinks

Table 6-9. Deleted Per 1997 Update

Table 6-10. Deleted Per 1997 Update

Table 6-11. Mass And Energy Release Rates For Peak Reverse Differential Pressure

Table 6-12. Allowance Leakage Area for Various Reactor Coolant System Break Sizes

Table 6-13. TMD Element Input Data

Table 6-14. TMD Flow Path Input Data

Table 6-15. Calculated Maximum Peak Pressures In Lower Compartment Elements Assuming Unaugmented Flow

Table 6-16. Calculated Maximum Peak Pressures In The Ice Condenser Compartment Assuming Unaugmented Flow

Table 6-17. Calculated Maximum Differential Pressures Across The Operating Deck Assuming Unaugmented Flow

Table 6-18. Calculated Maximum Differential Pressures Across The Upper Crane Wall Assuming Unaugmented Flow

Table 6-19. Containment Sump Volume Vs. Time Peak Containment Pressure Transient

Table 6-20. Containment Sump Volume Vs. Elevation

Table 6-21. Sensitivity Studies For D.C. Cook Plant

Table 6-22. Mass and Energy Releases into Steam Generator Enclosure

Table 6-23. TMD Input Data - 2 Node Steam Generator Enclosure

Table 6-24. Peak Differential Pressures - 2 Node Steam Generator Enclosure

Table 6-25. TMD Input Data - 9 Node Steam Generator Enclosure

Table 6-26. Peak Differential Pressure - 9 Node Steam Generator Enclosure

Table 6-27. Mass and Energy Release Rates Into Pressurizer Enclosure

Table 6-28. TMD Input Data - 2 Node Pressurizer Enclosure

Table 6-29. TMD Input Data - 4 Node Pressurizer Enclosure

Table 6-30. Mass and Energy Release Rates Into Reactor Cavity

Table 6-31. Reactor Cavity Analysis Volumes - Cold Leg Break

Table 6-32. Reactor Cavity Analysis Flow Paths - Cold Leg Break

Table 6-33. Reactor Cavity Design Pressures

Table 6-34. Deleted Per 2010 Update

Table 6-35. Deleted Per 2010 Update

Table 6-36. Deleted Per 2010 Update

Table 6-37. Deleted Per 2010 Update

Table 6-38. Deleted Per 2010 Update

Table 6-39. Deleted Per 2010 Update

Table 6-40. Deleted Per 1997 Update

Table 6-41. Deleted Per 1997 Update

Table 6-42. Deleted Per 1997 Update

Table 6-43. Deleted Per 1997 Update

Table 6-44. Deleted Per 1997 Update

Table 6-45. Deleted Per 1997 Update

Table 6-46. Deleted Per 1997 Update

Table 6-47. Mass and Energy Release Rates for Steam Line Rupture. 2.4 ft² Double-Ended Break at 3479 MWt (rated thermal power plus measurement uncertainty)

Table 6-48. Deleted Per 1997 Update

Table 6-49. Deleted Per 1997 Update

Table 6-50. Deleted Per 1997 Update

Table 6-51. Deleted Per 1997 Update

Table 6-52. Deleted Per 1997 Update

Table 6-53. Deleted Per 1997 Update

Table 6-54. Deleted Per 1997 Update

Table 6-55. Deleted Per 1997 Update

Table 6-56. Deleted Per 1997 Update

Table 6-57. Deleted Per 1997 Update

Table 6-58. Double Ended Pump Suction Guillotine Max SI

Table 6-59. DCP/Double Ended Pump Suction Guillotine Min SI

Table 6-60. Deleted Per 2000 Update.

Table 6-61. Mass and Energy Release Rates For Minimum Post-LOCA Containment Pressure

Table 6-62. Minimum Post-LOCA Containment Pressure Broken Loop Accumulator Flow to Containment

Table 6-63. Containment and Active Heat Sink Data for Peak Reverse Differential Pressure

Table 6-64. Structural Heat Sink Data For Minimum Post-LOCA Containment Pressure

Table 6-65. Structural Heat Sink Data for Peak Reverse Differential Pressure

Table 6-66. Containment and Active Heat Sink Data for Minimum Post-LOCA Containment Pressure
McGuire and Catawba

Table 6-67. Deleted Per 2000 Update.

Table 6-68. Air Return Fans and Hydrogen Skimmer Fans Failure Analysis

Table 6-69. Deleted Per 1990 Update

Table 6-70. Containment Spray Pump Design Parameters

Table 6-71. Containment Spray Heat Exchanger Operating Parameters

Table 6-72. Containment Spray System Single Failure Analyses

Table 6-73. Failure Mode and Effects Analysis - Containment Spray System - Active Components

Table 6-74. Potential Bypass Leakage Paths through Containment Isolation Valves

Table 6-75. Annulus Ventilation System Post Accident Respose

Table 6-76. Dual Containment Characteristics

Table 6-77. Containment Isolation Valve Data

Table 6-78. Comparison of Containment Purge System With Branch Technical Position CSB 6-4, Revision
2

Table 6-79. Applicable Codes, Standards and Guides Used in the Design of the Electric H2 Recombiner
Historical information in italics below required to be revised.

Table 6-80. Electric Hydrogen Recombiner Typical Parameters

Table 6-81. Containment Hydrogen Sample and Purge System Design Data

Table 6-82. Deleted Per 2006 Update

Table 6-83. Deleted Per 2006 Update

Table 6-84. Deleted Per 1991 Update

Table 6-85. Deleted Per 1991 Update

Table 6-86. Deleted Per 1991 Update

Table 6-87. Emergency Core Cooling System Component Parameters

Table 6-88. ECCS Relief Valve Data

Table 6-89. Motor Operated Isolation Valves In ECCS

Table 6-90. Materials Employed For Emergency Core Cooling System Components

Table 6-91. Failure Mode and Effects Analysis - Emergency Core Cooling System - Active Components

Table 6-92. Single Active Failure Analysis For Emergency Core Cooling System Components

Table 6-93. Sequence Of Changeover Operation From Injection To Recirculation

Table 6-94. Emergency Core Cooling System Recirculation Piping Passive Failure Analysis. Long Term Phase

Table 6-95. Safety Related Solenoid Valves Inside Containment Below Elevation 571'0"

Table 6-96. Active Valves Inside Containment Below Elevation 571'0"

Table 6-97. Emergency Core Cooling System Shared Functions Evaluation

Table 6-98. Normal Operating Status Of Emergency Core Cooling System Components For Core Cooling

Table 6-99. Parameters for Boron Precipitation Analysis

Table 6-100. Comparison of Control Room Area Protection Against Toxic Gas Hazards With Regulatory Guide 1.95, Revision 1, January 1977

Table 6-101. Comparison of Control Room Habitability Protection Against Toxic Gas Hazards Described in Regulatory Guide 1.78, Revision 0, June 1974

Table 6-102. Ice Condenser Elemental Iodine Removal Efficiency¹

Table 6-103. Process Lines Subject to Augmented Inservice Inspection

Table 6-104. Wall Panel Design Loads¹

Table 6-105. Ice Basket Load Summary

- Table 6-106. Summary of Stresses in Basket Due to Design Loads
- Table 6-107. Ice Basket Material Minimum Yield Stress
- Table 6-108. Allowable Stress Limits (D + OBE) For Ice Basket Materials
- Table 6-109. Allowable Stress Limits (D + SSE), (D + DBA) For Ice Basket Materials
- Table 6-110. Allowable Stress Limits (D + SSE + DBA) For Ice Basket Materials
- Table 6-111. Ice Basket Clevis Pin Stress Summary
- Table 6-112. Ice Basket Mounting Bracket Assembly Stress Summary
- Table 6-113. Ice Basket Plate Stress Summary
- Table 6-114. Ice Basket U-Bolt Stress Summary
- Table 6-115. Ice Basket - Basket End Stress Summary
- Table 6-116. Ice Basket Coupling Screw Stress Summary. 3 Inch Elevation¹
- Table 6-117. Ice Basket Coupling Screw Stress Summary. 12 Foot Elevation⁽¹⁾
- Table 6-118. Ice Basket Coupling Screw Stress Summary. 24 Foot Elevation¹
- Table 6-119. Ice Basket Coupling Screw Stress Summary. 36 Foot Elevation¹
- Table 6-120. Crane and Rail Assembly Design Loads
- Table 6-121. Refrigeration System Parameters
- Table 6-122. Lower Inlet Door Design Parameters and Loads
- Table 6-123. Top Deck Design Parameters and Loads
- Table 6-124. Summary of Results. Upper Blanket Door Structural Analysis — LOCA
- Table 6-125. Intermediate Deck Design Parameters and Loads
- Table 6-126. Summary of Waltz Mill Tests
- Table 6-127. Ice Condenser Temperature Instrumentation
- Table 6-128. Ice Condenser Allowable Limits¹
- Table 6-129. Summary of Catawba Loads-Tangential Case Obtained Using The Two-Mass Dynamic Model
- Table 6-130. Summary of Catawba Loads-Radial Case Obtained Using the Two-Mass Dynamic Model
- Table 6-131. Summary of Load Results of Five Non-Linear Dynamic Models
- Table 6-132. Summary of Parameters Used In The Seismic Analysis

Table 6-133. Selection of Steels in Relation to Prevention of Non-Ductile Fracture of Ice Condenser Components

Table 6-134. Swivel Bracket Stress Summary (Ref.19) Load Case IV

Table 6-135. Containment Coatings

Table 6-136. Cruciform Cable Suspension System Design/Test Load Summary

Table 6-137. External Coupling Ring and Rivet Design Load/Stress Summary

Table 6-138. Ice Basket Load Summary - Basic Design Loads (2000 Lb. Basket)

List of Figures

Figure 6-1. Minimum Containment Sump pH Following a Design Basis LOCA

Figure 6-2. Sensitivity of Peak Pressure to Air Compression Ratio

Figure 6-3. Steam Concentration in a Vertical Distribution Channel

Figure 6-4. Peak Compression Pressure Versus Compression Ratio

Figure 6-5. Upper Compartment Compression Pressure Versus Energy Release for Tests at 110% and 200% of Initial DBA Blowdown Rate

Figure 6-6. Peak Containment Pressure Transient – Pressure

Figure 6-7. Peak Containment Pressure Transient - Upper Containment Temperature

Figure 6-8. Peak Containment Pressure Transient - Lower Containment Temperature

Figure 6-9. Peak Containment Pressure Transient - Sump Temperature

Figure 6-10. Peak Containment Pressure Transient - Ice Melted

Figure 6-11. Containment Spray Return Drains from Air Return Pit Fans

Figure 6-12. Containment Spray Return Drains from Air Return Pit Fans

Figure 6-13. Drain Piping Arrangement Refueling Canal

Figure 6-14. Ice Melted Versus Energy Release for Tests at Different Blowdown Rates

Figure 6-15. Upper Compartment Peak Compression Pressure Versus Blowdown Rate for Tests with 175% Energy Release

Figure 6-16. Peak Reverse Differential Pressure Transient

Figure 6-17. Peak Reverse Differential Pressure Transient

Figure 6-18. Pressure Increase Versus Deck Area from Deck Leakage Tests

Figure 6-19. Energy Release at Time of Compression Peak Pressure from Full-Scale Section Test with 1-Foot Diameter Baskets

Figure 6-20. Peak Containment Temperature Transient - Lower Containment Temperature

Figure 6-21. Peak Containment Temperature Transient - Break Compartment Temperature

Figure 6-22. Deleted Per 1997 Update

Figure 6-23. Typical Upper and Lower Compartment Pressure Transient for Break Compartment Having a DEHL Break

Figure 6-24. Typical Upper and Lower Compartment Pressure Transient for Break Compartment Having a DECL Break

Figure 6-25. Plan at Equipment Rooms Elevation

Figure 6-26. Compartment Section View

Figure 6-27. Plan View at Ice Condenser Elevation - Ice Condenser Compartments

Figure 6-28. Layout of Containment Shell

Figure 6-29. TMD Code Network

Figure 6-30. Nine Volume Nodalization of the Steam Generator Enclosure

Figure 6-31. Double Ended Steam Line Break in Steam Generator Enclosure

Figure 6-32. Double Ended Steam Line Break in Steam Generator Enclosure

Figure 6-33. Double Ended Steam Line Break in Steam Generator Enclosure

Figure 6-34. Double Ended Steam Line Break in Steam Generator Enclosure

Figure 6-35. Double Ended Steam Line Break in Steam Generator Enclosure

Figure 6-36. Two Volume Nodalization of the Steam Generator Enclosure

Figure 6-37. Two Volume Nodalization of the Pressurizer Enclosure

Figure 6-38. Four Volume Nodalization of the Pressurizer Enclosure

Figure 6-39. Developed View of the TMD Code Network for the Reactor Cavity Analysis

Figure 6-40. Flowpath Connections for the Reactor Cavity Analysis

Figure 6-41. Containment Model for the Reactor Cavity Analysis

Figure 6-42. Reactor Vessel Nozzle Break Restraints

Figure 6-43. Reactor Cavity Analysis, Element 1

Figure 6-44. Reactor Cavity Analysis, Element 2

Figure 6-45. Reactor Cavity Analysis, Element 3

Figure 6-46. Reactor Cavity Analysis, Element 4

Figure 6-47. Reactor Cavity Analysis, Element 5

Figure 6-48. Reactor Cavity Analysis, Element 6

Figure 6-49. Reactor Cavity Analysis, Element 7

Figure 6-50. Reactor Cavity Analysis, Element 8

Figure 6-51. Reactor Cavity Analysis, Element 9

Figure 6-52. Reactor Cavity Analysis, Element 10

Figure 6-53. Reactor Cavity Analysis, Element 11

Figure 6-54. Reactor Cavity Analysis, Element 12

Figure 6-55. Reactor Cavity Analysis, Element 13

Figure 6-56. Reactor Cavity Analysis, Element 14

Figure 6-57. Reactor Cavity Analysis, Element 15

Figure 6-58. Reactor Cavity Analysis, Element 16

Figure 6-59. Reactor Cavity Analysis, Element 17

Figure 6-60. Reactor Cavity Analysis, Element 18

Figure 6-61. Reactor Cavity Analysis, Element 19

Figure 6-62. Reactor Cavity Analysis, Element 20

Figure 6-63. Reactor Cavity Analysis, Element 32

Figure 6-64. Reactor Cavity Analysis, Element 33

Figure 6-65. Reactor Cavity Analysis, Element 34

Figure 6-66. Reactor Cavity Analysis, Element 35

Figure 6-67. Reactor Cavity Analysis, Element 36

Figure 6-68. Reactor Cavity Analysis, Element 37

Figure 6-69. Reactor Cavity Analysis, Element 38

Figure 6-70. Reactor Cavity Analysis, Element 39

Figure 6-71. Reactor Cavity Analysis, Element 40

Figure 6-72. Reactor Cavity Analysis, Element 41

Figure 6-73. Reactor Cavity Analysis, Element 42

Figure 6-74. Reactor Cavity Analysis, Element 43

Figure 6-75. Reactor Cavity Analysis, Element 44

Figure 6-76. Reactor Cavity Analysis, Element 45

Figure 6-77. Reactor Cavity Analysis, Element 46

Figure 6-78. Reactor Cavity Analysis, Element 47

Figure 6-79. Reactor Cavity Analysis, Element 53

Figure 6-80. Reactor Cavity Analysis, Element 54

Figure 6-81. Hot Leg Double Ended Guillotine Break

Figure 6-82. Hot Leg Double Ended Guillotine Break

Figure 6-83. Cold Leg Double Ended Guillotine Break

Figure 6-84. Cold Leg Double Ended Guillotine Break

Figure 6-85. Hot Leg Single Ended Split Break

Figure 6-86. Hot Leg Single Ended Split Break

Figure 6-87. Cold Leg Single Ended Split Break

Figure 6-88. Cold Leg Single Ended Split Break

Figure 6-89. Comparison of Satan to Henry Fauske

Figure 6-90. Comparison of Satan to Moody Subcooled

Figure 6-91. Zaloudek Measured Data Versus Modified Zaloudek Correlation

Figure 6-92. Zaloudek Short Tube Data

Figure 6-93. Exit Plane Quality as a Function of Upstream Pressure for Saturated Liquid

Figure 6-94. Henry ANL 7740 Data

Figure 6-95. Loft Tests 809 and 813 Gage P-1

Figure 6-96. Deleted Per 2001 Update

Figure 6-97. Deleted Per 2001 Update

Figure 6-98. Deleted Per 2001 Update

Figure 6-99. Deleted Per 2001 Update

Figure 6-100. Deleted Per 2001 Update

Figure 6-101. Deleted Per 2001 Update

Figure 6-102. Illustration of Choked Flow Characteristics

Figure 6-103. Flow Diagram of Containment Air Return Exchange & Hydrogen Skimmer System

Figure 6-104. Reactor Building Plan at Elev. 565 + 3 Hydrogen Skimmer System

Figure 6-105. Reactor Building Hydrogen Skimmer System

Figure 6-106. Containment Air Return Fan Performance Curve

Figure 6-107. Hydrogen Skimmer Fan Performance Curve

Figure 6-108. Areas of Potential Hydrogen Pockets

Figure 6-109. Flow Diagram of Containment Spray System

Figure 6-110. Containment Spray Pump Performance Curve

Figure 6-111. Recirculation Sump Screen Assembly (UNIT 1)

Figure 6-112. Containment Piping Penetration Valve Arrangements

Figure 6-113. Containment Piping Penetration Valve Arrangements

Figure 6-114. Containment Piping Penetration Valve Arrangements

Figure 6-115. Containment Piping Penetration Valve Arrangements

Figure 6-116. Flow Diagram of Containment Valve Injection Water System

Figure 6-117. Fuel Transfer Tube

Figure 6-118. Model B Electric Hydrogen Recombiner-Cutaway

Figure 6-119. Recombiner Control System Schematic

Figure 6-120. Flow Diagram of Containment Hydrogen Sample & Purge System

Figure 6-121. Deleted Per 1991 Update

Figure 6-122. Deleted Per 1991 Update

Figure 6-123. Deleted Per 1991 Update

Figure 6-124. Deleted Per 2004 Update

Figure 6-125. Deleted Per 2006 Update

Figure 6-126. Deleted Per 2006 Update

Figure 6-127. Deleted Per 2003 Update

Figure 6-128. Flow Diagram of Safety Injection System

Figure 6-129. Flow Diagram of Safety Injection System

Figure 6-130. Flow Diagram of Safety Injection System

Figure 6-131. Flow Diagram of Safety Injection System

Figure 6-132. Safety Injection System

Figure 6-133. Residual Heat Removal Performance Curve

Figure 6-134. Centrifugal Charging Pump Performance Curve

Figure 6-135. Safety Injection Pump Performance Curve

Figure 6-136. Safety Injection/Residual Heat Removal System Process Flow Diagram

Figure 6-137. Ice Condenser

Figure 6-138. Isometric of Ice Condenser

Figure 6-139. Floor Structure

Figure 6-140. Wear Slab Top Surface Area Showing Typical Coolant Piping Layout

Figure 6-141. Lattice Frame Orientation

Figure 6-142. Load Distribution For Tangential Seismic And Blowdown Loads In Analytical Model

Figure 6-143. Lattice Frame

Figure 6-144. Lattice Frame Analysis Model

Figure 6-145. Typical Bottom Ice Basket Assembly

Figure 6-146. Combinations of Concentric Axial Load and Distribution Load

Figure 6-147. Crane Assembly

Figure 6-148. Crane Rail Assembly

Figure 6-149. Refrigerant Cycle Diagram

Figure 6-150. Glycol Cycle to Each Containment

Figure 6-151. Schematic Flow Diagrams of Air Cooling Cycle

Figure 6-152. Air Handling Unit Support Structure

Figure 6-153. Deleted Per 2010 Update

Figure 6-154. Lower Inlet Door Assembly

Figure 6-155. Details of Lower Inlet Door Showing Hinge, Proportioning Mechanism Limit Switches and Seals

Figure 6-156. Inlet Door Frame Assembly

Figure 6-157. Inlet Door Panel Assembly

Figure 6-158. Lower Inlet Door Shock Absorber Assembly

Figure 6-159. Four Loop Ice Condenser Lower Support Structure Conceptual Plan and Sections

Figure 6-160. Four Loop Ice Condenser Lower Support Structure General Assembly

Figure 6-161. Ansys Model Assembly

Figure 6-162. Finite Element Model of Postal Frame

Figure 6-163. Schematic Diagram of Force Applied to Three Pier Lower Support Structure

Figure 6-164. Force Transient Hot Leg Break

Figure 6-165. DLF Spectra Hot Leg Break Force Transient

Figure 6-166. Top Deck Test Assembly

Figure 6-167. Details of Top Deck Door Assembly

Figure 6-168. Intermediate Deck Door Assembly

Figure 6-169. Air Distribution Duct

Figure 6-170. Air Distribution Duct

Figure 6-171. Phase Diagram for Na₂B₄O₇ - .10 H₂O System at One Atmosphere

Figure 6-172. Ice Bed Compaction Versus Time

Figure 6-173. Test Ice Bed Compaction Versus Ice Bed Height

Figure 6-174. Total Ice Compaction Versus Ice Bed Height

Figure 6-175. Ice Condenser RTD Location

Figure 6-176. Block Diagram: Ice Condenser Temperature Monitoring System

Figure 6-177. Door Monitoring Zones

Figure 6-178. Wiring Diagram: "Y" Switch

Figure 6-179. Wiring Diagram: "X" Switches Lower Inlet Doors

Figure 6-180. Deleted Per 2001 Update

Figure 6-181. Model of Horizontal Lattice Frame Structure

Figure 6-182. Group of Six Interconnected Lattice Frames

Figure 6-183. Lattice Frame Ice Basket Gap

Figure 6-184. Typical Displacement Time History for 12 Foot Basket with End Supports - Pluck Test

Figure 6-185. Non Linear Dynamic Model

Figure 6-186. 3 Mass Tangential Ice Basket Model

Figure 6-187. 9 Mass Radial Ice Basket Model

Figure 6-188. 48 Foot Beam Model

Figure 6-189. Phasing Mass Model of Adjacent Lattice Frame Bays

Figure 6-190. Phasing Study Model, 1 Level Lattice Frame 300 Degrees Non-Linear Model

Figure 6-191. Typical Crane Wall Displacement

Figure 6-192. Typical Ice Basket Displacement Response

Figure 6-193. Typical Ice Basket Impact Force Response

Figure 6-194. Typical Crane Wall Panel Load Response

Figure 6-195. Wall Panel Design Load Distribution Obtained Using the 48-Foot Beam Model Tangential Case

Figure 6-196. Wall Panel Design Load Distribution Obtained Using the 48-Foot Beam Model Radial Case

Figure 6-197. Ice Basket Swivel Bracket Assembly

Figure 6-198. Block Ice Minimum Restriction Basket Assembly

Figure 6-199. CNS-1 Double-Ended LBLOCA Mass and Energy Release Analyses

Figure 6-200. CNS-1 Double-Ended LBLOCA Mass and Energy Release Analyses

Figure 6-201. CNS-1 Double-Ended LBLOCA Mass and Energy Release Analyses

Figure 6-202. CNS-1 Double-Ended LBLOCA Mass and Energy Release Analyses

Figure 6-203. Deleted Per 2000 Update.

Figure 6-204. Upper and Lower Compartment Pressure, Min. Pressure Analysis

Figure 6-205. Upper Compartment Heat Removal Rate, Min. Pressure Analysis

Figure 6-206. Lower Compartment Heat Removal Rate, Min. Pressure Analysis

Figure 6-207. Upper and Lower Compartment Temperature, Min. Pressure Analysis

Figure 6-208. Ice Bed Heat Removal Rate, Min. Pressure Analysis

Figure 6-209. Heat Removal Rate by Lower Compartment Drain, Min. Pressure Analysis

Figure 6-210. Heat Removal Rate by Sump and Spray, Min. Pressure Analysis

6.0 Engineered Safety Features

THIS IS THE LAST PAGE OF THE TEXT SECTION 6.0.

THIS PAGE LEFT BLANK INTENTIONALLY.

6.1 Engineered Safety Feature Materials

6.1.1 Metallic Materials

6.1.1.1 Materials Selection and Fabrication

Typical materials specifications used for components in the Engineered Safety Features (ESF) are listed in [Table 6-1](#), Engineered Safety Feature Materials. In some cases, this list of materials may not be totally inclusive. However, the listed specifications are representative of those materials used. Materials utilized are procured in accordance with the materials specification requirements of the ASME Boiler and Pressure Vessel Code, Section III, plus applicable and appropriate Addenda and Code Cases.

Even though fracture toughness was not required by the ASME Code, fracture toughness requirements were imposed on the accumulators which were identified as the only ferritic material actually used in Catawba's engineered safety features systems. The material met the ASME Code for the Catawba components.

The welding materials used for joining the ferritic base materials of the ESF conform to or are equivalent to ASME Material Specifications SFA 5.1, 5.2, 5.5, 5.17, 5.18, and 5.20. The welding materials used for joining nickel-chromium-iron alloy in similar base material combination and in dissimilar ferritic or austenitic base material combination conform to ASME Material Specifications SFA 5.11 and 5.14. The welding materials used for joining the austenitic stainless steel base materials conform to ASME Material Specifications SFA 5.4 and 5.9. These materials are tested and qualified to the requirements of the ASME Code, Section III and Section IX rules and are used in procedures which have been qualified to these same rules. The methods utilized to control delta ferrite content in austenitic stainless steel weldments are discussed in Section [5.2.3](#).

All parts of components in contact with borated water are fabricated of or clad with austenitic stainless steel or equivalent corrosion resistant material. The integrity of the safety-related components of the ESF is maintained during all stages of component manufacture. Austenitic stainless steel is utilized in the final heat treated condition as required by the respective ASME Code, Section II, material specification for the particular type or grade of alloy. Furthermore, it is required that austenitic stainless steel materials used in the ESF components be handled, protected, stored, and cleaned according to recognized and accepted methods which are designed to minimize contamination which could lead to stress corrosion cracking. The rules covering these controls are stipulated in Westinghouse process specifications, which are discussed in Section [5.2.3](#). Additional information concerning austenitic stainless steel, including the avoidance of sensitization and the prevention of intergranular attack, can be found in Section [5.2.3](#). No cold worked austenitic stainless steels having yield strengths greater than 90,000 psi are used for components of the ESF within the Westinghouse standard scope. Westinghouse supplied ESF components within the containment that would be exposed to core cooling water and containment sprays in the event of a loss-of-coolant accident utilize materials listed in [Table 6-1](#). These components are manufactured primarily of stainless steel or other corrosion resistant material. The integrity of the materials of construction for ESF equipment when exposed to post design basis accident (DBA) conditions has been evaluated. Post DBA conditions were conservatively represented by test conditions. The test program (Reference [1](#)) performed by Westinghouse considered spray and core cooling solutions of the design chemical compositions, as well as the design chemical compositions contaminated with corrosion and deterioration products which may be transferred to the solution during recirculation. The effects

of sodium (free caustic), chlorine (chloride), and fluorine (fluoride) on austenitic stainless steels were considered. Based on the results of this investigation, as well as testing by ORNL and others, the behavior of austenitic stainless steels in the post DBA environment will be acceptable. No cracking is anticipated on any equipment even in the presence of postulated levels of contaminants, provided the core cooling and spray solution pH is maintained at an adequate level. The inhibitive properties of alkalinity (hydroxyl ion) against chloride cracking and the inhibitive characteristic of boric acid on fluoride cracking have been demonstrated.

Information concerning the degree to which the materials used comply with Regulatory Guides 1.31, 1.37, and 1.44 are discussed in Section [5.2.3.4](#).

6.1.1.2 Composition, Compatibility, and Stability of Containment and Core Spray Coolants

The vessels used for storing ESF coolants include the cold leg accumulators and the refueling water storage tank.

The cold leg accumulators are carbon steel clad with austenitic stainless steel. Because of the corrosion resistance of these materials, significant corrosive attack on the storage vessels is not expected.

The cold leg accumulators are filled with borated water and pressurized with nitrogen gas. The nominal boron concentration, as boric acid, is approximately 2800 ppm (cycle specific limits are given in the Core Operating Limits Report). Samples of the solution in the accumulators are taken periodically for checks of boron concentration. Principal design parameters of the accumulators are listed in [Table 6-87](#).

The refueling water storage tank is a source of borated cooling water for injection. The nominal boron concentration, as boric acid, is approximately 2800 ppm (cycle specific limits are given in the Core Operating Limits Report), which is below the solubility limit at freezing. The temperature of the refueling water is maintained above 70°F. Principal design parameters of the refueling water storage tank are given in Section [9.2.7](#).

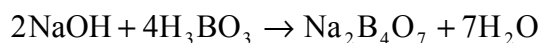
The method of establishing containment spray and recirculation sump pH following a LOCA is discussed in Section [6.2.2](#) and Section [6.2.3](#). Information concerning hydrogen release by the corrosive gas concentrations within the containment following a LOCA is discussed in Section [6.2.5](#).

6.1.1.2.1 Post Accident Chemistry

The soluble acids and bases identified within the containment are boric acid and sodium tetraborate. Boron in the form of boric acid is present in the reactor coolant system, accumulators and refueling water storage tank. Boron and sodium hydroxide in the form of sodium tetraborate are present in the ice.

Boron in the form of boric acid (H_3BO_3) is found in the reactor coolant system, in the accumulators and refueling water storage tank. Refer to [Table 6-2](#) for concentrations used in the post accident chemistry analysis.

Sodium tetraborate ($Na_2B_4O_7$) is an additive in the ice of the ice condenser. Sodium tetraborate ice consists of sodium hydroxide, NaOH, boric acid, H_3BO_3 and water combined as follows:



The ice bed holds a minimum 2.13×10^6 pounds of ice having a minimum boron concentration, per Technical Specifications, of 1800 ppm. The NaOH/B ratio is 1.85. Hence, there are 3834 pounds of boron and 7093 pounds of sodium hydroxide contained in the ice.

6.1.1.2.2 Final Post Accident Chemistry

The time dependent lower bound values of the containment sump pH following a postulated design basis accident were calculated. The results of the calculations are shown in Figure [6-1](#). Within a minute after event initiation, the post LOCA containment sump rises above 7.0 and remains above 7.0 for the duration of the event. The equilibrium value of lower bound containment sump pH of 7.72 is reached at the end of ice melt. The minimum transient value of lower bound post LOCA containment sump pH is 7.37. At all times following the postulated design basis accident, the containment sump pH is 7 or higher.

A conservative upper bound value of containment sump pH is calculated by assuming only melted ice in the sump. The reactor coolant and the boric acid solution from the Refueling Water Tank and Cold Leg Accumulators is ignored. Therefore, the upper bound of 9.2 is very conservative. This is below the values of pH associated with significant effect on corrosion of aluminum and zinc, as well as caustic corrosion of stainless steel components.

In summary, stress-corrosion cracking of austenitic stainless steel components and excessive hydrogen by corrosion of aluminum and galvanized components is avoided.

The assumptions used in the calculations are presented in [Table 6-2](#). The pH is determined using the titration curves for boric acid with sodium hydroxide presented in WCAP-7153-A (Reference [2](#)) and NUREG/CR-5950 (Reference [5](#)).

6.1.2 Organic Materials

6.1.2.1 Coatings and Paint in Westinghouse Scope

Quantification of significant amounts of protective coatings on Westinghouse supplied components located inside the Containment building is given in [Table 6-3](#); the painted surfaces of Westinghouse supplied equipment comprise a small percentage of the total painted surfaces inside the Containment.

For large equipment requiring protective coatings (specifically itemized in [Table 6-3](#)), Westinghouse specifies or approves the type of coating systems utilized; requirements with which the coating system must comply are stipulated in Westinghouse process specifications, which supplement the equipment specifications. For these components, the generic types of coatings used are zinc silicate or epoxy based primer with or without chemically-cured epoxy modified phenolic top coat.

The remaining equipment requires protective coatings on much smaller surface areas and is procured from numerous vendors; for this equipment, Westinghouse specifications require that high quality coatings be applied using good commercial practice. [Table 6-3](#) includes identification of this equipment and total quantities of protective coatings on such equipment.

The total exposed surface area is approximately 3450 square feet and the average thickness is approximately 0.005 inches.

Protective coatings for use in the reactor containment have been evaluated as to their suitability in post DBA conditions. Tests have shown that certain epoxy and modified phenolic systems are satisfactory for in containment use. This evaluation (Reference [3](#)) considered resistance to

high temperature and chemical conditions anticipated during a LOCA, as well as high radiation resistance.

Information regarding compliance with Regulatory Guide 1.54 is discussed below. Further compliance information has been submitted to the NRC for review (via letter NS-CE-1352 dated February 1, 1977, to Mr. C. J. Heltemes, Jr., Quality Assurance Branch, NRC, from Mr. C. Eicheldinger, Westinghouse PWRSD, Nuclear Safety Dept.) and accepted (via letter dated April 27, 1977, to Mr. C. Eicheldinger from Mr. C. J. Heltemes, Jr.).

Regulatory Guide 1.54

Quality Assurance Requirements for Protective Coatings Applied to Water-Cooled Nuclear Power Plants (6/73)

Discussion

Westinghouse nuclear steam supply system equipment located in the containment building is separated into four categories to identify the applicability of this regulatory guide to various types of equipment. These categories of equipment are as follows:

1. Category 1 - Large equipment
2. Category 2 - Intermediate equipment
3. Category 3 - Small equipment
4. Category 4 - Insulated/stainless steel equipment

A discussion of each equipment category follows:

1. Category 1 - Large Equipment

The Category 1 equipment consists of the following:

- a. Reactor coolant system supports (supplied by Duke Power).
- b. Reactor Coolant pumps (motor and motor stand).
- c. Accumulator tanks.
- d. Manipulator crane.

Since this equipment has a large surface area and is procured from only a few vendors, it is possible to implement tight controls over these items. Westinghouse specifies stringent requirements for protective coatings on this equipment through the use of a painting specification in our procurement documents. This specification defines requirements for:

- a. Preparation of vendor procedures.
- b. Use of specific coatings systems which are qualified to ANSI N101.2.
- c. Surface preparation.
- d. Application of the coating systems in accordance with the paint manufacturer's instructions.
- e. Inspections and nondestructive examinations.
- f. Exclusion of certain materials.
- g. Identification of all nonconformances.
- h. Certifications of compliance.

The vendor's procedures are subject to review by Westinghouse engineering personnel, and the vendor's implementation of the specification requirements is monitored during the Westinghouse quality assurance surveillance activities.

This system of controls provides assurance that the protective coatings will properly adhere to the base metal during prolonged exposure to a post-accident environment present within the containment building.

2. Category 2 - Intermediate Equipment

- a. Seismic platform and tie rods.
- b. Reactor internals lifting rig.
- c. Head lifting rig.
- d. Electrical cabinets.

Since these items are procured from a large number of vendors, and individually have very small surface areas, it is not practical to enforce the complete set of stringent requirements which are applied to Category 1 items. However, Westinghouse does implement another specification in our procurement documents. This specification defines to the vendors the requirements for:

- a. Use of specific coating systems which are qualified to ANSI N101.2.
- b. Surface preparation.
- c. Application of the coating systems in accordance with the paint manufacturer's instructions.

The vendor's compliance with the requirements is also checked during the Westinghouse quality assurance surveillance activities in the vendor's plant. These measures of control provide a high degree of assurance that the protective coatings will adhere properly to the base metal and withstand the postulated accident environment within the containment building. Westinghouse has not taken credit for this in calculating the amount of paint which might peel or flake off in the post accident environment.

3. Category 3 - Small Equipment

The Category 3 equipment consists of the following:

- a. Transmitters
- b. Alarm Horns
- c. Small Instruments
- d. Valves
- e. Heat Exchanger Supports

Since these items are procured from several different vendors, and the total exposed surface area is very small ([Table 6-3](#): < 1300 ft²) it is not necessary to enforce the complete set of stringent requirements of the Category 1 items. For purposes of estimating the amount of paint that might peel or flake off, Westinghouse has assumed that all of this material might come off, and the average thickness is approximately 0.005 inches.

4. Category 4 - Insulated or Stainless Steel Equipment

Category 4 equipment consists of the following:

- a. Steam generators - covered with rigid reflective insulation, or flexible fiberglass blanket insulation.
- b. Pressurizer - covered with rigid reflective insulation.
- c. Reactor pressure vessel - covered with rigid reflective insulation.
- d. Reactor cooling piping - stainless steel.
- e. Reactor coolant pump casings - stainless steel.

Since Category 4 equipment is insulated or is stainless steel, no painted surface areas are exposed within the containment. Therefore, this regulatory guide is not applicable for Category 4 equipment.

6.1.2.2 Coatings and Paint in Duke Scope

Duke complies with Regulatory Guide 1.54, Quality Assurance Requirements for Protective Coatings Applied to Water-Cooled Nuclear Power Plants.

The original coating materials and coating systems were specified by Engineering and applied by the Duke Power Construction Department to all structures within the containment and the Containment Vessel. The coating systems were qualified for radiation exposure, pressure, temperature, and water chemistry exposure during a DBA in accordance with ANSI N101.2.

Carboline coating materials are now used for maintenance of the existing coating systems and for any new applications. These coating systems are specified by Engineering and applied by the Duke Power Maintenance Department. The Carboline coating materials have been qualified over the existing Mobil/Valspar coatings as a mixed system and as a new coating system for radiation exposure, pressure, temperature, and water chemistry exposure during a DBA in accordance with ANSI N101.2.

The original, maintenance, and new coating systems defining temperature limitations, surface preparation, type of coating, and dry film thickness are tabulated on [Table 6-135](#).

The elements of the Catawba Coatings Program are documented in a Nuclear Generation Department - Administrative Procedure AD-EG-ALL-1640. The Catawba Coatings Program includes periodic condition assessments of Service Level I coatings used inside containment. As localized areas of degraded coatings are identified, those areas are evaluated for repair or replacement, as necessary.

9,300 square feet of unqualified coatings inside the containment have been evaluated for impact on the ECCS Sump Strainer and its ability to support ECCS recirculation & containment spray functions. See Section [6.3](#) & [6.5](#) for details of the evaluation.

6.1.2.3 Quantities of Organic Materials Inside Containment

Organic Materials that exist within the Containment in significant amounts are identified and quantified in [Table 6-4](#).

6.1.3 Polyethylene Material

6.1.3.1 High Density Polyethylene (HDPE)

Typical materials specifications used for components in the Engineered Safety Features (ESF) are listed in [Table 6-1](#), Engineered Safety Feature Materials. 12" HDPE materials utilized in the RN system are procured in accordance with the requirements of References [6](#), [7](#), and [8](#).

6.1.4 References

1. "Behavior of Austenitic Stainless Steel in Post Hypothetical Loss of Coolant Accident Environment," WCAP - 7798-L (Proprietary) and WCAP-7803 (Non-Proprietary), January 1972.
2. WCAP-7153-A, "Investigation of Chemical Additives for Reactor Containment Sprays", April 1975. (Non-Proprietary)
3. Picone, L. F., "Evaluation of Protective Coatings for Use in Reactor Containments", WCAP-7825, December, 1971.
4. M. S. Tuckman (Duke) letter dated November 11, 1998 to Document Control Desk (NRC), "Response to Generic Letter 98-04: Potential Degradation of the Emergency Core Cooling System and the Containment Spray System After a Loss-of-Coolant Accident Because of Construction and Protective Coating Deficiencies and Foreign Material in Containment," Catawba Nuclear Station, Unit 1 and 2 Docket Nos. 50-413, 414.
5. E.C. Beahm, R.A. Lorenz, C.F. Weber, Iodine Evolution and Control, NUREG/CR-5950, ORNL/TM-12242 R3, December 1992.
6. Catawba Nuclear Station, Units 1 and 2, Docket Numbers 50-413 and 50-414, Request for Relief Number 06-CN-003, Use of Polyethylene Materials in Nuclear Safety Related Piping Applications, Dated October 26, 2006.
7. Catawba Nuclear Station, Units 1 and 2, Relief 06-CN-003 Use of Polyethylene Material in Nuclear Service Water Applications (TAC Nos. MD3729 and MD3730), Dated September 12, 2008.
8. Catawba Nuclear Station, Units 1 and 2, Relief 06-CN-003 For Use of Polyethylene Material in Buried Service Water Piping (TAC Nos. ME0234 and ME0235), Dated May 27, 2009.

THIS IS THE LAST PAGE OF THE TEXT SECTION 6.1.

THIS PAGE LEFT BLANK INTENTIONALLY.

6.2 Containment Systems

6.2.1 Containment Functional Design

6.2.1.1 Containment Structure

6.2.1.1.1 Design Bases

Note:

This section of the FSAR contains information on the design basis and design criteria for the Reactor Building **Steel (primary) Containment**. Additional information that may assist the reader is provided in Design Basis Specification for the Reactor Building Structures (CNS-1144.00-00-0010).

The containment vessel steel shell is designed for dead loads, construction loads, design basis accident loads, external pressure, seismic loads and penetration loads as described in Section [3.8.2.3](#). The applicable loading combinations considered are listed in [Table 3-37](#).

The design basis accident internal pressure is 15 psig. The effects of pipe rupture in the primary coolant system, up to and including a double-ended rupture of the largest pipe as well as rupture of the main steam line, are considered in determining the peak accident pressure.

The maximum design external pressure is 1.5 psig. This is greater than the internal vacuum created by an accidental trip of a portion of the Containment Spray System during normal operation. The Containment Pressure Control System is discussed in Section [7.6](#).

The internal structures of the containment vessel are also designed for subcompartment differential accident pressures. The accident pressures considered are due to the same postulated pipe ruptures as described above for the containment vessel. A 40 percent margin is applied to these calculated differential pressures. A tabulation of the calculated as well as the design pressures (including the 40 percent increase) is given in [Table 3-47](#).

The other simultaneous loads in combination with the accident pressures and the applicable load factors are given in [Table 3-32](#). For a further description of these loads see Section [3.8.3.7](#).

The functional design of the Containment is based upon the following accident input source term assumptions and conditions:

1. The design basis blowdown energy of 324.2×10^6 Btu and mass of 498,200 lb put into the Containment.
2. The hot metal energy is considered.
3. A reactor core power of 3479 MWt (rated thermal power plus measurement uncertainty) used for decay heat generation.
4. The minimum Engineered Safety Features performance (i.e., the single failure criterion applied to each safety system) comprised of the following:
 - a. The ice condenser which condenses steam generated during a LOCA thereby limiting the pressure peak inside the Containment (see Section [6.7](#)).
 - b. The Containment Isolation System which closes those fluid penetrations not serving accident consequence limiting purposes (see Section [6.2.4](#)).

- c. The Containment Spray System which sprays cool water into the Containment atmosphere, thereby limiting the pressure peak (particularly in the long term - see Section [6.2.2](#)).
- d. The Annulus Ventilation System which produces a slightly negative pressure within the annulus, thereby precluding outleakage and relieving the post-accident thermal expansion of air in the annulus (see Sections [6.2.3](#) and [9.4.9](#)).
- e. The air return fans which return air to the lower compartment.
- f. The Residual Heat Removal System, which provides a portion of the spray water to the Containment Spray System following realignment to sump recirculation, see Section [6.2.2](#).

Refer to Section [6.2.1.1.3.1](#) for the peak Containment pressure transient analysis where the above assumptions are discussed and utilized.

The Containment is designed to ensure that an acceptable upper limit of leakage of radioactive material is not exceeded under design accident conditions. For purposes of integrity, the Containment may be considered as the Containment Vessel and the Containment Isolation System. This structure and system are directly relied upon to maintain Containment integrity. The Annulus Ventilation System and Reactor Building function to keep outleakage minimal (the Reactor Building also serves as a protective structure), but are not factors in determining the design leak rate.

Although the Containment System incorporates the Annulus Ventilation System to maintain a negative pressure in the annulus as described in Section [6.2.3](#), assurance of Containment leak-tightness does not depend upon this system at any time. The design leak rate is the same whether or not this system is in operation. This leak rate is a property of the Containment Vessel alone, as verified by tests described in Section [6.2.1.6](#). The effect of the Annulus Ventilation System may be considered a margin of conservatism built into the leak rate as the system collects, delays and filters gases leaking from the Containment Vessel. The Containment Isolation System serves to maintain Containment integrity in the event of a fluid penetration leak. The design evaluation of this system is presented in Section [6.2.4.3](#), and testing and inspection of this system are discussed in Section [6.2.4.4](#) and in the Technical Specifications.

The Containment is specifically designed to meet the intent of the applicable General Design Criteria listed in Section [3.1](#). This Section ([6.2.1](#)), [Chapter 3](#), and other portions of [Chapter 6](#) present information showing conformance of design of the Containment and related systems to these criteria.

The ice condenser is designed to limit the Containment pressure below the design pressure for all reactor coolant pipe break sizes up to and including a double-ended severance. Characterizing the performance of the ice condenser requires consideration of the rate of addition of mass and energy to the Containment, as well as the total amounts of mass and energy added. Analyses have shown that the accident which produces the highest blowdown rate into an Ice Condenser Containment results in the maximum Containment pressure rise. That accident is the double-ended severance of a reactor coolant pipe.

Post-blowdown energy releases can also be accommodated without exceeding Containment design pressure.

6.2.1.1.2 Design Features

Consideration is given to subcompartment differential pressure resulting from a design basis accident in Section [6.2.1.2](#). If a design basis accident were to occur due to a pipe rupture in one of these relatively small volumes, the pressure would build up at a faster rate than in the Containment, thus imposing a differential pressure across the wall of these structures.

Parameters affecting the assumed capability for post-accident pressure reduction are discussed in Section [6.2.1.1.3](#).

There are five conditions which have a potential for resulting in a net external pressure on the Containment:

1. Rupture of a hot or high pressure process pipe in the annulus.
2. Inadvertent Containment Spray System initiation during normal operation.
3. Inadvertent Containment air return fan initiation during normal operation.
4. Containment purge fan operation with Containment purge inlet valves closed.
5. Containment air release fan pressure controller failure resulting in fan not shutting off properly.

The Containment design of 1.5 psig negative is not violated in the first four above listed cases due to either equipment limitations or design features, but violation is possible in the fifth case. The maximum Containment purge fan differential pressure is 0.75 psig, which would produce a 0.75 psig negative pressure in the Containment with the purge inlet valves closed. The containment air release fan is capable of pulling a negative pressure in containment beyond design limits if allowed to run unchecked.

The guard pipe for hot penetrations is discussed in Section [3.9](#). This design feature provides a path to the Containment for the fluid from a rupture in the annulus region.

Inadvertent spray or air return fan operation is precluded by design features consisting of an additional set of Containment pressure sensors, which prevent operation of either of these systems when the Containment pressure is below 0.25 psig positive. The logic of these sensors is presented in Section [7.6.4](#).

Failure of the containment air release fan to properly shut off is not a credible scenario because of system design features and administrative controls in place to prevent this event. System control logic is designed to automatically shut off the fan when containment pressure reaches 0 psig. The OAC response to a low pressure alarm ensures a VQ release is terminated if in progress and in cases where the OAC is inoperable the pressure is monitored on a thirty minute frequency during releases. These controls are utilized to ensure the pressure stays within the Tech Spec limit of 0.1 psig negative.

The codes and standards applied for the design of both the containment vessel and the interior structures are listed in [Table 3-31](#).

The Containment consists of a Containment Vessel and a separate Reactor Building enclosing an annulus. The Containment Vessel is a freestanding welded steel structure with a vertical cylinder, hemispherical dome, and a flat circular base. The Reactor Building is a reinforced concrete structure, similar in shape to the Containment Vessel. The design of these structures is described in Section [3.8.1.1](#) for the Reactor Building and Section [3.8.2.1](#) for the Containment Vessel.

The design pressure for the Containment is 15 psig, and the design temperature is 250°F. The environmental qualification (EQ) limit for most equipment in containment is 340°F. All

equipment in containment, that is within the scope of 10 CFR 50.49, has been qualified to meet its design function for all post-accident environmental conditions for which it must operate. (The Peak Containment Temperature Transient is discussed in Section [6.2.1.1.3](#)). The design basis accident leakage rate is 0.2 percent/24 hr for the first 24 hours of the accident and 0.1 percent/24 hr thereafter. The design methods used to ensure integrity of the Containment internal structures and subcompartments with respect to accident pressure pulses are described in Section [3.8.3.4](#).

HISTORICAL INFORMATION NOT REQUIRED TO BE REVISED

The type of Containment used for the Catawba Nuclear Station was selected for the following reasons:

- 1. The Ice Condenser Containment can accept large amounts of energy and mass inputs and maintain low internal pressures and leakage rates. A particular advantage of the ice condenser is its passive actuation not requiring an actuation system signal.*
- 2. The Ice Condenser Containment combines the required integrity, compact size, and a carefully considered advanced design desirable for a nuclear station.*
- 3. The double-enclosure concept affords minimal interaction between the Containment Vessel (leakage barrier) and the Reactor Building (protective structure), a margin of conservatism in leakage rate from the use of two structures plus the Annulus Ventilation System, and a reduction of gaseous and particulate radioactive release due to annulus mixing and holdup prior to filtering and release.*

The regions where appreciable quantities of water may be trapped and prevented from returning to the containment recirculation sump are listed in [Table 6-5](#) along with their approximate volumes. Not listed in this table are regions below the operating floor which begin to fill as the sump level rises.

The available NPSH for the containment spray pumps and the residual heat removal pumps was calculated ignoring any pressure in the containment above atmospheric. Only a minimum amount of static head due to water level above the sump floor was included. This minimum level is the amount of water that must be present in order to transition into the recirculation mode of ECCS operation.

Return of containment spray solution from the upper compartment to the recirculation sump is discussed in Section [6.2.1.1.3](#).

The ice condenser components are described in Section [6.7](#) along with a discussion of the test programs that have been conducted to qualify these components for use in the ice condenser. Section [6.7](#) also includes an analysis of the expected reduction in the mass of the ice due to sublimation during normal plant operation as well as a discussion on the ice condenser condensing capability during a loss-of-coolant accident.

The Ice Condenser Containment, incorporating forced circulation of the Containment atmosphere together with the Containment Spray System, ensures the functional capability of Containment for as long as necessary following an accident. The peak internal design pressure (15.0 psig) of the Containment is greater than the peak compression pressure (7.57 psig) occurring as the result of the complete blowdown of the reactor coolant through any rupture of the Reactor Coolant System, up to and including the hypothetical double-ended severance of the largest reactor coolant pipe. The design pressure is not exceeded during any subsequent long term pressure transient.

6.2.1.1.3 Design Evaluation

6.2.1.1.3.1 Loss of Coolant Accident

The time history of conditions with an Ice Condenser Containment during a postulated loss of coolant accident can be divided into 2 periods for calculational purposes:

1. The initial reactor coolant blowdown, which for the largest assumed pipe break occurs in approximately 30 seconds.
2. The post blowdown phase of the accident which begins following the blowdown and extends several hours after the start of the accident.

During the first few seconds of the blowdown period of the Reactor Coolant System, containment conditions are characterized by a rapid pressure and temperature increase. It is during this period that the peak differential pressures and blowdown loads occur. To calculate these transients, a detailed spatial and short time increment analysis is necessary. This analysis is performed with the TMD computer code, with the calculation time of interest extending up to a few seconds following the accident initiation.

Physically, tests at the ice condenser Waltz Mill test facility have shown that the blowdown phase represents that period of time in which the lower compartment air and a portion of the ice condenser air are displaced and compressed into the upper compartment and the remainder of the ice condenser. The Containment pressure at or near the end of blowdown is governed by this air compression process.

Containment pressure during the post blowdown phase of the accident is calculated with the GOTHIC 4.0/DUKE code, which models the Containment structural heat sinks and Containment safeguards systems.

Compression Ratio Analysis

As blowdown continues following the initial pressure peak from a double ended cold leg break, the pressure in the lower compartment again increases, reaching a peak at or before the end of blowdown. The pressure in the upper compartment continues to rise from the beginning of blowdown and reaches a peak which is slightly lower than the lower compartment pressure. After blowdown is complete, the steam in the lower compartment continues to flow through the doors into the ice bed compartment and is condensed.

The primary factor in producing this upper compartment pressure peak and, therefore, in determining the design pressure, is the displacement of air from the lower compartment into the upper compartment. The ice condenser quite effectively performs its function of condensing virtually all the steam that enters the ice beds. Essentially, the only source of steam entering the upper Containment is from leakage through the drain holes and other leakage around crack openings in hatches in the operating deck separating the lower and upper portions of the Containment building.

A method of analysis of the compression peak pressure was developed, based on the results of full-scale section tests. This method consists of the calculation of the air mass compression ratio, the polytropic exponent for the compression process, and the effect of steam bypass through the operating deck on this compression.

The compression peak pressure in the upper Containment for the Catawba design is calculated to be 7.57 psig (for an initial air pressure of 0.3 psig). This compression pressure includes the effect of a pressure increase of 0.4 psi from steam bypass and also for the effects of the dead-ended volumes. The nitrogen partial pressure from the accumulators is not included since this nitrogen is not added to the Containment until after the compression peak pressure has been

reduced, which is after blowdown is completed. This nitrogen is considered in the analysis of pressure decay following blowdown as presented in the long term performance analysis. In the following sections, a discussion of the major parameters affecting the compression peak will be discussed. Specifically, they are air compression, blowdown energy, blowdown rate, and steam bypass.

Air Compression Process Description

The volumes of the various Containment compartments determine directly the air volume compression ratio. This is basically the ratio of the total active Containment air volume to the compressed air volume during blowdown. During blowdown, air is displaced from the lower compartment and compressed into the ice condenser beds and into the upper Containment above the operating deck. It is this air compression process which primarily determines the peak in Containment pressure, following the initial blowdown release. A peak compression pressure of 7.57 psig is based on the Catawba design compartment volumes shown in [Table 6-6](#). [Figure 6-2](#) shows the sensitivity of the compression peak pressure with different air compression ratios.

The actual Waltz Mill test compression ratios were found by performing air mass balances before the blowdown and at the time of the compression peak pressure, using the results of three special full-scale section tests. These three tests were conducted with an energy input representative of the plant design.

In the calculation of the mass balance for the ice condenser, the compartment is divided into two sub-volumes; one volume representing the flow channels and one volume representing the ice baskets. The flow channel volume is further divided into four sub-volumes, and the partial air pressure and mass in each sub-volume is found from thermocouple readings of the air that is saturated with steam at the measured temperature. From these results, the average temperature of the air in the ice condenser compartment is found, and the volume occupied by the air at the total ice condenser pressure is found from the equation of state as follows:

$$V_a = \frac{M_a R_a T_a}{P} \quad \text{Equation 1}$$

where:

- V_a = Volume of ice condenser occupied by air (ft³)
- M_a = Mass of air in ice condenser compartment (lbm)
- T_a = Average temperature of air in ice condenser (°R)
- P = Total ice condenser pressure (lbf/ft²)

The partial pressure and mass of air in the lower compartment are found by averaging the temperatures indicated by the thermocouples located in that compartment and assuming saturation conditions. For these three tests, it was found that the partial pressure, and hence the mass of air in the lower compartment, was zero at the time of the compression peak pressure.

The actual Waltz Mill test compression ratio is then found from the following:

$$C_r = \frac{V_1 + V_2 + V_3}{V_3 + V_a} \quad \text{Equation 2}$$

where:

- V_1 Lower compartment volume (ft³)
- V_2 Ice condenser compartment volume (ft³)
- V_3 Upper compartment volume (ft³)

The polytropic exponent for these tests is then found from the measured compression pressure and the compression ratio calculated above. Also considered is the pressure increase that results from the leakage of steam through the deck into the upper compartment.

The compression peak pressure in the upper compartment for the tests or Containment design is then given by

$$P_3 = P_o (C_r)^n + \Delta P_{\text{deck}} \quad \text{Equation 3}$$

where:

- P_3 = Compression peak pressure (psia)
- C_r = Volume compression ratio
- P_o = Initial containment pressure, 15.0 psia
- n = Polytropic exponent
- ΔP_{deck} = Pressure increase caused by deck leakage (psi)

Using the method of calculation described above, the compression ratio is calculated for the three full-scale section tests. From the results of the air mass balances, it was found that air occupied 0.645 of the ice condenser compartment volume at the time of peak compression, or,

$$V_a = 0.645V_2 \quad \text{Equation 4}$$

The final compression volume includes the volume of the upper compartment as well as part of the volume of air in the ice condenser. The results of the full-scale section tests ([Figure 6-3](#)) show a variation in steam partial pressure from 100 percent near the bottom of the ice condenser to essentially zero near the top. The thermocouples and pressure detectors confirm that at the time when the compression peak pressure is reached, steam occupies less than half of the volume of the ice condenser. The analytical model used in defining the Containment pressure peak uses upper compartment volume plus 64.5 percent of the ice condenser air volume as the final volume. This 64.5 percent value was determined from appropriate test results.

The calculated volume compression ratios are shown in [Figure 6-4](#), along with the compression peak pressures for these tests. The compression peak pressure is determined from the measured pressure, after accounting for the deck leakage contribution. From the results shown in [Figure 6-4](#), the polytropic exponent for these tests is found to be 1.13.

For the Catawba design, the volume compression ratio, not accounting for dead-ended volume effect, is calculated using the data in [Table 6-13](#):

- V_1 is the sum of elements 1-6, 27, 31, 33, and 50-53
- V_2 is the sum of elements 7-24 and 40-45
- V_3 is the sum of elements 25, 38, 39, and 46-49

$$C_r = \frac{273,218 + 110,522 + 717,101}{717,101 + 0.645 \times 110,522}$$

Equation 5

$$C_r = 1.396$$

The peak compression pressure, based on an initial containment pressure of 15.0 psia, is then given by Equation 3 as:

$$P_3 = 15.0(1.396)^{1.13} + 0.4$$

$$P_3 = 22.27 \text{ psia or } 7.57 \text{ psig}$$

This peak compression pressure includes a pressure increase of 0.4 psi from steam bypass through the deck. The effect of the dead-ended compartment volumes is to trap additional air, and thus reduce the compression ratio and the above calculated peak pressure.

Sensitivity To Blowdown Energy

The sensitivity of the upper compartment compression pressure peak versus the amount of energy released is shown in [Figure 6-5](#). This figure shows the magnitude of the peak compression pressure versus the amount of energy released in terms of percentage of Reactor Coolant System energy release. These data are based on test results in which each of the tests were run at 110 percent and 200 percent of the initial blowdown rate equivalent to the maximum coolant pipe break flow.

These test results indicate the very large capacity of the ice condenser for additional amounts of energy with only a small effect on compression peak pressure. For example, during testing, 100 percent energy release gave a pressure of about 6.8 psig, while an increase up to 220 percent energy release gave an increase in peak pressure of only about 2 psi. It is also important to note that maldistribution of steam into different sections of the ice condenser would not cause even the small increase in peak pressure that is shown in [Figure 6-5](#). For every section of the ice condenser which may receive more energy than that of the average section, there are other sections which receive less energy. Thus, the compression pressure in the upper compartment would be indicated by the test performance based on 100 percent energy release, rather than either the maximum energy release section or the minimum energy release section.

[Figure 6-14](#) gives some insight as to the very large capacity for energy absorption of the ice condenser, as obtained from test results. [Figure 6-14](#) is a plot of the amount of ice melted versus the amount of energy released, based on test results at different energies and blowdown rates. These test results indicate that a 200 percent energy release melts only about 74 percent of the ice, while 100 percent energy release melts only 37 percent of the ice. Thus, even for energy release considerably in excess of 200 percent, there would still be a substantial amount of ice remaining in the condenser.

Effect of Blowdown Rate

[Figure 6-15](#) shows the effect of blowdown rate upon the final compression pressure in the upper compartment as obtained from test results. [Figure 6-15](#) is based on a series of tests, all of which had the plant design ice condenser configuration, but with the important difference that all of these tests were run with 175 percent of the Reactor Coolant System energy release quantity. There are two important effects to note from [Figure 6-15](#). First, the magnitude of the compression peak pressure in the upper compartment is low (about 7.7 psig) for the reactor plant design blowdown rate. Second, even an increase in this rate up to 200 percent blowdown rate produces only a small increase in the magnitude of this peak pressure (about 1 psi).

Effect of Steam Bypass

The mass of steam which leaks through the operating deck into the upper Containment is a function of the relative flow areas and loss coefficients of the deck and inlet doors to the ice condenser, the mass of steam input to the lower compartment at the time of peak compression pressure, and the mass of steam stored in the lower compartment at the time of peak compression pressure.

Following is a discussion of the results of four full-scale section tests which were conducted at Waltz Mill to measure the effect of deck leakage on the final compression peak pressure, and the calculational technique used to obtain the maximum allowable deck leakage area.

The effect of deck leakage on upper Containment pressure has been verified by a series of four special, full-scale section tests. These tests were all identical, except different size deck leakage areas were used.

The results of these tests are given in [Figure 6-18](#), which includes two curves of test results. The slope of the increase in pressure at the end of blowdown is approximately 0.107 psi/ft² in the range of interest for deck leakage area. Each curve shows the difference in upper compartment pressure between one test and another resulting from a difference in deck leakage area. One curve shows the increase in upper compartment pressure at the end of the boiler blowdown (after the compression peak pressure, at about 50 seconds in these tests), and the second curve shows the increase in upper compartment peak pressure, (about 10 seconds in these tests). It should be noted that the pressure at the end of blowdown is less than the peak upper compartment pressure, which occurred at about 10 seconds for the reference blowdown test.

The containment pressure increase due to deck leakage is directly proportional to the total amount of steam leakage into the upper compartment. The amount of this steam leakage is, in turn, proportional to the amount of steam released from the boiler minus the inventory of steam remaining in the lower compartment. Notably, the increase in upper compartment compression peak pressure is substantially less than the increase in upper compartment pressure at the end of blowdown. This is because the peak compression pressure occurs before the boiler has released all of its energy, and the measured increase in peak compression pressure due to increased deck leakage, is proportionately reduced. For the case of the station design, the final peak compression pressure is conservatively assumed to occur when the Reactor Coolant System has released 75 percent of its total energy. This value is selected as a reference value, based on the results of a number of tests conducted with different blowdown rates and total energy releases, as shown in [Figure 6-19](#). The actual deck leakage coefficient is therefore,

$$\frac{\Delta P_{\text{deck}}}{A_{\text{bypass}}} = 0.107 \times 0.75 = 0.080 \text{ psi/ft}^2$$

The above equation was revised in the 2000 update.

The divider barrier, including the enclosures over the pressurizer, steam generators, and reactor vessel, is designed to provide a reasonably tight seal against leakage. Holes are purposely provided in the bottom of the refueling cavity and in the containment air return fan room to allow water from sprays in the upper compartment to drain to the sump in the lower compartment. Potential leakage paths exist at all the joints between the operating deck, the pump access hatches, and reactor vessel enclosure slabs. The total of all deck leakage flow areas is approximately 5 square feet. The effect of this potential leakage path is small and is found to be:

$$\Delta P_{\text{deck}} = 5 \times 0.080 = 0.4 \text{ psi}$$

In the event that the Reactor Coolant System break flow is so small that it would leak through these flow paths without developing sufficient differential pressure (1 lbf/ft²) to open the ice condenser doors, steam from the break slowly pressurizes the Containment. The Containment Spray System has sufficient capacity to maintain pressure well below design for this case.

The method of analysis used to obtain the maximum allowable deck leakage capacity as a function of the primary system break size is as follows:

During the blowdown transient, steam and air flow through the ice condenser doors and also through the deck bypass area into the upper compartment. For the Containment, this bypass area is composed of two parts: a known leakage area of 2.3 ft², with a geometric loss coefficient of 1.5 through the deck drainage holes, located at the bottom of the refueling canal and at the containment air return fan pit, and an undefined deck leakage area with a conservatively small loss coefficient of 2.5. A resistance network similar to that used in TMD is used to represent 6 lower compartment volumes, each with a representative portion of the deck leakage and the lower inlet door flow resistance. Flow area is calculated for small differential pressures on the lower inlet doors and across the operating deck. The resultant deck leakage rate and integrated steam leakage into the upper compartment is then calculated. The lower inlet doors are initially held shut by the cold head of air behind the doors (approximately one pound per square foot). The initial blowdown from a small break opens the doors and removes the cold head on the doors. With the door differential removed, the door position is slightly open. An additional pressure differential of one pound per square foot is then sufficient to fully open the doors. The nominal door opening characteristics are based on test results.

One analysis conservatively assumed that flow through the postulated leakage paths is pure steam. During the actual blowdown transient, steam and air representative of the lower compartment mixture leak through the holes, thus, less steam would enter the upper compartment. If flow were considered to be a mixture of liquid and vapor, the total leakage mass would increase, but the steam flow rate would decrease. The analysis also assumed that no condensing of the flow occurs due to structural heat sinks. The peak air compression in the upper compartment for the various break sizes is assumed, with steam mass added to this value to obtain the total Containment pressure. Air compression for the various break sizes is obtained from previous full-scale section tests conducted at Waltz Mill.

The allowable leakage area for the following Reactor Coolant System (RCS) break sizes was determined: DE, 0.6 DE, 3 ft², 0.5 ft², 8 inch diameter, 6 inch diameter, 2.5 inch diameter and 0.5 inch diameter. For break sizes 3 ft² and above, a series of deck leakage sensitivity studies were made to establish the total steam leakage to the upper compartment during the blowdown transient. This steam was added to the peak compression air mass in the upper compartment to calculate a peak pressure. Air and steam were assumed to be in thermal equilibrium, with the air partial pressure increased over the air compression value to account for heating effects. For these breaks, sprays were neglected. Reduction in compression ratio by return of air to the lower compartment was conservatively neglected. The results of this analysis are shown in [Table 6-12](#). This analysis is confirmed by Waltz Mill tests conducted with various deck leaks equivalent to over 50 ft² feet of deck leakage for the double-ended blowdown rate and is shown in [Figure 6-18](#).

For breaks 0.5 ft² and smaller, the effect of Containment sprays was included. The method used is as follows: for each time step of the blowdown, the amount of steam leaking into the upper compartment was calculated to obtain the steam mass in the upper compartment. This steam was mixed with the air in the upper compartment, assuming thermal equilibrium with air. The air

partial pressure was increased to account for air heating effects. After sprays were initiated, the pressure was calculated based on the rate of accumulation of steam in the upper compartment.

This analysis was conducted for the 0.5 ft², 8 inch, 6 inch and 2.5 inch break sizes, assuming one spray pump operating (3400 gpm at 100° F). As shown in [Table 6-12](#), the 6 inch and the 8 inch breaks are the limiting cases for this range of break sizes.

A second, more realistic, method was used to analyze the 0.5 ft² and the 8 inch diameter breaks. This analysis assumed a 30 percent air, 70 percent steam mixture flowing through the deck leakage area. This is conservative considering the amount of air in the lower compartment during this portion of the transient. Operation of the deck fan increases the air content of the lower compartment, thus increasing the allowable deck leakage area. Based on the LOTIC code analysis, a structural heat removal rate of over 6000 Btu/sec from the upper compartment is indicated. Therefore, a steam condensation rate of 6 lbm/sec was used for the upper compartment. The results indicate that with one spray pump operating and a deck leakage area of 50 ft², the peak Containment pressure is below design pressure.

In this deck leakage sensitivity study, the 0.5 inch break is not sufficient to open the ice condenser inlet doors. For this break size, the upper containment spray is sufficient to condense the break steam flow. The deck leakage sensitivity study employs conservative assumptions to maximize the steam content in upper containment. As such, it should not be viewed as reflecting the actual plant behavior (with regard to ice condenser door behavior or containment pressurization) following Reactor Coolant System breaks.

In conclusion, it is apparent that there is a substantial margin between the design deck leakage area and that which can be tolerated without exceeding containment design pressure.

Long Term Containment Pressure Analysis

The GOTHIC 4.0/DUKE (Reference [47](#)) code is used to determine the containment response to high-energy line breaks. It solves the conservation equations for mass, energy, and momentum for multi-component two-phase flow. These equations are solved numerically on a finite-volume mesh made up of numerous computational cells. The code features a nodalization scheme in which lumped parameter, one-, two-, and three-dimensional analysis or any combination of these may be performed.

GOTHIC includes finite-difference conduction models for passive thermal conductors. Concrete walls and structural steel within the containment building are simulated with these models. The various mechanical components in the emergency safeguards systems, such as valves, heat exchangers, spray nozzles, and air return fans are also modeled.

Ice condenser heat transfer is calculated explicitly in the GOTHIC code. It is assumed that the ice remains at its initial temperature until it melts. The ice mass and surface area in each node is adjusted to account for the melted ice in each time increment. It is assumed that the ice remains in cylindrical columns within each node.

There are four different regions in an ice condenser containment building. These are the lower containment, upper containment, ice condenser, and dead-ended compartments. Slightly different modeling approaches are utilized in each of these four regions in the GOTHIC ice condenser containment model to accurately and efficiently calculate the containment response. The validation of the GOTHIC ice condenser model is presented in Reference [45](#), along with a discussion of the overall methodology utilized.

Peak Containment Pressure Transient

The following are major input assumptions used in the GOTHIC analysis for the pump discharge pipe rupture case, with the steam generators considered as an active heat source for the

Catawba Nuclear Station Containment. Note the flow values used in the containment analyses have been reduced by approximately 2% to account for the frequency variation of $\pm 2\%$ allowed by the Technical Specifications.

1. Minimum safeguards are employed in all calculations, i.e., one of two spray pumps and one of two spray heat exchangers, one of two RHR pumps and one of two RHR heat exchangers providing flow to the core, one of two safety injection pumps and one of two centrifugal charging pumps, and one of two air return fans.
2. 2.132×10^6 lbs. of ice initially in the ice condenser (Basis for Technical Specification limit). This ice is distributed with 1.808×10^6 lbs. in rows 1 through 7 (mean of 1196 lbs. per basket), and 3.240×10^5 lbs. in rows 8 and 9 (mean of 750 lbs. per basket).
3. The blowdown, reflood, and post reflood mass and energy releases described in Section [6.2.1.3](#) are used.
4. Nitrogen from the accumulators in the amount of 6459 lbm is included in the calculations.
5. Nuclear service water temperature of 96°F is used on the spray heat exchanger and the component cooling heat exchanger. See FSAR Section [9.2.5](#) for Service Water temperature transient. The RWST water temperature was modeled at 110°F.
6. The air return fan is effective approximately 10 minutes after the high-high containment pressure setpoint is reached.
7. An ice condenser bypass area of 5.0 ft² is assumed. Of this area, 2.3 ft² is accounted for by the containment spray return drains. The remaining 2.7 ft² is unspecified.
8. The initial conditions in the Containment are a temperature of 95°F in the lower and dead-ended volumes and a temperature of 60°F in the upper volume. All volumes are at a pressure of 0.4 psig.
9. Pump flow rates versus time given in [Table 6-7](#) were used during the cold leg recirculation phase. A Containment spray flow is not assumed during the injection phase from the RWST.
10. Containment structural heat sinks are assumed with conservatively low heat transfer rates. (See [Table 6-8](#)).
11. The operation of one Containment spray heat exchanger ($UA = 1.155 \times 10^6$ Btu/hr-°F) for containment cooling and the operation of one RHR heat exchanger ($UA = 1.67 \times 10^6$ Btu/hr-°F) for core cooling. The RHR flow is cooled by component cooling flow which is cooled, in turn, by its own heat exchanger ($UA = 3.62 \times 10^6$ Btu/hr-°F).
12. The air return fan returns air at a rate of 39,200 cfm from the upper to lower compartment.
13. Containment spray flow from the RWST is not assumed. Containment spray is initiated taking suction from the building sump following RWST low level with an operator action time delay. A containment spray flow rate of 3323 gpm is assumed to initiate at 3963 seconds.
14. A power level of 3479 MWt (rated thermal power plus measurement uncertainty) is used in the calculations.
15. Subcooling of ECC water from RHR heat exchanger is assumed.
16. Deleted Per 2006 Update.
17. The component cooling water flow rate to the RHR heat exchanger is 4900 gpm.
18. Deleted Per 2006 Update.

With these assumptions, the heat removal capability of the containment is sufficient to absorb the energy releases and still keep the maximum calculated pressure below the acceptance criterion of 14.68 psig. This criterion, which is below the containment design pressure, is the pressure to which containment leak rate testing is done per the Containment Leak Rate Testing Program.

The following plots are provided for the limiting case, the pump discharge break for Unit 1 with Feeding Steam Generators (FSG):

[Figure 6-6](#), Containment pressure transient

[Figure 6-7](#), Upper compartment temperature transient

[Figure 6-8](#), Lower compartment temperature transient

[Figure 6-9](#), Active Sump temperature transient

[Figure 6-10](#), Ice melt vs. time

[Table 6-19](#) gives total sump volume versus time. Comparing this table with [Table 6-20](#), which gives the total sump volume versus elevation, the sump elevation versus time can be determined.

As can be seen from [Figure 6-6](#) the maximum calculated Containment pressure is 14.18 psig occurring at approximately 14,700 seconds. The value for the maximum pressure is calculated using NRC approved methodology and is revised periodically to support plant operational activities. Thus, the UFSAR value for the maximum pressure may differ from the value contained in the plant Technical Specifications. However, the UFSAR value shall be less than or equal to the Technical Specifications value.

Structural Heat Removal

Provision is made in the Containment pressure analysis for heat storage in interior and exterior walls. Each wall is divided into a number of nodes. For each node, a conservation of energy equation expressed in finite difference form accounts for transient conduction into and out of the node and temperature increases within the node. [Table 6-8](#) is a summary of the Containment structural heat sink and material property data used in the peak containment pressure transient analysis.

The heat transfer coefficient to the containment structure is based primarily on the work of Uchida. An explanation of the manner of application is given in Reference [47](#).

Fluid Impingement on Ice Condenser Doors

Section [3.6](#) contains a discussion of the design provisions made to preclude the direct impingement of a stream of fluid from high energy lines in the lower compartment upon the ice condenser lower inlet doors.

Containment Spray Return to Sump

Following a LOCA, containment spray water returns from the upper containment to the lower containment via several paths:

1. Spray which falls into the ice condenser drains out through the twelve inch drains by which melted ice escapes.
2. Spray which falls into the air return fan pit (outside the crane wall between the ends of the ice condenser) drains out through one six inch pipe into the side of the refueling canal and through two four inch diameter pipes. The six inch line is illustrated in [Figure 6-11](#) and [Figure 6-12](#). The two four inch lines go directly to lower containment.

3. Spray which falls into the refueling canal drains out through six lines, each eight inches in diameter, from the refueling canal to the lower containment. These lines are illustrated in [Figure 6-13](#).
4. Spray which falls on the operating deck around the refueling canal could accumulate to a depth of three inches before spilling over the curb surrounding the refueling canal. This curb is to prevent material on the operating deck from accidentally entering the canal. This accumulated water is prevented from entering the air return fan pit by a pair of six inch high curbs on either side of the refueling canal. The three inch height difference between the fan pit curbs and the refueling canal curbs forces water to preferentially overflow into the refueling canal and also provides a margin to accommodate minor wave motion without spillover into the pit.

An analysis of the spray return drains has been made to show that they are adequately sized for maximum normal and auxiliary containment spray flow. It has also been shown that a water head of approximately 9 feet in the refueling canal is sufficient to establish a steady state drainage between the upper and lower compartments. This water head is well within the capacity of the refueling canal.

The administrative controls which ensure that the ice condenser floor drains and the refueling canal drains are open during normal operation are discussed in the Technical Specifications as described in Section [6.2.1.6.2](#).

Air Return Fans

Air return fans, located in the upper compartment in pits at elevation 605' between the crane wall and the Containment vessel wall as shown in [Figure 6-103](#) and [Figure 6-104](#) are provided to return air from the upper compartment into the lower compartment after the initial high energy line break blowdown. Two full capacity fans, designed to criteria applicable to safeguards operation in the post-accident Containment environment, are provided for this purpose. All essential components of the Containment Air Return System are designed to withstand the Safe Shutdown Earthquake.

Test results (Reference [44](#)) indicate the air returns to the lower compartment by natural convection without the air return fan. The fans are provided to enhance ice condenser removal of heat and fission products by maintaining forced convection flow through it.

After the Containment pressure has been reduced the ice condenser and Containment spray are capable of maintaining the pressure below design with the assumption of steam generation by residual energy until the ice bed is completely melted. If core steam generation is assumed after complete ice melt, the Containment Spray System maintains the pressure below design with the return fans circulating air through the Containment volume.

An air return system failure analysis is provided in [Table 6-68](#). Each fan has a capacity of 40,000 cfm. Both fans motors are started 9±1 minutes after Containment pressure reaches the high-high setpoint. The fans blow air from the upper compartment to the lower compartment, thereby returning the air which was displaced by the blowdown to the lower compartment. An isolation damper is provided on the discharge of each fan. The damper acts as a barrier between the upper and lower compartments to prevent reverse flow which would bypass the ice condenser. The damper is normally closed and remains closed throughout initial blowdown following a postulated high energy line break. The damper motor is actuated 10 seconds after the Containment high-high pressure setpoint is reached but the damper is prohibited from opening until such time as the pressure differential between the upper and lower compartments is less than 0.5 psi with the lower compartment positive to the upper compartment. The pressure differential permissive is accomplished through a differential pressure switch with

normally closed contacts located in the damper motor start circuit. A back draft damper is also provided at the discharge of each fan to serve as a check valve. For conservative calculations, both the isolation damper and check damper are considered open when pressure equalization between lower and upper compartments has taken place. Fan discharge flow is past radial walls and into the fan rooms. Flow enters the lower compartment through ports in the fan room crane wall. These ports provide for equalization of pressure between the lower compartment and dead ended volumes. After discharge into the lower compartment, the air flows, together with steam leaving the break, through the lower inlet doors into the ice condenser compartment where the steam portion of the flow is condensed. The air flow returns to the upper compartment through the intermediate and upper doors of the ice condenser compartment. The fans operate continuously after actuation, circulating air through the Containment volume, provided that Containment pressure is above the Containment Pressure Control System termination permissive.

The air return fans have sufficient head to overcome the divider barrier differential pressure (a maximum of 11.55 psf) resulting from steam flow and fan air flow entering the ice condenser through the lower inlet doors. The fans are provided with both normal and emergency Class 1E power. Fan "A" of each unit is supplied power from emergency diesel generator "A" of that unit. Fan "B" of each unit is supplied emergency power from emergency diesel generator "B" of that unit. The isolation damper provided at each air return fan discharge is sized to withstand the maximum differential pressure across the divider barrier. Adequate design margin is used to ensure structural and operating integrity.

The performance curve for the air return fans is shown on [Figure 6-106](#). The air return fan safety class and code class requirements are given in [Table 3-4](#).

In response to NRC Bulletin 2003-01, "Potential Impact of Debris Blockage on Emergency Sump Recirculation at Pressurized Water Reactors," Catawba has the option of starting one air return fan at a containment pressure of 1 psig during certain small break LOCA (SBLOCA) transient events.

The containment SBLOCA analysis demonstrates that operation of one air return fan between 1 and 3 psig in containment will not result in a malfunction of the Air Return System. During a SBLOCA event, the differential pressure between upper and lower containment remains well below the isolation damper actuator and air return fan design limits. The manual start of one air return fan does not interfere with automatic operation as described above or impact the diesel generator load sequencing as described in the UFSAR section 8.3, "Onsite Power Systems."

Hydrogen Skimmer Fans

Hydrogen skimmer fans, located in the upper compartment between the crane wall and the Containment vessel at elevation 646' as shown in [Figure 6-103](#) and [Figure 6-105](#), were originally provided to prevent the accumulation of hydrogen in restricted areas within the Containment resulting from a loss-of-coolant accident assuming no credit for the effects of LOCA induced turbulence and natural convection. The potential areas of hydrogen pocketing are shown on [Figure 6-108](#). Hydrogen pocketing is prevented by continuously drawing air out of each of the above areas. Two full capacity fans, designed to criteria applicable to safeguards operation in the post-accident Containment environment, are provided for this purpose. Piping, rather than sheet metal duct, is utilized in the hydrogen skimmer system to eliminate a possible rupture of the air conduit that could provide a path for bypassing the ice condenser during a high energy line break blowdown.

With the elimination of the design basis LOCA hydrogen release per 10CFR50.44, the requirements for hydrogen control systems to mitigate such release during a design basis

accident were eliminated. 10CFR50.44 still requires all pressurized water reactors with ice condenser containments to provide supplemental hydrogen control system to control hydrogen generated from a metal-water reaction for a beyond design basis degraded core accident. Technical Specification (TS) Amendments 219/214 were issued March 1, 2005 eliminating those TS requirements consistent with guidance provided by Technical Specification Task Force (TSTF) Traveler TSTF-447, Rev. 1.

A hydrogen skimmer system failure analysis is provided in [Table 6-68](#). Each hydrogen skimmer fan has a capability of 4260 cfm. This ensures that the flow rates given in [Figure 6-103](#) can be met. There is a normally closed, motor-operated valve on the hydrogen skimmer header to prevent ice condenser bypass during initial blowdown. Since this valve is electric motor operated, and is normally closed, it fails as-is or closed, should the unit experience a high-energy line break. After a containment high high pressure signal and 9 +/- 1 minute delay, the motor operated valve starts to open. Once the motor operated valve has started to open, the hydrogen skimmer fan will start. Thus ice condenser bypass through this path is not possible during the initial blowdown. Since only one of the two redundant hydrogen skimmer trains needs to operate, one of these valves may malfunction (stay closed after blowdown) with no loss to unit safety. The hydrogen skimmer fans operate continuously after actuation.

The performance curve for the hydrogen skimmer fans is shown on [Figure 6-107](#). The hydrogen skimmer fan safety class and code class requirements are given in [Table 3-4](#).

The hydrogen skimmer system has redundant piping and is powered from corresponding redundant Class 1E power supplies.

Deleted Per 2006 Update.

Containment Pressure Control System

Catawba Nuclear Station has no containment vacuum relief system. Instead, a pressure sensing system prevents actuation of the Containment Spray and Air Return Fan Systems when Containment pressure is below the start permissive and halts operation when the containment pressure decreases below the termination permissive. This Containment Pressure Control System is described in section [7.6](#). This system prevents inadvertent containment spray and inadvertent initiation of the containment air recirculation fans, the only causes of a sudden vacuum inside the Containment.

As an added precaution, the refueling water storage tank is kept heated between 70°-100°F. This operating condition is stated in Technical Specification 3.5.4. The Containment Air Release and Addition System takes care of small differences in containment pressure relative to atmospheric pressure, and is described in Section [9.5.10](#).

Peak Reverse Differential Pressure Transient

The LOTIC-2 computer code, described in Reference [24](#), is used to calculate the reverse differential pressure across the operating deck. In order to calculate a maximum reverse differential pressure, the following assumptions were made:

1. The dead-ended compartment volumes adjacent to the lower compartment (fan and accumulator rooms, pipe trenches, etc.) were assumed to be swept of air during initial blowdown. This is a conservative assumption, since this maximizes the air mass forced into the upper ice bed and upper compartment, thus raising the compression pressure. In addition, it minimizes the mass of the noncondensibles in the lower compartment. With this modeling, the dead-ended volume is included with that of the lower compartment.

2. The minimum Containment temperatures are assumed in the various subcompartments. This maximizes the air mass forced into the upper containment. It also increases the heat removal capability of the cold lower compartment structures.
3. The maximum temperature, 100°F, is assumed in the RWST. This helps raise the upper Containment temperature and pressure higher for a longer period of time.
4. The upper Containment spray flowrates used are runout flows. This assumption remains bounding following removal of the containment spray auto-start signal.
5. A summary of the Containment parameters is given in [Table 6-63](#) and [Table 6-65](#).
6. The Westinghouse ECCS model (Reference [7](#), Appendix A) is used for structural heat transfer.
7. The mass and energy release data is given in [Table 6-11](#).
8. Ice condenser doors are assumed to act as check valves, allowing flow only into the ice condenser.
9. It is conservatively assumed that the only available flow path for flow between the upper and lower compartments was through the air return fan system. The resistance (K/A^2) for this path is calculated to be 0.0072 ft⁴.

With these assumptions, the maximum reverse pressure differential across the operating deck is calculated to be 0.95 psi. [Figure 6-16](#) and [Figure 6-17](#) present the upper and lower compartment pressure and temperature transients.

6.2.1.1.3.2 Loss of Coolant Accident at Low Power and Reduced Containment Temperature

The long term containment transient calculation was reevaluated for McGuire Nuclear Station using the LOTIC-1 computer code with initial containment temperature of 60°F and reduced power. This calculation was assuming postfroth core power was 5% of ESDR (Engineered Safeguards Design Rating) power, (ESDR power is 3579 MWt, and is a value used for the original design of the plant) and the initial temperature in the upper, lower and dead ended compartments was 60°F. It should be noted that this calculation has the following conservatisms:

1. The blowdown, reflood, and froth mass and energy release were done at 100% of ESDR power. ESDR power is 3579 MWt, and is a value used for the original design of the plant.
2. All structural heat sinks were at temperatures consistent with the current analyses.

For this case, the ice bed melted out at approximately 67,500 seconds. The peak pressure following ice bed meltout was less than 4.0 psig. Since design pressure is 15.0 psig, this transient results in insignificant consequences with respect to demonstration of containment structural integrity. Due to the similarities between the two stations, this analysis is applicable to Catawba.

6.2.1.1.3.3 Steam Line Break

Analyses are performed with the GOTHIC 4.0/DUKE code (Reference [47](#)) to determine the pressure and temperature response of the containments following a steam line break.

The purpose for calculating the containment response following a steam line break is to determine if the temperature in lower containment is higher than the environmental qualification requirements established for components in that area. Due to the extended release of

superheated steam from the steam generators (in both the Westinghouse D5 design and the BWIFSG design), it is expected that temperatures in lower containment will be higher for a steam line break than for any LOCA.

The steam line break containment response is calculated for 360 seconds in each case run. The long-term containment response is not calculated because once the affected steam generator is isolated, the release of steam to the containment is essentially finished.

Peak Containment Temperature Transient

The following input assumptions used in the GOTHIC analyses for the steamline breaks analyzed for the Catawba Nuclear Station Containment:

1. Minimum safeguards are employed.
2. 2.132×10^6 lbs. of ice initially in the ice condenser.
3. The mass and energy releases described in Section [6.2.1.4](#) were used. Since these rates are considerably less severe than those of the Reactor Coolant System double-ended break, and their total integrated energy is not sufficient to cause ice bed melt out, the containment pressure transients generated for the Reactor Coolant System breaks will be limiting. However, since the steamline break blowdowns are superheated, the lower compartment temperature transients calculated in this analysis will be limiting.
4. The initial conditions in the Containment are a temperature of 135°F in the lower and dead-ended compartments, a temperature of 100°F in the upper compartment, and a temperature of 30°F in the ice condenser. All components are at a pressure of 0.3 psig.
5. Containment structural heat sinks and material property data are presented in [Table 6-8](#).
6. A series of cases were run to determine the limiting case break, as described in Section [6.2.1.4](#).
7. The heat transfer coefficients to the containment structures are based on the based on the work of Uchida. This is based on guidelines given in Reference [48](#).

Results

The lower containment volume-averaged temperature profiles for three different steam line break sizes are shown in [Figure 6-20](#). It is clear that the highest peak temperatures result from the largest break size. Once the ice condenser drain flow initiates, the temperatures in lower containment decrease to about 250°F. Since the largest break size (2.4 ft²) results in a larger, faster release of energy to containment, it is the limiting case. A peak lower containment volume-average temperature of 297°F is reached in this case. In [Figure 6-21](#), the peak temperature in the break compartment is shown for the 2.4 ft² break. The peak temperature reached in this compartment is 317°F.

6.2.1.2 Containment Subcompartments

6.2.1.2.1 Design Basis

Consideration is given in the design of the Containment internal structures to localized pressure pulses that could occur following a loss-of-coolant accident. If a loss-of-coolant accident were to occur due to a pipe rupture in these relatively small volumes, the pressure would build up at a rate faster than in the overall Containment, thus imposing a differential pressure across the walls of the structures.

These subcompartments include the steam generator enclosure, pressurizer enclosure, and the reactor cavity. Each compartment is designed for the largest blowdown flow resulting from the severance of the largest connecting pipe within the enclosure or the blowdown flow into the enclosure from a break in an adjacent region.

The extent to which pipe restraints are used to limit the break area of pipe ruptures is presented in Section [3.9](#) and Section [3.6](#).

The preliminary calculated differential compartment pressures are increased by a minimum of 40 percent for the design of interior structure walls, slabs, and component supports. The final calculated differential compartment pressures and component support loads due to final calculated differential pressures are in all cases less than those used for design.

The subcompartment pressurization, following a loss-of-coolant accident, was considered in the design of the interior structure. Subsequent to this design a revised postulated pipe break criteria was introduced in Section [3.6](#). The subcompartment pressurizations resulting from loss-of-coolant accident are not applicable unless they affect the design of containment, as described in this section, but represent an upper bound for loading resulting from a postulated pipe break.

The basic performance of the Ice Condenser Reactor Containment System has been demonstrated for a wide range of conditions by the Waltz Mill Ice Condenser Test Program. These results have clearly shown the capability and reliability of the ice condenser concept to limit the Containment pressure rise subsequent to a hypothetical loss-of-coolant accident.

To supplement this experimental proof of performance, a mathematical model has been developed to simulate the ice condenser pressure transients. This model, encoded as computer program TMD (Reference [1](#)), provides a means for computing pressures, temperatures, heat transfer rates, and mass flow rates as a function of time and location through the Containment. This model is used to compute pressure differences on various structures within the Containment, as well as the distribution of steam flow as the air is displaced from the lower compartment. Although the TMD code can calculate the entire blowdown transient, the peak pressure differences on various structures occur within the first few seconds of the transient.

6.2.1.2.2 Design Features

Subcompartment free volumes were calculated based on the actual net volume available for each subcompartment. When calculating the input data all obstructions to vent areas are subtracted to obtain the net areas for flow paths connecting adjacent subcompartments. Insulation and HVAC ducts which may collapse under pressure are assumed to remain in place. This results in smaller volumes and vent areas conservatively producing higher calculated differential subcompartment pressures.

6.2.1.2.3 Design Evaluation

The mathematical modeling in TMD is similar to that of the SATAN blowdown code (Reference [50](#)) in that the analytical solution is developed by considering the conservation equations of mass, momentum, and energy, and the equation of state, together with the control volume technique for simulating spatial variation. The governing equations for TMD are given in Reference [1](#)

The moisture entrainment modifications to the TMD code are discussed, in detail, in Reference [1](#). These modifications consist of incorporating the additional entrainment effects into the momentum and energy equations.

As part of the review of the TMD code, additional effects are considered. Changes to the analytical model required for these studies are described in Reference [1](#). These studies consist of:

- Spatial acceleration effects in ice bed.
- Liquid entrainment in ice beds.
- Upper limit on sonic velocity.
- Variable ice bed loss coefficient.
- Variable door response.
- Wave propagation effects.

Additionally, the TMD code has been modified to account for fluid compressibility effects in the high Mach number, subsonic flow regime. Also, the effects of 15% ice condenser basket flow channel blockage on subcompartment differential pressure has been taken into account as described in Reference [52](#).

Experimental Verification

The performance of the TMD code was verified against the 1/24 scale air tests and the 1968 Waltz Mill tests. For the 1/24 scale model, the TMD code was utilized to calculate flow rates to compare against experimental results. The effect of increased nodalization was also evaluated. The Waltz Mill test comparisons involved a reexamination of test data. In conducting the reanalyses, representation of the 1968 Waltz Mill test was reviewed with regard to parameters such as loss coefficients and blowdown time history. The details of this information are given in Reference [1](#).

The Waltz Mill Ice Condenser Blowdown Test Facility was reactivated in 1973 to verify the ice condenser performance with the following redesigned plant hardware scaled to the test configuration:

1. Perforated metal ice baskets and new design couplings.
2. Lattice frames sized to provide the correct loss coefficient relative to plant design.
3. Lower support beamed structure and turning vanes sized to provide the correct turning loss relative to the plant design.
4. No ice baskets in the lower ice condenser plenum opposite the inlet doors.

The result of these tests was to confirm that conclusions derived from previous Waltz Mill tests have not been significantly changed by the redesign of plant hardware. The TMD code has, as a result of the 1973 test series, been modified to match ice bed heat transfer performance. Detailed information on the 1973 Waltz Mill test series is found in Reference [22](#).

Application to Station Design (General Description)

As described in Reference [1](#), the control volume technique is used to spatially represent the Containment. The Containment is divided into 53 elements to give a detailed representation of the local pressure transient on the Containment shell and internal concrete structures. This division of the Containment is similar for all ice condenser units.

The Catawba Containment has been divided into elements as shown in [Figure 6-25](#) through [Figure 6-28](#). The interconnection between Containment elements in the TMD code is shown schematically in [Figure 6-29](#). Flow resistance and inertia are lumped together in the flow paths connecting the elements shown. The division of the lower compartment into 6 volumes occurs at the points of greatest flow resistance, i.e., the four steam generators, pressurizer, and refueling cavity.

Each of these lower compartment sections delivers flow through doors into a section behind the doors and below the ice bed. Each vertical section of the ice bed is, in turn, divided into three elements. The upper plenum, between the top of the ice bed and the upper doors, is represented by an element. Thus, a total of thirty elements (elements 7 through 24 and 38 through 49) are used to simulate the ice condenser. The six elements at the top of the ice bed, between bed and upper doors, deliver to element number 25, the upper compartment. Note that cross flow in the ice bed is not accounted for in the analysis; this yields the most conservative results for the particular calculations described herein. The upper reactor cavity (element 33) is connected to the lower compartment volumes and provides cross flow for pressure equalization of the lower compartments. The less active compartments, called dead-ended compartments (elements 26 through 32, 34 through 37, and 50 through 53) outside the crane wall are pressurized by ventilation openings through the crane wall into the fan compartments.

For each element in the TMD network, the volume, initial pressure, and initial temperature conditions are specified. The ice condenser elements have additional inputs of mass of ice, heat transfer area, and condensate layer length. For each flow path between elements, flow

resistance is specified as a loss coefficient "K", a friction loss " $f \frac{L}{D}$ ", or a combination of the

two based on the flow area specified between elements. Friction factor, equivalent length, and hydraulic diameter are specified for the friction loss. Additionally, input for each flow path includes the area ratio (minimum area/maximum area) which is used to account for compressibility effects across flow path contractions. The code input for each flow path is the flow path length used in the momentum equation. The ice condenser loss coefficients have been based on the 1/4 scale tests representative of the current ice condenser geometry. The test loss coefficient was increased to include basket roughness effects and to include intermediate and top deck pressure losses. The loss coefficient is based on removal of door port flow restrictors. To better represent short term transients effects, the opening characteristics of the lower, intermediate, and top deck ice condenser doors have been modeled in the TMD code. The Containment geometric data for the elements and flow paths used in the TMD code is confirmed to agree with the actual design by Duke and Westinghouse. An initial Containment pressure of 0.3 psig was assumed in the analysis. Initial containment pressure variation about the assumed 0.3 psig value has only a slight effect on the initial pressure peak and the compression ratio pressure peak. TMD input data is given in [Table 6-13](#) and [Table 6-14](#).

The reactor coolant blowdown rates used in these cases are based on the SATAN analysis of a double-ended rupture of either a hot or a cold leg reactor coolant pipe utilizing a discharge coefficient of 1.0. The blowdown analysis is presented in Section [6.2.1.3](#).

A number of analyses have been performed to determine the various pressure transients resulting from hot and cold leg reactor coolant pipe breaks in any one of the six lower compartment elements. The analyses were performed using the following assumptions and correlations:

1. Flow was limited by the unaugmented critical flow correlation.
2. The TMD variable volume door model, which accounts for changes in the volumes of TMD elements as the door opens, was implemented.
3. The heat transfer calculation used was based on performance during the 1973-1974 Waltz Mill test series. A higher value of the ELJAC parameter has been used, and an upper bound on calculated heat transfer coefficients has been imposed. (See Reference [22](#).)

4. One hundred percent moisture entrainment was assumed.
5. Compressibility effects due to flow area contractions were modeled.

[Figure 6-23](#) and [Figure 6-24](#) are representative of the typical upper and lower compartment pressure transients that result from a hypothetical double-ended rupture of a reactor coolant pipe for the worst possible location in the lower compartment of the Containment, i.e., hot leg and cold leg breaks in element 1.

Initial Pressures

Results of the analysis for Catawba are presented in [Table 6-15](#) through [Table 6-18](#). The peak pressures and peak differential pressures resulting from hot and cold leg reactor coolant pipe breaks in each of the 6 lower compartment control volumes were calculated.

[Table 3-47](#) presents the maximum calculated differential pressures between the various elements in the TMD network.

[Table 6-15](#) presents the maximum calculated pressure peaks resulting from hot and cold leg double ended pipe breaks. Generally, the maximum peak pressure within a lower compartment element results when the pipe break occurs in that element. A cold leg break in element 1 creates the highest pressure peak, also in element 1, of 18.2 psig. The maximum peak pressures in the ice condenser compartments are listed in [Table 6-16](#). The maximum peak pressure in each of the ice condenser sections is found in the lower plenum element of the section. The peak pressure was calculated to be 12.5 psig in element 40 for a cold leg break. [Table 6-17](#) and [Table 6-18](#) list the maximum differential pressures across the operating deck and the upper crane wall, respectively. The maximum differential pressure across the operating deck, 16.4 psi, occurred between element 1 and element 25 for a cold leg break. The maximum consideration is given to the calculation of subcompartment pressures (and pressure differentials) for cases other than the design basis double ended reactor coolant pipe rupture in the lower compartment.

Sensitivity Studies

A series of TMD runs for D. C. Cook investigated the sensitivity of peak pressures to variations in individual input parameters for the design basis blowdown rate and 100 percent entrainment. This analysis used a DEHL break in element 6 of D. C. Cook. [Table 6-21](#) presents the results of this sensitivity study.

As part of the short-term Containment pressure analysis of ice condenser units, the pressure response to both DEHL and DECL breaks are routinely considered for each of the loop compartments. Differences in blowdown parameters, such as initial Containment conditions, compartment geometry, unit rated power, etc., can have different relative effects on the Containment pressure response to a break in each location. Differences in blowdown mass/energy release and release rates are of major importance to the Containment pressure response.

For D. C. Cook, the peak differential pressure occurs in loop compartment 6, and is associated with the DEHL break whereas, for Catawba, the peak differential pressure occurs in loop compartment 1, and is associated with the DECL break. These results can, to a large extent, be attributed to the relative differences in DEHL and DECL blowdowns for the two stations as discussed in the response to Question 12 of the D. C. Cook FSAR Amendment 45. In particular, the DECL blowdown is directly influenced by the initial core outlet temperature. The higher core outlet temperature for Catawba results in earlier flashing of the hot leg and upper plenum fluid at a higher system pressure, thereby resulting in a greater subcooled blowdown from the vessel side of the DECL break.

The humidity level in the Catawba Containment at the time of a design basis accident, a double-ended hot leg break in compartment 1, has no significant effect on the initial pressure transient. The difference between peak operating deck pressure differentials calculated by TMD for 100 percent initial relative humidity and zero initial humidity is less than 0.5 percent.

Choked Flow Characteristics

The data in [Figure 6-102](#) illustrate the behavior of mass flow rate as a function of upstream and downstream pressures, including the effects of flow choking. The upper plot shows mass flow rate as a function of upstream pressure for various assumed values of downstream pressure. For zero back pressure ($P_d = 0$), the entire curve represents choked flow conditions with the flow rate approximately proportional to upstream pressure, P_u . For higher back pressure, the flow rates are lower until the upstream pressure is high enough to provide choked flow. After the increase in upstream pressure is sufficient to provide flow choking, further increases in upstream pressure cause increases in mass flow rate along the curve for $P_d = 0$. The key point in this illustration is that flow rate continues to increase with increasing upstream pressure, even after flow choking conditions have been reached. Thus choking does not represent a threshold beyond which dramatically sharper increases in compartment pressures could be expected because of limitations on flow relief to adjacent compartment.

The phenomenon of flow choking is more frequently explained by assuming a fixed upstream pressure and examining the dependence of flow rate with respect to decreasing downstream pressure. This approach is illustrated for an assumed upstream pressure of 30 psia as shown in the upper plot with the results plotted vs. downstream pressure in the lower plot. For fixed upstream conditions, flow choking represents an upper limit flow rate beyond which further decreases in back pressure do not produce any increase in mass flow rate.

The augmented choked flow relationship utilized in TMD is based on experimental data obtained for choked two-phase flow through long tubes, short tubes, and nozzles, as presented in Figure 1-8 of Reference [1](#). The short tube data was cited by Henry and Fauske in Reference [2](#). In that article, they report that the compressible discharge coefficient representing actual measured critical flow rates for single-phase flow through sharp-edged orifices is also representative of single-phase flow through short tubes. Henry and Fauske conclude that an identical discharge coefficient may be applied to two-phase flow through these geometries, which defines the actual critical flow rates through the two geometries to be the same. On this basis, since the augmented choked flow correlation has been based on short-tube data, it should be applicable to sharp-edged orifices as well. The similarity of critical mass flows through sharp-edged orifices and short tubes is also noted in Reference [3](#).

Carafano and McManus, Reference [4](#), have published data for the two-phase flow of air-water and steam-water mixtures. Actually, water vapor was present in the gas phase of the so-called air-water test, making it, in fact, an air-steam-water test. The data presented in Reference [3](#) demonstrates that the ratio of experimental air-steam-water critical flow values to homogeneous equilibrium model predictions is greater than the ratio of steam-water experimental critical flow values to homogeneous equilibrium model predictions. Therefore, augmentation factors derived by comparing steam-water data to the homogeneous equilibrium model may be used in air-steam-water calculations.

Steam Generator

The most severe break possible in the upper cavity of the steam generator enclosure is a double-ended break of the steam line pipe at no-load conditions. The worst break location is considered to be at the steam generator nozzle-to-piping junction which is downstream of the

flow-limiting nozzle. This is the only location in the upper cavity where the steam line is not enclosed by a continuous guard pipe. A full guillotine break is assumed at this location.

However, full flow area is not developed because pipe rupture restraints and guides are used to restrict the movement of the ruptured pipe after rupture. An energy absorbing restraint system involving the process pipe, a continuous guard pipe, internal pads between the process pipe and the guard pipe, a load transfer structure on the guard pipe, an energy absorber, and a load transfer structure on the building is designed to limit the pipe movement such that the maximum total flow area from the break is 3.05 square feet. The postulated pipe rupture is at the weld of the process pipe to the steam generator nozzle. This break is covered by the guard pipe. The guard pipe is limited in its upward travel to less than 6 inches due to postulated ruptures by a crush pipe energy absorber device. The flow area is thus limited to the annular area between the steam generator nozzle and the guard pipe. This gives a flow area of 3.05 ft².

For Unit 1, the guard pipe covering the nozzle weld has been removed. Consequently, the break opening area is limited not by the annular area between the guard and process pipes as described above. Instead, the break is limited by restricting the upward motion of the piping. In this case, the break opening area is determined by the vertical motion and the inside circumference of the 32" diameter process pipe. The same energy absorbing system described above used to limit the break opening area. The flow area of 3.05 sq. ft. is effectively maintained.

The blowdown for the break is given in [Table 6-22](#). Insulation is assumed to remain intact during blowdown. The TMD code, using the compressibility factor and assuming unaugmented critical flow, is used to calculate the pressure transients. The configuration of the steam generator enclosures is shown in [Figure 1-14](#) through [Figure 1-17](#). The nodalization of the steam generator enclosure where the break occurs is shown in [Figure 6-36](#). The adjacent steam generator enclosure is similarly divided into two nodes. The input data for the enclosures is given in [Table 6-23](#). Loss coefficients are calculated based on methods outlined in Reference [21](#). The peak differential pressures across the steam generator vessels and the enclosure are given in [Table 6-24](#).

A nodalization study was also performed. The number of nodes in the break enclosure and the adjacent enclosure was increased from two to nine. The nodalization used in each of the enclosures is shown in [Figure 6-30](#). The input data is given in [Table 6-25](#). The peak differentials across the steam generator vessel and the enclosure are given in [Table 6-26](#).

The major pressure differentials in the asymmetric direction occur when the blowdown rate changes. This is illustrated in [Figure 6-31](#) through [Figure 6-34](#). The pressure differential across the roof of the enclosure is shown in [Figure 6-35](#).

As is shown in [Table 6-22](#), step changes in blowdown rate were used in this analysis. This is unrealistic (but conservative), since it would take some time to accelerate the break flow. Because of this conservatism, there is a tendency to magnify the inertial peaks.

Comparing the results between the two node and the nine node steam generator models, it can be seen that a decrease in pressure occurs when the number of nodes is increased. Review of the 2 node model results indicated that one of the nodes contained pressure gradients because of the coarseness of the nodalization. The refined nodalization of the 9 node model minimizes nodal pressure gradients, resulting in more accurate calculation of peak pressures. Further nodalization of the enclosure would introduce node boundaries which are fictitious with respect to real geometric boundaries, and is, therefore, not necessary. On this basis, the 9 node model is the most accurate representation of the steam generator compartments, and the resulting differential pressures from this model are used to establish design pressures for the

compartment. As [Figure 6-31](#) through [Figure 6-34](#) show, the steady state peaks are fairly low and should not significantly affect the design.

The peak positive values of the differential pressures would cause a loading on the steam generator support that would tend to oppose the loads calculated in the dynamic analysis. The peak negative values of the differential pressures would cause a loading on the supports that would tend to increase the loads calculated in the dynamic analysis. However, the small value of this negative differential pressure (less than 1 psid) and the short duration of the peaks (less than .1 seconds) should not significantly influence the support loadings. All subsequent peaks in differential pressure are less than initial peaks and occur after the maximum loading conditions on the steam generator supports.

Pressurizer

The largest break possible in the pressurizer enclosure is a double ended break of the 6 inch spray line from the reactor coolant pump outlet. The break location is assumed to be at the top of the enclosure, based on an investigation of postulated break locations for the spray line. The blowdown data is given in [Table 6-27](#). Insulation is assumed to remain intact during blowdown. The TMD code, using the compressibility factor and assuming unaugmented critical flow, is used to calculate the pressure transients. The configuration of the pressurizer enclosure is shown on [Figure 1-14](#) through [Figure 1-16](#). The nodalization of the pressurizer enclosure is shown in [Figure 6-37](#). The input data for the enclosure is given in [Table 6-28](#). Loss coefficients are calculated based on methods outlined in Reference [21](#). The peak differential pressure for node 1 is 18.3 psi at 0.35 sec. and the peak differential pressure for node 2 is 18.0 psi at 0.35 sec. A nodalization sensitivity study was also performed. The number of nodes in the enclosure were increased from 2 to 4. This nodalization is shown in [Figure 6-38](#). The input data is given in [Table 6-29](#). The peak differential for node 1, across the roof of the enclosure, was 18.4 psi at 0.35 sec. The peak differential between nodes 2 to 4 and the upper compartment was 17.6 psi at 0.35 sec. The peak differentials between the nodes around the enclosure, nodes 2 to 4, were always less than 0.2 psi.

Reactor Cavity

The TMD computer code with the unaugmented, homogeneous, critical flow correlation and the previously described compressible subsonic flow correlation, was used to calculate pressure transients in the reactor cavity region.

The critical mass flow rate correlation utilized assumes a homogeneous mixture of air, steam and water. Data which show comparisons between measured critical mass flow rates and predictions, using the homogeneous critical flow model at low pressures, have been analyzed. Specifically, an equation which augments the homogeneous model critical mass flow rates has been developed which provides a conservative lower bound on experimental critical mass flow rates. The factor applied to homogeneous model flow rates is $(1.2 - .2X)$, where X is the quality of the upstream compartment. Although critical mass flow rates obtained using the augmentation factor are conservative with respect to experimental data, the results presented herein are based on unaugmented, homogeneous model, critical flow.

Nodalization sensitivity studies were performed before the analysis was begun. The total number of nodes used varied from 6 to 54. In the 6-element model, no detail of the reactor vessel annulus was involved, and for that reason, the model was discarded. Subsequent model changes primarily involved greater detail in the reactor vessel annulus. First, the annulus was divided into two vertical and eight circumferential regions. Next, some additional detail was added in the nozzle region, resulting in a 32-element model. A change to a 44 element model was made by increasing to three vertical and eight circumferential regions. The total integrated

pressure in the reactor cavity changed only slightly because of the change from 32 to 44 elements. The next change, to 54 elements, produced the model shown, with detailed modeling around the broken nozzle. This increase caused virtually no change in the integrated pressure. The additional elements from 48 to 52 are external to the reactor cavity (ice condenser). Additional elements were added to account for all real area changes in the immediate vicinity of the break (i.e., elements 53 and 54 were added to model the broken loop inspection port volume and the broken loop pipe annulus, respectively).

Any further nodalization in the region near the break would introduce fictitious boundaries between elements.

The nodal scheme around the reactor vessel produces a very accurate post-accident pressure profile because of its design. Element 3 is a small element inside the primary shield, which can receive all of the flow from the break element. If it were made any larger, it would contain internal flow losses due to turning and would, thus, contain a pressure gradient. If it were made any smaller, it could not receive all of the flow from the break element. The four elements numbered 33, 34, 45, and 46 are made small to minimize internal pressure variation, and the elements farther from the break are made larger because pressure gradients are low in those regions.

[Figure 6-39](#) shows the general configuration of the reactor vessel annulus nodalization. [Figure 6-40](#) shows the flow path connections for the 54 element model of the unit. [Figure 6-41](#) illustrates the positions of some of the compartments (21-24). The upper containment is represented by compartment 32. The ice condenser is modeled as five elements (48-52), neglecting any flow distribution effects. The break occurs in compartment 1, immediately around a nozzle. The corresponding pipe annulus is represented by compartment 54. The upper reactor cavity is compartment 47, the lower reactor cavity is compartment 2, and the remainder of the elements, as shown on [Figure 6-39](#), are in the reactor vessel annulus. Compartments 15, 42, and 16 are really adjoining compartments 17, 43, and 18 respectively. Thus, compartment 13 is on the opposite side of the vessel from the assumed break. Element 53 represents the inspection port volume above the break. Elements 5, 36, 38, 39, 40, 41, 42, 43, and 44 represent the neutron detector shafts.

[Figure 1-10](#) through [Figure 1-17](#) show the general arrangement of equipment and structures in the reactor cavity area.

The break opening area calculation for reactor vessel nozzle breaks is performed in two stages. First, conservative estimates of reactor vessel motion and loop displacements based on past analytical experience are chosen and used to calculate an estimated break area. Second, an analysis is performed using that area to verify that the assumptions used in the estimate are conservative.

The break opening area of 85 square inches used in the analysis was determined using conservatively estimated displacements. The reactor coolant loop analysis and reactor vessel dynamic analysis were then performed using specific Catawba parameters. The reactor vessel pipe rupture analysis includes the transient forcing functions resulting from loop hydraulic forces, reacting at the vessel nozzles, reactor pressure vessel internals hydraulic loadings, asymmetric reactor cavity pressure forces, and dead weight. The loop analysis is described in Section [3.9](#).

The reactor vessel supports have been evaluated considering the above defined loads and it has been confirmed that the reactor vessel support design meets the requirements specified in Section [5.4.14](#). [Figure 6-42](#) shows the details of the reactor vessel nozzle break restraints.

The detailed LOCA analyses indicate the following peak displacements:

1. The reactor vessel displaces horizontally 0.074 inches directly away from the break location.
2. The reactor vessel vertical and rotational displacements cause an upward vertical displacement of 0.037 inches at the nozzle.
3. The broken end of the pipe displaces 0.34 inches axially away from the nozzle, 0.65 inches laterally and 0.47 inches vertically downward.

These peak displacements are combined to confirm the break opening area. Since all of the peak displacements would not occur simultaneously, this combination produces a conservative estimate of break opening area. The break area calculated for a reactor vessel inlet nozzle break is 37 square inches. A similar LOCA analysis of a reactor vessel outlet nozzle break indicates a break area of 32 square inches. These calculations of break area verify the adequacy of the original break area assumption and demonstrate conservatism in the calculated response of the system.

The mass and energy release rates are presented in [Table 6-30](#).

Pressurization of the reactor cavity can occur for a postulated pipe break either at the inlet or outlet vessel nozzle terminal ends. The cavity is analyzed based on a limited area circumferential rupture at these locations. The break types and locations are consistent with the analysis discussed in Section [3.6](#). The break locations and types are chosen on the basis of detailed fatigue and stress analyses, and do not include hot leg and cold leg breaks within the cavity wall penetration.

[Table 6-31](#) and [Table 6-32](#) provide the volumes, flow paths, lengths, diameters, flow areas, resistance factors and the area ratio information for the elements and their connections. Loss coefficients are calculated using the methods outlined in Reference [21](#).

The inspection port plugs are removed during normal unit operation, and are, thus, assumed to be removed at the start of the accident. All insulation is assumed in place and uncrushed during the entire transient. All obstructions to vent areas such as ventilation ducting and electrical cables are conservatively assumed to be in place during the entire transient. Therefore, no credit is taken for movable objects in the analysis.

[Figure 6-43](#) through [Figure 6-80](#) show representative pressure transients for the break compartment, the upper and lower reactor cavities, the inspection port volume and pipe annulus near the break, the upper containment and the reactor vessel annulus. These plots demonstrate that the pressure gradient is steep near the break location and is very gradual farther away from the break. This indicates that the model must be very detailed close to the break location, but less detail is required with increasing distance.

Design pressures and calculated peak pressures for the reactor cavity volumes are presented in [Table 6-33](#).

Accumulator Nitrogen Supply Line Break

Nitrogen is supplied to the accumulators at a maximum pressure of 700 psig through a supply line one inch in diameter. If the supply line should break, a double-ended blowdown through the ruptured pipe would release the nitrogen present at 700 psig in the accumulators and in the nitrogen supply system. The nitrogen supply is normally isolated and depressurized. The assumption that the nitrogen in all four accumulators is released as a result of one pipe break maximizes the upper bound of the break. Because a 1 inch pipe is involved, the effective break area is only 0.01 ft² for a double-ended break. As a result, the blowdown rate is limited to a peak value of 22.8 lb/sec immediately following the break. As the blowdown proceeds the nitrogen pressure in the accumulators decreases, reducing the blowdown rate. A compartment

pressure response analysis using the TMD code has shown that the blowdown rate is slow enough that no significant pressure differentials are developed between compartments.

Overall, 10,000 lbm of nitrogen are released from the accumulators and the nitrogen supply system during the blowdown. This results in a pressure increase of 1.75 psi in the Containment.

6.2.1.3 Mass and Energy Release Analysis for Postulated Loss-of Coolant Accidents

This analysis presents the mass and energy releases to the containment subsequent to a hypothetical loss-of-coolant accident (LOCA). The release rates are calculated for pipe failure at three distinct locations:

1. Hot leg (between vessel and steam generator)
2. Pump suction (between steam generator and pump)
3. Cold leg (between pump and vessel)

The LOCA transient is typically divided into four phases:

1. Blowdown - includes the period from accident occurrence (when the reactor is at steady state operation) to the time when the total break flow stops.
2. Refill - period of time when the lower plenum is being filled by accumulator and safety injection water. (This phase is conservatively neglected in computing mass and energy releases for containment evaluations.)
3. Reflood - begins when the water from the lower plenum enters the core and ends when the core is completely quenched.
4. Post-Reflood - describes the period following the reflood transient. For the pump suction and cold leg breaks, a two-phase mixture exits the core, passes through the hot legs, and is superheated in the steam generators. After the broken loop steam generator cools, the break flow becomes two phase.

6.2.1.3.1 Short Term Mass and Energy Release Data

From the hot and cold leg studies, the design basis mass and energy release rates have been finalized. The mass and energy release rate transients for all the design cases are given in [Figure 6-81](#) through [Figure 6-88](#). All cases are generated from the SATAN-V break model consisting of Moody-Modified Zaloudek critical flow correlations applied at the break element. Since no mechanistic constraints have been established for full guillotine pipe rupture, an instantaneous pipe severance and disconnection is assumed for all transients. Assumptions specific to the presented transients are as follows:

For the hot leg mass and energy release rate transient to loop compartments:

[Figure 6-81](#) and [Figure 6-82](#)

A double ended guillotine type break.

A break located just outside the biological shield.

A break located in the worst loop.

A six node upper plenum model.

A 16 node broken hot leg pipe model.

A discharge coefficient (C_D) equal to 1.0

A power condition of 3479 MWt (rated thermal power plus measurement uncertainty) with $T_{hot} = 623.9$ F and $T_{cold} = 561.3$ F.

For the cold leg mass and energy release rate transient to loop compartments:

[Figure 6-83](#) and [Figure 6-84](#)

A double ended guillotine type break.

A break located just outside the biological shield.

A break located in the worst loop.

A six node upper plenum model.

A 16 node broken hot leg pipe model.

A discharge coefficient (C_D) equal to 1.0

A power condition of 3479 MWt (rated thermal power plus measurement uncertainty) with $T_{hot} = 623.9$ F and $T_{cold} = 561.3$ F.

For hot leg mass and energy release rate transients to subcompartments:

[Figure 6-85](#) and [Figure 6-86](#)

A single ended split type break.

A break just outside the hot leg nozzle.

A break in the pressurizer loop.

A six node upper plenum model.

A 16 node broken hot leg pipe model.

A discharge coefficient (C_D) equal to 1.0

A power condition of 3479 MWt (rated thermal power plus measurement uncertainty) with $T_{hot} = 623.9$ F and $T_{cold} = 561.3$ F.

For the cold leg mass and energy release rate transient to subcompartments:

[Figure 6-87](#) and [Figure 6-88](#)

A single ended split type break.

A break just outside the cold leg nozzle.

A break located in the worst loop.

A six node upper plenum model.

A 16 node broken hot leg pipe model.

A discharge coefficient (C_D) equal to 1.0

A power condition of 3479 MWt (rated thermal power plus measurement uncertainty) with $T_{hot} = 623.9$ F and $T_{cold} = 561.3$ F.

For the mass and energy release rate transient to the pressurizer enclosure, a 6 inch spray line pipe break was considered ([Table 6-27](#)).

1. A guillotine type break modeled as a 0.147 ft² split in the cold leg at the pump discharge (area of the six inch pressurizer spray feed line) and a 0.087 ft² split in the top of the pressurizer (area of 4 inch spray nozzle).
2. Valves in spray lines are assumed to be open.
3. No pipe resistance for the feed line considered.
4. A power condition of 3479 MWt (rated thermal power plus measurement uncertainty) with $T_{hot} = 623.9$ F and $T_{cold} = 561.3$ F.
5. A discharge coefficient (C_D) equal to 1.0.

6.2.1.3.1.1 Energy Sources

The energy sources include:

1. Reactor coolant system
2. Accumulators
3. Pumped injection
4. Decay heat
5. Core stored energy
6. Primary metal energy
7. Secondary metal energy
8. Steam generator secondary energy
9. Secondary transfer of energy (feedwater into and steam out of the steam generator secondary)

The inventories are presented at the following times, as appropriate:

1. Time zero (initial conditions)
2. End of blowdown time (EOB)
3. End of refill time (EOE)
4. End of reflood time (EOF)
5. End of analysis. (EOFIL)

The methods and assumptions used to release the various energy sources are given in Reference [33](#).

The following items ensure that the core energy release is conservatively analyzed for maximum containment pressure:

1. Maximum expected operating temperature
2. Allowance in temperature for instrument error and dead band (+4°F)
3. Margin in volume (1.4 percent)
4. Allowance in volume for thermal expansion (1.6 percent)
5. Allowance for calorimetric error (2 percent of ESDR). ESDR is 3579 MWt, and is a value used for the original design of the plant.
6. Conservatively modified coefficients of heat transfer
7. Allowance in core stored energy for effect of fuel densification
8. Margin in core stored energy

6.2.1.3.1.2 Description of Blowdown Model

Mass and energy release rate transients generated for the TMD pressure calculation are supported by an extensive investigation of short term blowdown phenomena. The SATAN-V code was used to predict early blowdown transients. The study concerned a verification of the conservatism of SATAN-V calculated transients. This verification was accomplished through two approaches: a review of the validity of the SATAN-V break model and a parametric study of significant physical assumptions.

The SATAN-V code uses a control volume approach to model the behavior of the Reactor Coolant System resulting from a large break in a main coolant pipe.

Release rate transients are determined by the SATAN-V break model which includes a critical flow calculation and an implicit representation of pressure wave propagation.

The SATAN-V critical flow calculation employs appropriately defined critical flow correlations applied for fluid conditions at the break element. For the early portion of blowdown, subcooled, saturated and two phase critical flow regimes are encountered. SATAN-V uses the Moody (Reference 5) correlation for saturated and two phase fluid conditions, and a slight modification of the Zaloudek (Reference 6) correlation for the subcooled blowdown regime.

Since most short term blowdown transients are characterized by a peak mass and energy release rate that occurs during a subcooled condition, the Zaloudek application is particularly significant. The Zaloudek correlation is modified to merge the Moody predicted mass velocities at saturation in the break element. This correlation appears in the critical flow routine of SATAN-V in the form:

$$G_{\text{crit}} = CK1 \sqrt{(5.553 \times 10^5)(P - C_1 P_{\text{sat}})}$$

where:

$$G_{\text{crit}} = \text{critical flow} \left(\frac{\text{lb}_m}{\text{sec ft}^2} \right)$$

$$P = \text{reservoir pressure (psia)}$$

$$P_{\text{sat}} = \text{reservoir saturation pressure psia}$$

$$C_1 = \text{constant (where } 0.5 < C_1 < 1)$$

$$. = \frac{0.1037}{1 - C_1} = \text{constant adjusted such that when } P = P_{\text{sat}}, G_{\text{crit}} \text{ from Zaloudek matches the SATAN-V Moody critical flow calculated at zero quality. For the present analysis, } C_1 \text{ equals 0.9 and CK1 equals 1.018. The modification also more conservatively accounts for the phenomena of increasing mass velocity with increasing degrees of subcooling. The slope of the subcooled } G \text{ versus } P \text{ curve is steeper for the modified correlation.}$$

The low quality portion of the SATAN-V critical flow model is presented in [Figure 6-89](#). The Moody saturation line corresponds to the condition upstream in the break element where quality equals zero and pressure equals saturation pressure. Thus when pressure equals saturation pressure in the break element the Zaloudek and Moody critical flow values are equal. When pressure exceeds saturation pressure in the break element, the modified Zaloudek is used for the critical flow calculation. The steep slope of the Zaloudek G versus P line indicates the conservative treatment of the subcooling effect.

Comparison to Other Critical Flow Models

The Henry-Fauske critical flow correlation was considered for comparison (References 2, 8 and 9). This correlation models flow nonequilibrium via an approach which includes an empirical parameter. This parameter describes the deviation from equilibrium mass transfer, and depends on flow geometry. The value is selected for a particular configuration based on the range of throat equilibrium qualities. The value for constant area ducts is used in the present analysis. This choice is based on the worst possible double ended break geometry described below.

For cold leg and hot leg breaks, the majority of the flow, about 65 percent, comes from the vessel side of the break. For this side, the geometry may be described as an entrance nozzle and a straight pipe of approximate 12 feet in length, and with a diameter of 29 inches. This length of pipe represents the distance from the reactor vessel to the periphery of the biological shield. No double ended break can occur within the biological shield because of the restricted movement within the pipe annulus. Hence the constant area value is appropriate.

Like the SATAN-V model, the Henry-Fauske correlation yields a G_{crit} in terms of upstream conditions and, like the SATAN-V model, it also exhibits a steeper slope of the G versus P line for subcooled conditions. As can be seen in [Figure 6-89](#), the Henry-Fauske saturated liquid line is below the Moody saturated line (SATAN-V model) for pressures greater than about 1000 psia. For short term blowdown calculations, the significant pressure region is from 1000 psia to 1800 psia, with increased emphasis on subcooled conditions for the 1000 psia end. Subcooled mass velocity versus pressure is given for the two fluid temperatures corresponding to $P_{sat} = 1000$ and $P_{sat} = 1800$. It is clear from the figure that the slope of the Zaloudek G versus P line is steeper in both cases. This increased sensitivity coupled with the higher value for Moody at saturation causes the SATAN-V model to predict higher mass velocities. Hence the SATAN-V model is a more conservative treatment of critical flow than the Henry-Fauske model.

In the original FLASH model (Reference [10](#)), the Moody correlation was extended to subcooled conditions. This treatment is employed in many blowdown codes and thus it is appropriate to compare the SATAN-V model to these values. This is illustrated in [Figure 6-90](#). Again the Zaloudek treatment yields higher mass velocities and the SATAN-V model is more conservative.

Comparison to Experimental Data

The margin included in the modified Zaloudek prediction of subcooled critical flow rates is demonstrated by a review of experimental subcooled critical flow data. [Figure 6-91](#) and [Figure 6-92](#) present a plot of measured versus predicted critical flow values for Zaloudek's own data (References [6](#) and [11](#)). The figures indicate that when the modified correlation is applied to Zaloudek's data, the predicted critical flow values are significantly higher than measured flow rates.

The margin associated with the SATAN-V critical flow calculation may also be demonstrated by a review of the low quality data presented by Henry (Reference [9](#)). Exit plane quality, in terms of the Moody model, is determined as a function of upstream conditions by assuming an isentropic expansion to exit plane (i.e., critical) pressure. The lowest exit plane qualities where the Moody model is applied in the SATAN-V code occur for expansion from saturated liquid conditions. A plot of these are shown in [Figure 6-93](#). For exit plane qualities above the line, the Moody model is used in the SATAN-V code. Below the line, the Modified Zaloudek model is used.

Henry's comparison between data and model shows that for the range of exit plane quality greater than 0.02, the Moody model overpredicts the data, hence is conservative.

For the region below 0.02, it is appropriate to compare Henry's results with the Modified Zaloudek model, as used in the SATAN-V code. This is done in [Figure 6-94](#) for all of Henry's data points. As can be seen, the Zaloudek model overpredicts the flow. A discharge coefficient of 0.6 would be more reasonable than the 1.0 value used in SATAN-V.

Application to Transient Conditions

The Zaloudek correlation was developed for stagnation (reservoir) pressure and quasi-steady state critical flow conditions. It is extended to application in the SATAN-V break element and transient flow conditions. This extension is justified because of the following considerations.

The pressure in the break element differs from the value in a nearby large volume because of three effects:

1. Pressure drop due to friction.
2. Pressure drop due to spatial acceleration (momentum flux).
3. Pressure drop due to the transient.

The friction term in the reactor application is quantifiable; this term is less important than the other two. The sensitivity of the break flow rate to fluid friction was evaluated via a parametric study. For the purposes of this study, an analysis was made wherein the frictional resistance between the vessel and the break was reduced from the design values by a factor of one hundred. Over the period from 0.0 to 60 milliseconds (which includes the peak break flow), the integrated mass flow differed by less than 18 lbs from the design friction case; the total release over this period was about 5000 lbs.

Spatial acceleration is the major source of pressure drop upstream of the break between the reservoir and the pipe, causing steep pressure gradients in the approach region to critical flow. This term is not calculated explicitly in the SATAN-V code. Spatial acceleration is accounted for by the use of critical flow correlations (Zaloudek or Moody) which contain this effect. No credit is taken for pressure drop due to spatial acceleration for elements other than the break element. Hence, the pressure calculated by SATAN-V may be interpreted as a stagnation pressure, which is the appropriate pressure for the Zaloudek and Moody models.

Prior to the occurrence of the peak release rate, the break element and upstream reservoir pressures differ as a result of the transient described by pressure wave propagation. The applicability of the SATAN-V break model to this situation is verified by the code's ability to match recorded semiscale transients. SATAN simulations of LOFT transients support the SATAN-V transient calculation. [Figure 6-95](#) presents a comparison of LOFT pressure transient recorded near the break to the SATAN-V model of the LOFT break element transient. The graphs demonstrate the ability of the SATAN-V code to track pressure waves in the broken pipe.

Moreover, the critical flow correlation is implemented in the present analysis by combining the correlation with the appropriate momentum equation. This provides a model for predicting break flow acceleration vis-a-vis a quasi-steady simulation. This is found to have little effect on Containment pressure but is a more physical representation.

Thus, the SATAN-V break model is supported by subcooled critical flow data, by comparison to other correlations, and by the ability to simulate short term transients.

Parametric Studies

With confirmation of the conservatism of the SATAN-V break model, a series of parametric studies were undertaken to identify the blowdown transient corresponding to the most severe TMD results. A series of basic sensitivities were first studied to set the scope of the more detailed investigations. The assumptions of break size, break type and break location were considered. The results of this analysis were evaluated using the TMD code.

Break Size, Type and Location

As part of the short term blowdown investigation, a parametric study was made to determine the effect of break size, type, and location on short term mass and energy release rates. A range of break sizes, from a break area corresponding to the main coolant pipe area to a break area of twice the pipe area, was considered. Also considered were possible break locations in the hot leg, the pump suction leg, and the cold leg. From this study, it was determined that the double

ended break area yielded the highest release rate transients, and that the pump suction leg break location resulted in much less severe mass and energy release rates. Thus, short term blowdown transients and corresponding Containment pressure transients are presented for hot leg and cold leg double ended guillotine breaks.

A sensitivity study to determine the effect of break type on short term blowdown has been performed. The study consisted of a series of short term blowdowns for both guillotine and split type breaks. For a double ended break area, the split type break resulted in less severe mass and energy release transients than were observed for guillotine type breaks. The observed double ended sensitivity is reversed for single ended breaks. Release rate transients are less severe for single ended guillotine type breaks than for single ended split type breaks.

The sensitivities presented above are explainable in terms of the inherent differences between split and guillotine type breaks. The guillotine break models a complete separation of the ends of the broken pipe, while the split break maintains the flow path through the broken pipe. Because physical separation of the ends exists for guillotine breaks throughout the blowdown transient, a significant difference is observed between pressures at the approach regions to the ends of the break. In particular, for a double ended guillotine break, the pressure at the vessel side of the break may exceed the loop side pressure by 300 psi. Communication allowed by the split break then acts to bring the approach region pressure to an intermediate value between the two pressures observed at the ends of the guillotine break.

By bringing the approach region pressure to an intermediate value, the release rates are reduced for split type breaks of twice the coolant pipe area. Flow from the vessel end of the break is limited by a choked condition at the nozzle and thus is relatively unaffected by the lower pressure in the break element. The intermediate pressure for the split, however, is higher than occurs at the loop end of the guillotine break. As a result, the pressure gradient driving loop side flow is reduced.

For breaks of an area equal to the coolant pipe area, the split break acts to increase release rates. The sensitivity is reversed because a choked flow condition does not prevail at the vessel nozzle. The intermediate pressure again reduces the loop side pressure gradient and thus the loop side flow. However, the intermediate pressure results in a vessel side pressure gradient which is higher than occurs for the single guillotine type break. Because a choked flow condition does not exist at the nozzle, an increase in vessel side flow results from the higher pressure gradient. Since the vessel supplies at least 2/3 of the flow to the break, an overall increase in the total mass flow rate is observed for the single ended split type break.

The influence of break location on TMD peak pressure was considered by generating blowdown transients for possible worst break locations. The results indicated that a double ended break in the pump suction leg was clearly less severe for short term blowdown release rates and that no such clear decision could be made between hot and cold leg breaks.

More detailed parametric studies were continued for the cold leg and the hot leg double ended guillotine breaks. The two locations produce intrinsically different TMD pressure responses and therefore must be dealt with in separate parametric surveys.

Hot Leg Nodal Configuration

A study of the SATAN-V nodal configuration has been applied to the hot leg double ended guillotine break. It was found that for this break, the nodal configuration of the broken hot leg and the upper plenum are significant to short term transients. Spatial convergence was achieved for the upper plenum after the addition of four nodes to the standard SATAN-V two node upper plenum model. These nodes are hemispherical shells arranged concentrically from the broken hot leg nozzle, and approximate the propagation of the pressure wave in the upper

plenum. They are significant in that they specify the inertial response of the upper plenum. Spatial convergence was demonstrated, because doubling the number of nodes yielded less than one percent deviation in break flow at all times.

Sensitivity to nodal configuration in the broken hot leg pipe was also investigated. Models with from 4 to 16 nodes were used to generate transients. Increasing the number of nodes was found to give a better simulation of pressure wave propagation in the pipe.

Cold Leg Studies

The cold leg break transient was also reviewed in terms of significant parameters.

The Reactor Coolant System behavior is different for cold leg breaks, and the peak Containment pressure occurs later for cold leg breaks. The following studies were performed:

1. Nodal Configuration

For the cold leg break, the nodal configuration of the broken cold leg and the downcomer is significant to the transient. Spatial convergence was achieved with the addition of three additional nodes to the standard SATAN-V model. These are annular rings arranged concentrically from the broken cold leg nozzle and model propagation of the pressure wave in the downcomer.

As in the hot leg sensitivity, from 4 to 16 pipe node models were tried for the cold leg transient. Again, more nodes give a better simulation of the pressure wave propagation in the broken pipe.

2. Pump Modeling

For the time period of interest, the variation in pump inlet density and pump speed are small. This model was found to have no effect.

6.2.1.3.2 Long Term Mass and Energy Release Data

Large break LOCA analyses have been performed to generate mass and energy release boundary conditions for determining the long term containment response to a rupture of the RCS piping. Reference [45](#) presented the long term mass and energy release analysis methodology. Since the Catawba Nuclear Station has an ice condenser containment, the peak pressure following a rupture of the RCS piping will not occur during the blowdown phase. The peak pressure occurs after ice meltout during the post-reflood phase of the event. The RELAP5/MOD3.1DUKE computer code is used to generate boundary conditions for the containment pressure response analyses from the initiation of the piping break through the blowdown, refill, reflood, and post reflood phases of the long term analysis. The RELAP5/MOD3.1DUKE code is derived from RELAP5/MOD3.1 (Reference [46](#)) which was developed by EG&G Idaho under NRC sponsorship.

Three double-ended guillotine pipe break locations are examined; hot leg, cold leg pump suction, and cold leg pump discharge. Split breaks and breaks of lesser flow area are not examined because it is well recognized that these breaks will not yield the limiting containment pressure. The mass and energy release boundary conditions generated from these break locations are used as input to the GOTHIC code (Reference [47](#)) to calculate the containment pressure response.

Both the Feeding Steam Generators (FSG) and the Catawba Model D5 steam generators are analysed. Since the FSG analysis is bounding, only the FSG analysis representative of Catawba Unit 1 is presented.

6.2.1.3.2.1 Computer Code

The RELAP5/MOD3.1DUKE code models the steady-state and transient behavior of a hydraulic system that may contain a mixture of steam, water, non-condensable gas or nonvolatile solute. The fluid system is modeled by discretizing the system into control volumes (nodes) joined by momentum cells (junctions). The hydraulic flow field treats the liquid and steam phases as separate fluids in a nonhomogeneous, non-equilibrium manner, solving the mass, energy and momentum equations for each phase. Constitutive relationships are used to define flow regimes and to model interphase drag, vapor generation and interphase heat and mass transfer, and horizontal and vertical stratification. Empirical relationships are used to model convective heat transfer, energy partitioning between phases, choked flow and two-phase wall friction. The code supports simulation of the primary system, secondary system, feedwater train, automatic control systems and core neutronics. Available component models include reactor point kinetics, pumps, valves, heat structures, heat exchangers, turbines, separators and accumulators.

6.2.1.3.2.2 LOCA Simulation Models

Reference 45 describes the RELAP5 nodalization used in the LOCA analyses. The vessel, piping and steam generator nodalization are of sufficient detail to assure that the requirements of ANS-56.4-1983 (Reference 48) are met (i.e., break flow quality is not overpredicted, and core-to-coolant, metal-to-coolant, and SG-to-coolant heat transfer will conservatively predict high containment peak pressures).

6.2.1.3.2.3 Critical Flow Model

The RELAP5 Ransom and Trapp critical flow model (Reference 46) is used as the break flow model. Flow discharge coefficients are applied so as to provide break flow results equivalent to that of the Moody/Henry-Fauske critical flow models.

6.2.1.3.2.4 Initial Conditions

The initial conditions for the RELAP5 LBLOCA mass and energy release analyses were chosen with consideration for the guidance presented in Reference 48. The intent is to select initial conditions that will maximize the stored energy in the primary and secondary coolant systems and thus contribute to a conservatively high peak pressure in the containment response analysis. The initial conditions in the RELAP5 mass and energy release analyses are listed below.

| PARAMETER | ANS GUIDANCE | RELAP5 Mass and Energy Analyses |
|------------------|---|---|
| Core power level | \geq licensed power level plus an uncertainty allowance | Rated Thermal Power (3469 MWt for Unit 1, 3411 MWt for Unit 2) plus measurement uncertainty (0.3% for Unit 1, 2% for Unit 2) = 3479.22 MWt. |

| PARAMETER | ANS GUIDANCE | RELAP5 Mass and Energy Analyses |
|---|--|--|
| Core inlet temperature | \geq normal operating temperature for the selected power level plus upward adjustment for uncertainties | Nominal + 4° F |
| RCS pressure | \geq normal operating pressure for the selected power level plus allowance for uncertainties | Nominal + 60 psi uncertainty allowance. |
| RCS flow | No guidance | High design flow rate plus 2.2% uncertainty. |
| S/G pressure | \geq normal operating pressure plus uncertainty allowance. | S/G pressure will be determined by RELAP5 initialization for power level and T_{AVG} . |
| Pressurizer level | \geq maximum normal operating level plus uncertainty allowance. | Nominal + 9%. |
| S/G water level | \geq normal level associated with selected power level plus uncertainty allowance. | 10% uncertainty allowances will be applied. |
| Safety injection tank pressure and water level | Normal operating values with allowances for uncertainties biased to produce maximum containment pressure. | Low initial pressure and liquid volume. |
| Safety injection tank temperature | Normal operating value with allowance for uncertainties biased to produce maximum containment pressure. | High temperature. |
| Refueling water storage tank (RWST) liquid volume | Choose ECCS flows and delay times in accordance with single-failure criteria to produce highest peak containment pressure. | Low RWST inventory and early recirculation switchover are selected to minimize the heat sink effect of a large volume of cold water. |
| Main feedwater temperature | No guidance. | High MFW temperature is assumed in order to maximize the heat source effect of the SG. |

6.2.1.3.2.5 Boundary Conditions - Energy Sources

The energy released into containment by a pipe break is that energy that is (a) initially contained in the primary and secondary coolant systems fluids and the metal components of the system boundaries and the sensible heat stored in the core, plus (b) that additional energy that is produced and released subsequent to the break as a result of continued fission, fission product and actinide decay and metal-water reaction. This section describes how the energy sources are accounted-for in the analyses.

RCS and SG Inventory

The volume of the RCS piping system is increased by 1% to account for the increased inventory due to thermal expansion. Also, zero SG tube plugging is assumed.

RCS and SG Metal

Heat structures are assumed to be in thermal equilibrium with the coolant in which they are in contact.

Core Stored Energy

A core time-of-life is selected such that the combined effects of the core stored energy and decay heat release will provide a core stored energy release that bounds all core loadings for any point in the fuel cycle.

Fission Energy

The RELAP5 kinetics model, coupled with reactivity feedback from moderator density, Doppler, and boron, is used to determine the delayed neutron fission power as a function of time. Consistent with most standard LBLOCA modeling practices, all control rods are assumed to remain out of the core throughout the simulations. Therefore, the reactor is brought subcritical with the available reactivity feedback effects. The most dominant negative feedback during blowdown is moderator density, while boron is dominant during the refill phase. The positive feedback (Doppler feedback) introduced by decreasing fuel temperature during blowdown is also significant. All of these effects are modeled. The analyses performed to generate this function examine several combinations of burnup, enrichment, and time-in-cycle. The combination which results in the least negative reactivity feedback function has been chosen for conservatism.

Because a point kinetics model is not capable of calculating spatial power distributions, nodal reactivities are flux-weighted to obtain a single reactivity value for use in the point kinetics model. A bounding beginning-of-cycle (BOC) β_{eff} is used for conservative moderator density feedback since end-of-cycle β_{eff} would provide a non-conservatively high Doppler effect greater than the increased feedback effect of a BOC β_{eff} .

Fission Product and Actinides Decay

Radioactive decay of fission products and actinides is based on the ANSI/ANS-5.1-1979 standard with 2σ uncertainty.

Metal-Water Reaction Rate

Heat resulting from exothermic metal-water reaction is considered. A simplified metal-water reaction is used to conservatively bound the expected reaction. The model assumes a total amount of clad reaction to be 1% of the amount that would be generated due to reaction of all of the cladding in the active region of all of the fuel rods. The metal-water reaction is assumed to begin when the PCT determined by a Chapter [15.6.5](#) LBLOCA analysis, exceeds 1800°F and

follows a parabolic rate. The hydrogen generated by the reaction is added to the containment atmosphere as a non-condensable gas.

6.2.1.3.2.6 Boundary Conditions - Assumptions

Limiting Single Failure

A loss of one train of Engineered Safeguards due to a diesel generator failure at the beginning of the accident is the limiting single-failure for LBLOCAs. This assumption is based on the knowledge that peak containment pressure for a LBLOCA occurs in the post-reflood phase of the event, when decay heat is the primary heat source and ECCS core cooling and containment spray are utilized for heat removal.

Break Location

The break is modeled to occur in the loop containing the pressurizer. However, since peak pressure occurs in the long-term post-reflood period, peak pressure results are not sensitive to the broken loop selection.

Emergency Core Cooling System Injection Flow

The initiation time for ECCS is assumed to be consistent with the UFSAR [Table 7-15](#) delay time. No direct spilling of injection flow to containment is assumed for the hot leg break and cold leg pump suction break case. ECCS injection flow spillage is accounted for in the cold leg pump discharge break case. To maximize break flow energy, a high value is selected for ECCS suction temperature during injection.

RWST Depletion and ECCS Switchover

The available RWST inventory is minimized. Net flow from the RWST is tracked and switchover (manual action) to recirculation initiated when the RWST level has decreased to a minimum volume corresponding to the low level alarm setpoint. ND suction is switched first, then NV and NI pumps are switched following the low-low level alarm.

Operator actions and delay times for pump realignments are accounted for with conservative allowances.

RCP Trip

RCPs are assumed to trip simultaneously with the main turbine and loss of offsite power (LOOP).

RCP Two-Phase Multipliers

The RELAP5 pump component model adds pump head to the mixture momentum equation. To account for degradation due to two-phase flow, when void fractions are such that little head is developed, homologous difference curves are provided. Appropriate curves for the CNS RCPs, based on experimental data, are included in RELAP5 and used in the analyses. For two-phase flow with void fractions where the pumps are able to develop head, multipliers based on void fraction are applied.

SG Post-Trip Level Control

Main feedwater flow is assumed to continue until the feedwater isolation valves close. Post-trip SG level is then controlled by auxiliary feedwater flow (CA) under manual control.

Auxiliary Feedwater Flow Rates and Temperature

Auxiliary feedwater temperature is conservatively maximized for increased secondary to primary heat transfer. One of the motor-driven auxiliary feedwater pumps is unavailable due to loss of one ESF train. The Technical Specifications and UFSAR values for startup and loading of the available diesel generator is assumed for the delay in availability of the available diesel generator.

Post-Trip SG Pressure Control

The main steam isolation valves (MSIV) and main steam PORVs are assumed to close on the containment high-high pressure signal resulting from the LBLOCAs. Operator action is assumed for any subsequent main steam PORV operation to reduce SG pressure in accordance with procedural guidance.

Cold Leg Accumulator Nitrogen

Nitrogen used to pressurize the safety injection accumulators is assumed to be discharged into the RCS cold legs and subsequently into the containment.

Containment Backpressure

Containment backpressure affects mass and energy release rates during the reflood and post-reflood phases. However, the RELAP5 code used for the mass and energy release analysis is not coupled to the GOTHIC code used for the containment pressure analysis. GOTHIC output is input to RELAP5 in an iterative manner, until converged. Conservatively high back pressures are used.

Refill Assumption

Refilling of the reactor vessel is an integral part of the RELAP5 analysis. This modeling approach has a minor impact on long-term containment response.

6.2.1.3.2.7 Cold Leg Recirculation Boundary Conditions

When the minimum water volume in the RWST is depleted, the lo-level alarm will actuate, and the operator must switch the ECCS pumps suction source over from the RWST to the containment sump. Containment Sump level is verified via redundant, safety-powered level switches prior to swap to ensure adequate inventory is available to support sustained sump recirc.

Transfer to Cold Leg Recirculation Sequence Timing

According to the current EOPs, the alignment of the ND system to the sump will be performed first following RWST low level, then the realignment of the NI and NV systems follow the RWST low-low level alarm. Containment spray is aligned to the sump after ND has been transferred to the sump. There is time required to transfer the ND, NI, and NV pump suction and also operator action delay time. Therefore, for a portion of this time frame, the ECCS pumps will have the RWST as their suction source. The length of time required to complete each pump realignment has been conservatively minimized.

ECC Flow Rates During Cold Leg Recirculation

[Table 6-7](#) shows typical minimum ECC flow rates for CNS. The hot leg and pump suction break analyses utilize data shown for the no-spilling simulation, and the cold leg pump discharge break analyses utilize data shown for the with-spilling simulation.

ECC Temperature During Cold Leg Recirculation

ECCS temperature following switchover is dependent on several factors, one of which is the sump temperature. Since sump temperature is computed by GOTHIC and not by RELAP5, it must be determined through a GOTHIC/RELAP5 iterative process.

6.2.1.3.2.8 Result of Mass and Energy Release Analyses

Various break locations are analyzed. The results show that the cold leg pump discharge break case generates the highest total integrated break vapor mass and energy release (Figures [6-199](#) to [6-202](#)).

Of the postulated RCS break locations, the hot leg break has the least vent path resistance. As a result, that break path results in the highest blowdown mass and energy release rates. However, following blowdown, the cold leg pump suction break case has a greater energy release rate due to the fact that the coolant picks up additional heat from an SG. Much later, during the cold leg recirculation phase, the mass and energy release rates of the cold leg pump discharge break case exceed those of the cold leg pump suction and the hot leg breaks due to ECCS spillage. As a result of these characteristics and of the heat removal capability of the containment cooling systems, the cold leg pump discharge break produces the limiting LBLOCA peak pressure.

6.2.1.4 Mass and Energy Release Analysis for Postulated Secondary System Pipe Ruptures Inside Containment

6.2.1.4.1 Pipe Break Blowdowns Spectra and Assumptions

A series of steam line breaks were analyzed to determine the most severe break condition for containment temperature and pressure response. The following assumptions were used in these analyses:

1. Breaks ranging in size from 0.4 ft² to 2.4 ft² were analyzed. Due to the rapid steam line isolation, breaks larger than 2.4 ft² produce mass and energy releases that are similar to the 2.4 ft² break due to the presence of the steam generator outlet nozzle flow restriction.
2. Prior to tube bundle uncover, the blowdown from the broken steam line is assumed to be dry saturated steam; i.e., no water entrainment was assumed. Following tube bundle uncover, the blowdown from the broken steam line is assumed to be superheated steam.
3. Steam line isolation is completed 1 second after the isolation setpoint is reached. The isolation signal is generated by a high-high containment pressure signal. A conservatively fast closure time for the main steam isolation valves and no electronic delay are assumed in order to speed tube bundle uncover.
4. All breaks are initiated from 3479 MWt (rated thermal power plus measurement uncertainty). Since the amount of superheat that occurs is limited by the temperature of the primary fluid flowing through the tubes, maximizing hot leg temperature will result in higher enthalpy releases to the containment. The high initial power level, with the essentially constant cold leg temperature program, results in a higher steam generator inlet temperature in the primary system. For steam line breaks inside containment, reactor trip, safety injection, and steam line isolation signals are generated on high containment pressure trips, which are not significantly influenced by the initial power level. Steam line breaks initiated from power levels less than full power are less limiting since a lower initial power level would result in lower steam generator inlet temperatures.

5. A total of six break sizes were analyzed. Prior to MSIV closure, these breaks model blowdown from one steam generator to one end of the break (forward flow) and from three steam generators to the other end of the break (reverse flow). Subsequent to MSIV closure, forward flow continues from the one steam generator through one side. Reverse flow is rapidly terminated since the isolated steam generators do not continue to blow down. The specific break sizes analyzed are 0.4 ft², 0.6 ft², 0.86 ft², 1.1 ft², 1.4 ft², and 2.4 ft².
6. The failure of one train of safety injection was assumed for all cases. In addition, a loss of offsite power was assumed for the containment analysis.
7. The mass and energy releases described in this section have been calculated to beyond the point at which the limiting parameter, containment temperature, has reached its peak value. Further releases will eventually be terminated by operator action, although no explicit assumption is made in the analysis about the time at which this occurs.
8. Main feedwater is assumed to be in manual control and thus is maintained at its initial rate until feedwater isolation occurs concurrent with reactor trip. No credit is taken for the rapid depressurization of the steam generator that would increase main feedwater flow and delay tube bundle uncover. A closure time of 1 second is assumed for the main feedwater isolation valves.
9. The Auxiliary Feedwater System is actuated by a safety injection signal due to high containment pressure. A delay of 60 seconds is assumed to speed tube bundle uncover in the faulted steam generator. The mass addition to the faulted steam generator is conservatively determined by assuming that the Auxiliary Feedwater System is instantaneously pumping at maximum capacity with the flow rate calculated from the feedwater system head curves and the system line resistance as a function of steam generator pressure.

6.2.1.4.2 Break Flow Calculations

The following is a description of the break flow modeling of the blowdown of the steam generators and plant steam piping:

1. Break flows and enthalpies from the steam generators are calculated using RETRAN-02 (Reference [49](#)). Blowdown mass and energy releases determined using the RETRAN code include the effects of core power generation, main and auxiliary feedwater additions, engineered safeguards systems, reactor coolant system metal, and reverse steam generator heat transfer.
2. The contribution to the mass and energy releases from the secondary plant steam piping is included in the mass and energy release values in [Table 6-47](#) for the limiting break size of 2.4 ft². For all ruptures, the steam piping volume blowdown begins at the time of the break and continues until the entire piping inventory is released. The flow rate is determined using the Moody correlation, the pipe cross-sectional area, and the steam pressure. Reverse flow from the intact steam generators continues until steam line isolation.

The blowdown model is discussed further in Section 4.0 of Reference [45](#).

6.2.1.4.3 Single Failure Effects

The single failure of one train of safety injection is assumed in order to minimize the injection of cold, borated water to the primary system. This single failure maximizes hot leg temperature which in turn maximizes the enthalpy of the steam released into the containment.

6.2.1.5 Minimum Containment Pressure Analysis for Performance Capability Studies of Emergency Core Cooling System

The Containment pressure analysis is performed with the LOTIC-2 code (Reference [24](#)). The transient pressure computed by the LOTIC-2 code is used for the purpose of computing the reflood transient.

The Westinghouse LOTIC (LONg-Term Ice Condenser) code (Reference [24](#)) has the capability to properly describe the post-blowdown period in the ice condenser containment. Not only are the upper, lower, and ice condenser volumes described, but also the ice condenser is divided into six circumferential sections, each with two vertical divisions. In this way maldistribution and sectional burnout effects can be studied as well as the changing volume distribution during the depletion of the ice bed. The code also describes the performance of the air recirculation fan in returning upper compartment air to the lower compartment. Coupling of residual and component cooling heat exchangers is provided to give an accurate indication of performance for these heat exchangers. The spray heat exchanger performance is also accurately modeled in the transients. The basic equations used are the standard transient mass and energy balances and the equations of state used in any containment transient, but appropriately coupled to the multi-volume ice condenser containment. The code also considers accumulator gas added to the containment and the displacement of free volume by the refueling water storage tank volume.

The LOTIC code uses the control volume technique to represent the physical geometry of the system. Fundamental mass and energy equations are applied to the appropriate control volumes and solved by suitable numerical procedures. The initial conditions of the containment by compartment are specified before blowdown. Ice melt is calculated for the blowdown period based on the mass and energy released to the containment. After the RCS blowdown, the basic LOTIC code assumption made is that the total pressure in all compartments is uniform. This assumption is justified by the fact that after the initial blowdown of the RCS the remaining mass and energy released from this system into the containment are small and very slowly changing. The resulting flow rates between compartments will also be relatively small. These small flow rates are unable to maintain significant pressure differentials between the containment compartments.

The Containment backpressure used for the ECCS analysis presented in Section [15.6.5](#) is presented in [Figure 6-204](#). The Containment backpressure is calculated using the methods and assumptions described in Reference [24](#). Input parameters, including the Containment initial conditions, Containment volume, passive heat sink materials, thicknesses, and surface areas, and starting time and number of Containment cooling systems used in the analysis, are described below.

6.2.1.5.1 Mass and Energy Release Data

The mass/energy releases to the Containment during the blowdown and reflood portions of the limiting break transient are presented in [Table 6-61](#) and are calculated by W COBRA/TRAC (Reference [51](#)). The mass and energy releases from the broken loop accumulator are given in [Table 6-62](#).

6.2.1.5.2 Initial Containment Internal Conditions

Containment data and initial conditions used in the analysis are presented in [Table 6-66](#). As detailed in Reference [44](#), it has been determined that containment parameters assumed in the minimum containment pressure analysis need not be the same as the Limiting Conditions for Operation (LCO) as defined in the Containment Technical Specifications. The LCOs in the Technical Specifications often represent extreme conditions that are not typically encountered

during normal operation. In addition, the LCOs associated with the Containment Technical Specifications are based upon containment integrity and equipment operability considerations, not ECCS performance considerations. Consequently, some LBLOCA EM (evaluation model) values were chosen as being representative of limiting conditions during normal full power operation, and others were set at the Technical Specification LCO value. In all cases the combination of containment parameter values were chosen to assure that the overall calculation of containment pressure during a LBLOCA would be conservative.

6.2.1.5.3 Containment Volume

The volume used in the analysis is 1,209,341 ft³.

6.2.1.5.4 Active Heat Sinks

The Containment Spray System, the Ice Condenser and the Air Return Fan System operate to remove heat from the Containment. Containment spray operation is a conservative assumption following removal of automatic spray actuation.

Pertinent data for these systems, which were used in the analysis, are presented in [Table 6-63](#).

The sump temperature was not used in the analysis because the maximum peak cladding temperature occurs prior to initiation of the recirculation phase for the Containment Spray System.

6.2.1.5.5 Steam-Water Mixing

Water spillage rates from the broken loop accumulator as given in [Table 6-62](#) are determined as part of the core reflooding calculation and are included in the LOTIC-2 calculational model.

6.2.1.5.6 Passive Heat Sinks

The passive heat sinks used in the analysis and their thermophysical properties are given in [Table 6-64](#).

6.2.1.5.7 Heat Transfer to Passive Sinks

The upper and lower compartment pressure response for the Best Estimate LBLOCA reference transient (DECLG, $C_D = 1.0$) is presented in [Figure 6-204](#). The upper and lower compartment heat removal rates are given in Figures [6-205](#) and [6-206](#) respectively. The heat transfer model used is described in Reference [24](#). [Figure 6-207](#) presents the temperature transient in both the upper and lower compartments. The heat removal from the ice bed, lower compartment drain, containment spray, and the sump are provided in [Figure 6-208](#), [Figure 6-209](#), and [Figure 6-210](#).

6.2.1.5.8 Other Parameters

All parameters having a substantial effect on the minimum containment pressure analysis have been discussed or referenced in the preceding sections.

6.2.1.6 Testing and Inspection

6.2.1.6.1 Preoperational Testing

Prior to initial fuel loading, certain tests are conducted to ensure the functional capability of the Containment and associated structures, systems, and components. Section [14.4](#) discusses the

preoperational tests and gives, for each test, the purpose, a description of the test method, and the acceptance criteria. The specific tests pertaining to the containment functional design are:

Containment Spray System Functional Test
Containment Structural Integrity Test
Containment Initial Integrated Leak Rate Test
Containment Air Return System Functional Test
Ice Condenser System Functional Test
Containment Divider Barrier Leakage Area Verification Test

6.2.1.6.2 Periodic Inservice Surveillance

During plant operation certain tests and inspections are conducted to ensure the functional capability of the Containment and associated structures, systems, and components. The Catawba Technical Specifications discusses the periodic inservice surveillance tests and inspections and gives, for each test or inspection, the acceptance criteria, the operational mode(s) in which these criteria are applicable, the actions(s) to be taken in the event the criteria are not satisfied, and the surveillance requirements necessary to demonstrate satisfaction of the criteria. The specific tests and inspection items pertaining to the Containment functional design are:

Containment Integrity
Containment Leakage
Internal Pressure
Air Temperature
Containment Vessel Structural Integrity
Reactor Building Structural Integrity
Containment Spray System
Ice Condenser
Ice Condenser Doors
Divider Barrier Personnel Access Doors
Divider Barrier Equipment Hatches
Containment Air Return System
Ice Condenser Floor Drains
Refueling Canal Drains
Divider Barrier Seal

Bases for the periodic inservice surveillance tests and inspections are given in the Bases for the Technical Specifications.

6.2.1.7 Instrumentation Requirements

Instrumentation is provided in the Containment to remotely monitor the following post-accident conditions:

1. Pressure
2. Sump Level
3. Radiation Level

These monitors, whose readout is located in the Control Room, are designed to remain functional and on scale for environmental conditions resulting from any postulated accident. Operational and testing requirements for the sump level and pressure monitors are presented in Section [3.11](#).

6.2.2 Containment Heat Removal Systems

Adequate containment heat removal capability for the Ice Condenser Reactor Containment is provided by the Ice Condenser (Section [6.7](#)), the Air Return Fan System and the Containment Spray System whose components operate as described in Section [6.2.2.2](#).

The Containment Spray System consists of two trains of redundant equipment. There are six spray headers per unit. Two headers are supplied by each containment spray pump the other two are supplied by separate ND pumps. Each train consists of two spray headers supplied by one containment spray pump and its associated heat exchanger, one spray header supplied by a residual heat removal pump, and required piping and valves. All of the spray headers are located in upper containment and contain a sufficient number of spray nozzles to deliver adequate flow and maximum coverage of upper containment for pressure suppression following an accident. The system is manually initiated from the recirculation sump after ND pumps switchover to the sump.

Minimum Engineered Safety Feature performance of the Containment Heat Removal Systems is achieved with the following:

1. Ice Condenser (Section [6.7](#).)
2. One train of the Containment Air Return Fan System, (Section [7.6.10](#))
3. One train of the Containment Spray System
4. One train of the Residual Heat Removal (ND) System (Sections [5.4](#) and [6.3](#)).

6.2.2.1 Design Bases

The primary design basis for the Containment Spray System is to spray cool water into the containment atmosphere when appropriate in the event of a loss-of-coolant accident and thereby ensure that the containment pressure cannot exceed the containment shell design pressure of 15.0 psig. This protection is afforded for all pipe break sizes up to and including the hypothetical instantaneous circumferential rupture of the reactor coolant loop resulting in unobstructed flow from both pipe ends. The Containment Spray System supplements the ice condenser until all the ice is melted by which time the residual spray headers are also available to remove energy directly from the Containment. The system is designed to provide a means of removing containment heat without loss of functional performance in the post-accident containment environment and operate without benefit of maintenance for the duration of the time required to restore and maintain containment conditions at atmospheric pressure. Although the water in the core after a loss-of-coolant accident is quickly subcooled by the Emergency Core Cooling System (Section [6.3](#)), the design heat removal capability of the Containment Spray System is based on the conservative assumption that the core residual heat is released to the containment as steam which eventually melts all ice in the ice condenser. The heat sources and amounts of energy for which the spray system is designed are listed in Section [4.2](#).

The secondary design basis for the Containment Spray System is the suppression of steam partial pressure in the upper volume due to operating deck leakage from a small break. The requirement is that the Containment Spray System be able to absorb the steam leakage through the operating deck at the maximum possible long-term deck differential pressure of one pound per square foot equivalent to the ice condenser door opening differential pressure.

The Containment Spray System is designed to withstand the safe shutdown earthquake and the operational basis earthquake without loss of function. It is an Engineered Safety Feature System and satisfies ANS Safety Class 2 requirements. The Containment Spray System will

maintain its integrity and will not suffer loss of ability to perform its minimum required function due to normal operation, faults of moderate frequency, infrequent faults, or limiting faults.

Sufficient redundancy for all supporting systems necessary for minimum operational requirements of the Containment Spray System is provided and complies with the single failure criteria for engineered safety features. Separate divisions of essential raw cooling water supply, power equipment, heat exchangers, pumps, valves, and instrumentation are provided in order to have two completely separated trains.

The system is provided with overpressure protection that could result from temperature changes or interconnection with other systems operating at higher pressures.

Provisions for inservice and preoperational testing of this system are described in Section [6.2.2.4](#).

6.2.2.2 System Design

The Containment Spray System consists of two separate trains of equal capacity with each train independently capable of meeting system requirements. Each train consists of a residual spray header as well as a pump, heat exchanger, and two ring headers with nozzles, isolation valves and associated piping, instrumentation and controls. Independent electrical power supplies are provided for equipment in each containment spray train. In addition each train is provided with electrical power from separate emergency diesel generators in the event of a loss of offsite electrical power. The flow diagram for this system is presented in [Figure 6-109](#).

All of the piping, valves, pumps, and additional equipment which form the pressure boundary of the containment spray system are purchased and fabricated in accordance with the applicable edition of the ASME Boiler and Pressure Vessel Code, Section III, Class 2. In addition the system is designed to meet the requirements of General Design Criteria 38, 39, and 40 of Appendix A of 10CFR 50. The system design also complies with NRC Regulatory Guides 1.1, 1.26, 1.29, and 1.82 as described in Section [1.7](#).

During normal operation, all of the equipment is idle and the spray header isolation valves are closed. Upon system activation during a LOCA, adequate containment cooling is provided by the Containment Spray Systems whose components operate in sequential modes. These modes are: 1) after the refueling water storage tank has been drained to the low level alarm, recirculation of water from the containment sump through the containment spray pumps, through the containment spray heat exchangers and back to the containment. 2) This spray is useful in reducing sump water temperatures and increases the effective life of the ice; diversion of a portion of the recirculation flow from the Residual Heat Removal System through the residual spray headers if required by procedure. The spray water from the containment and RHR spray systems will be returned from the upper compartment to the lower compartment through six 8 inch drains in the bottom of the refueling canal.

The Containment Spray System will be actuated manually from the control room. The Containment Spray System provides two redundant heat removal trains. The operator manually actuates the system as required, controls for positioning all valves to their operating positions and starting the pumps. RHR spray operation is initiated manually when required by the operator and only if 1) the Emergency Core Cooling System is operating in the recirculation mode, 2) more than 50 minutes have passed since the initiation of the accident, and 3) containment pressure exceeds a setpoint. Assuming a large break LOCA with one train of Engineered Safeguards failed, the remaining ND Auxiliary Spray header is not required to maintain containment pressure within design values.

The interlocks associated with the Containment Spray Pumps are discussed in Section [7.6.4](#). With the exception of the Containment Spray Pump Motors, there are no pressure switches or permissive devices used in such a way that would preclude automatic and manual operation of pump/motor combination.

As described in Section [6.2.2.3](#), the design of the Containment Spray System meets applicable General Design Criteria which assure no loss of capability to perform required safety functions. Following an accident, the Containment Spray System will remain capable of operation to perform its minimum required function.

Those portions of the Containment Spray System located outside of the containment which are designed to circulate, during post accident conditions, radioactively contaminated water collected in the containment meet the following requirements:

1. Shielding within guidelines of 10CFR 20 and 10CFR 100.
2. Collection of discharges from pressure relieving devices.
3. Remote means for isolating any sections under anticipated malfunction or failure conditions.
4. Means to detect and control radioactivity leakage into the environs to limits consistent with guidelines set forth in 10CFR 20 and 10CFR 100.

Design Criteria are discussed in [Chapter 3](#) and a summary of Codes and other criteria applicable to components of the Containment Spray System are given in [Table 3-4](#). Provisions for preoperational and inservice testing of this system are described in Section [6.2.2.4](#).

Component Description

Pumps

The Containment Spray System flow is provided by two centrifugal type pumps driven by electric motors. The motors, which can be powered either normally or from an emergency source are direct coupled and non-overloading to the end of the pump curve. The design head of the Containment Spray Pumps is sufficient to ensure rated capacity with a minimum level in the containment sump when pumping against a head equivalent to the sum of the design pressure of the containment, the elevational head between the pump discharge and the uppermost spray nozzles, and the equipment and piping friction losses. Manufacturer performance testing of each pump yielded 3400 gpm flow at a head of 400 ft. See [Table 6-70](#) for additional design parameters and [Figure 6-110](#) characteristic curves.

The residual heat removal pumps can also provide flow to the Containment Spray System are described in Section [5.4.7](#) and Section [6.3](#). Each residual heat removal pump can provide about 2000 gpm for upper containment spray.

The residual heat removal pumps which also can provide flow to the Containment Spray System are described in Section [5.4.7](#) and Section [6.3](#). Each residual heat removal pump can provide about 2000 gpm for upper containment spray; however, RHR spray operation is not required for design basis accident mitigation. (Unit 2 Only)

The containment spray pumps are vertical shaft pumps. Pump motor parameters are as follows:

| | |
|------------------|------|
| Motor horsepower | 500 |
| Service factor | 1.25 |
| Motor voltage | 4000 |

| | |
|-------|----|
| Phase | 3 |
| cycle | 60 |

Heat Exchangers

Containment Spray Heat Exchangers are of the vertical shell and tube type with tubes rolled and welded to the tube sheet. Borated water from either the refueling water storage tank or the containment sump circulates through the shell side while the service water from the RN system circulates through the tubes. Design parameters are presented in [Table 6-71](#).

Piping

All Containment Spray System piping in contact with borated water is austenitic stainless steel. All piping joints are welded except for the flanged connection at the pump and relief valves. Flanged connections may also be installed in the heat exchanger drain piping.

Spray Nozzles and Ring Headers

Each pair of containment spray headers provides approximately 3400 gpm and contain a total of approximately 223 hollow cone ramp bottom nozzles, each of which is capable of a design flow of 15.2 gpm with a 40 psi differential pressure. These nozzles have a 3/8 inch spray orifice and are not subject to clogging by particles up to 1/4 inch in maximum dimension. The nozzles produce a mean drop size of approximately 700 microns in diameter at rated system conditions. The spray solution is completely stable and soluble at all temperatures of interest in the containment and therefore will not precipitate or otherwise interfere with nozzle performance. Each nozzle is independently oriented to maximize coverage of the containment volume inside the crane wall.

Each residual spray header contains 133 nozzles. These headers have the same design characteristics as those associated with the containment spray pumps.

Refueling Water Storage Tank

During the injection phase immediately following a LOCA, the containment spray is not supplied from the refueling water storage tank. Containment spray is manually actuated from the sump during the recirculation phase of the LOCA.

Material Compatibility

All parts of the Containment Spray System in contact with borated water are austenitic stainless steel or equivalent corrosion-resistant material.

Containment Recirculation Sump

The lower compartment of containment collects ice condenser melt, reactor coolant system spill (including ECCS injection water), and containment spray fluid (via the refueling canal) and provides the water for the ECCS recirculation phase. One suction line removes fluid from the lowest elevation of containment (with the exception of the incore instrument tunnel) for one train of the residual heat removal pumps and containment spray pumps. An adjacent suction line supplies the redundant residual heat removal pump and containment spray pump. The ends of these suction lines are enclosed by a Containment Recirculation Sump Strainer Assembly as shown in [Figure 6-111](#).

The strainer assembly is located between the polar crane wall and the containment vessel. Piping subject to breaks that result in need for recirculation capabilities are located inside the crane wall and are thus isolated from the recirculation sump strainer assembly. This physical isolation protects the strainer assembly from pipe whip and jet impingement, and also eliminates

air entrainment in the recirculating fluid caused by jet effects on the liquid surface. In addition the crane wall keeps insulation and other debris directly generated by the break from getting into the annular region where the sump is located. The approach velocity inside the crane wall is very low. This allows a long time for any debris that might be produced in this area to settle to the floor. The identified flow passages through the crane wall consist of a number of used and unused pipe sleeves that penetrate the crane wall. These sleeves are above the floor elevations. Due to the very low velocities inside the crane wall, the height from the floor to the invert elevation of the lowest pipe sleeves acts as an effective trash barrier for dense debris. There are sufficient unused pipe sleeves to ensure adequate flow from inside the crane wall to the annular sump area.

The design of the containment recirculation sump strainer assembly complies with the recommendations of Regulatory Guide 1.82 as discussed in Section 1.7. The basis for PWR licensees to demonstrate compliance with the above regulatory requirements and commitments is documented in GL 2004-02, "Potential Impact of Debris Blockage on Emergency Recirculation during Design Basis Accidents at Pressurized-Water Reactors".

Potential sources of post-accident debris have been held to a minimal amount through appropriate design, procurement and operation of the plant. The following potential sources of debris have been minimized as far as practical:

1. A general housekeeping inspection, which is performed at the end of each shutdown, is designed to assure that there are no unnecessary materials inside containment that have the potential to become debris capable of blocking the recirculation sump strainer.
2. Unqualified coatings inside containment have been limited as much as practical.
3. Thermal insulation used on hot piping is resistant to forming particulate debris due to a pipe break accident.
4. There are no structures designed to be displaced by accident pressure to provide vent area.
5. Sand plugs were not used inside containment at Catawba.
6. The recirculation sump strainer is protected from debris generated by other non-safety-related equipment by the crane wall which has relatively small, submerged pipe sleeves which provide flow from the pipe break to the screen assemblies.

The design adequacy of the recirculation sump strainer has been verified as acceptable through Duke's response to Generic Letter 04-02, "Potential Impact of Debris Blockage on Emergency Recirculation during Design Basis Accidents at Pressurized Water Reactors". The Generic Letter response (including RAI responses and Supplemental Content Guide) includes evaluations pertaining to minimum sump inventory, NPSH margins, chemical effects, debris loading, etc.

See Section [6.3.2.9](#) for further discussion on the design of the recirculation sump strainer and compliance with G.L. 04-02.

6.2.2.3 Design Evaluation

Performance of the containment heat removal systems is evaluated through analyses of the design basis accident and various other cases described in [Chapter 15](#) and Section [6.2.1](#). The analyses were performed using the GOTHIC code and show that containment systems are capable of keeping the containment pressure below the design pressure of 15 psig even when it is assumed that only minimum engineered safety features are operating. Presented in Section [6.2.1](#) is a description of the analytical methods and models which were used along with

verification of pertinent items from Waltz Mill tests, and curves showing the calculated performance of important variables following the design basis loss-of-coolant accident.

The design basis accident results in a required containment spray flow rate of 3323 gpm using 100°F constant temperature essential raw cooling water for the heat exchangers.

The Containment Spray System provides two full capacity heat removal systems each of which is capable of delivering the design flow of 3400 gpm and, thereby, removing heat at the rate which will preclude an increase of the containment pressure above 15.0 psig. All spray headers and spray nozzles are located inside the containment in the upper compartment and will withstand, without loss of function or maintenance, the post accident containment environment. The remainder of the system which includes all active components, is located in the auxiliary building and therefore are not affected by wind, tornado, or snow and ice conditions.

The design is based on the spray water being raised to the saturation temperature of the containment in falling through the steam-air mixture within the building. The minimum fall path of the droplets is approximately 75 ft. from the spray ring headers to the operating deck. The actual fall path is long due to the trajectory of the droplets sprayed out from the ring headers nozzles.

The Containment Spray System operates independently of other engineered safety features. For extended operation in the recirculation mode, water can be supplied to the residual spray headers through the Residual Heat Removal pumps and Residual Heat Removal exchangers. One Containment spray system train provides adequate heat removal capability to limit Containment pressure below design (see Section [6.2.1.3](#)). Residual spray may be initiated manually and only after switchover to the recirculation mode and no earlier than 50 minutes after initiation of the LOCA if desired by procedure. At this time one ND pump can provide sufficient residual spray as well as adequate core flow via the high head (one centrifugal charging and one safety injection) pumps. The Residual Spray may be required due to high containment pressure. High containment pressure would be indicated to the operator via safety-related redundant pressure indication in the control room. (See Section [6.3.3](#) for the performance evaluation of the ND pumps in their core cooling function.)

An analysis has been made of all active components of the system to show that the failure of any single active component will not prevent fulfilling the design function. This analysis is summarized in [Table 6-72](#). A single failure in the Residual Heat Removal System will not prevent long-term use of the spray system. The analyses of the loss-of-coolant accident presented in [Chapter 15](#) reflect the single failure analysis. Each of the spray trains provides complete backup for the other.

An analysis of the spray return drains located in the refueling canal has been made to show that they are adequately sized for a maximum RHR and containment spray flow. It was shown that a water head of approximately 9 feet in the refueling canal is sufficient to establish a steady-state drainage between the upper and lower compartment. This water head is well within the capacity of the refueling canal.

The passive portion of the spray systems located within the containment are designed to withstand, without loss of functional performance, a post accident containment environment and to operate without benefit of maintenance. The spray headers which are located in the upper containment volume are separated from the reactor and primary coolant loops by the operating deck and inner wall of the ice bed. These spray headers are therefore protected from missiles originating in the lower compartment.

In accordance with Regulatory Guide 1.1, the plant and piping layout of the Containment Spray System ensures that the pump net positive suction head (NPSH) requirements are met at

maximum calculated runout conditions with the Containment Spray Pumps taking suction from the containment sump. The NPSH available from the containment sump is calculated using the maximum credible sump water temperature 200°F with no credit taken for containment overpressure. Only a minimum amount of static head due to water level above the sump floor is included. This minimum level is the amount of water that must be present in order to initiate spray from the containment sump. For additional details of the analysis refer to [Table 6-70](#) and the RHR pump NPSH analysis. (See Section [6.3.2.2](#).)

Proper initial fill and venting of the Containment Spray System ensures that loss of NPSH, pump cavitation, gas binding, or water hammer will not occur in Containment Spray if spray is initiated. The containment spray system was evaluated for gas accumulation for Generic Letter 2008-01. The Generic Letter 2008-01 evaluation concluded that system procedures and design are adequate to maintain the Containment Spray System sufficiently full of water to ensure operability.

A Failure Mode and Effects Analysis of the Containment Spray System is provided as [Table 6-73](#).

This evaluation shows that the Containment Spray System can withstand expected conditions during the 40-year life of the plant without loss of capability to perform the required safety functions. Specifically, the system achieved this by having been designed to meet applicable General Design Criteria as follows:

1. The system can withstand the effects of natural phenomena as required by General Design Criterion 2.
2. The system is designed to accommodate the effects of and be compatible with the environmental conditions associated with normal operation, maintenance, testing, and postulated accidents including loss of coolant as required by General Design Criterion 4.
3. The system is not shared with another nuclear power unit as required by General Design Criterion 5.
4. The system is designed to be capable of being inspected and tested to ensure reliability throughout their life as required by General Design Criteria 39 and 40.

6.2.2.4 Testing and Inspections

Italicized text below is HISTORICAL INFORMATION, NOT REQUIRED TO BE REVISED.

Performance tests of the active components in the system were performed in the manufacturer's plant and will be followed by in-place preoperational testing. Capability is provided to test initially and subsequently on a routine basis to the extent practical the operational startup sequence and performance capability of the Containment Spray System including the transfer to alternate power sources. Capability to test periodically the delivery capacity of the Containment Spray System at a position as close to the spray header as is practical is provided. Also, the spray nozzles can be tested for obstruction. As part of the preoperational test program, the containment spray nozzles will be verified to be unobstructed by introducing smoke or air into the containment spray headers. The smoke or air will be introduced into the headers through a test connection on each header. The test connections are shown on [Figure 6-109](#).

A preoperational Engineered Safety Feature (ESF) Functional Test will be performed which will include measuring the response time of ESF components.

Initially, the Containment Spray System will be hydrostatically tested at the applicable code test pressure. Preoperational test abstracts are described in [Chapter 14](#) in topic 14.0.

All periodic tests of individual components or the complete Containment Spray System will be controlled to ensure that plant safety is not jeopardized and that undesirable transients do not occur.

The Containment Spray System is designed to comply with ASME Section XI, Inservice Inspection of Nuclear Power Plant Components.

6.2.2.5 Instrumentation Requirements

The Containment Spray System is actuated manually from the control room. The operation of the Containment Spray Systems is verified by instrument readout in the control room. Pump motor breakers energize indicating lights on the control panel to show power is being supplied to the pump motors. Status lights on the main control panel indicate valve position and are energized independently of the valve actuation signal.

Locally mounted instruments monitor containment spray pump suction and discharge pressure, heat exchanger inlet temperature and the flow in the test line from the pumps to the RWST. The total pump discharge flow and heat exchanger outlet temperature are indicated on the main control board.

The system is designed for seismic Category I conditions. The instrumentation and associated interconnected wiring and cables are physically and electrically separated so that a single event cannot cause malfunction of the entire system.

6.2.2.6 Materials

All parts of the Containment Spray System in contact with borated water are austenitic stainless steel or equivalent corrosion-resistant material. None of these materials produce radiolytic or pyrolytic decomposition products that will interfere with this or other engineered safety features.

6.2.3 Secondary Containment Functional Design

6.2.3.1 Design Bases

The design bases for the secondary containment are (1) to assure that an effective barrier exists and is maintained for gases and fission products that may leak from the primary containment and (2) to insure retention in the secondary containment for clean-up by the Annulus Ventilation System prior to being released to the atmosphere.

Section [9.4.9.1](#) provides the design bases and a description of the Annulus Ventilation System.

The Reactor Building provides a secondary containment boundary for the Annulus Ventilation System. All penetrations are sealed so that the negative annulus pressure may be maintained. A checklist is provided in [Table 6-74](#) which considers all containment piping penetrations and indicates those that must be considered potential bypass leak paths. The valves on these potential bypass leak path penetrations are tested in accordance with 10CFR 50, Appendix J. The Reactor Building is designed to withstand an internal or external pressure of 3 psig. This pressure is considered in combination with seismic forces and other loads defined in Section [3.8.1.3](#).

The secondary containment is designed for periodic inspection and functional testing required by the Technical Specifications.

Also, in accordance with 10 CFR Part 50.34, paragraph c and d; 10 CFR Parts 73.46, 73.50, and 73.55 paragraph (d) 8 and as committed to in the Catawba Nuclear Station Security Plan,

the upper and lower annulus doors will be locked and maintained under security card key access control. Door position indication and annunciation of door alarms is provided for in the Central and Secondary Alarm Stations.

6.2.3.2 System Design

The Reactor Building description and design criteria including codes and standards is completely furnished in Section [3.8.1](#). Additional information is provided in [Table 6-76](#). The structural outline of the Reactor Building is furnished in [Figure 3-243](#). Additional plans and sections are shown in [Figure 1-10](#) through [Figure 1-18](#).

6.2.3.3 Design Evaluation

Analyses of conditions in the containment and performance of the Annulus Ventilation System following a design basis LOCA have been performed. These analyses determined the ability of the Annulus Ventilation System to draw and maintain the necessary vacuum in the annulus. The analyses were performed for the following three design basis LOCA scenarios.

- 1) Design basis LOCA with the failure of one train of the Annulus Ventilation System to start and run. This corresponds to a design basis LOCA or rod ejection accident with a Minimum Safeguards failure. The effects of this failure include a delay in the time to draw a sufficiently negative pressure in the annulus and a lower Annulus Ventilation recirculation flow rate in the long-term,
- 2) Design basis LOCA with one Annulus Ventilation Pressure Transmitter failing high. This results in the full flow from the affected Annulus Ventilation train being exhausted even when the setpoint to begin modulation of the exhaust flow is reached. The effects of this failure include a high Annulus Ventilation exhaust flow rate until the affected train is secured.
- 3) Design basis LOCA with no failures of the Annulus Ventilation System. This is associated with two design basis LOCA scenarios. In one scenario, the single failure is failure of cooling water flow through a Residual Heat Removal or Containment Spray Heat Exchanger. The second scenario includes an initially closed control room outside air intake.

The pressure, temperature, and mass of annulus air is calculated by the Fortran IV program CANVENT for the entire accident transient, including the steady state conditions prior to the initiating event. The containment is divided into three regions, where standard equations of heat transfer are applied. No heat or mass transfer between regions is assumed except in the annulus. The steady state, pre-accident temperatures are determined by an interactive process until successively calculated temperatures differ by less than some small predetermined amount. The post-DBA transient conditions are calculated using the finite differences technique.

The following assumptions are made for simplification and/or conservatism:

1. The containment is divided into three regions. The temperature of each region is uniform within that region.
2. There are no temperature gradients in the vertical or circumferential directions. Thus, the model is one dimensional with heat transfer occurring only in the radial directions.
3. All physical properties (e.g., heat capacity, thermal conductivity, emissivity, and density) are independent of temperature, except the density of air in the annulus.
4. The air in the annulus behaves as an ideal gas and is uniformly mixed.

5. Direct radiative heat transfer to the annulus atmosphere is included. Solely to this purpose, the air in the annulus is taken to include water vapor. The amount of water vapor assumed to be in the annulus corresponds to a temperature inside the annulus of 95°F and a relative humidity of 100%.
6. Radiative heat transfer occurs between the concrete reactor building and the steel containment building and between each of these surfaces and the annulus atmosphere. The surfaces are treated as gray bodies with a parallel, flat plate geometry.
7. The equation for the heat transfer coefficient for the upper containment to annulus air, treating the dome as a horizontal plate, is $h = .22 (\Delta t)^{1/3}$. Similarly, treating the ice condenser and lower containment sections as vertical plates, the heat transfer coefficient to annulus air is $h = .19 (\Delta t)^{1/3}$.
8. For the transfer of heat from the containment air to the containment shell, a heat transfer coefficient that increases linearly in time from 8 Btu/hr - ft² - °F to some maximum value is assumed, followed by exponential decay at a rate of .025 sec⁻¹ to some long-term value. The steady-state calculations are based on the natural convection heat transfer coefficients previously mentioned.
9. Circulation of refrigerating air in the ice condenser air ducts ceases at the initiation of the accident. Therefore, before the accident, heat is transferred to the refrigerating air by forced convection; whereas, after the accident the mechanism is natural convection. The use of a forced convection heat transfer coefficient is eliminated by assuming the ice condenser walls are at the same temperature as the refrigerating air.
10. The annulus ventilation fan comes on instantaneously at full speed at a time determined by signal response times and fan characteristics. Partial flow before this time is not considered.
11. For all design basis LOCA scenarios, the airflow from all available Annulus Ventilation fans initially is discharged to the unit vent stack. This EXHAUST mode of operation continues until the annulus pressure is reduced to the Annulus Ventilation pressure transmitter setpoint of approximately -1.67 in.w.g. Once this setpoint is reached for all scenarios except that including a pressure transmitter failure only that portion of the fan discharged airflow required to maintain the annulus pressure at the pressure transmitter setpoint is discharge to the unit vent stack. The remaining airflow is recirculated to the annulus. For the design basis LOCA with a pressure transmitter failure, the affected Annulus Ventilation train continues in the EXHAUST mode with the full fan flow discharged to the unit vent stack for 2.5 hours after the initiating event. At that time the control room operators trip the affected Annulus Ventilation fan. The unaffected Annulus Ventilation train modulates fan discharge airflow between EXHAUST and RECIRCULATION to maintain the annulus pressure at the pressure transmitter setpoint.
12. Leakage across the concrete reactor building from the environment into the annulus is assumed. The leak rate reaches its maximum when the annulus pressure reaches the setpoint of the Annulus Ventilation pressure transmitter (-1.67 in.w.g.) for all design basis LOCA scenarios except the one including a pressure transmitter failure. The design basis value of the reactor building leak rate is calculated based on the outside air being at a 99th percentile low temperature. This value is used to calculate the reactor building leak rate at all other annulus pressures on incompressible flow. At no time is credit taken for leakage across the reactor building from the annulus to the environment.
13. Thermal contact resistances are neglected.

14. For each of the three regions, heat transfer areas are lumped into one of three categories based on the inside radius of the containment shell, the midpoint of the annulus, and the midpoint of the reactor building. This is assumed in order to avoid the continuous variation of area with radius associated with cylindrical geometry.
15. Outside temperatures remain unchanged during the course of the accident. For steady-state calculations, the surface of the reactor building is at the outside temperature. For the post-accident transient, the Reactor Building is considered an adiabatic wall.
16. The expansion of the containment shell, due to the pressure and temperature increase within, is calculated assuming each region is freestanding and independent of any other region.
17. The outside air initially is assumed to be at the 99th percentile low temperature.

Post accident airflow rates of the Annulus Ventilation System for the scenarios noted above are presented in [Table 6-75](#). The analyses of radiological consequences of the design basis rod ejection accident and LOCA are reported in Sections [15.4.8.3](#) and [15.6.5.3](#), respectively. The Minimum Safeguards scenario (one unavailable Annulus Ventilation train) is limiting for all radiation doses following the design basis rod ejection accident. The scenario involving post operation of both Annulus Ventilation trains is limiting for all radiation doses following the design basis LOCA.

6.2.3.4 Tests and Inspections

Preoperational and periodic tests are described in [Chapter 14](#) and the Technical Specifications respectively.

6.2.3.5 Instrumentation Application

The Annulus Ventilation System instrumentation and controls are discussed in Section [7.6.14](#).

6.2.4 Containment Isolation System

The Containment Isolation System provides the means of isolating fluid systems that pass through Containment penetrations such that any radioactivity that may be released into the Containment following a postulated design basis accident will be confined. The Containment Isolation Systems are Engineered Safety Features required to function following a design basis event to isolate nonsafety-related fluid systems penetrating the Containment. There is no single system for complete Containment isolation, but isolation design is achieved by applying acceptable common criteria to penetrations in many different fluid systems, injecting water at a higher pressure than Containment design pressure between the seats of double disk gate valves, and by using Containment pressure to provide Containment isolation signals as described below to actuate appropriate valves.

6.2.4.1 Design Bases

Note:

This section of the FSAR contains information on the design bases and design criteria of this system/structure. Additional information that may assist the reader in understanding the system is contained in the design basis document (DBD) for this system/structure.

The design bases for the Containment Isolation Systems include provisions for the following:

1. A double barrier at the Containment penetration in those fluid systems that are not required to function following a design basis event.
2. Automatic and leaktight closure of those valves required to close for Containment integrity following a design basis event to minimize release of any radioactive material.
3. A means of leak testing barriers in fluid systems that serve as Containment isolation.
4. The capability to periodically test the operability of Containment isolation valves.
5. A Containment Valve Injection Water System to inject water between the seats of double disk gate valves at a pressure higher than Containment design pressure, thus preventing leakage past these valves and reducing potential off-site dose following the postulated accident.
6. Diversity in containment isolation signals as required per Regulatory Guide 1.141 is achieved by utilizing a combination of ECCS initiation, high pressure, and high radiation signals.
7. Containment isolation valve control wiring has been engineered to preclude automatic reopening of containment isolation valves when the isolation signal is reset.

Phase A Containment isolation is initiated by means of a Containment High Pressure Signal (ST). An ST occurs on a containment pressure of 1 psig as sensed by two out of four containment high pressure sensors or upon receipt of a Safety Injection Signal (SS). Phase B Containment isolation occurs on a Containment High-High Pressure Signal (SP). An SP occurs on a containment pressure of 3 psig as sensed by the same instrumentation mentioned above. [Table 3-104](#) gives the specific isolation signals for each containment isolation valve.

The instrumentation circuits that generate ST and SP are described in Section [7.3](#). The inclusion of the Main Steam Isolation Signal as a Containment isolation signal is not necessary as the radiological releases due to a steam line break are within acceptable guidelines. Main steam and main feedwater isolation are initiated by the Main Steam Isolation Signal as described in [Chapter 7](#).

Due to the high radiation potential of the Liquid Radwaste System, its two penetrations at the containment floor sumps and the ventilation unit condensate drains are set to close on a high radiation signal.

Each Containment penetration which is not required to function following a design basis accident has at least two automatic isolation barriers; one barrier is located outside the Containment and one inside the Containment. An automatic barrier is either a closed system, an automatic valve, or an automatic valve with seal water injection.

The following criteria and definitions are used in the design of the Containment Isolation System to assure that the above barrier design is met:

1. Containment isolation valves, operators, and piping are designed to withstand internal conditions of the process piping and external conditions due to post-LOCA temperature, pressure, humidity, and radiation.
2. All valves and equipment which are considered to be isolation barriers are classified as Safety Class 2. The containment isolation system conforms to all guidelines of Regulatory Guide 1.26 as described in Section [3.2.2](#) and [Table 3-3](#).
3. All automatic valves that are actuated by containment isolation signals also have controls in the control room for manual actuation.

4. A closed system outside the Containment designed in accordance with criteria 1, 2, and 3 above, meets the following requirements:
 - a. It does not communicate with the atmosphere outside the Containment.
 - b. Its safety class is the same as for Engineered Safety Features Systems, either class B or C.
 - c. The internal design pressure and temperature must be no less than Containment design pressure and temperature.
5. A closed system inside the Containment designed in accordance with criteria 1, 2, and 3, meets the following requirements:
 - a. It does not communicate with either the Reactor Coolant System or the reactor Containment atmosphere.
 - b. Its safety class is the same as for Engineered Safety Features Systems.
 - c. It will withstand external pressure and temperature equal to Containment design pressure and temperature.
 - d. It will withstand accident temperature, pressure, and fluid velocity transients, and the resulting environment.
 - e. It is missile protected.

Note: Any system not completely meeting the requirements of Criteria 4 and 5 is considered an open system.

6. A check valve inside the Containment incoming lines is considered to meet or exceed the criteria for:
 - a. A remote manual valve; or
 - b. An automatic valve.
7. A locked closed valve is equivalent to an automatic valve.
8. Lines which, due to safety considerations, must remain in service subsequent to certain accidents shall be provided with at least one remote-manual isolation valve.
9. The Containment Valve Injection Water System is provided with two trains, one for valves powered from A train diesel and one for valves powered by B train diesel. This prevents the possibility of both inside and outside isolation valves not sealing due to a single failure.
10. The piping of the Containment Valve Injection Water System has a design pressure the same as the valves it supplies and is Safety Class 2. Relief valves set at 150 psig are provided in the unlikely event of backleakage past two check valves in series.
11. Assured makeup water is provided to the Containment Valve Injection Water System from the essential headers of the Nuclear Service Water System, which is capable of supplying makeup water for 30 days following the postulated LOCA.

The Containment Isolation System minimizes the leakage of radioactive materials through the pipes penetrating the Containment in the event of a design basis accident. Double barrier protection is provided on lines that are part of the reactor coolant pressure boundary or are connected directly to the Containment atmosphere to assure that no single credible failure or malfunction of an active Component shall result in a loss of isolation function. Lines that do not fall into the above categories are provided with a single barrier. The barriers are of three types:

1. Type I

Lines that are part of the reactor coolant pressure boundary and penetrate the primary reactor Containment are provided with valves as follows:

- a. One locked closed isolation valve inside and one locked closed isolation valve outside Containment, or
- b. One automatic isolation valve inside and one locked closed isolation valve outside Containment, or
- c. One locked closed isolation valve inside and one automatic isolation valve outside Containment. A check valve is not used as the automatic isolation valve outside Containment, or
- d. One automatic isolation valve inside and one automatic isolation valve outside Containment. A check valve is not used as the automatic isolation valve outside Containment.

The above provisions satisfy General Design Criterion 55.

2. Type II

Lines that connect directly to the Containment atmosphere and penetrate the primary reactor Containment are provided with the following isolation valves:

- a. One locked closed isolation valve inside and one locked closed isolation valve outside Containment, or
- b. One automatic isolation valve inside and one locked closed isolation valve outside Containment, or
- c. One locked closed isolation valve inside and one automatic isolation valve outside Containment. A check valve is not used as the automatic isolation valve outside Containment, or
- d. One automatic isolation valve inside and one automatic isolation valve outside Containment. A check valve is not used as the automatic isolation valve outside Containment.

These provisions satisfy General Design Criterion 56.

3. Type III

Lines that penetrate the primary reactor Containment and are neither part of the reactor coolant pressure boundary nor connected directly to the Containment atmosphere have at least one isolation valve, located outside the Containment, which is (a) automatic, (b) locked closed, or (c) capable of remote manual operation. A check valve is not used as the automatic isolation valve.

These provisions satisfy General Design Criterion 57.

In conformance to General Design Criterion 54, the piping systems and related components penetrating the Containment are provided with leak detection, isolation, and Containment capabilities having redundancy, reliability, and performance capabilities that reflect the importance to safety of isolating these fluid systems. The Containment leakage test program provides for periodic testing to determine if valve leakage is within allowable design limits and to test the operability of the isolation valve and associated components. Gate valves tend to leak air at quantities higher than that which is acceptable for bypass leakage through a penetration. These valves are injected with water between the seats at a pressure higher than Containment

Design pressure. This water is injected automatically on an engineered safety signal from the Containment Valve Injection Water System, thus preventing leakage of the Containment atmosphere through those valves and reducing the potential offsite dose following the postulated accident. These valves are exempt from air leak rate testing, since the water prevents Containment atmosphere from leaking past the valve. Isolation valves are located as close as practical to the Containment. All automatic valves are designed with a failure position that provides the greatest safety.

Instrument lines for process instrumentation that penetrates the Containment employ excess flow check valves outside Containment and appropriate orificing inside Containment to maintain Containment integrity in accordance with Regulatory Guide 1.11. Instrument lines for Containment pressure sensing also penetrate the Containment. These lines are provided with remotely operated class IE solenoid valves located just outside the containment vessel for isolation purposes. This design conforms to Regulatory Guide 1.11.

Administrative controls or locks are used to assure that manual Containment isolation valves are in the closed positions whenever conditions of the plant are such that automatic isolation is required.

Isolation check valves are designed and/or installed to have their disc seated whenever the differential pressure across the seat is zero.

Penetrations for process piping, instrumentation lines, ventilation ducts, and electrical lines are designed to withstand Containment design pressure and temperature as well as any forces due to differential expansion between piping systems and the structure. Where required, bellows are provided between piping and the Containment wall to prevent excessive forces on the piping or on the Containment.

Compliance with Regulatory Guide 1.141 is discussed below.

Regulatory Guide 1.141

Containment Isolation Provisions for Fluid Systems (Rev. 0)

Discussion

Westinghouse design provisions for containment isolation include isolation signals for (a) containment isolation phase A, (b) containment isolation phase B, and (c) containment ventilation isolation. Each of these isolation signals can be initiated automatically, by instrumentation which sense key plant parameters, or by manual operator action at the main control board. The means utilized to initiate the various containment isolation signals are itemized below.

1. Containment isolation phase A
 - a. safety injection signal
 - 1) VN-CN-11377A
 - 2) low pressurizer pressure
 - 3) high containment pressure
 - b. manual safety injection initiation
 - c. manual containment isolation phase A initiation
2. Containment isolation phase B
 - a. high-high containment pressure

- b. manual containment isolation phase B initiation
- 3. Containment ventilation isolation
 - a. high containment air particle monitor activity (not an Engineered Safety feature)
 - b. high containment radio gas monitor activity (not an Engineered Safety feature)
 - c. Deleted Per 2007 Update
 - d. safety injection signal
 - 1) low pressurizer pressure
 - 2) high containment pressure
 - e. manual safety injection initiation
 - f. manual containment isolation phase A initiation
 - g. manual containment isolation phase B initiation

Implementation of the isolation signals is such that all non-essential containment penetrations are isolated on a containment isolation phase A signal. These non-essential containment penetrations include those connected to the reactor coolant pressure boundary and containment atmosphere. Non-essential containment penetrations that are part of the containment ventilation system are also isolated on a containment ventilation isolation signal. Containment isolation phase B is utilized to automatically isolate certain essential containment penetrations.

To evaluate the merit of including containment radiation as an initiating signal for containment isolation phase A, a study was performed to evaluate if containment isolation on high radiation would occur earlier in the transient than due to the present containment isolation logic. The study evaluated the spectrum of design basis accidents and concluded that in all cases, except for small reactor coolant system leaks (i.e., leaks resulting from an approximately 3/8 inch or smaller diameter rupture), the present logic would isolate containment prior to high containment radiation. For small reactor coolant system leaks, the reactor coolant system pressure may be maintained by operation of the normal charging system and safety injection initiation may not occur to initiate containment isolation phase A. This type of accident is characterized by the release of reactor coolant with a low specific activity. If the reactor coolant was at the technical specification activity level at the initiation of the transient, it would take approximately two hours before containment isolation would occur on high radiation assuming a 100 gpm leak rate. For this category of accident, credit has traditionally been taken for operator action to diagnose the rupture and take action within this time period, including manual initiation of containment isolation phase A if appropriate, to mitigate the consequences of the rupture. Based on this study, Westinghouse concludes that the present initiation logic for containment isolation phase A is sufficient to ensure timely isolation of non-essential containment penetrations for the present category of design bases accidents.

Although not required for the present category of design basis accidents, containment isolation phase A initiation on containment radiation may have merit relative to certain postulated accidents (e.g., loss of all heat sink or loss of all AC power) outside the present design basis. However, modifying the present containment isolation phase A initiation logic to include containment radiation also has a potential disadvantage in that containment isolation phase A initiation during normal plant operation due to spurious high containment radiation will subject the plant to an abnormal transient with the potential for reactor trip. Another potential disadvantage is that containment isolation phase A initiation following a small reactor coolant system leak may reduce operator flexibility to mitigate this category of accident by isolation nonessential containment penetrations that connect to the reactor coolant pressure boundary.

Consequently, any modification to add containment radiation as an initiation signal for containment isolation phase A should minimize the potential for spurious initiation and maximize operator flexibility to mitigate small reactor coolant system leaks.

In summary, the present Westinghouse containment isolation initiation logic is sufficient for the present category of design basis accidents. The present containment isolation phase A initiation logic is sufficiently diverse and fast acting to preclude any benefit from including containment radiation. Containment radiation indication and alarms in the control room are available to aid the operator in determining whether containment isolation phase A should be manually initiated. The present containment ventilation isolation logic on containment radiation ensures that non-essential airborne release paths are isolated on high containment radiation. If the present design basis is expanded to include postulated accidents for which there may be benefits in automatic containment isolation phase A initiation on high containment radiation, this modification must be implemented to optimize plant safety while minimizing impact on plant availability. It should be noted that if the present design basis is expanded to include these postulated accidents, other accident mitigation systems may require modification.

6.2.4.2 System Design

6.2.4.2.1 Containment Isolation Systems

No single piping and instrumentation diagram shows all of the Containment penetrations; however, they are clearly shown on all piping and instrumentation diagrams for systems. All automatic valves that will operate in the event of a Containment isolation signal are clearly identified. A diagram showing the location of valves in relation to the Containment wall for fluid systems penetrating Containment is shown in [Figure 6-112](#). This figure also shows the arrangement of the valving system and type of valves used in each fluid system penetration. Each fluid penetration is listed with the service it performs on [Table 6-77](#). The table lists for each penetration the normal flow direction, valve arrangement from [Figure 6-112](#), the automatic actuating signal for the valves, normal, shutdown, and accident valve position, valve position upon failure of actuation systems, the penetration line size, seismic classification of equipment associated with the penetration, and the reference FSAR System Flow Diagram. The parameter associated with Containment isolation is high Containment pressure. The parameter associated with main steam and feedwater isolation is low steam pressure. Channel separation is provided for all automatic isolation valves. All automatic isolation valves have position indicating lights in the Control Room to show the open and closed positions.

Potential bypass leak paths through Containment isolation valves are identified and evaluated in [Table 6-74](#).

ANSI standard N271-1976, Section 4.4.4, specifies the requirements for containment isolation valve closure times.

The power sources for each valve actuator can be determined from [Table 6-77](#) (Note 4).

The sequencing system for loading the onsite emergency electrical generators is designed to actuate all valves receiving an engineered safety features actuation signal within adequate time to supply ECCS and auxiliary pumps after the switch to emergency onsite electrical power signal is accomplished.

The Containment Purge System (as described in Section [9.4.5](#)) reduces radioactivity levels in the containment as well as in the Incore Instrumentation Room by taking in fresh air from the outside and exhausting containment air through cleanup filters prior to discharge to atmosphere through the unit vent stack. Expected Containment Purge System usage is described in Section

[9.4.5.2](#) and is further limited by the Station Technical Specifications. The Containment Purge System (VP) is designed to meet the requirements outlined in Branch Technical Position CSB 6-4, Revision 1, dated December 1978. A comparison of the system to CSB 6-4, Revision 2, dated July 1981 is given in [Table 6-78](#). Other systems similar in function as well as in design requirements are the Containment Air Release and Addition System (VQ) and Containment Hydrogen Sample and Purge System (VY). The VP and VQ Systems containment penetrations are provided with isolation valves capable of 5 second closure. The VY System Containment penetrations are provided with isolation valves capable of 10 second closure. The VP and VY Systems containment isolation valves are locked closed in modes one through four in accordance with the Technical Specifications because they have never been adequately demonstrated to close under design basis accident conditions.

Airborne fission products in the ECCS Pump Room should be effectively contained by filters located in the Auxiliary Building Ventilation System (VA). In addition, the VA System contains radiation monitors in the unit vent stacks which check the radiation level in the ECCS Pump Room. This system is discussed further in Section [9.4.3](#). The VA System in conjunction with the area radiation monitor (see Section [12.3](#)), located at El. 522' and 543' in the ECCS Pump Rooms should satisfactorily serve to detect leakage in the engineered-safety-feature systems.

As described below adequate protection is provided for piping, valves, and vessels against dynamic effects and missiles which might result from plant equipment failures, including a LOCA.

Isolation valves inside the Containment are located between the secondary shield and the inside Containment wall. The secondary shield serves as the missile barrier. Any missile barriers for isolation valves and piping, or vessels which provide one of the isolation barriers outside the Containment, consist of structural steel and concrete which forms walls and floors of adjacent buildings, either the Auxiliary Building or Doghouses.

Piping, isolation valves, and actuators in the Containment Isolation System outside Containment are located inside a Seismic Category 1 enclosure complex, and are located as close as practical to the Containment wall; i.e., in almost all cases, isolation valves will be located immediately after the penetration assembly. There will, however, be exceptions, such as the case of the main steam lines which require a series of safety valves before the isolation valve. Also, there will be some exceptions due to normal structural design arrangements. Actual lengths of pipe from penetrations to the isolation valves outside Containment have been kept to a minimum.

The isolation arrangement of the fuel transfer tube, shown in [Figure 6-117](#) consists of a transfer tube closure and a blind flange, enclosing the transfer tube. The blind flange contains two 'O' - ring grooves and a pressure tap which runs through the blind flange to the annulus between the two 'O' -rings. When assembled preparatory to reactor operation, the blind flange is bolted to the transfer tube closure and the annulus between the seals is pressurized to ensure that both seals are functioning. The seal is further tested when test pressure is introduced into the containment.

When these tests have been satisfactorily completed, the fuel transfer tube is isolated from the containment. The transfer tube closure and the blind flange are considered to be the containment boundary and, therefore, General Design Criterion 56 does not apply to the transfer tube penetration and an isolation valve is not required.

A manual valve is provided on the transfer tube outside the containment. However, its basic function is not to provide Containment isolation. At the beginning of refueling, during filling of the refueling pool, this valve is maintained closed until a common water level is reached in the

refueling pool and the spent fuel pool. Then the valve is opened to allow the transfer of fuel. This valve KF122 is open during normal operation to provide source of water from spent fuel pool to SSF transfer pump.

It is a physical impossibility for the transfer tube closure to fall under either GDC 56 or 57 since the closure is neither a "line that connects directly to the containment atmosphere", nor a "line" at all. In point of fact, the transfer tube closure does not even come in contact with the fuel transfer tube. The purpose of the transfer tube closure is identical to that of any access closure in containment, i.e., to provide necessary access into containment only at appropriate times. Therefore, the transfer tube closure is intended and designed to fall into the "access openings" category of GDC 50. Because the transfer tube closure falls under GDC 50, it is also designed to meet GDC 51, 52, and 53. As specifically stated in GDC 53, ". . . periodic testing at containment design pressure of the leaktightness of penetrations which have resilient seals. . ." must be accommodated in the design. 10CFR 50, Appendix J, Section 11.G.1 specifically states that Type B testing applies to "containment penetrations whose design incorporates resilient seals." Since the transfer tube closure is a containment penetration designed with resilient seals, it has therefore been designed to meet GDC 53 testing requirements using Type B testing discussed in 10CFR 50, Appendix J.

Fluid lines which must remain open subsequent to a design basis accident, such as lines serving ESF systems, do not have Containment isolation valves that are automatically closed by the Containment Isolation Signals, Safety Injection Signal, or Main Steam Isolation Signal. Each of these penetrations has a minimum of one remote-manual operated isolation valve outside Containment.

Provisions made to assure the operability of the isolation valve system under an accident environment satisfy the requirements for redundancy, independence, and testability. The valving system is designed for pressures equal to or greater than the Containment pressure. A comprehensive testing and inspection program (see Technical Specifications) assures that these components will operate for the time period required in the post-design basis accident conditions of temperature, pressure, humidity, radiation, or seismic phenomena. The proper design basis accident environmental conditions are listed in the design specifications for all components that are part of the Containment Isolation System. Vendor factory testing is performed on a prototype of these components to assure their adequacy under these conditions.

Air or motor-operated valves are used for the automatic isolation valves. Air-operated valves are designed to assume the position of greater safety upon loss of air. Motor-operated valves are powered from the emergency power sources.

Remote manual control of the automatically actuated Containment isolation valves is provided.

Automatic valves are installed in lines that must be immediately isolated after an accident. Those lines which must remain in service after an accident have at least one remote manual valve.

Hot and cold penetration design and analyses are presented in Section [3.6.2.4](#), Mechanical Penetrations. Special penetrations such as main steam, main feedwater, and sump recirculation line penetrations are described in detail under this section.

The integrity of the isolation valves system and connecting lines under the dynamic forces resulting from inadvertent closure while at operating conditions (e.g., main steam lines) is assured by the performance of static and dynamic analysis on the piping, valves and restraints.

The supports and restraints are applied such that integrity is assured and pipe stresses and support reactions are within allowable limits. Valves, in nonsafety-related systems where function permits, are normally positioned closed to minimize any release following a design basis event. Those valves that are required to change position following a design basis event are equipped with valve operators to move the valve rapidly.

Containment isolation valves and operators inside the Containment are designed to withstand a maximum integrated radiation dose of 2×10^8 rads during the life of the plant.

Containment isolation valves that are located inside the Containment are designed to function under the pressure-temperature conditions of both normal operation and that during the design basis event. The pressure-temperature condition used for valve design under normal operation is 14.7 psia and 120°F. The pressure-temperature condition used for valve external design under accident conditions is 15 psig and 300°F.

6.2.4.2.2 Containment Valve Injection Water System

The Containment Valve Injection Water System (NW) is shown in [Figure 6-116](#). It prevents leakage of containment atmosphere past certain gate valves used for containment isolation following a LOCA by injecting seal water at a pressure exceeding containment accident pressure between the two seating surfaces of the flex wedge valves. The system consists of two independent, redundant trains; one supplying gate valves that are powered by the A train diesel and the other supplying gate valves powered by the B train diesel. This separation of trains prevents the possibility of both containment isolation valves not sealing due to a single failure.

Each train consists of a surge chamber which is filled with water and pressurized with nitrogen. One main header exits the chamber and splits into several headers. A solenoid valve is located in the main header before any of the branch headers which will open after 60 second delay on ST signal. Each of the headers supply injection water to containment isolation valves located in the same general location, and close on the same engineered safety signal. A solenoid valve is located in each header which supplies seal water to valves closing on SP signal. These solenoid valves open after a 60 second delay on SP signal. Since a ST signal occurs before a SP signal, the solenoid valve located in the main header will already be injecting water to Containment isolation valves closing on ST signal. This leaves an open path to the headers supplying injection water on SP signal. The delay for the solenoid valves opening is to allow adequate time for the slowest gate valve to close, before water is injected into the valve seat.

Individual solenoid valves are provided for the NI and NS containment isolation valves receiving seal water injection. Following a postulated accident one or more of the NI or NS containment isolation valves may be open. These solenoid valves will receive a signal to open, following a ST signal and once its associated containment isolation valve has closed. If the containment isolation valve subsequently opens, its associated NW solenoid valve closes. Thus after a ST signal, the NW solenoid valve will be open when its containment isolation valve is closed and vice versa.

One header for each train penetrates the Containment. The NW Containment isolation valve on the outside of the Containment opens on ST signal, allowing seal water to be injected to those containment isolation valves located inside the Containment. Inside Containment, solenoid valves isolate the headers that supply injection water to those valves closing on SP signal. The solenoid valves open after a 60 second delay on SP signal.

Makeup water is provided from the Demineralized Water Storage Tank for testing and adding water to the surge chamber during normal plant operation. Assured water is provided from the

essential header of the Nuclear Service Water System. This supply is assured for at least 30 days following a postulated accident. If the water level in the surge chamber drops below the low-low level or if the surge chamber nitrogen pressure drops below the low-low pressure after a ST signal, a solenoid valve in the supply line from the Nuclear Service Water System will automatically open and remains open, assuring makeup to the NW system at a pressure greater than 110% of peak Containment accident pressure.

The NW system is designed to meet all Regulatory and Testing requirements set forth in 10CFR 50, Appendix J and ASME Code Section IX.

Where the potential exists to overpressurize containment penetration piping due to thermal expansion of the fluid trapped in the penetration piping, overpressure protection is provided. Overpressure protection is provided to relieve the pressure buildup caused by the heatup of a trapped volume of incompressible fluid between two positively closing valves (due to containment temperature transient) back into containment where an open relief path exists. This open relief path could be the relief valve on any normally aligned component, or to the Reactor Coolant System (NC) itself.

Each containment penetration is classified as one of the following:

1. Penetration configuration which requires relief devices
2. Penetration configuration which does not require relief devices

The criteria used to classify penetrations are as follows:

1. Penetrations requiring relief protection
 - a. Penetrations consisting of normally closed, metal to metal seat gate or globe valves both inside and outside containment, unless excluded on some other basis. (See Item 2.)
 - b. Same as 1a except one of the valves could be a soft seat globe valve.
 - c. Penetrations consisting of automatic closure gate and/or globe valves (S, T, P, or other safety signal) both inside and outside containment unless excluded on some other basis (see Item 2).
 - d. Penetrations consisting of automatic closure gate valves served by the Containment Valve Injection Water (NW) System (and actuated by S, T, P, or other safety signal) both inside and outside containment.
2. Penetrations for which the overpressure protection feature is considered unnecessary, and thus is not provided include the following:
 - a. Penetrations including a check valve for the inside isolation valve, through which the pressure increase could flow unimpeded to a relief device located elsewhere along the system, or through soft seated valve(s) per Category 2.d.
 - b. Penetrations which, during normal operation, contain fluid at a temperature higher than containment peak accident temperature, and thus whose isolation would not result in thermal expansion following the accident.
 - c. Penetrations which, during normal operation, contain air, steam, or other compressible gas mixtures, and thus whose isolation would not result in gross overpressurization due to thermal expansion following the accident. This feature can also be accomplished by draining water or oil filled lines during normal power operation.
 - d. Penetrations which utilize at least one soft seated valve capable of slight leakage or displacement to accommodate thermal expansion following the accident. For instance,

this feature is attributed to diaphragm, butterfly, and soft seat plug valves. Diaphragm and butterfly valves are prone to leak-by at high differential pressure, while plug valve leakage may be a combination of leak-by, stem leakage, and plug displacement.

- e. Penetrations which utilize a single isolation device either inside or outside containment and thus are incapable of being overpressurized.
- f. Equipment Decontamination (WE) piping judged to be adequate to withstand heatup due to 8015 psia design pressure.

6.2.4.3 Design Evaluation

The Containment structure and the Containment penetrations form an essentially leak-tight barrier. Allowable leak rates from the Containment under design pressure condition are discussed in Section [6.2.1](#). Testing provisions and performance are also discussed in Section [6.2.1](#). Whenever practicable, isolation valves outside Containment which are normally open and required to close on a signal to isolate the Containment are designed to fail closed.

In determining potential bypass leak paths following a LOCA, a liquid seal between two isolation valves is not assumed. Rather, the liquid seal is maintained by the line terminating in a seismic Class 1 tank or normally closed valve. Neither is it assumed that liquid pressure in the "sealed lines" will always equal or exceed containment pressure. No single failure will prevent bypass leakage control including failure of one safety channel of isolation valves to close. Through line leakage is still precluded since no seal is assumed between the two isolation valves. Following isolation valve closure, design valve leakage rates will be sufficiently low to preclude loss of liquid seals.

In order that no single, credible failure or malfunction will result in loss of isolation capability, the closed piping systems, both inside and outside the Containment, and various types of isolation valves provide a double barrier.

The isolation valve and actuators are located as close as practical to the Containment and protected from missile damage. This minimizes the potential hazards that could be experienced by the system.

The integrity of the isolation valve system and connecting lines under the dynamic forces resulting from inadvertent closure under operating conditions is assured, based upon required static and dynamic analysis.

The supports and restraints are applied such that pipe stresses and support reactions are within allowable limits as defined in Section [3.9.2](#).

Two trains of injection water are provided in the Containment Valve Injection Water System. This will prevent the loss of injection water or loss of sealing capability should one train of Containment isolation valves fail to close. Makeup water can be assured from the Nuclear Service Water System for 30 days following the postulated LOCA.

6.2.4.4 Testing and Inspection

Each valve is designed to be tested periodically during normal operation or during shutdown conditions to verify its operability and ability to meet closing requirements. Phase A containment isolation testing of the Containment Purge Ventilation and Hydrogen Purge Systems is not performed since these valves are sealed closed in Modes 1-4.

A program of test inspection requirements for containment isolation is presented in the Technical Specifications. Similar tests are performed prior to operation as discussed in [Chapter 14](#).

Gate valves served by the Containment Valve Injection Water System do not receive a conventional Type C leak rate test using air as a test medium.

The Containment Isolation valves served by the Containment Valve Injection Water System together with the NW systems are tested simultaneously. Containment isolation valves are leak rate tested by injecting seal water from the Containment Valve Injection Water System to the containment isolation valves (Note that one to all Containment Isolation valves can be tested simultaneously so that effect on plant operation and radiation exposure can be minimized. With the containment isolation valve closed, the leakage is determined by measuring flow rate of seal water out of the containment valve injection water surge chamber. The leakage rate from all containment isolation valves is totaled for each train. The total leakage from each train should not exceed Technical Specifications. To assure that seal water is in fact taking place, seal water flow is verified with the containment valve in the open positions and then seal water flow is verified to be reduced when the containment isolation valve is closed. This alternate to Type C leak rate testing with air is allowed by NRC 10CFR 50, Appendix J.

6.2.5 Combustible Gas Control in Containment

Following a design basis accident, hydrogen gas may be generated inside the containment by reactions such as zirconium metal with water, corrosion of materials of construction and radiolysis of aqueous solution in the core and sump. Means are provided to adequately mix the containment atmosphere after a design basis accident to ensure that hydrogen concentration will not be a concern.

The Thermal Electric Hydrogen Recombiners were originally provided as the primary means for controlling hydrogen gas. With the elimination of the design basis LOCA hydrogen release per 10CFR50.44, the requirements for hydrogen control systems to mitigate such a release during a design basis accident were eliminated. The Hydrogen Sample and Purge System is provided to sample the containment atmosphere after the severe accident to assess the degree of core damage and if necessary provide an alternate means of controlling the hydrogen concentration within the containment during such an event.

Mixing of containment atmosphere following a Loss-of-Coolant Accident is provided by the Containment Air Return and Hydrogen Skimmer System described in Section [6.2.1](#).

6.2.5.1 Design Bases

6.2.5.1.1 Electric Hydrogen Recombiners

Historical information in italics below not required to be revised.

The following is the original design bases that applied to the electric hydrogen recombiners: (Technical Specification 3.6.7 was eliminated by Unit 1 License Amendment 219 and Unit 2 License Amendment 214)

- 1. The recombiners are designed to sustain all normal and accident loads including SSE and pressure transients from a design basis loss-of-coolant accident.*
- 2. The recombiners are protected from damage by missiles or jet impingement from broken pipes.*

3. *The recombiners are located in the containment such that they process a flow of containment air containing hydrogen at a concentration which is approximately typical of the average concentration throughout the containment. No dedicated penetrations are necessary for post accident hydrogen processing, hence no isolation provisions are required to meet NUREG-0694.*
4. *The recombiners are located away from high velocity air streams such as could emanate from fan cooler exhaust ports or protected from direct impingement of such high velocity air streams by suitable barriers such as walls or floors.*
5. *The recombiners are designed for a lifetime of forty years, consistent with that of the plant.*
6. *All materials used in the recombiners are selected to be compatible with the environmental conditions inside the reactor containment during normal operation or during accident conditions.*
7. *Process capacity is such that the containment hydrogen concentration will not exceed 4 volume percent based on the NRC TID release model as indicated in NRC Regulatory Guide 1.7, "Control of Combustible Gas Concentrations in Containment Following a Loss-of-Coolant Accident.*
8. *Two redundant electric hydrogen recombiners meet the single failure criterion.*
9. *The electric hydrogen recombiner design provides for periodic inspection and testing.*

6.2.5.1.2 Containment Hydrogen Purge System

The Containment Hydrogen Purge System is designed to be manually initiated. Redundancy is not required for the Containment Hydrogen Purge System, since it is a backup system to the Hydrogen Mitigation System.

6.2.5.2 System Design

After a loss of coolant accident the Containment Air Return and Hydrogen Skimmer System described in Section [6.2.1](#), will mix the containment atmosphere to prevent local concentration of hydrogen from building up.

6.2.5.2.1 Electric Hydrogen Recombiners

Historical information in italics below not required to be revised.

The applicable codes, standards and guides used in the design of the electric hydrogen recombiner are listed in [Table 6-79](#). A typical electric hydrogen recombiner is shown in [Figure 6-118](#). The recombiner units are located in the containment upper compartment such that a flow of containment air containing hydrogen at a concentration which is generally typical of the average concentration throughout the containment is processed.

To meet the requirements for redundancy and independence, two recombiners are provided. Each recombiner is powered from a separate safeguards bus, and is provided with a separate power panel and control panel. There exists no interdependency between this system and the other safeguard systems.

The recombiner consists of an inlet preheater section, a heater-recombination section, and a discharge mixing chamber. The preheater section consists of a shroud placed around the central heater section to take advantage of heat conduction through the walls to preheat the incoming air. The heater section consists of a thermally insulated vertical metal duct with electric

resistance metal sheathed heaters. Four vertically stacked electric heater assemblies are integral to the heater section with each assembly containing individual heating elements. The discharge mixing chamber consists of the mixing chamber and exhaust louvers. The recombiner is provided with an outer enclosure to protect the unit from containment spray water.

The unit is manufactured of corrosion resistant, high temperature material. The electric hydrogen recombiner uses commercial type electric resistance heaters sheathed with Incoloy-800 which is an excellent corrosion resistant material for this service. These recombiner heaters operate at significantly lower power densities than in commercial practice.

Containment atmosphere is circulated through the recombiner by natural circulation. Air is drawn into the recombiner and passes first through the preheater section which serves the dual function of reducing heat losses from the recombiner and of preheating the air. The warmed air passes through an orifice plate and then enters the electric heater section where it is heated to approximately 1150-1400°F, a temperature sufficient to cause hydrogen recombination with the containment oxygen. Tests have verified that the recombination is not a catalytic surface effect associated with the heaters but occurs due to the increased temperature of the process gases. Since the phenomenon is not a catalytic effect, saturating of the unit by fission products will not occur. [Table 6-80](#) gives the recombiner design parameters. Operation of the recombiner is done manually from a control panel located outside the containment. The recombiner power supply panel and control panel are shown schematically in [Figure 6-119](#). The power panel for the recombiner contains an isolation transformer plus an SCR controller to regulate power into the recombiner. This equipment is not exposed to the post-loss-of-coolant accident environment. To control the recombination process, the correct power input which will bring the recombiner above the threshold temperature for recombination will be set on the controller. The correct power required for recombination depends upon containment atmosphere conditions and will be determined when recombiner operation is required. Thermocouples are installed in each hydrogen recombiner to verify heater operation during testing and periodic checkouts of the recombiners. The heater plate temperature measured by the thermocouples is displayed on the Hydrogen Recombiner Heater Temperature Monitor Panels.

Reference [43](#) provides a description of the testing of a full scale prototype electric hydrogen recombiner.

6.2.5.2.2 Containment Hydrogen Purge System

The Containment Hydrogen Purge System is shown in [Figure 6-120](#).

The Containment Hydrogen Purge System consists of a containment hydrogen purge inlet blower, which blows air from the Auxiliary Building through a 4 inch pipe into the upper compartment of the containment. Another 4 in pipe originating in the upper compartment of the containment purges air from the containment to the annulus. A control valve located in the line can be throttled from the control room to the desired purge rate. The purged air from the containment mixes with the air in the annulus. The recirculation ductwork of the Annulus Ventilation System guarantees a mix in the annulus volume prior to discharge, thus reducing the offsite dose. Since the annulus is kept at a negative pressure flow through the purge line can always be assured. The design flow of the hydrogen purge inlet blower is 100scfm. The blower has sufficient developed head to overcome piping losses and containment pressure. Redundancy is not required for the Containment Hydrogen Purge System, since it is a backup system to the redundant hydrogen igniters. The hydrogen purge inlet blower and valves required for operation are manually operated from the control room.

Since the VY lines are closed at all times during power operation, Branch Technical Position CSB 6-4 does not apply to this system.

Equipment design data is presented in [Table 6-81](#). for the Containment Hydrogen Purge System. Piping between containment isolation valves meet ASME III class 2 codes.

6.2.5.3 Design Evaluation

6.2.5.3.1 Deleted Per 2006 Update

6.2.5.3.2 Containment Hydrogen Sample and Purge System

The Containment Hydrogen Purge and Sample System (VY) is used to monitor the hydrogen concentration inside containment after a severe accident involving core damage. Samples of Containment air are obtained via the Containment hydrogen/oxygen sample lines to the Post Accident Containment Sample (PACS) panel located in the auxiliary building.

The containment hydrogen analyzer system continuously monitors the hydrogen concentration inside containment. Maintaining close surveillance of the containment atmosphere hydrogen concentration will provide indication that the hydrogen igniters are operating effectively.

Additional discussion is provided in UFSAR Section [1.8.1.20](#), and UFSAR section [9.3.2](#).

The Hydrogen Purge System will be utilized only in the highly improbable event that the Hydrogen Mitigation System fails to control hydrogen concentration.

The containment hydrogen purge inlet blower is designed to purge at the rate of 100 scfm.

The Containment Hydrogen Sampling and Purge Systems were originally supplied assuming a double failure of the hydrogen recombiners. To protect the Containment Hydrogen Sample and Purge Systems from single failure would indicate a hypothesized triple failure. This requirement would be highly inconsistent with other safety systems and the triple failure is not considered feasible.

6.2.5.3.3 Deleted Per 2006 Update

6.2.5.3.3.1 Deleted Per 2006 Update

6.2.5.3.3.2 Deleted Per 2006 Update

6.2.5.3.3.3 Deleted Per 2006 Update

6.2.5.3.3.4 Deleted Per 2006 Update

6.2.5.3.3.5 Deleted Per 2006 Update

6.2.5.4 Tests and Inspections

6.2.5.4.1 Electric Hydrogen Recombiners

Historical information in italics below not required to be revised.

The electric hydrogen recombiners have undergone extensive testing in the Westinghouse development program. These tests encompassed the initial analytical studies, laboratory proof-of-principal tests and full scale prototype testing. The full scale prototype tests included the effects of:

1. *Varying hydrogen concentrations*
2. *Alkaline spray atmosphere*
3. *Steam effects*
4. *Convection currents*
5. *Seismic*

A detailed discussion of these tests is given in Reference [43](#).

Preoperational tests and inspections will be performed to assure the capability of the recombiner to perform its function. Testing will be performed to verify operation of the control system and to verify functional performance of the heaters to the required temperature level.

6.2.5.4.2 Containment Hydrogen and Purge System

The Containment Hydrogen Purge System is preoperationally tested to verify the capability to discharge to the annulus.

Preoperational testing of the Containment Hydrogen Sampling System is described in UFSAR section [1.8.1.20](#) and [9.3.2.4](#).

6.2.5.5 Instrumentation Requirements

Historical information in italics below not required to be revised.

The recombiners do not require any instrumentation inside the containment for proper operation. Thermocouples are provided, but are not necessary to assure proper operation of the recombiners. The proper amount of air flow through the recombiner is fixed by the orifice plate built into the recombiner.

The Containment Hydrogen Sample and Purge Systems are manually operated. Flow indication is provided where necessary.

6.2.5.6 Materials

6.2.5.6.1 Electric Recombiner

Historical information in italics below not required to be revised.

The materials of construction for the electric recombiner are selected for their compatibility with the post-LOCA environment. The major structural components are manufactured from 300-Series stainless steel. Incoloy-800 is used for the heater sheaths and Inconel-600 for other parts such as the heat duct, which operates at high temperature.

There are no radiolytic or pyrolytic decomposition products from these materials.

6.2.5.6.2 Containment Hydrogen Sample and Purge System

All Piping and valves in the Containment Hydrogen Sample and Purge System are made of carbon steel.

6.2.5.7 Supplemental Hydrogen Control System/Hydrogen Mitigation System/Hydrogen Ignition System

The licensing requirements, relative to the provisions for hydrogen control, prescribed in 10CFR 50.44 have evolved from numerous deliberations among the Nuclear Regulatory Commission (NRC), the Advisory Committee on Reactor Safeguards (ACRS), the NRC staff, and utilities. The NRC's requirement for ice condenser containments is that a supplemental hydrogen control system be provided so that the consequences of the hydrogen release generated during the more probable degraded core accident sequences do not involve a breach of containment nor adversely affect the functioning of essential equipment.

As part of research activities, Duke Power in cooperation with Tennessee Valley Authority (TVA) and American Electric Power (AEP) investigated alternative measures of hydrogen control. As a result of these studies, a hydrogen ignition system (HIS) has been installed in Catawba Units 1 & 2 to provide adequate safety margins in controlling the consequences of degraded core accidents.

SYSTEM DESCRIPTION

The HIS is a system of thermal igniters and ancillary equipment installed within the containment of Catawba Units 1 & 2. The igniters are designed to ensure a controlled burning of hydrogen in the unlikely event that excessive quantities of hydrogen are generated as a result of a postulated degraded core accident. The HIS is designed to promote the combustion of hydrogen in a manner such that containment integrity is maintained.

Deleted Per 2006 Update.

The HIS utilizes hydrogen igniters manufactured by Tayco Engineering, Inc. The igniter is powered directly from a 130VAC source. Each igniter assembly consists of a 1/8-inch thick steel enclosure which contains all electrical connections and partially encloses the igniter. This enclosure meets National Electrical Manufacturers Association (NEMA) Type 4 specifications for watertight integrity under various environmental conditions including exposure to water jets. The sealed enclosure incorporates a spray shield to reduce water impingement on the glow plug from above. In addition, the hydrogen igniter system is designed to meet seismic Category I requirements.

Igniter Power Supply

The igniters in the HIS are equally divided into two redundant groups, with separate circuits and circuit breakers per group. The number of igniters on each circuit can range from 1 to 6. Igniters located at elevations near the flood level (those in the pipe chase area) are on dedicated circuits. Each group has independent and separate control power and igniter locations to ensure adequate coverage in the event of a single failure. The system is manually actuated from the auxiliary building.

The igniters are powered from the Class 1E AC power system that has normal and alternate power supply from offsite sources. In the event of a loss of offsite power, the igniters would be powered from the emergency diesel generators. Group A igniters receive power from the train A diesels and Group B igniters from the train B diesels. A train igniters can also be manually aligned to be powered from the SSF Diesel Generator, via 1E MCC EMXS. This alignment is controlled by operations procedures during certain scenarios as required to meet commitments made in response to Generic Safety Issue GSI-189. This alternate alignment is not required for operability of the EHM system.

Igniter Coverage

The hydrogen mitigation system consists of 70 igniter assemblies distributed throughout the upper, lower, dead-ended, and ice condenser compartments. Following the onset of a degraded core accident, any hydrogen that is produced would be released into lower containment. There are forty six (46) igniters installed in lower containment locations. Any hydrogen not burned in lower containment would be carried up through the ice condenser and into its upper plenum. Because steam would be removed from the mixture as it passes through the ice bed, thus concentrating the hydrogen, mixtures that were non-flammable in the lower containment would tend to become flammable in the ice condenser upper plenum. Controlled burning in the upper plenum is preferable to burning in the upper containment because the upper plenum burns involve smaller quantities of hydrogen per burn. Duke has taken advantage of the beneficial characteristics of combustion in the upper plenum and has distributed twelve (12) igniters around it. These igniters are located in a staggered fashion alternately between the crane wall and the containment shell wall sides of the upper plenum at almost equally spaced aximuthal locations. Twelve (12) igniters have been installed to handle any accumulation of hydrogen in the upper containment.

System Actuation

The EHM system will be energized by procedure when a LOCA inside containment has been verified or when containment pressure is > 3.0 psig.

Surveillance Testing

To ensure that the hydrogen mitigation system will function as intended, a surveillance testing program has been established. On a quarterly basis, the igniter system will be energized and current and voltage readings of the igniter circuits will be taken at the emergency lighting panelboards. If the power consumption does not compare favorably with that measured during previous testing, the igniters on the affected circuit will be individually inspected to ensure their operability. In addition to power consumption measurements, the igniter temperatures will be measured at specified intervals.

6.2.6 Containment Leakage Testing

Primary containment leakage tests and containment isolation system valve operability tests will be performed periodically to verify that leakage from the containment is maintained within acceptable limits set forth in the Containment Leak Rate Testing Program. The types of leakage tests are as follows:

1. Type A Test

A test to verify the leakage integrity of the containment structure. To this end, a measurement will be taken of the containment system overall integrated leakage rate under conditions representing DBA containment pressure and system alignments.

2. Type B Test

A pneumatic test intended to detect or measure leakage across pressure-retaining or leakage-limiting boundaries other than valves, such as; (a) containment penetrations whose design incorporates resilient seals, gaskets, sealant compounds, expansion bellows, or flexible seal assemblies; (b) seals, including door operating mechanism penetrations, which are part of primary containment; and (c) doors and hatches with resilient seals or gaskets except for seal welded doors.

3. Type C Test

A pneumatic test to measure containment isolation valve leakage rates.

These tests are performed in compliance with the requirements of 10CFR 50.54(o) and 10CFR 50, Appendix J, Option B, as modified by approved exemptions. The program shall be in accordance with the guidelines contained in NEI 94-01, "Industry Guideline for Implementing Performance-Based Option of 10CFR Part 50, Appendix J" Revision 3-A, dated July 2012, and the conditions and limitations specified in NEI 94-01 Revision 2-A, dated October 2008. The details of this testing are located in the Containment Leak Rate Testing Program.

6.2.6.1 Containment Integrated Leak Rate Test

The maximum allowable containment leakage rate for the Catawba Nuclear Station is 0.30 weight percent per day as specified in the Containment Leak Rate Testing Program. During the test the Containment is isolated and pressurized in accordance with Appendix J of 10CFR 50 and the Technical Specification requirements. When test pressure is reached, the Containment is isolated from its pressure source and the following parameters are recorded at periodic intervals:

1. Containment absolute pressure
2. Dry bulb temperatures
3. Dew Point Temperature or Relative Humidity
4. Absolute Ambient Atmospheric Pressure
5. Liquid Levels (that can affect containment free air volume)
6. Superimposed Flow (during the leak rate verification test)

During the test, ventilation inside the Containment is operated as necessary to enhance an even air temperature distribution. The test data is processed at periodic intervals during the test to determine test status and leakage conditions. If it appears that the leakage is excessive, the pressure plateau is either maintained on the test or aborted to perform repairs. After a prescribed time period and assurance of leak test rate, the pressure is slowly bled off to verify the leak rate measurement. This is accomplished by precise measurement of a flow which causes a change in the weight of air in the Containment that is in the same order of magnitude as the allowable leakage rate. Test Methods and Formulas used in computing the integrated leak rate are based on the formulas found in ANSI/ANS – 56.8 – 2002, "Containment System Leakage Testing Requirements" and NEI 94-01, "Industry Guideline for Implementing Performance-Based Option of 10CFR Part 50, Appendix J" Revision 3-A, dated July 2012, with the applicable conditions and limitations specified in NEI 94-01 Revision 2-A, dated October 2008. Acceptance criteria are in the Technical Specifications.

Deleted paragraph in 2017 update.

6.2.6.2 Containment Penetration Leakage Rate Test

Type B leakage rate tests are performed on all electrical, equipment, and personnel hatch penetrations in accordance with 10CFR 50 Appendix J (Option B). The test pressure, test frequencies and acceptance criteria are specified in the Containment Leak Rate Testing Program. Leakage rates are determined by pressure loss or makeup flow methods.

[Table 6-77](#) provides a list of all containment penetrations.

All bellows on mechanical penetrations are subject to a local structural integrity test by pressurizing the volume between the two ply bellows to 3-5 psig to verify no detectable leakage. Otherwise, the assembly must be tested with the containment side of the bellows assembly

pressurized to conditions representing DBA containment pressure. The bellows test frequency and other acceptance criteria are specified in the Containment Leak Rate Testing Program.

During the performance of each Type A test, the test connections on all bellows are uncapped. This assures that the volume between the two ply bellows is vented to the annulus during performance of this test. At the completion of this test, all of the test connections are capped except for the main steam and feedwater penetration outer bellows test connections which remain uncapped and vented to the annulus.

The testing program for bellows on mechanical penetrations is the same as was previously reviewed and approved by the NRC for McGuire (NUREG-0422, Supplement 1, May 1978).

6.2.6.3 Containment Isolation Valve Leakage Rate Test

Type C leakage rate tests are conducted for each penetration identified in [Table 6-74](#) as a potential bypass leakage path in accordance with 10CFR50 Appendix J (Option B). Each valve or set of valves subject to Type C testing is tested by pressurizing with air or nitrogen on one side of the valve while the other side is opened to atmospheric pressure. Leakage rates are determined by pressure loss or makeup flow methods. Test pressure, test frequency and acceptance criteria are specified in the Containment Leak Rate Testing Program.

6.2.6.4 Scheduling and Reporting of Periodic Tests

Periodic Type A, B and C leakage rate tests are performed, and the results reported as specified in 10CFR50, Appendix J, NEI 94-01 Rev 2-A/3-A, and the Containment Leak Rate Testing Program.

6.2.6.5 Special Testing Requirements

Inleakage from the Reactor Building is checked preoperationally and periodically as required by the Technical Specifications. A discussion of the Annulus Ventilation System is provided in Section [6.2.3](#).

The effectiveness of fluid filled systems is verified by use of the systems during normal operation or periodic testing to show operability and the ability to develop required pressures.

Any major modification or replacement of a component which is part of the primary reactor containment, performed after the preoperational leakage rate test, will be followed by a Type A, B or C test as required by NEI 94-01 Rev 2-A/3-A.

6.2.7 References

1. "Ice Condenser Containment Pressure Transient Analysis Method," *WCAP-8077* (Proprietary) and *WCAP-8078* (Non-Proprietary) March, 1973.
2. Henry, R. E., and Fauske, H. K., "The Two-Phase Critical Flow of One-Component Mixtures in Nozzles, Orifices and Short Tubes," *Journal of Heat Transfer*, May, 1971, pp. 179-187.
3. Isbin, H. S., Fauske, H. K., Petrick, M., Robbins, C. H., Smith, R. W., Szawlequcz, S. A., and Zaloudek, F. R., *Proc. of the Third Intl. Conf. for the Peaceful Uses of Atomic Energy, Geneva, Switzerland, Aug.-Sept., 1964*.
4. Carofano, G. C., and McManus, H. N., "An Analytical and Experimental Study of the Flow of Air-Water and Steam-Water Mixtures In a Coverging-Diverging Nozzle," *Progress in Heat & Mass Transfer*, Volume 2, pp. 395-417.

5. F. J. Moody, "Maximum Flow Rate of Single Component, Two-Phase Mixture," *ASME publication, Paper No. 64-HT-35*.
6. F. R. Zaloudek, "Steam-Water Critical Flow From High Pressure Systems," *Interim Report HW-68936*, Hanford Works, 1964.
7. Bordelon, F.M., Massie, H.W., Jr., and Zordan, T.A., " Westinghouse Emergency Core Cooling System Evaluation Model - Summary", *WCAP-8339*, June, 1974.
8. R. E. Henry, "A Study of One-and Two-Component, Two-Phase Critical Flows at Low Qualities," *ANL-7430*.
9. R. E. Henry, "An Experimental Study of Low-Quality, Steam-Water Critical Flow at Moderate Pressures," *ANL-7740*.
10. F. W. Kramer, "FLASH - A Digital Computer Code for the Loss of Coolant Accident Analyses," *WCAP-1678*, January, 1961.
11. F. R. Zaloudek, "The Critical Flow of Hot Water Through Short Tubes," *HW-77594*, Hanford Works, 1963.
12. Dittus, F. W., and L. M. K. Boelter, University of California (Berkeley), *Publs. Eng.*, 2, 433 (1930).
13. Jens, W. H., and P. A. Lottes, "Analysis of Heat Transfer, Burnout, Pressure Drop, and Density Data for High Pressure Water," USAEC Report *ANL-4627*, 1951.
14. Bergles, A. E., and W. M. Rohsenow, "The Determination of Forced-Convection Surface-Boiling Heat Transfer," *ASME Paper No. 63-HT-22*, 1963.
15. Macbeth, R. V., "Burnout Analysis, Pt. 2, The Basis Burn-out Curve", U. K. Report *AEEW-R 167*, Winfrith (1963). Also Pt. 3, "The Low-Velocity Burnout Regimes," *AEEW-R 222* (1963); Pt. 4, "Application of Local Conditions Hypothesis to World Data for Uniformly Heated Round Tubes and Rectangular Channels", *AEEW-R 267* (1963).
16. D. M. McEligot, L. W. Ormand and H. C. Perkins, Jr., "Internal Low Reynolds - Number Turbulent and Transitional Gas Flow with Heat Transfer", *Journal of Heat Transfer*, 88, 239-2465 (May 1966).
17. W. H. McAdam, *Heat Transmission*, McGraw-Hill 3rd edition, 1954, p. 172.
18. Dougall, R. S., and W. M. Rohsenow, Film Boiling on the Inside of Vertical Tubes with Upward Flow of Fluid at Low Quantities, *MIT Report 9079-26*.
19. Cunningham, W. P., and H. C. Yeh, "Experiments and Void Correlation for PWR Small-Break LOCA Conditions", *Transactions of American Nuclear Society*, Vol. 17, Nov. 1973, pp. 369-370.
20. Grim, N. P., and Colenbrander, H. G. C., "Long Term Ice Condenser Containment Code - LOTIC Code," *WCAP-8354* (Proprietary) and *WCAP-8355* (Non-Proprietary), July, 1974.
21. Idel'Chik, I. E., *Handbook of Hydraulic Resistance*, Translated from Russian, Published by the USAEC, 1966.
22. "Final Report Ice Condenser Full-Scale Section Tests at the Waltz Mill Facility", *WCAP-8282*, February, 1974.
23. Wallace, G. B., et al., "Two Phase Flow and Boiling Heat Transfer," *Quarterly Progress Report (July-September, 1974) NYD-3114-4*.

24. Hsieh, T. and Raymund, M., "Long Term Ice Condenser Containment Code - LOTIC Code," *WCAP-8354, Supplement 1 (Proprietary)* and *WCAP-8355, Supplement 1 (Non-Proprietary)*, June 1975.
 25. Letter from T. M. Novak (NRC) to H. B. Tucker (DPC) dated October 14, 1982. Enclosure: Safety Evaluation Report On Response To I.E. Bulletin 80-04.
 26. "MARVEL-A Digital Computer Code for Transient Analyses of a Multi-loop PWR System", *WCAP-8843, NS-CE-1627, 12/8/77*.
 27. C. Eicheldinger, Letter of 10/27/76, No. NS-CE-1250.
 28. C. Eicheldinger, Letter of 6/14/77, No. NS-CE-1453.
 29. C. Eicheldinger, Letter of 12/7/77, No. NS-CE-1626.
 30. John F. Stolz, Letter of 5/3/78, "Evaluation of Proposed Supplement to WCAP-8354 (LOTIC-3).
 31. Land, R. E., "Mass and Energy Release Following a Steam Line Rupture," *WCAP-8822, September 1976*.
 32. Hsieh, T. and Liparulo, N. J., "Westinghouse Long Term Ice Condenser Containment Code LOTIC-3 Code", *WCAP 8354 Supplement 2(Proprietary)*, February, 1979.
 33. "Westinghouse LOCA Mass and Energy Release Model for Containment Design - March 1979 Version", *WCAP - 10325-P-A, May 5, 1983 (Proprietary)*, *WCAP-10326-A, May 5, 1983 (Non-Proprietary)*.
 34. Deleted Per 2001 Update.
 35. "Westinghouse ECCS Evaluation Model-1981 Version", *WCAP 9220-P-A*, February, 1982.
 36. Shepard, R. M., Massie, H. W., Mark, R. H., and Docherty, P. J., "Westinghouse Mass and Energy Release Data for Containment Design", *WCAP-8264-P-A (Proprietary)* and *WCAP-8312-A, Revision 1, June, 1975 (Non-Proprietary)*.
 37. Alden Research Laboratory, "Assessment of Flow Characteristics within Reactor Building Using a Scale Model for McGuire Nuclear Station," May 1978.
 38. Deleted Per 2006 Update.
 39. Deleted Per 2006 Update.
 40. Deleted Per 2006 Update.
 41. Deleted Per 2006 Update.
 42. Deleted Per 2006 Update.
- Historical information below in in italics not required to be revised.
43. *J. F. Wilson "Electric Hydrogen Recombiner for PWR Containments", WCAP-7709, (proprietary) and WCAP-7820, supplements 1, 2, 3, 4 and 5 (Non-proprietary).*
 44. W Letter, *DAP-92-034, DCP-92-026* to DPC, June 9, 1992.
 45. Duke Power Company, McGuire Nuclear Station, Catawba Nuclear Station, Mass and Energy Release and Containment Response Methodology, *DPC-NE-3004-PA*, November 1997.
 46. RELAP5/MOD3 Code Manual, Volumes 1 to 5, *NUREG/CR-5535, EGG-2596 (Draft)*, June 1990.

47. GOTHIC Containment Analysis Package, Version 4.0, RP3048-1, Prepared for Electric Power Reserach Institute, Numerical Applications, Inc., September 1993
48. ANSI/ANS-56.4-1983, American National Standard Pressure and Temperature Transient Analysis for Light Water Reactor Containments, American Nuclear Society, December 23, 1983.
49. EPRI, "RETRAN-02: A Program for Transient Thermal-Hydraulic Analysis of Complex Fluid Flow Systems," EPRI NP-1850-CCM, Revision 6.1, June, 2007.

HISTORICAL INFORMATION IN ITALICS BELOW NOT REQUIRED TO BE REVISED

50. *Bordelon, F.M., et al, "SATAN-IV Program: Comprehensive Space Time Analysis of Loss of Coolant," WCAP-8302, June 1974.*
51. "Code Qualification Document for Best Estimate LOCA Analysis," WCAP-12945-P-A (Proprietary), Volume I, Revision 2, and Volumes II-V, Revision 1, and WCAP-14747 (Non-Proprietary), Westinghouse Electric Company, March 1998.
52. W Letter, WOG-ICMG-99-011 to Ice Condenser Minigroup Representative, May 7, 1999
53. Letter to the U.S. Nuclear Regulatory Commission from T.P. Harrall dated October 13, 2008, titled "Duke Energy Carolinas, LLC (Duke) Oconee Nuclear Station, Units 1, 2 & 3, Docket Nos. 50-269, 50-270, 50-287, McGuire Nuclear Station, Units 1 & 2, Docket Nos. 50-369, 50-370, Catawba Nuclear Station, Units 1 & 2, Docket Nos. 50-413, 50-414, Generic Letter 2008-01, 9-Month Response.
54. R.M. Shepard, et al, SATAN-V Program: Westinghouse Mass and Energy Release Data for Containment Design, WCAP-8264-P-A-R1, August 1975

THIS IS THE LAST PAGE OF THE TEXT SECTION 6.2.

THIS PAGE LEFT BLANK INTENTIONALLY.

6.3 Emergency Core Cooling System

6.3.1 Design Bases

The Emergency Core Cooling System is designed to cool the reactor core and provide shutdown capability following initiation of the following accident conditions:

1. Loss of Coolant Accident (LOCA) including a pipe break or a spurious relief or safety valve opening in the RCS which would result in a discharge larger than that which could be made up by the normal make-up system.
2. Rupture of a control rod drive mechanism causing a rod cluster control assembly ejection accident.
3. Steam or feedwater system break accident including a pipe break or a spurious relief or safety valve opening in the secondary steam system which would result in an uncontrolled steam release or a loss of feedwater.
4. A steam generator tube rupture.

The primary function of the ECCS is to remove the stored and fission product decay heat from the reactor core during accident conditions.

The ECCS provides shutdown capability for the accidents above by means of boron injection. It is designed to tolerate a single active failure (short term) or single active or passive failure (long term). It can meet its minimum required performance level with onsite or offsite electrical power and under simultaneous Safe Shutdown Earthquake loading.

The ECCS consists of the centrifugal charging, safety injection and residual heat removal pumps, low pressure cold leg injection accumulators, RHR heat exchangers, and the refueling water storage tank, along with the associated piping, valves, instrumentation and other related equipment.

See Section [1.3.1](#) for comparison of the Catawba ECCS with similar designs at other facilities.

The design bases for selecting the functional requirements of the ECCS are derived from Appendix K limits for Fuel Cladding Temperature following any of the above accidents delineated in 10CFR 50.46. The subsystem functional parameters are selected to integrate so that the Appendix K requirements are met over the range of anticipated accidents and single failure assumptions.

Reliability of the ECCS has been considered in selection of the functional requirements, selections of the particular components and location of components and connected piping. Redundant components are provided where the loss of one component would impair reliability. Valves are provided in series where isolation is desired and in parallel when flow paths are to be established for ECCS performance. Redundant sources of the ECCS actuation signal are available so that the proper and timely operation of the ECCS will not be inhibited. Sufficient instrumentation is available so that a failure of an instrument will not impair readiness of the system. The active components of the ECCS are powered from separate buses which are energized from offsite power supplies.

In addition, redundant sources of auxiliary onsite power are available through the use of the emergency diesel generators to assure adequate power for all ECCS requirements. Each diesel is capable of driving all pumps, valves and necessary instruments associated with one train of the ECCS.

Spurious movement of a motor operated valve due to the actuation of its positioning device coincident with a LOCA has been analyzed and found not credible for consideration.

The elevated temperature of the sump solution during recirculation is well within the design temperature of all ECCS components. In addition, consideration has been given to the potential for corrosion of various types of metals exposed to the fluid conditions prevalent immediately after the accident or during long term recirculation operations.

Environmental testing of ECCS equipment inside the containment, which is required to operate following a loss of coolant accident, is discussed in Section [3.11](#).

6.3.2 System Design

The Emergency Core Cooling System (ECCS) components are designed such that a minimum of three low pressure cold leg accumulators, one charging pump, one safety injection pump, and one residual heat removal pump together with their associated valves and piping will assure adequate core cooling in the event of a design basis loss of coolant accident. The redundant onsite emergency diesels assure adequate emergency power to all electrically operated components in the event that a loss of offsite power occurs simultaneously with a loss of coolant accident, assuming a single failure in the emergency power system such as the failure of one diesel to start.

6.3.2.1 Schematic Piping and Instrumentation Diagrams

Flow diagrams of the ECCS are shown in [Figure 6-128](#) through [Figure 6-132](#).

Process flow diagram [Figure 6-136](#) (sheets 1 through 4) shows the flow rate thru the ECCS under injection, cold-leg recirculation, and hot-leg recirculation operating modes.

A complete listing of ECCS valve interlocks is presented in [Table 6-89](#).

A description of the automatic features and interlocks used in different modes of system operation are listed below.

1. The safety injection ("S") signal is received by the following equipment in the ECCS to initiate cold leg injection (for a complete listing of pumps and valves that receive an "S" signal see [Table 3-103](#) and [Table 3-104](#)):
 - a. Centrifugal charging pumps (CCP's) start.
 - b. Valves in the CCP's suction header isolate the volume control tank and align to the refueling storage tank.
 - c. CCP's discharge aligned to cold leg injection lines.
 - d. Normal charging path valves close.
 - e. The safety injection pumps start.
 - f. The residual heat removal pumps start.
 - g. Refueling water storage tank recirculation is terminated and the makeup line to the spent fuel pool is isolated.
2. Automatic switchover of the residual heat removal pumps (RHRP's) from injection mode to recirculation involves the following.
 - a. The suction valves from the sump open when 2 of 4 low level transmitters indicate a low level in the RWST in conjunction with an "S" signal.

- b. The isolation valves from the refueling water storage tank close after the sump valves are open.
3. Manual switchover of the suction of the safety injection pumps and the centrifugal charging pumps requires the following interlocks be satisfied.
 - a. The containment recirculation sump isolation valve is open.
 - b. The RHRP's suction lines must be isolated from the reactor coolant system.
 - c. The safety injection pumps miniflow line must be closed.
4. The manual switchover of the containment spray pumps require the following interlocks be satisfied.
 - a. The containment recirculation sump isolation valve is open.
 - b. The line from the refueling water storage tank to the pump suction line is closed.

6.3.2.2 Equipment and Component Descriptions

The component design and operating conditions are specified as the most severe conditions to which each respective component is exposed during either normal plant operation, or during operation of the ECCS. For each component these conditions are considered in relation to the code to which it is designed. By designing the components in accordance with applicable codes, and with due consideration for the design and operating conditions, the fundamental assurance of structural integrity of the ECCS components is maintained. Components of the ECCS are designed to withstand the appropriate seismic loadings in accordance with their safety class as given in [Table 3-4](#).

Pertinent design and operating parameters for the components of the ECCS are given in [Table 6-87](#). The codes and standards to which the individual components of the ECCS are designed are listed in [Table 3-3](#).

The operability of two independent ECCS subsystems ensures that sufficient emergency core cooling capability will be available in the event of a LOCA assuming the loss of one subsystem through any single failure consideration. Either subsystem operating in conjunction with the accumulators is capable of supplying sufficient core cooling to limit the peak cladding temperatures within acceptable limits for all postulated break sizes. In addition, each ECCS subsystem provides long-term core cooling capability in the recirculation mode during the accident recovery period.

All ECCS equipment has been designed to perform its system operating function for at least 1 year without any periodic maintenance. The two independent ECCS subsystems/or trains allow maintenance to be performed on any pump, if it is necessary, during long-term operation.

Accumulator gas pressure is monitored by indicators and alarms. The operator can take action when required to maintain plant operation within the requirements of the technical specification covering accumulator operability.

ECCS pumps are seismically qualified by a combination of analysis and tests including structural and operability analysis. Each pump is tested in the vendor's (Westinghouse) shop to verify hydraulic and mechanical performance. Performance is again checked at the plant site during preoperational system checks and quarterly per ASME Code. Pump design is specified, with strong consideration given to shaft critical speed, bearing, and seal design. Thermal transient and 100-hour endurance tests have been completed on the centrifugal charging and the safety injection pumps. Addition rotor dynamics tests have been performed on the

centrifugal charging pumps which are used in the highest speed applications. A thermal transient analysis has been performed on the RHR pump; this analysis is supported by the vendor's test on a similar design.

Endurance and leak determination testing has been completed on the mechanical seals by the seal supplier. The testing included various temperature, pressure, radiation, and boric acid concentration levels. The conditions were all substantially elevated over those expected during normal or post-accident conditions.

The reliability program extends to the procurement of the ECCS components so that only designs which have been proven by past use in similar applications are acceptable for ECCS application. For example, the equipment specification for the ECCS pumps (safety injection, centrifugal charging, and residual heat removal pumps) required them to be capable of performing their long-term cooling function for 1 year. The same type of pumps have been used extensively in other operating plants. The performance and capability of pumps of the same type has been adequately demonstrated by their reliable and recurrent use during normal power and cooldown operation at other Westinghouse plants such as Zion, D.C. Cook, Trojan, and Farley. Reliability tests and inspections (see Section [6.3.4.2](#)) further confirm their long-term operability. Nevertheless, design provisions would allow some maintenance on ECCS pumps, if necessary, during long-term operations.

Proper initial fill and venting of the ECCS ensures that loss of NPSH, gas binding, pump cavitation, or water hammer will not occur in ECCS lines if injection flow is initiated. High point vents in the ECCS lines are provided for proper venting of lines and pumps. The accessible portions of the ECCS susceptible to gas accumulation are vented monthly per Technical Specification surveillance requirement 3.5.2.3. While these accessible portions do not represent all the highest points of the system, this practice has been reviewed and determined to be an acceptable means to ensure operability. Alternate means of ensuring the system is sufficiently filled to ensure operability may be used, for example, ultra sonic testing or high point sight glass observations, etc. The ECCS was evaluated for gas accumulation for Generic Letter 2008-01. The Generic Letter 2008-01 evaluation concluded that system procedures and design are adequate to maintain the ECCS sufficiently full of water to ensure operability.

The major mechanical components of the ECCS follow.

Cold Leg Injection Accumulators

The accumulators are pressure vessels partially filled with borated water and pressurized with nitrogen gas. During normal operation each accumulator is isolated from the Reactor Coolant System (RCS) by two check valves in series.

Should the RCS pressure fall below the accumulator pressure, the check valves open and borated water is forced into the RCS. Each accumulator is attached to one of the cold legs of the RCS. Mechanical operation of the swing-disc check valves is the only action required to open the injection path from the accumulators to the core via the cold leg.

Two cold leg accumulators serve as safety related sources of nitrogen which can be aligned to respective pressurizer power-operated relief valves' pneumatic actuators by the operator from the control room.

Connections are provided for remotely adjusting the level and boron concentration of the borated water in the accumulator during normal plant operation when required. Accumulator water level may be adjusted either by draining to the FWST through the NI test headers or draining through the Nuclear Sampling lines to the liquid radwaste system, or by pumping

borated water from the refueling water storage tank to the accumulator. Samples of the solution in the accumulators are taken periodically for checks of boron concentration.

Accumulator pressure is provided by a supply of nitrogen gas, and can be adjusted as required during normal plant operation; however, the accumulators are normally isolated from this nitrogen supply. Gas relief valves on the accumulators protect them from pressures in excess of design pressure.

The accumulators are located within the containment but outside of the secondary shield wall which protects them from missiles.

Accumulator gas pressure is monitored by indicators and alarms. The operator can take action when required to maintain plant operation within the requirements of the technical specification covering accumulator operability.

Residual Heat Removal Pumps

The residual heat removal pumps are started automatically on receipt of an "S" signal. The residual heat removal pumps deliver water to the RCS from the refueling water storage tank during the injection phase and from the containment sump during the recirculation phase. Each residual heat removal pump is a single stage vertical centrifugal pump.

A minimum flow bypass line is provided for the pumps to recirculate and return the pump discharge fluid to the pump suction should these pumps be started with their normal flow paths blocked. Once flow is established to the RCS, the bypass line is automatically closed. This line prevents deadheading of the pumps and permits pump testing during normal operation.

The residual heat removal pumps are discussed further in [Chapter 5](#). A pump performance curve is given in [Figure 6-133](#).

Centrifugal Charging Pumps

The charging pumps are started automatically on receipt of an "S" signal and are automatically aligned to take suction from the refueling water storage tank during injection. During recirculation, suction is provided from the residual heat removal pump and heat exchangers.

These pumps deliver flow to the RCS at the prevailing RCS pressure. Each centrifugal charging pump is a multistage diffuser design, barrel-type casing with vertical suction and discharge nozzles. A minimum flow bypass line is provided on each pump. An "S" signal closes valves to isolate the normal charging line and volume control tank and opens the charging pump/refueling water storage tank suction valves to align the high head portion of the ECCS for injection.

The generation of the "S" signal does not automatically close the isolation valves on the minimum flow bypass line.

The pump deadheading problem is a valid concern for the charging pumps as operating these pumps at or above their shutoff head would lead to failure of the pumps due to overheating. The miniflow path for the centrifugal charging pumps is opened and closed by the operator according to specific guidelines in the various emergency procedures.

Duke has provided the NRC with the Westinghouse generic analysis which concludes that non-automatic isolation of the mini-flow line is acceptable. It found that negligible flow degradation resulted provided the line is isolated in accordance with the emergency operating procedures. This analysis was transmitted in H. B. Tucker's letter of 10/26/83 to H. R. Denton.

The charging pumps may be tested during power operation in a normal charging alignment.

A pump performance curve for the centrifugal charging pump is presented in [Figure 6-134](#).

Safety Injection Pumps

The safety injection pumps are started automatically on receipt of an "S" signal. These pumps deliver water to the RCS from the refueling water storage tank during the injection phase and from the containment sump via the residual heat removal pumps and heat exchangers during the recirculation phase. Each high head safety injection pump is driven directly by an induction motor.

A minimum flow bypass line is provided on each pump discharge to recirculate flow to the refueling water storage tank in the event that the pumps are started with the normal flow paths blocked. This line also permits pump testing during normal plant operation.

The SI pump common miniflow line, while non-nuclear safety, is protected from high and medium energy line breaks, tornadoes, and is located in a seismic category 1 building. Should the line rupture, redundant safety related, Class 1E powered isolation valves are located upstream and can be closed by the operator to isolate the failure.

The line itself is only used during inservice testing of the SI pumps and during the initial injection phase following receipt of an SI signal. The line is isolated during the switchover from injection to cold leg recirculation. Two parallel valves in series with a third, downstream in a common header, are provided in this line. These valves are manually closed from the control room as part of the ECCS realignment from the injection to the recirculation mode. A pump performance curve is shown in [Figure 6-135](#).

Residual Heat Exchangers

The residual heat exchangers are conventional shell and U-tube type units. During normal cooldown operation, the residual heat removal pumps recirculate reactor coolant through the tube side while component cooling water flows through the shell side. During emergency core cooling recirculation operation, water from the containment sump flows through the tube side. The tubes are seal welded to the tubesheet.

A further discussion of the residual heat exchangers is found in Section [5.4.7](#).

Valves

Design parameters for valves used in the ECCS are given in [Table 6-87](#), [Table 6-88](#), [Table 6-89](#), and [Table 6-90](#).

Design features employed to minimize valve leakage include:

1. Where possible, packless valves are used.
2. Other valves which are normally open, except check valves and those which perform a control function, are provided with backseats to limit stem leakage.
3. Normally closed globe valves are installed with recirculation fluid pressure under the seat to prevent stem leakage of recirculated (radioactive) water.
4. Relief valves are enclosed, i.e., they are provided with a closed bonnet.

Motor-Operated Valves

The seating design of all motor-operated valves is a flexible wedge design. This design releases the mechanical holding force during the first increment of travel so that the motor operator works only against the frictional component of the hydraulic unbalance on the disc and the packing box friction. The disc is guided through its full travel to prevent chattering and to provide ease of gate movement. The seating surfaces are hard faced to prevent galling and to reduce wear.

Where a gasket is employed for the body to bonnet joint, it is either a fully trapped, controlled compression, spiral wound gasket with provisions for seal welding, or it is of the pressure seal design with provisions for seal welding. The valve stuffing boxes are designed with a lantern ring leakoff connection to minimize external packing leaks.

Manual Globes, Gates and Check Valves

Gate valves employ a wedge design and are straight through. The wedge is either split or solid. All gate valves have backseat and outside screw and yoke.

Globe valves, "T" and "Y" style are full ported with outside screw and yoke construction.

Check valves are spring loaded lift piston types for sizes 2 inches and smaller, swing type for size 2-1/2 inches and larger. Stainless steel check valves have no penetration welds other than the inlet, outlet and bonnet. The check hinge is serviced through the bonnet.

The stem packing and gasket of the stainless steel manual globe and gate valves are similar to those described above for motor-operated valves. Carbon steel manual valves are employed to pass non-radioactive fluids only and therefore do not contain the double packing and seal weld provisions.

Cold Leg Injection Accumulator Check Valves (Swing-disc)

The accumulator check valve is designed with a low pressure drop configuration with all operating parts contained within the body.

Design considerations and analyses which assure that leakage across the check valves located in each accumulator injection line will not impair accumulator availability are as follows:

1. During normal operation the check valves are in the closed position with a nominal differential pressure across the disc of approximately 1650 psi for Cold Leg Injection Accumulators. Since the valves remain in this position except for testing or when called upon to open following an accident and are therefore not subject to the abuse of flowing operation or impact loads caused by sudden flow reversal and seating, they do not experience significant wear of the moving parts and are expected to function with minimal back-leakage. This back-leakage can be checked via the test connection as described in Section [6.3.4](#).
2. When the RCS is being pressurized during the normal plant heatup operation, the check valves are tested for leakage as soon as there is a stable differential pressure of about 100 psi or more across the valve. This test confirms the seating of the disc and whether or not there has been an increase in the leakage since the last test. When this test is completed, the accumulator discharge line motor-operated isolation valves are opened and the RCS pressure increase is continued. There should be no increase in leakage from this point on since increasing reactor coolant pressure increases the seating force and decreases the probability of leakage.
3. The experience derived from the check valves employed in the emergency injection systems indicates that the system is reliable and workable; check valve leakage has not been a problem. This is substantiated by the satisfactory experience obtained from operation of the Robert Emmett Ginna and subsequent plants where the usage of check valves is identical to this application.
4. The accumulators can accept some in-leakage from the RCS without affecting availability. Continuous inleakage would require, however, that the accumulator water volume be adjusted accordingly with Technical Specifications requirements.

Relief Valves

Relief valves are installed in various sections of the ECCS to protect lines which have a lower design pressure than the RCS. The valve stem and spring adjustment assembly are isolated from the system fluids by a bellows seal between the valve disc and spindle. The closed bonnet provides an additional barrier for enclosure of the relief valves. [Table 6-88](#) lists the systems relief valves with their capacities and setpoints.

Butterfly Valves

Each residual heat removal heat exchanger discharge line has an air-operated butterfly valve which is normally open and is designed to fail in the open position. The actuator is arranged such that air pressure on the diaphragm overcomes the spring force, causing the linkage to move the butterfly to the closed position. Upon loss of air pressure, the spring returns the butterfly to the open position. These valves are left in the full open position during normal operation to maximize flow from this system to the RCS during the injection mode of the ECCS operation. In addition, these valves receive an "S" signal that vents the air operator. These valves are used during normal Residual Heat Removal System (RHRS) operation to control cooldown flowrate.

Each residual heat removal heat exchanger bypass line has an air-operated butterfly valve which is normally closed and is designed to fail closed. These valves are used during normal cooldown to avoid thermal shock to the residual heat exchanger.

Specific Emergency Core Cooling System Parameters are given in [Table 6-87](#).

NPSH

The Emergency Core Cooling System is designed so that adequate net positive suction head is provided to system pumps in accordance with Regulatory Guide 1.1. To demonstrate that adequate NPSH is provided for the ECCS pumps, the most limiting conditions are considered.

ECCS pump specifications require that the pumps be operable below a specified maximum NPSH value. Pump vendors have verified that the required NPSH for the ECCS pumps is less than the maximum specified NPSH through testing in accordance with the criteria established by the Hydraulic Institute Standards. Further, from the pump head/flow and NPSH required characteristics curves that have been derived from the testing, Westinghouse subsequently confirmed that adequate NPSH is available based on the actual system piping layouts, and conservatively calculated maximum pumps runout verified by preoperational testing.

Adequate net positive suction head is shown to be available for all pumps as follows:

Residual Heat Removal Pumps

The net positive suction head of the residual heat removal pumps is evaluated for normal shutdown operation, and for both the injection and recirculation modes of operation for the design basis accident. The recirculation mode of operation gives the limiting NPSH requirement for the residual heat removal pumps, and the NPSH available is determined from the following equation:

$$\text{NPSH actual} = (\text{h}) \text{ containment pressure} - (\text{h}) \text{ vapor pressure} + (\text{h}) \text{ static head} - (\text{h}) \text{ loss}$$

NPSH margin will be increased over time by increasing sump pool level and decreasing pool vapor pressure (decreasing temperature).

To evaluate the adequacy of the available NPSH, several conservatism's are applied:

1. No increase in Containment pressure from that present prior to the accident is assumed.
2. The Containment sump fluid temperature is assumed to be 200°F.

3. For the maximum calculated runout flow case of approximately 3980 gpm, the static elevation head is calculated from the minimum sump inventory necessary to initiate pump suction from the containment sump instead of the available water level. The assumption of minimum water level in the containment recirculation sump is conservative and also decouples the NPSH calculations from the actual containment sump level or Refueling Water Storage Tank level considerations.
4. The worst case head loss to pump suction is determined by considering possible single failure, single train operation, and dual train evaluation with conservatively assumed junction factors.
5. The Limiting NPSH available is calculated early in the event at the time of realignment of the pump suction to the ECCS Sump pool from the RWST, and conservatively assumes that most of the debris in the pool that can transport to the strainer has already done so. In actuality, the transport paths for a significant portion of this debris are long and circuitous, which would delay arrival at the strainer surface.

Related details of ECCS Sump Strainer design, performance and head loss are given in Section [6.3.2.9](#), "Generic Letter 2004-02".

6. A second case for RHR pump NPSH has been performed to conservatively bound a non-mechanistic assumed RH pump runout flow of 5300 gpm coincident with maximum Containment Spray pump flow. This case was performed in response to an NRC hypothetical question that required calculating NPSH at ND pump "runout" flow of 5300 gpm in addition to the "maximum calculated runout flow" as contained in Item 3 (the first case). In reality, RHR pump flow rates of this high magnitude are observed only during preoperational testing or refueling conditions when the pump suction is aligned from the Refueling Water Storage Tank and the discharge head is significantly reduced. Such a reduction in back pressure results from flow paths that do not utilize the ECCS flow paths with their associated friction losses due to piping and numerous RHR system flow orifices. This value was not cited in the NRC discussion in such a way that it was necessary to demonstrate compliance with Reg Guide 1.1, but rather to resolve SER Confirmatory Item 22 (NPSH Analysis).

Per SER Supplement 2 section 6.3.4.1 Preoperational Testing: "In the SER, the applicant stated that the available refueling water storage tank (FWST) inventory provides...an available net positive suction head (NPSH) for all the ECCS pumps in their highest flow configuration with adequate margin above the required value. In a letter dated January 11, 1983, the applicant provided a detailed analysis of the residual heat removal pump's NPSH calculations using conservative assumptions. The applicant showed that for a runout flow of 5300 gpm the available NPSH would be 24 ft while the required NPSH is 23.0 ft. Therefore, the staff finds the NPSH analysis acceptable and considers Confirmatory Issue 22 to be resolved.

For this conservative hypothetical case, credit is taken for approximately 2 feet of water (100,000 gallons) on the containment floor which is roughly half of the minimum injected volume from the RWST. In fact, the figure of a minimum 2 feet in the containment is still a reasonable and conservative assumption because in the case of a LOCA requiring sump recirculation, there will be a higher level due to partial ice melt in addition to FWST injected water. The sump recirculation pipes are 18 in. diameter and take suction horizontally off the floor, so there will be greater than 2 feet to cover the pipes and ensure adequate suction conditions.

Safety Injection and Centrifugal Charging Pumps

The net positive suction head for the safety injection pumps and the centrifugal charging pumps is evaluated for both the injection and recirculation modes of operation for the design basis accident. The end of the injection mode gives the limiting NPSH requirement for the safety injection pumps and the centrifugal charging pumps, and the NPSH available is determined from the following equation:

$$\text{NPSH actual} = (h)\text{atmospheric pressure} - (h)\text{vapor pressure} + (h)\text{static head} - (h)\text{loss}$$

To evaluate the adequacy of the available NPSH, several conservatism's are applied:

1. The RWST fluid temperature is assumed to be 114°F, but analysis at 120°F and other temperatures show that friction losses are not significantly affected by temperature.
2. The static elevation head is calculated taking no credit for water level above the outlet nozzle on the RWST.
3. The head loss to pump suction is evaluated based on all pumps running at the maximum calculated runout flow with conservatively assumed junction factors.
4. The required NPSH for a pump is based on the pump running at its maximum calculated runout flow.

Elevations of the ECCS components are given in Section 1.2. Available and required NPSH for ECCS pumps are provided in Table 5-30 for the Residual Heat Removal Pump and Table 6-87 for the Safety Injection and Centrifugal Charging Pump. The actual available NPSH will always be greater than the calculated value, due in part to the contribution of velocity head term, which has been conservatively ignored in the NPSH equation selected for this evaluation.

Duke has performed confirmatory NSPH calculations, using a flow model (Woods) to evaluate multiple flow path conditions. Cases with minimum safeguards, maximum safeguards (all pumps operating), and any one pump failed with all other pumps in operation are included. ECCS system alignments for ECCS pumps and the Containment Spray pumps are modeled.

The Woods model results provide fluid conditions at the suction of the pumps, including flow velocities. NPSH available is most directly represented by the following equation:

$$\text{NPSH available} = (h)s_{pg} + (h)s_{pb} - (h)s_{pv} + (h)\text{velocity}$$

With,

- | | |
|--------------------|--|
| (h)s _{pg} | as the head in feet associated with gauge pressure at pump suction reference point |
| (h)s _{pb} | as the head in feet associated with barometric pressure at pump suction gauge |
| (h)s _{pv} | as the head in feet associated with vapor pressure at pump suction reference point |
| (h)velocity | as head in feet, given by flow velocity squared / (2 x gravitational acceleration) |

- No correction of elevation difference between suction gauge and suction reference point is required as suction gauge pressure is calculated by the analysis at the elevation of the suction reference point.
- In all cases, the velocity head is not significant, with respect to the results. It is at most approximately 4 feet in the case of 17 ft/sec flow at the suction reference of the Safety Injection pumps operating at 675 GPM.

The difference between the above NPSH representation and that reported from the Westinghouse calculations is the inclusion of the velocity term and the use of modeling results which translate the friction loss and suction source fluid level differential elevation head to direct suction reference point conditions.

Westinghouse performed the original calculation before these systems were installed. Those results are validated by the more recent and detailed confirmatory calculations. Newer purchased Centrifugal Charging pump elements (namely a 1983 shop test and a 2001 shop test) show NPSH required values higher than those in the Westinghouse evaluation. However, even with these updated pump's NPSH requirements considered the margin of NPSH available above the NPSH required remains substantial. UFSAR Table 6-87 is updated for the Centrifugal Charging pump entries to reflect parenthetically the updated NPSH required and NPSH available numbers resulting from the revised calculation and updated pump data.

Containment Spray pump NPSH data (required and available) was not originally included in the UFSAR and is now provided in Table 6-70. Residual Heat Removal pumps originally were shown to required 24 ft. with 2 ft. of water in the sump to demonstrate NPSH margin at 5300 GPM. Even though the maximum calculated runout flow for the RHR pumps is shown by the updated calculation to be significantly less than 5300 GPM due to friction losses in the piping, the RHR 5300 GPM runout case has been demonstrated to remain within original UFSAR results. The updated calculation for the Safety Injection pumps was shown to be bounded by the original, more conservative UFSAR results.

Cold Leg Injection Accumulator Motor-Operated Valve Controls

As part of the plant shutdown administrative procedures, the operator is required to close these valves. This prevents a loss of accumulator water inventory to the RCS and is done shortly after the RCS has been depressurized below approximately 1000 psig. The redundant pressure and level alarms on each accumulator would remind the operator to close these valves, if any were inadvertently left open. Power is disconnected after the valves are closed.

During plant startup, the operator is instructed via procedures to energize and open these valves prior to RCS pressure reaching approximately 1000 psig, the safety injection setpoint. Power is again disconnected after the valves are opened. Monitor lights in conjunction with an audible alarm will alert the operator should any of these valves be left inadvertently closed once the RCS pressure increases beyond the safety injection unblock setpoint.

The accumulator isolation valves are not required to move during power operation. For a discussion of limiting conditions for operation and surveillance requirements of these valves, refer to the Technical Specifications.

For further discussions of the instrumentation associated with these valves refer to Sections [6.3.5](#), [7.3.1.1.2](#) and [7.6.3](#).

Motor-Operated Valves and Controls

Remotely operated valves for the injection mode which are under manual control (i.e., valves which normally are in their ready position and do not require a safety injection signal) have their positions indicated on a common portion of the control board. If a component is out of its proper position, its monitor light will indicate this on the control panel. If at any time during operation one of these valves is not in the ready position for injection, this condition is shown visually on the board, and an audible alarm is sounded in the control room.

The ECCS delivery lag times are given in Section [15.1](#). The accumulator injection time varies as the size of the assumed break varies since the RCS pressure drop will vary proportionately to the break size.

Inadvertent mispositioning of a motor operated valve due to a malfunction in the control circuitry in conjunction with an accident has been analyzed and found not to be a credible event for use in design. This analysis is contained in Westinghouse report WCAP-8966 "Evaluation of Mispositioned ECCS Valves", September 1977. The mispositioning of the accumulator discharge isolation valves is prevented by interlocks and administrative controls (see FSAR Section [7.6.3](#) and Technical Specifications). Power is removed to the following Residual Heat Removal (RHR) System and Safety Injection (SI) System valve operators to preclude the possibility of mispositioning during operation.

| Valve Function | Number |
|---------------------------------|----------------|
| RHR pump discharge to cold legs | NI173A, NI178B |
| RHR pump discharge to hot legs | NI183B |
| SI pump suction from RWST | NI100B |

| | |
|---------------------------------------|----------------|
| SI pump common miniflow | NI147B |
| SI pump discharge to cold legs | NI162A |
| SI pump discharge to hot legs | NI121A, NI152B |
| A similar analysis applies to Unit 2. | |

The following design features for these valves have been provided:

1. Power can be restored from control room consistent with the time allowed for the valve to be operational; and
2. Redundant Class 1E valve position indication is provided in the control room; and
3. Technical Specification includes a list of all valves that have power removed, and the required position of these valves.

There are no single failures that could prevent the ECCS from performing its function for each mode of ECCS operation.

[Table 6-89](#) is a listing of motor operated isolation valves in the ECCS showing interlocks, automatic features and position indications. The purpose of the interlocks and automatic features for the valves in [Table 6-89](#) are listed below by function.

Cold Leg Accumulator Isolation Valves - Assures valves are open during power operation.

Residual Heat Removal System (RHRS) Suction from Refueling Water Storage Tank (RWST) - Prevents valves from opening during post accident recirculation operation of ECCS.

RHRS Pump Discharge to Centrifugal Charging Pump (CCP) [Safety Injection (SI) Pump] - Prevents flow of recirculation sump fluid to FWST, prevent possible overpressure of pipe during cooldown, permits alignment to supply SI & CCP pumps only during recirculation.

Containment Sump Valve - The interlocks prevent the control room operator from opening the sump valves and flooding containment with fluid from the reactor coolant system or the RWST. The automatic features override the interlocks and open the valve if the RWST level is low and an "S" signal has been generated (this prevents the sump valve from opening and flooding containment during refueling as the RWST is emptied into the refueling cavity).

CCP Normal Suction - Isolates normal charging sources after RWST is available to pumps.

Reactor Coolant System (RCS) to RHRS Isolation Valves - Interlocks prevent flow from RCS to RWST, spill of RCS to containment sump, potentially overpressuring CCP and SI pump suction lines, spraying RCS to containment via residual spray headers. Pressure interlocks prevent overpressure of the ND pump suction line.

SI Pump Miniflow - Interlocks prevent recirculation sump fluid from being pumped to RWST.

Containment Spray System Suction from RWST - Prevents spill of RWST fluid to containment sump via RHRS piping.

Containment Spray System Suction From Sump - Prevents spill of RWST fluid to containment sump and prevents containment spray with reactor coolant.

Residual Containment Spray - Prevents residual containment spray with reactor coolant.

6.3.2.3 Applicable Codes and Classifications

Applicable industry codes and classifications for ECCS are discussed in Section [3.9.3](#).

6.3.2.4 Material Specifications and Compatibility

Materials employed for components of the ECCS are given in [Table 6-90](#). Materials are selected to meet the applicable material requirements of the codes in [Table 3-3](#) and the following additional requirements:

1. All parts of components in contact with borated water are fabricated of or clad with austenitic stainless steel or equivalent corrosion resistant material.
2. All parts of components in contact (internal) with sump solution during recirculation are fabricated of austenitic stainless steel or equivalent corrosion resistant material.
3. Valve seating surfaces are hard faced with Stellite number 6 or equivalent to prevent galling and to reduce wear.
4. Valve stem materials are selected for their corrosion resistance, high tensile properties, and resistance to surface scoring by the packing.

6.3.2.5 System Reliability

Reliability of the ECCS is considered in all aspects of the system from initial design to periodic testing of the components during plant operation. The ECCS is a two train, fully redundant safeguard feature. The ECCS is a standby system, with the exception of the Centrifugal Charging Pumps (CCPs) which provide normal charging as part of the Chemical and Volume Control System (CVCS). The system has been designed and proven by analysis to withstand any single credible active failure during injection or either an active or a passive failure during recirculation and maintain the performance objectives desired in [Section 6.3.1](#). Two trains of pumps, heat exchangers, and flow paths are provided for redundancy while only one train is required to satisfy the performance requirements. The initiating signals for the ECCS are derived from independent sources as measured from process (e.g., low pressurizer pressure) or environmental variables (e.g., containment pressure). Redundant as well as functionally independent variables are measured to initiate the safeguards signals. Each train is physically separated and protected where necessary so that a single event cannot initiate a common failure. Power sources for the ECCS are divided into two independent trains supplied from the emergency buses from offsite power. Sufficient diesel generating capacity is maintained onsite to provide required power to each train. The diesel generators and their auxiliary systems are completely independent and each supplies power to one of the two ECCS trains.

The reliability program extends to the procurement of the ECCS components such that only designs which have been proven by past use in similar applications are acceptable for use. The quality assurance program as described in [Chapter 17](#) assures receipt of components only after manufacture and testing to the applicable codes and standards.

HISTORICAL INFORMATION NOT REQUIRED TO BE REVISED

The preoperational testing program assures that the systems as designed and constructed meet the functional requirements calculated in the design.

The ECCS is designed with the ability for on-line testing of most components so the availability and operational status can be readily determined.

In addition the integrity of the ECCS is assured through examination of critical components during the routine inservice inspection.

Catawba ECCS design is in compliance with regulatory position B.5 of RSB6-1. Of the three pairs of ECCS pumps, only the residual heat removal pumps (RHRP's) have suction piping that can supply water either from the refueling water storage tank (RWST) or directly from the

containment recirculation sump. The physical arrangement of this equipment has the RWST at grade elevation, the recirculation sump bottom approximately 41' below grade and RHRP suction approximately 68' below grade elevation. With all valves open, flow would be from the RWST to the sump and to the RHRP suction. Thus, this arrangement does not preclude automatic switchover.

There is one motor operated gate valve between the containment sump and each pump suction while the line from the RWST to each pump contains both a motor operated gate valve and a check valve. (Refer to [Figure 6-131](#), [Figure 5-17](#), and [Figure 9-62](#)) A pressure control bypass line to the FWST has been installed in parallel with the check valve on each train. Each bypass line contains a spring loaded check valve, FW96 on A train and FW97 on B train, designed to remain closed during sump recirculation conditions and open to relieve excess pressure to the FWST prior transfer to cold leg recirculation. The control pressure is determined in CNC-1223.21-00-0020, reference [24](#), in Section 6.7. The ND suction pressure control is required to assure that the generic letter 89-10 limits for motor operators on the containment sump isolation valves, NI185A and NI184B, are not exceeded during the transfer to cold leg recirculation in a small break LOCA scenario. CNC-1223.21-00-0021, reference [25](#), in Section 6.7 evaluated the ECCS and dose consequences of the pressure control bypass line installed around the check valves. Failure of the motor operated valves is analyzed in [Table 6-91](#) (items 13 and 14). This shows that assuming single failure, adequate core cooling is available and that the failure does not result in establishment of a path that would allow release of radioactive material to the environment.

A Failure Modes and Effects Analysis of the Emergency Core Cooling System is provided as [Table 6-91](#).

1. Active Failure Criteria

The ECCS is designed to accept a single failure following an accident without loss of its protective function. The system design will tolerate the failure of any single active component in the ECCS itself or in the necessary associated service systems at any time during the period of required system operations following the incident.

A single active failure analysis is presented in [Table 6-92](#), and demonstrates that the ECCS can sustain the failure of any single active component in either the short or long term and still meet the level of performance for core cooling.

Since the operation of the active components of the ECCS following a steam line rupture is identical to that following a loss of coolant accident, the same analysis is applicable and the ECCS can sustain the failure of any single active component and still meet the level of performance for the addition of shutdown reactivity.

2. Passive Failure Criteria

The following philosophy provides for necessary redundancy in component and system arrangement to meet the intent of the General Design Criteria on single failure as it specifically applies to failure of passive components in the ECCS. Thus, for the long term, the system design is based on accepting either a passive or an active failure.

Redundancy of Flow Paths and Components for Long Term Emergency Core Cooling

In design of the ECCS, Westinghouse utilizes the following criteria.

- a. During the long term cooling period following a loss of coolant, the emergency core cooling flow paths shall be separable into two subsystems, either of which can provide minimum core cooling functions and return spilled water from the floor of the containment back to the RCS.

- b. Either of the two subsystems can be isolated and removed from service in the event of a leak outside the containment.
- c. Adequate redundancy of check valves is provided to tolerate failure of a check valve during the long term as a passive component.
- d. Should one of these two subsystems be isolated in this long term period, the other subsystem remains operable.
- e. Provisions are also made in the design to detect leakage from components outside the containment, collect this leakage and to provide for maintenance of the affected equipment.
- f. Provision is made for diversion of a portion of the RHR pump flow from the low head injection path to auxiliary spray headers in the upper Containment volume. For this mode, the RHR pumps continue to supply recirculation flow from the Containment sump to the core via the safety injection and centrifugal charging pumps. The diversion of the RHR flow from the low head injection path to the auxiliary spray headers occurs only after the switchover to the recirculation mode and no earlier than 50 minutes after initiation of the LOCA. The procedure for initiating RHR spray flow is given in [Table 6-93](#). RHR spray is not credited in the LOCA analysis.

Thus, for the long term emergency core cooling function, adequate core cooling capacity exists with one flow path removed from service.

Subsequent Leakage From Components in Safeguards Systems

With respect to piping and mechanical equipment outside the containment, considering the provisions for visual inspection and leak detection, leaks will be detected before they propagate to major proportions. A review of the equipment in the system indicates that the largest sudden leak potential would be the sudden failure of a pump shaft seal. Evaluation of leak rate assuming only the presence of a seal retention ring around the pump shaft showed flows less than 50 gpm would result. Piping leaks, valve packing leaks, or flange gasket leaks have been of a nature to build up slowly with time and are considered less severe than the pump seal failure.

Excessive leakage flows via a floor drain from a faulted residual heat removal pump or containment spray pump to the RHRS (Residual Heat Removal System) and Containment Spray System room sump on elevation 522 feet.

Excessive leakage from a faulted safety injection pump or centrifugal charging pump, flows via a floor drain to Floor Drain Sump A (Unit 1) or Floor Drain Sump B (Unit 2). Both sumps are on elevation 537 feet. Sump level instrumentation and pumps in Floor Drain Sumps A & B are not safety related, therefore availability of these devices is not assumed. With no sump pumps operating, leakage from a safety injection or charging pump collects in one of the floor drain sumps.

If the sump overflows and the room fills to elevation 543 feet, additional leakage will drain to the 522 feet elevation and collect in the RHRS and Containment Spray System room sump. The RHRS and Containment Spray System room sump has four ASME III, Class 3 pumps and level instrumentation. High and high-high sump levels are alarmed and sump pump discharge volume is totalized in the control room. Once these alarms confirm excessive leakage, the measured flow rate at the discharge of each ECCS pump is used to determine which train is faulted. The faulted train is then isolated.

Assuming none of the RHRS and Containment Spray System room sump pumps are operating, the operator has at least 30 minutes from receipt of the high level alarm to isolate

the passive failure and prevent the sump from overflowing. However, with only one of the four Nuclear Safety Related sump pumps operating, the pump down rate exceeds the leakage rate.

Consequently, this arrangement precludes all ECCS pump areas from flooding due to passive ECCS failures during long-term cooling.

For a description of leak detection features of the Liquid Radwaste System and its compliance with the requirements of IEEE 279-1971, refer to Section [7.6.6](#).

The design pressure of the suction lines for the charging and safety injection pumps is appropriate for all modes of ECCS operation.

Larger leaks in the ECCS are prevented by the following:

- a. The piping is classified in accordance with ANS Safety Class 2 and receives the ASME Class 2 quality assurance program associated with this safety class.
- b. The piping, equipment and supports are designed to ANS Safety Class 2 seismic classification permitting no loss of function for the design basis earthquake.
- c. The system piping is located within a controlled area of the plant.
- d. The piping system receives periodic pressure tests and is accessible for periodic visual inspection.
- e. The piping is austenitic stainless steel which, due to its ductility, can withstand severe distortion without failure.

Based on this review, the design of the Auxiliary Building and related equipment is based upon handling of leaks up to a maximum of 50 gpm. Means are also provided to detect and isolate such leaks in the emergency core cooling flow path (Refer to Sections [5.4.7.2.5](#) and Section [6.2.4.2.1](#)).

A single passive failure analysis is presented in [Table 6-94](#). It demonstrates that the ECCS can sustain a single passive failure during the long term phase and still retain an intact flow path to the core to supply sufficient flow to maintain the core covered and remove decay heat. The procedure followed to establish the alternate flow path also isolates the component which failed.

The RHRS and Containment Spray System sump pumps will be stopped on receipt of an "S" signal from either unit and will start on high-high sump level which also provides an alarm in the main control room. As a result the volume that could accumulate in the RHRS and Containment Spray System sump prior to generation of an alarm is about 2500 gallons. The loss of this amount of fluid from the recirculation sump is insignificant.

Lag times for initiation and operation of the ECCS are limited by pump startup time and the loading sequence of these motors onto the safeguard buses. Most valves are normally aligned for safety injection initiation, therefore, valve opening time is not considered for these valves. In the case of a blackout a 10 second delay is assumed for diesel startup, then pumps and valves are loaded according to the sequencer. The valves will be applied to the buses in 11 seconds, the charging pumps in 12 seconds, the safety injection pumps in 15 seconds and the residual heat removal pumps in 20 seconds. These times refer to the maximum delay after satisfying the conditions for generation of an "S" signal assuming loss of offsite power. If there is no loss of offsite power, the same starting sequence is followed without delay, the first load being started upon receipt of the "S" signal.

Post Accident Flooding Consequences on ECCS Functions

The maximum post-accident flood level inside containment has been determined to be elevation 571' 0". The safety related control instrumentation below this elevation are the reactor coolant loop elbow flow rate instruments and the reactor coolant system wide range temperature RTD's. The flow rate instrumentation provides both control room indication and a reactor trip (on low flow in any one loop) neither of which is required after an accident (no operator actions taken on indication, and reactor trips due to safety injection signal). The RTD's are sealed units which are terminated above the flood level and therefore are not affected by submergence.

A list of safety related solenoid valves in containment that are below maximum flood elevation is presented in [Table 6-95](#). These solenoids perform one of two functions; namely, controlling air to air diaphragm operated valves and providing air to the lower personnel air lock inflatable seals. All of the air diaphragm operated valves are designed to assume their safety position on loss of air. All of the solenoids controlling the air supply are designed to vent the air diaphragm on loss of power. Therefore, even if control of these solenoid valves is lost the air operated valve will assume its correct position. The solenoids which supply air to the lower personnel air lock seals are designed to fail in the position which supplies air to the seals. None of these valves are required to be repositioned to perform short or long term ECCS functions.

A list of active valves in containment that are below maximum flood elevation is presented in [Table 6-96](#). The valves which will potentially be flooded are, except as noted, electric motor operated. These are assumed to fail in the position they are in when flooded. There is sufficient time for the ones which receive a safety signal to stroke to their safety positions before being flooded. None of these valves are required to be repositioned to perform short or long term ECCS functions.

As indicated on [Table 6-96](#), 17 valve operators were not qualified for submergence. These valves close on Containment Isolation Phase A (ST) signals. There is sufficient time for them to close before being flooded. To prevent possible repositioning after flooding, the valves motor controls circuits have been modified. One relay per train will be energized by a ST signal and mechanically latched in. Normally closed contacts from this relay will be wired between the limit switches and the open motor starter coils of valves of the corresponding train. These contacts will open on ST and prevent any spurious limit switch operation from repositioning the valves. These relays will have manual reset capability in the control room. Breakers and fuses are coordinated such that, in the case of faults caused by submergence, the faulted valve circuits will be isolated without adversely affecting the upstream class 1E power sources.

An additional valve, 1NI438A, has been identified as being approximately three feet below the final flood elevation. This valve is a normally closed, EMO which supplies nitrogen from a cold leg accumulator to a pressurizer PORV as a part of the low temperature overpressure protection system (LTOP). Since it is near the top of the flood elevation, it is not flooded during the time that cold leg accumulator injection is required and spurious operation if it were to occur after the valve is flooded presents no safety question.

Potential Boron Precipitation

Boron precipitation in the reactor vessel can be prevented by backflushing cooling water through the core. This reduces boil-off and the resulting concentration of boric acid in the water remaining in the reactor vessel.

Only a limited amount of hot leg injection flow is necessary to both remove decay heat at the switch-over time and dilute the core region boron concentration. Since one safety injection

pump, injecting through the hot legs, has more than enough flow capacity to meet this requirement, a direct flow path from the residual heat removal pumps to the hot legs need not be aligned.

In addition, simultaneous alignment of a residual heat removal pump for direct hot leg injection and auxiliary containment spray would result in insufficient spray because of the relative system resistance between the two flow paths. Therefore, if a particular residual heat removal pump is providing auxiliary containment spray to assist a containment spray pump in maintaining containment peak pressure within design limits, that same pump would not be aligned for direct hot leg injection.

Loss of one pump or one flow path will not prevent hot leg recirculation since two redundant flow paths are available for use.

In order for the operator to switch from cold leg recirculation to hot leg recirculation there are five valves which require power be reestablished before they can be repositioned. These valves are NI178B, NI173A, NI152B, NI162A, and NI121A. Valves NI173A and NI178B could require repositioning as early as 50 minutes after the start of the accident if residual containment spray is required. NI183B can have power restored if it is desired to establish a direct flow path from the residual heat removal pumps to the hot legs; however, this is not a required or credited function for accident mitigation. Power removal/restoration capability for all these valves has been added to the main control room. A similar analysis applies to Unit 2.

Monitoring of ECCS Degradation

Early warning of ECCS malfunctioning can provide more time to initiate any manual action which may be required by the operator. The ECCS instrumentation is discussed in Section [6.3.5](#). Alarms are provided in the control room to alert the operator of any ECCS degradation.

The RHR Heat Exchanger Outlet Flow transmitters are used to provide alarms to alert the operator to potential RHR (or ECCS) degradation. Refer to [Figure 5-17](#) and [Figure 5-18](#) for transmitters NDFT5190 and NDFT5180 respectively. Since these instruments measure the portion of RHR flow directed to the Reactor Coolant System (RCS), they are insensitive to miniflow and are effective for a wide range of circumstances (e.g. air entrainment, inadequate NPSH, etc.). The alarm setpoint will be 500 gpm or greater. Control room indication is provided by an annunciator, and an alarm is also provided by the plant process computer.

6.3.2.6 Protection Provisions

The provisions taken to protect the system from damage that might result from dynamic effects are discussed in Section [3.6](#). The provisions taken to protect the system from missiles are discussed in Section [3.5](#). The provisions to protect the system from seismic damage are discussed in Sections [3.7](#), [3.9](#) and [3.10](#). Thermal stresses on the RCS are discussed in Section [5.2](#).

6.3.2.7 Provisions For Performance Testing

Test lines are provided for performance testing of the ECCS system as well as individual components. These test lines and instrumentation are shown in [Figure 6-128](#) thru [Figure 6-132](#). Additional information on testing can be found in Section [6.3.4.2](#).

6.3.2.8 Manual Actions

The only manual action required by the operator for proper ECCS operation during the injection mode is the isolation of the CCP minimum flow bypass line when RCS pressure drops to 1500 psig. Operator action is also required to open the CCP minimum flow bypass line if RCS pressure increases to greater than 2000 psig. Only limited manual actions are required by the operator to realign the system for the cold leg and hot leg recirculation modes of operation. These actions are delineated in [Table 6-93](#).

The changeover from the injection mode to recirculation mode is initiated automatically and completed manually by operator action from the main control room. Protection logic is provided to automatically open the two Containment recirculation sump isolation valves and automatically close the two RHR/RWST isolation valves (FW27A and FW55B) when two of four refueling water storage tank level channels indicate a refueling water storage tank level less than a predetermined level in conjunction with the initiation of the engineered safeguards actuation signal ("S" signal). This automatic action aligns the two residual heat removal pumps to take suction from the containment sump and to deliver directly to the RCS. It should be noted that the residual heat removal pumps would continue to operate during this changeover from injection mode to recirculation mode.

The two charging pumps and the two safety injection pumps continue to take suction from the refueling water storage tank, following the above automatic action, until manual operator action is taken to align these pumps in series with the residual heat removal pumps.

The refueling water storage tank level protection logic consists of four level channels with each level channel assigned to a separate process control protection set. Four refueling water storage tank level transmitters provide level signals to corresponding normally de-energized level channel bistables. Each level channel bistable would be energized on receipt of a refueling water storage tank level signal less than the predetermined level setpoint.

A two out of four coincident logic is utilized in both protection cabinets A and B to ensure a trip signal in the event that two of the four level channel bistables are energized. This trip signal, in conjunction with the "S" signal, provide the actuation signal to automatically open the corresponding containment sump isolation valves.

The low-low refueling water storage tank level alarm informs the operator to initiate the manual action required to realign the charging and safety injection pumps for the recirculation mode. Containment Sump level is verified via redundant, safety-powered level switches prior to swap to ensure adequate inventory is available to support sustained sump recirculation.

The RWST Low level setpoint provides a volume above the no vortex level to account for the maximum RWST outflow during switchover with the most limiting single failure plus an allowance for instrument error. The "transfer allowance" is included in this volume.

The manual switchover sequence that must be performed by the operator is delineated in [Table 6-93](#). Following the automatic and manual switchover sequence, the two residual heat removal pumps would take suction from the containment sump and deliver borated water directly to the RCS cold legs. A portion of the residual heat removal pump A discharge flow would be used to provide suction to the two charging pumps which would also deliver directly to the RCS cold legs. A portion of the discharge flow from residual heat removal pump B would be used to provide suction to the two safety injection pumps which would also deliver directly to the RCS cold legs. As part of the manual switchover procedure ([Table 6-93](#)), the suctions of the safety injection and charging pumps are cross connected so that one residual heat removal pump can deliver flow to the Reactor Coolant System and both safety injection and charging pumps, in the event of the failure of the other residual heat removal pump.

A calculation based on this switchover procedure determined the FWST volume required for each step both with no failures and with the most restrictive single failure. The most restrictive single failure is failure of one of the RWST to RHR suction isolation valves (FW27A or FW55B) to close, thus maximizing RWST outflow during switchover.

The control room operator is assumed to require a maximum of 195 seconds to accomplish steps M1 through M7, 195 seconds for steps M8 through M18, and 300 seconds to accomplish step M22 through either M26.k. or M27.k. of the procedure.

The control board design and the layout of devices in the control room enhance the operator's ability to quickly locate and operate each of the devices required to complete the switchover to the recirculation procedure. The Standard Review Plan, Section [6.3](#) requires that the operator have at least 20 minutes to respond where manual actions are required following a LOCA.

The low level setpoint provides sufficient time for the operator to stop all ECCS pumps prior to reaching the RWST no vortex level assuming that the operator fails to respond for 20 minutes when there is no single failure. The control room operator is assumed to require 60 seconds to secure the ECCS pumps.

Deleted Per 2009 Update.

See Section [7.5](#) for process information available to the operator in the control room following an accident.

The consequences of the operator failing to act altogether will be loss of high head safety injection pumps and charging pumps.

6.3.2.9 Generic Letter 2004-02

The NRC initiated Generic Safety Issue (GSI)-191, "Assessment of Debris Accumulation on PWR Sump Performance," in 1996 based upon the findings that the amount of debris generated from a high energy line break and resulting head loss across the ECCS Sump Strainer could be greater than previously anticipated. This precursor to Generic Letter 2004-02 focuses on reasonable assurance that the provisions of Title 10 of the Code of Federal Regulations (10 CFR) Section 50.46(b)(5) are met. This rule requires maintaining long-term core cooling after initiation of the Emergency Core Cooling Systems. The objective of GSI-191 and the subsequent Generic Letter 2004-02 is to ensure that post accident debris blockage will not impede or prevent the operation of the Emergency Core Cooling Systems (ECCS) and Containment Spray System (CSS) in recirculation mode during LOCAs.

The Catawba Unit 1 and Unit 2 ECCS Sump Strainers were designed to meet the requirements of USNRC Generic Letter 2004-02, "Potential Impact of Debris Blockage on Emergency Recirculation During Design Basis Accidents at Pressurized-Water Reactors", including the guidance outlined in NEI 04-07, "Pressurized Water Reactor Sump Performance Evaluation Methodology", and its companion Safety Evaluation Report (SER).

In response to the NRC staff SER conclusions on NEI 04-07, the Pressurized Water Reactor Owners Group (PWROG) sponsored the development of the following Topical Reports (TRs):

- TR-WCAP-16406-P-A, "Evaluation of Downstream Sump Debris Effects in support of GSI-191," to address the effects of debris on piping systems and components.
- TR-WCAP-16530-NP-A, "Evaluation of Post-Accident Chemical Effects in Containment Sump Fluids to Support GSI-191," to evaluate the chemical effects which may occur post-accident in containment sump fluids.

- TR-WCAP-16793-NP-A, "Evaluation of Long Term Cooling Considering Particulate, Fibrous and Chemical Debris in the Recirculating Fluid," to address the effects of debris on the reactor core.

The NRC staff reviewed the TRs and found them acceptable to use (as qualified by the Limits and Conditions stated in the respective SERs).

ECCS Sump Strainer design considerations and exceptions to these documents are identified and justified in Catawba letters to NRC of February 29, 2008, April 30, 2008, August 13, 2012 and July 31, 2013. The NRC documented their acceptance of the Catawba responses and closeout of Generic Letter 2004-02 in a letter dated December 31, 2013 and accompanying Staff Review document.

Significant aspects of the Catawba Unit 1 and Unit 2 ECCS Sump Strainer design related to GL 2004-02 are described following:

Design Considerations

A fundamental function of the ECCS is to provide long term post-accident cooling of the core. This is accomplished by recirculating water that has collected at the bottom of the containment building (sump pool) through the reactor core following a break in the reactor coolant system piping. If a LOCA occurs, thermal insulation and other materials may be dislodged by the two-phase jet emanating from the broken RCS pipe. The debris may transport via flows coming from the RCS break or from the containment spray system to the sump pool following a LOCA. Once transported to the sump pool, the debris could be drawn towards the ECCS Sump Strainer which is designed to prevent debris from entering the Emergency Core Cooling Systems and the reactor core. If this debris were to clog the strainers, long term core cooling as well as containment cooling could be degraded and the potential for core damage and containment failure would increase.

It is possible that some fine debris could bypass the ECCS Sump Strainer and lodge in the reactor core. This could result in reduced core cooling and potential core damage.

Resolution of GSI-191 and subsequently Generic Letter 2004-02 involves two distinct but related safety concerns:

1. Potential clogging of the sump strainers that results in ECCS and/or Containment Spray Pump failure (due to inadequate NPSH available) or gross structural failure of the ECCS Sump Strainer; and
2. Potential clogging of flow channels within the reactor vessel because of debris bypass of the ECCS Sump Strainer (in-vessel effects).

Clogging at any point (the strainer, the downstream piping components or in the reactor vessel) can result in the loss of the long-term cooling safety function.

Design Description

The Containment Recirculation Sump Strainer Assembly is located on Elevation 552' of the Containment Reactor Building. The strainer assembly is outside the crane wall in the pipe chase between approximately 126° azimuth to 226° azimuth. The overall strainer assembly height above the containment building floor is lower than the predicted minimum containment water level for a small break LOCA. The strainer assembly is designed to withstand a safe shutdown earthquake.

The strainer modules ("Top-Hats") are made of two concentric cylinders formed from perforated plates for straining debris from the water. Each Top-Hat module has an outer diameter of 8 inches and an inner diameter of 6 inches with a length varying from approximately 24 to 45

inches. The strainer openings are 3/32 inch in diameter. Water will enter the Top-Hats through the perforated plates and flow horizontally within the annulus of each Top-Hat. Within the annulus of each Top-Hat is knitted wire mesh material which provides additional filtration for any debris that may enter. Upon exiting the Top-Hats, water will flow through a cruciform support plate and into the plenum boxes. Four series of plenum boxes direct flow to the two 18" ECCS recirculation phase suction lines. A cross over plenum attaches to each 'main' plenum at the center of the strainer assembly. Each 18" ECCS recirculation phase suction line inserts into its own strainer assembly main plenum water box.

The strainer design includes vortex suppressors above the Top-Hat strainer modules. The vortex suppressors are constructed of floor grating and install directly over the Top-Hats.

Break Selection:

The Catawba ECCS Sump Strainers were designed to accommodate the debris generation from a double-ended guillotine break of a primary loop. Break locations throughout the RCS were analyzed based on their debris generation and transport potential and the break selected is the limiting case for debris generation. This limiting break generates the highest quantity of fibrous debris and also transport the highest portion of that fibrous debris to the strainer. The bounding break location is on the Unit 1 B loop hot leg, adjacent to the steam generator. Breaks on the hot leg are generally more limiting than breaks on the crossover and cold legs due to their proximity to the adjacent loop hot leg piping. In addition, in terms of debris generation, breaks in Unit 2 are bounded by Unit 1 breaks since Unit 2 contains significantly less fibrous insulation within lower containment.

Secondary line breaks were not considered in the evaluation of debris generation. For debris generation, the smaller secondary side breaks inside the crane wall are bounded by the primary side breaks. Further, for a secondary system break inside containment, the steam release will terminate following isolation of feedwater to the faulted steam generator. For a design basis steam line break, the RCS remains intact and long term operation with the ECC Sump Strainer is not required.

Debris Generation:

There are three kinds of conventional debris assumed to be generated from the limiting break: failed insulation, failed coatings, and latent debris (i.e., placards, tags, labels, dust/dirt and lint). The insulation debris, coating debris and dust/dirt and lint debris generated during blowdown and transported to the ECCS Sump Pool can vary in size and texture, from pieces/clumps, to individual strands, to particulates. Additionally, large fiber clumps that do not transport to the strainer are conservatively assumed to partially erode over time into individual fiber strands, which do transport.

Several types of insulation systems are used inside containment within the Zone of influence (ZOI) of high energy breaks: Reflective Metal Insulation (RMI), Nukon® Low Density Fiberglass (LDFG) fiber insulation, and Thermal-Wrap® LDFG fiber insulation. Both jacketed and unjacketed LDFG fiber insulation systems are used. A spherical zone of influence is measured as a function of the pipe diameter and centered at the break location used for the debris generation analysis. The ZOI used for evaluation of RMI is 28.6D and the ZOI for Nukon® and Thermal-Wrap® LDFG is 17D regardless of the jacketing. These ZOIs are consistent with the recommendations of NEI 04-07 and the associated NRC Safety Evaluation.

The destroyed RMI is not buoyant and therefore does not pose a threat to the operation of the ECCS Sump strainer. Therefore, the quantity of RMI either within containment or destroyed due to a high energy line break is not considered a critical parameter with respect to ECCS Sump Strainer performance.

The maximum amount of LDFG fibrous debris generated in the limiting break was documented in Reference [24](#). NEI 04-07 and the associated NRC Safety Evaluation were used to determine this overall debris quantity. In addition, the predicted debris generated due to the LOCA jet is characterized by debris size (fines, small pieces, large pieces, and intact blankets). The amount of LDFG debris generated as well as the size distribution of the debris is based on the proximity of the insulation to the break. This characterization of debris is critical to the sump strainer analysis as the transportability and thus debris load on the ECCS Sump Strainer is dependent on debris size.

Coatings inside the Containment are classified as either qualified or unqualified for the purposes of debris generation analysis, which encompasses all of the coating systems used within Containment. Unqualified coatings in Containment are assumed to fail as particulates, in accordance with NEI 04-07 guidance. Qualified coatings are assumed to fail as particulates within a 5D ZOI based on the methodology outlined in WCAP-16568-P, "Jet Impingement Testing to Determine the Zone of influence (ZOI) for DBA-Qualified/Acceptable Coatings". The amount of qualified coatings is documented in Reference [25](#). For unqualified coatings, NEI 04-07 guidance directs utilities to assume 100% failure of unqualified coatings into transportable particulate. Catawba performed an alternative analysis utilizing EPRI OEM coatings failure data to refine the quantity of coatings assumed to fail. Utilizing this data, an overall volume of failed unqualified coatings was documented in Reference [27](#). All of the failed coatings are assumed to transport to the Sump Strainer as particulate debris.

Walkdowns were performed on each Unit to assess the quantity of dust, dirt, and lint per NEI 02-01 guidance and a bounding value of 200 lb was used in the debris generation evaluation. The actual results of the walkdowns indicated significantly less than 200 lb however, the use of this bounding value is consistent with guidance provided in NEI 04-07. The characterization of dust, dirt, and lint is also addressed in NEI 04-07. 15% of the overall quantity of dust, dirt, and lint on a mass basis is assumed to be lint with fibrous like behavior (30 lb or 12.5 ft³). The remainder of the debris (170 lb) is assumed to be dust/dirt which can be represented by particulate debris.

Placards, tags, labels and other miscellaneous latent materials in containment were included in the debris generation analysis consistent with NEI 04-07 guidance. Refinements to the tag and label analysis were performed to account for the torturous path labels in some locations would be required to traverse to transport to the ECCS Sump Strainer. The total surface area of tags and labels assumed to dislodge and transport to the ECCS Sump Strainer is documented in Reference [28](#). When determining actual strainer surface area blockage, this total is reduced by 25% to account for overlap and compression of the debris consistent with the NEI 04-07 guidance.

The following actions have been taken to minimize the potential for debris build-up on the ECCS Sump Strainers:

- Containment cleaning and inspection during each refueling outage
- Establishment of controls for the procurement, application and maintenance of Service Level 1 coatings inside containment
- Enhancements to administrative controls programs and equipment labeling processes

In addition to the conventional debris, chemical precipitates can form in the post-LOCA environment inside containment. The quantity of chemical precipitates that could form was estimated using the models and methodologies from WCAP-16530-NP-A. By executing this model using plant specific containment material inventories and environmental conditions, a bounding mass of chemical precipitates as well as a temperature at which the precipitates form

was determined and included in the scope for ECCS Sump Strainer head loss testing. The key material for this analysis is Aluminum inventory as documented in Reference [29](#).

Debris Transport to ECCS Sump:

The methodology used in the debris transport analysis was based on the NEI 04-07 guidance report for refined analyses, as modified by the NRC SER, as well as the refined methodologies suggested by the SER in Appendices III, IV, and VI. Assumptions used in the debris transport analysis are listed in Catawba's letter to NRC of February 29, 2008; deviations from NEI 04-07 guidance and their justification are also listed in that letter. The Computational Fluid Dynamics (CFD) calculation for recirculation flow in the ECCS Sump Pool was performed using Flow-3D® version 9.0. The assumptions used in the CFD model are also listed in the response to question 3(e)(2) of the February 29, 2008 letter. The transport fraction of each type of debris was determined using the velocity and Turbulent Kinetic Energy (TKE) profiles from the CFD model output, along with the initial distribution of debris. The quantity of debris that could experience erosion due to the break flow, spray flow, or ice melt drainage was determined. Catawba assumes (based on industry testing) that 10 percent of all LDFG that is destroyed but is too large to transport to the ECCS Sump Strainer erodes to individual fiber strands that are transportable. The overall transport fraction for each type of debris was calculated by combining each of the previous steps in a logic tree.

The design and placement of the ECCS Sump Strainer also provides for the filtration of large debris (i.e., fiber insulation clumps and pieces of RMI) entrained in the sump pool prior to reaching the strainer via passage of water through openings in the Crane Wall.

For the postulated limiting break, all fine debris (i.e., dust/dirt, lint, failed coatings particulates, and failed LDFG insulation fibers) was assumed to transport to the ECCS sump pool, and to the strainer itself. Upstream fine debris settling was not credited.

The debris Transport analysis is documented in Reference [26](#).

ECCS Sump Strainer Head Loss:

The ECCS Sump Strainer head loss is determined by combining the calculated clean strainer head loss (hydraulic losses through a clean top-hat module, plenums and waterboxes) with debris head losses obtained from prototype array testing that was performed to determine the cumulative head loss under fiber, particulate and chemical effects loading. The WCAP-16530-NP-A analysis described above predicts that chemical effects will not occur until the sump pool temperature cools to 165°F. As a result, for sump pool temperatures above 165°F, the conventional debris head loss is used while at temperatures below 165°F, the conventional debris combined with the chemical effects head loss is used. Both the conventional debris and chemical effects head losses were determined based on data obtained during prototype array head loss testing.

At the initiation of sump recirculation, the ECCS Sump Strainer is completely submerged and it is assumed a full conventional debris bed has formed on the strainer. No credit is taken for the time-dependent building of a debris bed as the ECCS Sump Strainer is placed in service. In addition, no credit is taken for the static head of water above the minimum height at which the ECCS Sump Strainer can be placed into service. These assumptions as well as additional conservative inputs for the RHR and CS pump calculation of NPSH margin are assumed as described in Sections [6.2.2.3](#) and [6.2.2.2](#).

Considering NPSH, as the ECCS sump pool cools during the ECCS Sump Strainer mission time, the decrease in sump pool temperature (and thus vapor pressure) will largely offset the effect of head loss across the ECCS Sump Strainer, particularly in the SBLOCA case

(considerably less debris would be generated and ECCS flow would be lower). However, as the pool cools and chemical precipitates form, the head loss across the strainer will increase. Thus, the design structural limit of the ECCS Sump Strainer also defines the acceptable head loss across the strainer and debris load. The ECCS Sump Strainer head loss throughout the required 30 day required mission time was determined via combination of testing and analytical methods and was found to be acceptable from both an NPSH and structural integrity perspective.

In addition to ECCS Sump Strainer head loss testing, additional tests were successfully performed to demonstrate the effectiveness of the ECCS Sump Strainers ability to resist air entrainment due to vortex formation, quantification of debris that bypasses the ECCS sump strainer, and the ability of the Catawba ECCS Sump Strainer to accommodate various conventional debris load combinations without forming a thin, high-density debris bed that can result in high head losses.

Strainer Bypass and Downstream Effects

Testing and analyses have been performed to quantify the amount of fibrous debris that could pass through the Top Hat perforated plates, the Debris Bypass Eliminators, and the gaps/openings in the strainer plenums. The results of the analyses show that the maximum total amount of fiber bypass during the ECCS mission time is significantly less than 15g/fuel assembly for the limiting Catawba unit. This limit is used as a criteria for implementing Closure Option 1 outlined in SECY-12-0093, "Closure Options for Generic Safety Issue 191, Assessment of Debris Accumulation on Pressurized-Water Reactor Sump Performance". Since Catawba is classified as an "Option 1" or "clean plant", WCAP 16793-NP, Revision 2 can be utilized to address in-vessel downstream effects.

This evaluation address blockage due to the physical debris that is assumed to bypass the ECCS Sump Strainer as well as chemical precipitants that can form. The methodology and models described in WCAP-16793-NP as well as the Limits and Conditions imposed in the Staff's SER were utilized and addressed to perform this in-vessel evaluation. The results of the evaluation conclude the accumulation and deposition of conventional debris and chemical precipitate debris at the reactor core will not challenge the ability to maintain post-accident Long Term Core Cooling (LTCC) at Catawba.

The effects of debris that bypasses the ECCS Sump Strainer was also evaluated on downstream ECCS components such as pumps, valves, orifices and heat exchangers. By utilizing testing performed by Duke Energy as well as the industry, it was determined the quantity and characteristics of debris that bypasses the Catawba ECCS Sump Strainer is below the expected concentration of debris found within the guidance of WCAP-1604-P, Revision 1. Utilizing the methodologies of WCAP-1604-P as well as addressing the Limits and Conditions contained within the Staff's SER, Catawba demonstrated that downstream ECCS components will not fail due to post-LOCA debris that passes through ECCS Sump Strainer components.

6.3.3 Performance Evaluation

Accidents which require ECCS operation

1. The accidental depressurization of the main steam system.
2. A loss of reactor coolant from small ruptured pipes or from cracks in large pipes.
3. A major reactor coolant system pipe rupture (LOCA).
4. A major secondary system pipe rupture.

5. A steam generator tube rupture.

Accidental Depressurization of the Main Steam System

The most severe core conditions resulting from an accidental depressurization of the main steam system are associated with an inadvertent opening of a single steam dump, relief or safety valve.

In the event of an accidental depressurization of the main steam system, the Safety Injection System is actuated by any of the following:

1. Two-out-of-four pressurizer low pressure signals.
2. Two-out-of-three containment high pressure signals.
3. Manual actuation.

A safety injection signal will rapidly close all feedwater control valves trip the main feedwater pumps, and close the feedwater isolation valves (upper and lower nozzles).

Following the actuation signal, the suction of the charging pumps is diverted from the volume control tank to the refueling water storage tank. The valves isolating the injection header are automatically opened. The charging pumps force boric acid solution from the RWST, through the header and injection line and into the cold legs of each loop. The safety injection pumps also start automatically but provide no flow when the RCS is at normal pressure. The passive injection systems and the low head system also provide no flow at normal RCS pressure.

Results and Conclusions of Accidental Depressurization of Main Steam System

The assumed steam release is typical of the capacity of any single steam dump relief or safety valve. The boric acid solution provides sufficient negative reactivity to maintain the reactor well below criticality. The transient is quite conservative with respect to cooldown, since no credit is taken for the energy stored in the system metal other than that of the fuel elements or the energy stored in the steam generators. Since the transient occurs over a period of about five minutes, the neglected stored energy is likely to have a significant effect in slowing the cooldown. The analysis shows that after reactor trip, assuming a stuck rod cluster control assembly, with offsite power available, and assuming a single failure in the ESF, there will be no consequential damage to the core or RCS.

Loss of Reactor Coolant from Small Ruptured Pipes or from Cracks in Large Pipes Which Actuate Emergency Core Cooling System

A loss of coolant accident is defined as a rupture of the Reactor Coolant System piping or of any line connected to the system. Ruptures of small cross section will cause expulsion of the coolant at a rate which can be accommodated by the charging pumps. For such a break the charging pumps would maintain an operational water level in the pressurizer permitting the operator to execute an orderly shutdown.

The maximum break size for which the normal makeup system can maintain the pressurizer level is obtained by comparing the calculated flow from the RCS through the postulated break against the charging pump makeup flow at normal Reactor Coolant System pressure, i.e., 2250 psia. A makeup flow rate from one centrifugal charging pump is adequate to sustain pressurizer level at 2250 psia for a 0.375 inch diameter break. This break results in a loss of approximately 17.5 lb/sec (127 gpm at 130°F and 2250 psia).

The safety injection signal stops normal feedwater flow by closing the main feedwater line isolation valves and initiates emergency feedwater flow by starting auxiliary feedwater pumps.

The analyses deal with breaks of up to 1.0 ft² in area, where the safety injection pumps play an important role in the initial core recovery because of the slower depressurization of the RCS.

The RCS depressurization and water level transients show that for a break of approximately 3.0 inch equivalent diameter, the transient is turned around and the core is recovering prior to accumulator injection. For a 4.0 inch equivalent diameter break, the core remains uncovered with a decreasing level until accumulator action. Thus, the maximum break size showing core recovery prior to accumulator injection will be approximately 3.0 inch equivalent diameter. Accumulator injection to the cold legs commences when pressure reaches approximately 585 psig.

During a normal startup or shutdown, an automatic SI actuation signal from low pressurizer pressure may be manually blocked.

Results and Conclusions from Analysis of Small Break LOCA

The analysis of this break has shown that the high head portion of the Emergency Core Cooling System, together with accumulators, provide sufficient core flooding to keep the calculated peak clad temperature below required limits of 10 CFR 50.46. Hence, adequate protection is afforded by the ECCS in the event of a small break LOCA.

Major Reactor Coolant System Pipe Ruptures (Loss of Coolant Accident)

A major loss of coolant accident is defined as a rupture 1.0 ft² or larger of the Reactor Coolant System piping including the double ended rupture of the largest pipe in the Reactor Coolant System or of any line connected to that system. The boundary considered for loss of coolant accidents as related to connecting piping is defined in Section [3.6](#).

Should a major break occur, depressurization of the Reactor Coolant System results in a pressure decrease in the pressurizer. Reactor trip occurs when the pressurizer low pressure reactor trip setpoint is reached. The Safety Injection System is actuated when the pressurizer low pressure safety injection actuation setpoints are reached. Reactor trip and safety injection system actuation are also provided by a high containment pressure signal. These countermeasures will limit the consequences of the accident in two ways:

1. Reactor trip and borated water injection provide additional negative reactivity insertion to supplement void formation in causing rapid reduction of power to a residual level corresponding to fission product decay heat.
2. Injection of borated water ensures sufficient flooding of the core to prevent excessive clad temperatures.

When the pressure falls below approximately 585 psig the cold leg injection accumulators begin to inject borated water.

For breaks up to and including the double ended severance of a reactor coolant pipe, the ECCS will limit the clad temperature to well below the melting point and assure that the core will remain in place and substantially intact with its essential heat transfer geometry preserved. See Section [15.6](#) tables for ECCS sequence of events.

Results and Conclusions for Major Reactor Coolant System Pipe Rupture

Conclusions - Thermal Analysis

For breaks up to and including the double ended severance of a reactor coolant pipe, the Emergency Core Cooling System will provide a high level of probability that the Acceptance Criteria as presented in 10CFR 50.46 are met. That is:

1. The calculated peak fuel element clad temperature provides margin to the requirement of 2200°F.
2. The amount of fuel element cladding that reacts chemically with water or steam does not exceed 1 percent of the total amount of Zircaloy in the reactor.
3. The clad temperature transient is terminated at a time when the core geometry is still amenable to cooling. The cladding oxidation limits of 17 percent are not exceeded during or after quenching.
4. The core temperature is reduced and decay heat is removed for an extended period of time, as required by the long-lived radioactivity remaining in the core.

Major Secondary System Pipe Rupture

The steam release arising from a rupture of a main steam pipe would result in energy removal from the RCS causing a reduction of coolant temperature and pressure. In the presence of a negative moderator temperature coefficient, the cooldown results in a reduction of core shutdown margin. There is an increased possibility that the core will become critical and return to power. A return of power following a steam pipe rupture is a potential problem. The core is ultimately shut down by the boric acid injection delivered by the Safety Injection System.

Minimum capability for injection of the boric acid solution is assumed corresponding to the most restrictive single failure in the safety injection system.

The actual modeling of the Safety Injection System in RETRAN-02 is described in Reference [13](#). The calculated transient delivery times for the borated water are listed in [Table 15-15](#). In all cases, borated safety injection from the RWST is preceded by unborated water which is swept from the lines.

For the cases where offsite power is assumed, the sequence of events in the Safety Injection System is the following: After the generation of the safety injection signal (appropriate delays for instrumentation, logic, and signal transport included), the appropriate valves begin to operate and the high head safety injection pump starts. In 19 seconds, the valves are assumed to be in their final position and the pump is assumed to be at full speed. This delay, described above, is inherently included in the modeling.

In cases where offsite power is not available, an additional 14 second delay is assumed to start the diesels and to load the necessary safety injection equipment onto them.

During a normal startup or shutdown, an automatic SI actuation signal from low pressurizer pressure may be manually blocked.

If a steamline rupture occurs while this SI actuation signal is blocked, steamline isolation will occur on high negative steam pressure rate. An alarm for steamline isolation will alert the operator of the accident.

Results and Conclusions of Major Secondary System Pipe Rupture

The analysis has shown that assuming a stuck RCCA with or without offsite power, and assuming a single failure in the engineered safeguards the core remains in place and intact. Radiation doses will not exceed 10CFR 100 guidelines.

Although DNB and possible clad perforation following a steam pipe rupture are not necessarily unacceptable and not precluded in the criterion, the above analysis shows that no DNB occurs for any rupture assuming the most reactive RCCA stuck in its fully withdrawn position.

Steam Generator Tube Rupture

The accident examined is the complete severance of a single steam generator tube assuming it to take place at power.

Assuming normal operation of the various plant control systems, the following sequence of events is initiated by a tube rupture:

1. Pressurizer low pressure and low level alarms are actuated and charging pump flow increases in an attempt to maintain pressurizer level. On the secondary side there is a steam flow/feedwater flow mismatch before the trip as feedwater flow to the affected steam generator is reduced due to the additional break flow which is now being supplied to that unit.
2. Continued loss of reactor coolant inventory leads to a reactor trip signal generated by low pressurizer pressure or overtemperature ΔT . Resultant plant cooldown following reactor trip leads to a rapid change of pressurizer level, and the safety injection signal, initiated by low pressurizer pressure follows soon after the reactor trip. The safety injection signal automatically terminates normal feedwater supply and initiates auxiliary feedwater addition. After reactor trip the break flow reaches equilibrium at the point where incoming safety injection flow is balanced by outgoing break flow. The resultant break flow persists from plant trip until the operator brings the primary system into pressure equilibrium with the ruptured steam generator.
3. The Steam Generator Leakage Monitor adjacent to the affected main steam line will alarm based on increased Nitrogen-16 activity.
4. The condenser off-gas radiation monitor will alarm, indicating a sharp increase in radioactivity in the secondary system and will automatically terminate steam generator blowdown.
5. The reactor trip automatically trips the turbine and, if offsite power is available, the steam dump valves open permitting steam dump to the condenser. In the event of a coincident station blackout, the steam dump valves would automatically close to protect the condenser. The steam generator pressure would rapidly increase resulting in steam discharge to the atmosphere through the steam generator safety and/or power operated relief valves.
6. Following reactor trip, the continued action of auxiliary feedwater supply and borated safety injection flow (supplied from the refueling water storage tank) provide a heat sink which absorbs some of the decay heat. Thus, steam bypass to the condenser, or in the case of loss of offsite power, steam relief to atmosphere, is attenuated during the time in which the recovery procedure leading to isolation is being carried out.
7. Safety injection flow results in increasing pressurizer water level. The time after trip at which the operator can clearly see returning level in the pressurizer is dependent upon the amount of operating auxiliary equipment.

Results and Conclusions of Steam Generator Tube Rupture

A steam generator tube rupture will cause no subsequent damage to the Reactor Coolant System or the reactor core. An orderly recovery from the accident can be completed even assuming simultaneous loss of offsite power.

Existing Criteria Used to Judge the Adequacy of the ECCS

Criteria from 10CFR 50.46

1. Peak clad temperature calculated shall not exceed 2200°F.

2. The calculated total oxidation of the clad shall nowhere exceed 0.17 times the total clad thickness before oxidation.
3. The calculated total amount of hydrogen generated from the chemical reaction of the clad with water or steam shall not exceed 0.01 times the hypothetical amount that would be generated if all of the metal in the clad cylinders surrounding the fuel, excluding the clad around the plenum volume, were to react.
4. Calculated changes in core geometry shall be such that the core remains amenable to cooling.
5. After any calculated successful initial operation of the ECCS, the calculated core temperature shall be maintained at an acceptable low value and decay heat shall be removed for the extended period of time required by long lived radioactivity remaining in the core.

Note: Using a best estimate large break LOCA evaluation model, there must be a high level of probability that the acceptance criteria of 10CFR 50.46 are met.

In addition to 10CFR 50.46, another accident has a more specific criterion as shown below.

For a major secondary system pipe rupture the added criteria is: Assuming a stuck RCCA with or without offsite power, and assuming a single failure in the engineered safeguards the core remains in place and intact.

Use of Dual Function Components

The ECCS contains components which have no other operating function as well as components which are shared with other systems. Components in each category are as follows:

1. Components of the ECCS which perform no other function are:
 - a. One low pressure accumulator for each loop which discharges borated water into its respective cold leg of the reactor coolant loop piping.
 - b. Two safety injection pumps, which supply borated water for core cooling to the RCS. (May be used during check valve testing and for cold leg accumulator makeup also.)
 - c. Associated piping, valves and instrumentation.
2. Components which also have a normal operating function are as follows:
 - a. The residual heat removal pumps and the residual heat exchangers: These components are normally used during the latter stages of normal reactor cooldown and when the reactor is held at cold shutdown for core decay heat removal. However, during all other plant operating periods, they are aligned to perform the low head injection function.
 - b. The centrifugal charging pumps: These pumps are normally aligned for charging service but are automatically aligned to the suction of the refueling water storage tank upon receipt of the safety injection signals. As a part of the Chemical and Volume Control System, the normal operation of these pumps is discussed in [Chapter 9](#).
 - c. The refueling water storage tank: This tank is used to fill the refueling canal for refueling operations. However, during all other plant operating periods it is aligned to the suction of the safety injection pumps, and the residual heat removal pumps.

An evaluation of all components required for operation of the ECCS demonstrates that either:

1. The component is not shared with other systems, or

2. If the component is shared with other systems, it is either aligned during normal plant operation to perform its accident function or, if not aligned to its accident function, two valves in parallel are provided to align the system for injection, and two valves in series are provided to isolate portions of the system not utilized for injection. These valves are automatically actuated by the safety injection signal.

[Table 6-97](#) indicates the alignment of components during normal operation, and the realignment required to perform the accident function.

In all cases of component operation, safety injection has the priority usage such that an "S" signal will override all other signals and start or align systems for injection.

Limits on System Parameters

The analyses show that the design basis performance characteristic of the ECCS is adequate to meet the requirements for core cooling following a loss of coolant accident with the minimum engineered safety feature equipment operating. In order to ensure this capability in the event of the simultaneous failure to operate any single active component, Technical Specifications are established for reactor operation.

Normal operating status of ECCS components is given in [Table 6-98](#).

The ECCS components are available whenever the coolant energy is high and the reactor is critical. During low temperature physics tests there is a negligible amount of stored energy in the coolant and low decay heat; therefore, an accident comparable in severity to accidents occurring at operating conditions is not possible and ECCS components are not as necessary for accident mitigation, although they are still required by the Technical Specification.

The principal system parameters and the number of components which may be out of operation in test, quantities and concentrations of coolant available, and allowable time in a degraded status are illustrated in the Technical Specifications. If efforts to repair the faulty component are not successful the plant is placed into a lower operational status i.e., hot standby to hot shutdown, hot shutdown to cold shutdown, etc.

Boron Precipitation Evaluation

An analysis has been performed to determine the maximum boron concentration in the reactor vessel following a hypothetical LOCA. This analysis used the method and assumptions described in Reference [2](#) with the principal input parameters given in [Table 6-99](#). The analysis considers the increase in boric acid concentration in the reactor vessel during the long term cooling phase of a LOCA, assuming a conservatively small effective vessel volume including only the free volumes of the reactor core and the upper plenum below the bottom of the hot leg nozzles. This assumption conservatively neglects the mixing of the boric acid solution with directly connected volumes, such as the reactor vessel lower plenum. The calculation of boric acid concentration in the reactor vessel considers a cold leg break of the Reactor Coolant System in which steam is generated in the core from decay heat while the boron associated with the boric acid solution is completely separated from the steam and remains in the effective vessel volume.

The results of the analysis show that the maximum allowable boric acid concentration established by the NRC, which is the boric acid solubility limit minus 4 weight percent, will not be exceeded in the vessel if hot leg injection is initiated approximately 6 hours after the LOCA occurs.

The safety injection flow to the Reactor Coolant System hot legs will exceed (assuming failure of one ECCS train) the decay heat mass boil off of approximately 35 lbm/sec. The recommended flow rate should be at least 46 lbm/sec. This hot leg flow will dilute the reactor vessel boron

concentration by passing relatively dilute boron solution from the hot leg through the vessel to the cold leg break location. Centrifugal charging pump flow will continue to be provided to the Reactor Coolant System cold legs and will preclude any boron concentration buildup in the vessel for breaks in the hot leg.

Potential boron precipitation is discussed in Section [6.3.2.5](#). A single active failure analysis is presented in [Table 6-92](#). A passive failure analysis is presented in [Table 6-94](#). In addition [Table 6-91](#) provides a failure mode and effects analysis.

Since the ECCS is designed to meet the single failure criterion, no back up means is required to be provided to prevent the buildup of boron concentration. All components of the ECCS are ANS Safety Class 2 and Seismic Category 1.

ECCS testing is discussed in Section [6.3.4](#).

6.3.4 Tests and Inspections

6.3.4.1 ECCS Performance Tests

HISTORICAL INFORMATION NOT REQUIRED TO BE REVISED

Preoperational Test Program at Ambient Conditions

Preliminary operational testing of the ECCS system as required by Regulatory Guide 1.79 (see Section [1.7](#) for discussion of position on this guide) can be conducted during the hot functional testing of the Reactor Coolant System following flushing and hydrostatic testing, with the system cold and the reactor vessel head removed. Provision is made for excess water to drain into the refueling canal. The ECCS is aligned for normal power operation. Simultaneously, the safety injection block switch is reset and the breakers on the lines supplying offsite power are tripped manually so that operation of the emergency diesels is tested in conjunction with the safety injection system. This test provides information including the following facets:

1. *Satisfactory safety injection signal generation and transmission.*
2. *Proper operation of the emergency diesel generators, including sequential load pickup.*
3. *Valve operating times.*
4. *Pump starting times.*
5. *Pump delivery rates at runout conditions (one point on the operating curve).*

Components

1. Pumps

Separate flow tests of the pumps in the ECCS systems are conducted during the operational startup testing (with the reactor vessel head off) to check capability for sustained operation. The centrifugal charging, safety injection, and residual heat removal pumps will discharge into the reactor vessel through the injection lines, the overflow from the reactor vessel passing into the refueling canal. Each pump is tested separately with water drawn from the RWST. Data is taken to determine pump head and flow at this time.

2. Accumulators

Each cold leg injection accumulator is filled with water from the RWST and pressurized with the MOV on the discharge line closed. The valve is opened and the accumulator allowed to discharge into the reactor vessel as part of the operational startup testing with the reactor cold and the vessel head off.

3. Containment Sump Strainer

Prototype testing was performed to determine the acceptability of the ECCS Sump Strainer design. The main objective of this test was to determine the head loss across a fully developed debris bed under various flow and debris conditions. In addition, tests were performed to:

- Ensure vortices and air ingestion would not occur.
- Quantify and characterize the amount of debris that bypasses the ECC Sump Strainer.
- Assess susceptibility to high density thin debris bed formation that can cause high head losses.

See Section [6.3.2.9](#) for a more detailed description on ECCS Sump Strainer design and testing.

6.3.4.2 Reliability Tests and Inspections

6.3.4.2.1 Description of Tests

Routine periodic testing of the ECCS components and all necessary support systems at power is performed. Valves which operate after a loss of coolant accident are operated through a complete cycle, and pumps are operated individually in this test on their miniflow lines except the charging pumps which are tested by their normal charging function. If such testing indicates a need for corrective maintenance, the redundancy of equipment in these systems permits such maintenance to be performed without shutting down or reducing load under certain conditions. These conditions include considerations such as the period within which the component should be restored to service and the capability of the remaining equipment to provide the minimum required level of performance during such a period.

The operation of the remote stop valve and the check valve in each accumulator tank discharge line may be tested by opening the remote test line valves just downstream of the stop valve and check valve respectively. Flow through the test line can be observed on instruments and the opening and closing of the discharge line stop valve can be sensed on this instrumentation.

Where series pairs of check valves form the high-pressure to low-pressure isolation barrier between the Reactor Coolant System (RCS) and Safety Injection System (SIS) piping outside the reactor containment, periodic testing of these check valves must be performed to provide assurance that certain postulated failure modes will not result in a loss of coolant from the low pressure system outside containment with a simultaneous loss of safety injection pumping capacity.

The SIS test line subsystem provides the capability for determination of the integrity of the pressure boundary formed by series check valves. The tests performed verify that each of the series check valves can independently sustain differential pressure across its disc, and also verify that the valve is in its closed position. The required periodic tests are to be performed after each refueling just prior to plant startup, after the RCS has been pressurized.

Lines in which the series check valves are tested are the safety injection pump cold leg injection lines and the residual heat removal pump cold leg injection lines.

To implement the periodic component testing requirements, Technical Specifications have been established. During periodic system testing, a visual inspection of pump seals, valve packings, flanged connections, and relief valves is made to detect leakage, inservice inspection provides further confirmation that no significant deterioration is occurring in the ECCS fluid boundary.

Design measures have been taken to assure that the following testing can be performed:

1. Active components may be tested periodically for operability (e.g., pumps on miniflow, certain valves, etc.).
2. An integrated system actuation test¹ can be performed when the plant is cooled down and the Residual Heat Removal System (RHRS) is in operation.

The ECCS will be arranged so that no flow will be introduced into the RCS for this test.

3. An initial flow test of the full operational sequence can be performed.

The design features which assure this test capability are specifically:

1. Power sources are provided to permit individual actuation of each active component of the ECCS.
2. The safety injection pumps can be tested periodically during plant operation using the minimum flow recirculation lines provided.
3. The residual heat removal pumps are used every time the RHRS is put into operation. They can also be tested periodically when the plant is at power using the miniflow recirculation lines.
4. The centrifugal charging pumps are either normally in use for charging service or can be tested periodically.
5. Remote-operated valves can be exercised during routine plant maintenance.
6. Level and pressure instrumentation is provided for each accumulator tank, for continuous monitoring of these parameters during plant operation.
7. Flow from each accumulator tank can be directed at any time through a test line to determine check valve leakage and to demonstrate operation of the accumulator motor-operated valves.
8. A flow indicator is provided in the safety injection pump header, and in the residual heat removal pump headers. Pressure instrumentation is also provided in these lines.
9. An integrated system test can be performed when the plant is cooled down and the RHRS is in operation. This test does not introduce flow into the RCS but does demonstrate the operation of the valves, pump circuit breakers, and automatic circuitry including diesel starting and the automatic loading of ECCS components of the diesels (by simultaneously simulating a loss of offsite power to the vital electrical buses).

Refer to the Technical Specifications for the selection of test frequency, acceptability of testing, and measured parameters. A description of the inservice inspection program is also included in the Technical Specifications. ECCS components and systems are designed to meet the intent of ASME Code Section XI for inservice inspection.

¹ Details of the testing of the sensors and logic circuits associated with the generation of a safety injection signal together with the application of this signal to the operation of each active component are given in Section [7.2](#).

6.3.5 Instrumentation Requirements

Instrumentation and associated analog and logic channels employed for initiation of Emergency Core Cooling System (ECCS) operation is discussed in Section [7.3](#). This section describes the instrumentation employed for monitoring ECCS components during normal plant operation and also ECCS post accident operation. All alarms are annunciated in the control room.

6.3.5.1 Temperature IndicationResidual Heat Exchanger Temperature

The fluid temperature at the inlet and outlet of each residual heat exchanger is monitored by locally mounted temperature indicators and recorded on the main control board.

6.3.5.2 Pressure IndicationSafety Injection Header Pressure

Safety injection pump discharge header pressure is indicated in the control room.

Accumulator Pressure

Duplicate pressure channels are installed on each accumulator. Pressure indication in the control room and high and low pressure alarms are provided by each channel.

SIS Test Line Pressure

Pressure in this line is measured by a locally mounted pressure indicator.

Residual Heat Removal Pump Discharge Pressure

Residual heat removal discharge pressure for each pump is indicated in the control room. A high pressure alarm is actuated by each channel.

6.3.5.3 Flow IndicationCharging Pump Injection Flow

Total charging pump injection flow is measured by a meter mounted in the common 4" injection header between the charging pump discharge and the individual cold leg injection lines. Readout is provided on the main control board.

Safety Injection Pump Header Flow

Flow through the safety injection pump header is indicated in the control room.

Residual Heat Removal Return Line Flow

Flow through each residual heat removal injection and recirculation header leading to the reactor cold legs is indicated in the control room. This instrumentation also controls total RHR flow during cooldown.

SIS Test Line Flow

Local indication of safety injection test line flow is provided.

Residual Heat Removal Hot Leg Injection Flow

The return flow from the residual heat removal loop to the reactor hot legs is indicated in the control room.

Safety Injection Pump Minimum Flow

A flow indicator is installed in the safety injection pump minimum flow line.

Residual Heat Removal Pump Minimum Flow

Differential pressure switches installed in each residual heat removal pump discharge header provide control for the valve located in the pump minimum flow line.

6.3.5.4 Level Indication

Refueling Water Storage Tank Level

Four water level wide range indicator channels and two narrow range instrument loops, which indicate in the control room, are provided for the refueling water storage tank. Any one narrow range instrument loop provides a high level alarm and make up level alarm. Any one wide range channel provides a pre lo level alarm, lo level alarm, or lo-lo level alarm. All of the RWST wide range level channels are connected so that 2/4 channels produce an additional alarm indicating low level, which is used to initiate automatic switchover of the residual heat removal pumps at low level for containment recirculation.

The high level alarm is provided to protect against possible overflow of the refueling water storage tank. The tank level at makeup alarm is provided to assure that a sufficient volume of water is always available in the refueling water storage tank in conformance with the Technical Specifications. The lo level alarm alerts the operator to initiate switchover of the RHR pumps. The low-low level alarm alerts the operator to initiate switchover of the suction of the NI and NV pumps. These are the last manual actions required to switchover the suction of the ECCS pumps to the containment recirculation sump.

In addition to the containment recirculation, the RWST Lo Level setpoint also de-energizes the RWST heaters. During outages, Mode 5, 6 and No Mode, it is desirable to maintain heating of the RWST even below the normal Lo Level setpoint. Therefore, during these modes the RWST Lo Level setpoint is reduced to 11% FWST level.

Deleted Per 2012 Update.

Accumulator Water Level

Duplicate water level channels are provided for each accumulator. Both channels provide indication in the control room and actuate high and low water level alarms.

Containment Water Level

The containment water level instrumentation provides continuous indication in the main control room. This instrumentation measures water level up to 20 feet above the bottom of containment (lowest floor elevation with exception of the incore instrument cavity). This is in excess of the maximum possible post-LOCA flood level. This instrumentation is nuclear safety related and is qualified to operate in the post accident environmental conditions. Also, two level switches per train are provided to annunciate when swap to sump is allowable for ECCS and NS.

6.3.5.5 Valve Position Indication

Valves which are controlled from the main control board show a green status light if the valve is closed and a red status light if open. In addition, all pumps and valves which are an integral part of, or associated with the Engineered Safeguards Systems (used for injection, containment spray and recirculation) have an operation/position status light. These monitor status lights are displayed on the main control board within easy view of the plant operator. When the plant is in normal, full power operation, the component monitor lights should not, in general, be lighted. The only time the monitor lights should be lighted is when the component operating mode changes to the off-normal condition. In addition to the lighting arrangement, certain critical valves have an annunciator to indicate and alarm a change to the off-normal operational mode.

Cold Leg Accumulator Isolation Valve Position Indication

The accumulator isolation valves are provided with red (closed) and green (open) position indicating lights located at the control switch for each valve. These lights are powered by valve control power and actuated by valve motor operator limit switches.

A monitor light that is on when the valve is not fully open is provided in an array of monitor lights for each of the accumulator isolation valves. This light is actuated by a valve motor-operated limit switch.

An alarm annunciator point is activated by both a valve motor-operator limit switch and by a valve position limit switch activated by stem travel whenever an accumulator valve is not fully open for any reason with the system at pressure (the pressure at which the safety injection block is unblocked is approximately 1900 psig). A separate annunciator point is used for each accumulator valve. This alarm will be recycled at approximately one hour intervals to remind the operator of the improper valve lineup.

6.3.6 References

1. Alden Research Laboratory, "Assessment of Flow Characteristics Within Reactor Building Using a Scale Model for McGuire Nuclear Station," May 1978.
2. Westinghouse Letter CLC-NS-309, C. L. Caso to T. M. Novak, April 1, 1975.
3. Nuclear Regulatory Commission, Letter to All Holders of Operating Licenses for Nuclear Power Reactors, from James G. Partlow, May 11, 1993, NRC Bulletin No. 93-02, "Debris Plugging of Emergency Core Cooling Suction Strainers."
4. Duke Power Company, Letter from D.L. Rehn to NRC, June 10, 1993, re: Response to NRC Bulletin No. 93-02, "Debris Plugging of Emergency Core Cooling Suction Strainers."
5. Duke Power Company, Letter from D.L. Rehn to NRC, September 16, 1993, re: Response to NRC Bulletin No. 93-02, "Debris Plugging of Emergency Core Cooling Suction Strainers," Supplemental Response.
6. Duke Power Company, Letter from D.L. Rehn to NRC, September 30, 1993, re: Response to NRC Bulletin No. 93-02, "Debris Plugging of Emergency Core Cooling Suction Strainers," Supplemental Response.
7. Duke Power Company, Letter from D.L. Rehn to NRC, December 15, 1993, re: Response to NRC Bulletin No. 93-02, "Debris Plugging of Emergency Core Cooling Suction Strainers," Supplemental Response.
8. Duke Power Company, Letter from D.L. Rehn to NRC, May 9, 1994, re: Response to NRC Bulletin No. 93-02, "Debris Plugging of Emergency Core Cooling Suction Strainers," Supplemental Response.
9. Duke Power Company, Letter from D.L. Rehn to NRC, June 2, 1994, re: Request for Additional Information on NRC Bulletin 93-02 (Debris Plugging of Emergency Core Cooling), TAC Nos. M86545 and M86546.
10. Nuclear Regulatory Commission, Letter from R.E. Martin to D.L. Rehn (DPC), June 10, 1994, re: Catawba, Units 1 and 2 - Response to NRC Bulletin 93-02, "Debris Plugging of Emergency Core Cooling Section Strainers" (TAC Nos. M86545 and M86546).
11. Nuclear Regulatory Commission, Letter to Holders of Operating Licenses for Nuclear Power Plants, Except Those Who Have Permanently Ceased Operations and Have Certified That Fuel Has Been Permanently Removed from the Reactor Vessel, from Jack W. Roe,

- October 7, 1997, "Assurance of Sufficient Net Positive Suction Head for Emergency Core Cooling and Containment Heat Removal Pumps (Generic Letter 97-04)."
12. Duke Power Company, Letter from M.S. Tuckman to the NRC, January 5, 1998, re: Response to Generic Letter 97-04, "Assurance of Sufficient Net Positive Suction Head for Emergency Core Cooling and Containment Heat Removal Pumps."
 13. "McGuire and Catawba Nuclear Stations, Multidimensional Reactor Transients and Safety Analysis Physics Parameters Methodology," DPC-NE-3001-PA, Duke Power Company, Revision 0a, May, 2009.
 14. Karassik, Igor; et al, copyright © 1986 Pump Handbook Second Edition, ISBN 0-07-033302-5.
 15. Letter to the U.S. Nuclear Regulatory Commission from T.P. Harrall dated October 13, 2008, titled "Duke Energy Carolinas, LLC (Duke) Oconee Nuclear Station, Units 1, 2 & 3, Docket Nos. 50-269, 50-270, 50-287, McGuire Nuclear Station, Units 1 & 2, Docket Nos. 50-369, 50-370, Catawba Nuclear Station, Units 1 & 2, Docket Nos. 50-413, 50-414, Generic Letter 2008-01, 9-Month Response.
 16. Letter J.M. Morris (Duke) to USNRC Document Control Desk, Subject: NRC Generic Letter 2004-02, "Potential Impact of Debris Blockage on Emergency Recirculation During Design Basis Accidents at Pressurized Water Reactors," dated February 29, 2008.
 17. Letter J.M. Morris (Duke) to USNRC Document Control Desk, Subject: Response to NRC Generic Letter 2004-02, "Potential Impact of Debris Blockage on Emergency Recirculation During Design Basis Accidents at Pressurized Water Reactors," dated April 30, 2008.
 18. Letter to the U.S. Nuclear Regulatory Commission from Regis Repko dated September 30, 2010, McGuire Nuclear Station Units 1 and 2 and Catawba Nuclear Station Units 1 and 2, "Draft Responses to NRC Request for Additional Information (RAI) related to Generic Letter 9GL) 2004-02 - Potential Impact for Debris Blockage on Emergency Recirculation During Design Basis Accidents at Pressurized Water Reactors".
 19. Letter to the U.S. Nuclear Regulatory Commission from Kelvin Henderson dated August 13, 2012, Catawba Nuclear Station Units 1 and 2, "Final Responses to NRC Request for Additional Information (RAI) related to Generic Letter (GL) 2004-02, "Potential Impact of Debris Blockage on Emergency Recirculation During Design Basis Accidents at Pressurized Water Reactors".
 20. Letter to the U.S. Nuclear Regulatory Commission from Kelvin Henderson dated May 13, 2013, Catawba Nuclear Station Units 1 and 2, "Closure Options for Generic Safety Issue (GSI)-191, "Assessment of Debris Accumulation on Pressurized-Water Reactor Sump Performance" in Resolution of Final Issues Related to Generic Letter (GL) 2004-02, "Potential Impact of Debris Blockage on Emergency Recirculation During Design Basis Accidents at Pressurized-Water Reactors".
 21. Letter to the U.S. Nuclear Regulatory Commission from Kelvin Henderson dated July 31, 2013, Catawba Nuclear Station Units 1 and 2, "Catawba Nuclear Station Closure Option 1 Response to In-Vessel Downstream Effects Request for Additional Information for Generic Safety Issue (GSI) 191, "Assessment of Debris Accumulation on Pressurized-Water Reactor Sump Performance" in Resolution of Final Issues Related to Generic Letter (GL) 2004-02, "Potential Impact of Debris Blockage on Emergency Recirculation During Design Basis Accidents at Pressurized-Water Reactors".

22. Letter from NRC to Kelvin Henderson dated December 31, 2013, Catawba Nuclear Station Units 1 and 2, "Closeout of Generic Letter, 2004-02 - Potential Impact of Debris Blockage on Emergency Recirculation During Design Basis Accidents at Pressurized Water Reactors".
23. NEI 04-07, Pressurized Water Reactor Sump Performance Evaluation Methodology
24. CNC-1223.11-00-0041, Fibrous Insulation Debris Generated due to a LBOCA Inside Containment.
25. CNC-1223.11-00-0037, GSI-191 ECCS Recirculation Sump NEI 04-07 Refined Analysis (Vendor Calc ALION-CAL-DUKE-2720-04)
26. CNC-1223.11-00-0038, GSI-191 ECCS Recirculation Sump NEI 04-07 Refined Analysis (Vendor Calc ALION-CAL-DUKE-2720-07)
27. CNC-1223.11-00-0047, Refinement of Unqualified Coating Failure Assumptions for Contribution to ECCS Sump Strainer Particulate Loads.
28. CNC-1223.11-00-0043, Catawba Units 1 and 2 Containment Buildings Tag and Label Reductions.
29. CNC-1223.01-00-0012, Aluminum Inventory Inside Containment.
30. CNC-1223.11-00-0042, Catawba Units 1 and 2 Containment Recirculation Sump Top-Hat Strainer Hydraulic Certification Report.

THIS IS THE LAST PAGE OF THE TEXT SECTION 6.3.

6.4 Habitability Systems

6.4.1 Design Bases

The Control Room Envelope Habitability System is comprised of the equipment, components, and the building enclosure that are provided to ensure a suitable environment is maintained for personnel and equipment in the control room envelope for safe, long-term occupancy during both normal and emergency operation of the plant. The design bases of the habitability system for the control room envelope includes:

1. The capability to withstand the safe shutdown earthquake,
2. The capability to function properly following any single active failure,
3. The capability to function during a design basis tornado,
4. The capability to detect and limit concentrations of chlorine gas as specified in Regulatory Guide 1.95 (see [Table 6-100](#)) or products of combustion entering the control room,
5. The capability to shield control room envelope personnel from radiation sources, such that exposure to personnel will not exceed the limits specified in General Design Criterion 19 of Appendix A to 10CFR 50,
6. The capability to detect and limit the introduction of airborne radioactive contamination into the control room envelope such that exposure to personnel will not exceed the limits specified in General Design Criterion 19 of Appendix A to 10CFR 50, and
7. The capability to permit safe shutdown of the plant from the control room following a loss-of-coolant accident (LOCA).

6.4.2 System Design

6.4.2.1 Definition of Control Room Envelope

The control room envelope is shared for the operation of both units, and includes the control room proper (elev. 594'), with the pressure boundary consisting of the control room walls, floors, roof, doors, and any penetrations of those in addition to the ductwork, lampers, filter units, and fan housings of the Control Room Area Ventilation System. The control room envelope requires continuous occupancy while other areas referred to as the control room area, (the mechanical equipment room, cable room, battery room, electrical penetration room (594' elev. only), switchgear rooms and motor control center rooms) require infrequent access.

All controls and displays necessary to bring the plant to a safe shutdown condition are included within the control room envelope or control room area. All necessary activities that must take place in the control room area are such that they can be completed within a short time.

6.4.2.2 Ventilation Systems

The Control Room Area Ventilation System design is described in detail in Section [9.4.1](#).

6.4.2.3 Leak Tightness

The pressurizing air flow rate necessary to maintain the control room envelope at a positive pressure is determined by the leakage characteristics of the control room envelope enclosure. Assuming a 1/32" crack around enclosure penetrations due to aging of the sealant and

assuming a 1/4" water gauge pressure differential between the control room and the Auxiliary Building, a pressurizing air flow rate of 1,590 cfm is calculated. A pressurizing air flow rate of 2,000 cfm is provided to ensure pressurization and to provide adequate design margin.

The control room is formed by the:

1. Reinforced concrete floor, roof and walls described in Section [3.8.4](#),
2. Seismic block walls described in Section [3.8.4](#),
3. Low leakage seals for all electrical lines and ventilation ducts penetrating the control room, and
4. Low leakage door seals.

The control room is virtually insensitive to wind effects since only a small portion of wall on the west side and the control room roof is exposed to the outside.

The roof, floor and a major portion of the walls of the control room are constructed of reinforced concrete. The remaining walls are of seismic concrete block construction with voids filled with concrete. Leakage paths are minimized with this type construction, thus, infiltration and exfiltration are negligible through this type construction.

Electrical and ventilation duct penetrations through the control room are provided with low leakage seals. Doors which penetrate the control room are provided with seals which exhibit low leakage characteristics.

During a postulated period when both intakes are closed, assuming a 1/32" crack around all duct openings, cable openings and door openings due to aging of the sealant, a 1/8" water gage pressure differential would cause a 1125 CFM leak rate. A pressure differential of 0.05" water gage, which would be a more realistic figure, would cause a 710 CFM leak rate. This is based on the fact that plant architectural design eliminates wind effects, thermal column effects, and barometric pressure changes.

6.4.2.4 Interaction With Other Zones and Pressure-Containing Equipment

Portions of the Auxiliary Building Ventilation Zone and the Service Building Ventilation Zone are adjacent to the control room envelope habitability area. The Auxiliary Building is adjacent to the control room envelope to the north and south, and the Service Building is adjacent to the control room envelope to the west. The remaining control room envelope interfaces are with other areas of the control complex. The control room envelope is pressurized and tested to verify that it is at least 1/8" greater in pressure than all adjacent areas. This assures that the transfer of toxic or radioactive gases into the control room envelope is prevented. Penetrations between the control room envelope and other zones are provided with low leakage seals.

Two ducts serving the electrical penetration rooms pass through the control room envelope. These ducts penetrate the control room envelope, but do not communicate with the control room envelope environment. One duct is a supply system which is conditioned and filtered in the same manner as the control room envelope supply system. The remaining duct is a return system operating at a slight negative pressure, thus, the potential leak path is into the duct system.

In general, pressure-retaining equipment or piping is not permitted in the control room envelope. Several small hand-held fire extinguishers are located within the area for local fire control. Several self-contained type breathing devices are located within the control room envelope. Areas of the Auxiliary Building and the Service Building which contain high-pressure equipment or piping have no direct interface with the control room envelope.

6.4.2.5 Shielding Design

Refer to Section [12.3.2](#).

6.4.3 System Operational Procedures

The control room envelope is served by the Control Room Area Ventilation System. The operation of the ventilation system is the same for all plant operational modes. The pressurization system utilizes filters as described in Section [12.3.3](#) for filtration of pressurizing air during all modes of plant operation.

Each outside air intake for the pressurizing system is monitored for the presence of radioactivity, chlorine, and products of combustion during all plant operation modes. Indication of a high radiation level, smoke or chlorine in the intakes is alarmed in the control room. Isolation of the affected intake(s) is initiated manually from the control room as required.

6.4.4 Design Evaluation

6.4.4.1 Radiological Protection

Refer to Section [15.0](#).

6.4.4.2 Toxic Gas Protection

A hazards analysis for toxic material is presented in Section [2.2](#). The habitability of the control room envelope was evaluated to determine if a site-related or off-site accident involving a release of hazardous chemicals exceeds the toxicity limits as specified in Regulatory Guide 1.78 (see [Table 6-101](#)). The survey has determined that the off-site storage and transportation of hazardous chemicals for industries in the vicinity of the plant is of sufficient distance (5 miles) from the plant that they do not present a hazard to the plant.

A review of onsite chemicals was also done to determine if any impact to control room envelope habitability existed. In general, it is not possible for gases to “leak” into the control room because the CNS control room is maintained at a positive pressure. However, if a gaseous substance were to get into the Control Room Area Ventilation (VC) System outside air intakes, it would eventually be discharged into the control room envelope unless it was filtered out by the VC system filter unit. Most chemicals stored at CNS are not gases and do not pose a toxic gas concern. The potential to generate hazardous fumes from the accidental mixing or spilling of these chemicals is assumed to be controlled under the site Chemical Control Program (EWP 7.0) and various design features, such as catchments and physical separation. There are, however, two gases used onsite that require review to determine if they pose a habitability concern. These gases are chlorine and carbon dioxide. Chlorine is a potential concern because of its highly toxic nature. Carbon dioxide is stored onsite in large quantities and has the potential to cause asphyxiation.

There are two potential sources of chlorine gas at CNS. One is from the accidental mixing of hypochlorite and sulfuric acid, and the other is from liquefied chlorine that is used for water treatment. The mixing of hypochlorite and sulfuric acid was considered a potential source of chlorine gas during initial startup because both of these chemicals were stored at the Water Chemistry Building in bulk quantities. However, hypochlorite is no longer stored at the Water Chemistry Building and there are no credible scenarios in which hypochlorite and sulfuric acid can mix. Therefore, this source of chlorine is no longer a concern at CNS.

An assessment was completed to determine if the present use of liquefied chlorine at CNS created a control room envelope habitability concern. Based on the guidance in Regulatory Guides 1.78 and 1.95, the quantities used onsite are small enough and stored/used at distances far enough from the control room envelope intakes that a control room envelope habitability issue is not created. Additionally, an evaluation of the likelihood of a chlorine release at the usage or storage locations showed that there are no credible accident scenarios that would allow a gaseous chlorine release to flow to and enter a control room envelope outside air intake.

Based on the limited quantities of chlorine used and stored at CNS, chlorine is not considered a control room envelope habitability concern. Chlorine detectors have been installed in the VC system to provide a defense-in-depth function against an accidental chlorine spill. These detectors are non-safety related instruments and do not have any automatic intake isolation function. There is, however, the capability for manual isolation of either outside air intake. The chlorine detection system will be controlled under the SLCs program.

Carbon dioxide is not a toxic gas but it could create a control room envelope habitability concern due to its asphyxiation potential. This substance is used in the fire suppression system for the diesels and the CA Pumps. The carbon dioxide used in the diesel fire suppression system is contained in two 7.5 ton tanks. The tanks are located on the 594 elevation in the east end of the Turbine Building (one tank in the Unit 1 Turbine Building and one tank in the Unit 2 Turbine Building). Because carbon dioxide is heavier than air, a spill within the Turbine Building would result in the gas falling into the Turbine Building basement through any number of large openings in the Turbine Building floor. Releases through the diesel fire system piping are not considered since the piping is empty except when the system is in service and pipe breaks during a diesel fire are not considered to occur concurrently.

The carbon dioxide used for the CA Pumps fire suppression system is contained in 36 cylinders located on the 543 elevation of the Auxiliary Building. Of these 36 cylinders, 18 are in the Unit 1 CA Pump room and 18 are in the Unit 2 CA Pump room. Each Pump room has 2 banks of 9 cylinders; one bank as a primary source and one bank as a backup source. A release from any of these cylinders or discharge headers would result in carbon dioxide either staying on the 543 elevation or falling to a lower elevation within the Auxiliary Building. Any carbon dioxide spill would be readily detectable by station personnel since carbon dioxide forms a visible white fog when released. This fog would alert station personnel to take the necessary actions to correct any leakage.

Based on the above reasoning, it is not credible to assume that carbon dioxide could get into a control room envelope intake. The fact that the control room envelope is normally pressurized prevents gases from "leaking" into the space through cracks or other opening. Therefore, carbon dioxide is not considered a control room envelope habitability concern.

6.4.5 Testing and Inspection

Italicized text below is HISTORICAL INFORMATION, NOT REQUIRED TO BE REVISED.

Preoperational tests are performed on the Control Area Ventilation System to ensure that all equipment meets the design criteria during all modes of operation. Periodic tests have been performed to demonstrate system readiness and operability, as required by the Technical Specifications.

In-place testing of the outside air pressurizing filter trains will be performed in accordance with test methods and acceptance criteria described in Regulatory Guide 1.52.

6.4.6 Instrumentation Requirements

Sufficient indications in the form of status lights and performance readouts are provided in the control room to evaluate the ventilation system operation and indicate system malfunctions. Refer to Section [7.8](#).

Chlorine, smoke, and radiation detectors are located in each outside air intake duct for the pressurizing system. These functions are described in Sections [6.4.3](#) and [9.4.1.1](#).

THIS IS THE LAST PAGE OF THE TEXT SECTION 6.4.

THIS PAGE LEFT BLANK INTENTIONALLY.

6.5 Fission Product Removal and Control Systems

6.5.1 Engineered Safety Feature (ESF) Filter Systems

The following filter systems perform safety-related functions following a DBA:

1. Annulus Ventilation System
2. Control Room Area Pressurizing System
3. Fuel Handling Area Exhaust System
4. Auxiliary Building Filtered Exhaust System

6.5.1.1 Design Bases

General Design Criteria 41, 42, and 43 of Appendix A to 10 CFR Part 50 requires that containment atmosphere cleanup systems be provided as necessary to reduce the concentration and quality of fission products released to the environment following a DBA and that these systems be designed to permit periodic inspection and testing. The Annulus Ventilation System is based on exhaust flow required to produce a negative pressure in the annulus within sixty seconds following receipt of an Engineered Safety Feature signal. Design bases of the Annulus Ventilation System are discussed in Section [9.4.9.1](#).

General Design Criterion 19 of Appendix A to 10CFR Part 50 requires adequate radiation protection to permit access and occupancy of the control room during and following the DBA. The Control Room Area Pressurizing System design bases are discussed in Section [9.4.1.1](#).

General Design Criteria 60 and 61 of Appendix A to 10CFR Part 50 require fuel storage and handling area filter systems be provided to control the release of fission products to the environment following the DBA and that these systems be designed to permit periodic inspection and testing. The Fuel Handling Area Exhaust System design bases are discussed in Section [9.4.2.1](#).

The Auxiliary Building Filtered Exhaust System design bases are discussed in Section [9.4.3.1](#).

Fission product removal capability of all ESF filter systems is based on the design, construction, operation, maintenance, and testing requirements of Regulatory Guide 1.52, Revision 2.

6.5.1.2 System Design

Design features of each ESF filter system are compared to the positions detailed in Regulatory Guide 1.52, Revision 2, in Tables [12-23](#), [12-24](#), [12-25](#) and [12-26](#). An alternate method is provided for each design item to which an exception is taken.

6.5.1.3 Design Evaluation

The ESF filter systems conform to the design criteria established in Regulatory Guide 1.52, Revision 2 as shown in Tables [12-23](#), [12-24](#), [12-25](#) and [12-26](#).

The Annulus Ventilation System safety evaluation is discussed in Section [9.4.9.3](#).

The Control Room Area Pressurizing System safety evaluation is discussed in Section [9.4.1.3](#).

The Fuel Handling Area Exhaust System safety evaluation is discussed in Section [9.4.2.3](#).

The Auxiliary Building Filtered Exhaust System safety evaluation is discussed in Section [9.4.3.3](#).

ESF filter systems ductwork is designed to withstand the Safe Shutdown Earthquake. Ductwork was leak tested during startup in accordance with Regulatory Guide 1.52, Revision 2, Position C.2.I.

6.5.1.4 Tests and Inspections

Preoperational testing and periodic inspection of ESF filter systems is in accordance with Regulatory Guide 1.52, Revision 2, Positions 3, 5, and 6.

Inspection and testing to demonstrate system readiness and operability is discussed in Sections [9.4.1.4](#), [9.4.2.4](#), [9.4.3.4](#), and [9.4.9.4](#) for each ESF filter system.

6.5.1.5 Instrumentation Requirements

Each ESF Filter system is provided with instrumentation as described in this section. Typical ESF filter system layout is shown in [Figure 12-30](#).

Local temperature indication is provided upstream and downstream of heater sections. Differential pressure gauges are provided across each individual filter bank to locally monitor resistance. Total filter train differential pressure transmitters are provided to give control room indication and high pressure alarm. Carbon absorber sections are provided with temperature transmitters to give Control Room indication of high temperature and fire alarm. Air flow monitors are provided downstream of filter systems giving Control Room indication of flow rate.

The Annulus Ventilation System and Auxiliary Building Filtered Exhaust System are actuated by Engineered Safety Feature signals discussed in Section [7.3](#).

The Control Room Area Pressurization System operates continuously.

The Fuel Handling Area Exhaust System Filter Train is actuated by radiation monitoring devices described in Section [9.4.2.2](#).

Instrumentation conforms to the recommendations of Regulatory Guide 1.52 as shown in Tables [12-23](#), [12-24](#), [12-25](#) and [12-26](#).

6.5.1.6 Materials

Materials used in all ESF filter systems are in accordance with the Regulatory Guide 1.52, Revision 1, "Component Design Criteria and Qualification Testing" Position. Adsorbent material is impregnated activated carbon qualified in accordance with ANSI N509, 1980, [Table 5-1](#).

While maintaining filter system capacity, use of gasket material and filter medium is minimized to preclude the interference of any radiolytic or pyrolytic products with system operation. System design incorporates 100% redundancy to ensure system integrity and availability.

6.5.2 Containment Spray Systems

The Containment Spray System is assumed to remove fission products following a design basis accident and credit is taken in the calculations of post LOCA radiation doses. No credit is taken for removal of fission products by the Containment Spray System following a rod ejection accident.

6.5.3 Fission Product Control Systems

6.5.3.1 Primary Containment

There is no primary containment ventilation system to control release of fission products following the DBA. The Annulus Ventilation System, serving the secondary containment, is the means of controlling release of fission products postulated to leak from the primary containment following the DBA.

6.5.3.2 Secondary Containment

The Annulus Ventilation System is designed primarily to remove fission products from the secondary containment atmosphere. The Annulus Ventilation System also serves to control the release of secondary containment fission products following the DBA as described in Section [9.4.9.3](#).

6.5.4 Ice Condenser as a Fission Product Cleanup System

No credit is taken for fission product removal by the ice condenser in the current license basis calculation of post accident-radiation doses. The information below is retained as a historical record.

HISTORICAL INFORMATION NOT REQUIRED TO BE REVISED

The Ice Condenser System is an Engineered Safety Feature designed to serve as a containment air purification and cleanup system. The Ice Condenser serves primarily as a large heat sink to readily reduce the containment temperature and pressure and condense the steam. For this purpose, ice is stored in a closed compartment between the lower and upper compartments of the Containment. The Containment is designed such that the only significant flow path from the lower to the upper compartment is through the ice bed. Immediately following a LOCA, a large pressure differential exists between the lower and upper compartment; thereby providing flow through the ice bed. Later in the transient flow is provided by two 40,000 cfm fans which circulate upper containment air into the lower compartment. The ice bed absorbs molecular iodine from the containment atmosphere. The removal is particularly effective as all air flow from the lower to the upper compartments must pass through the ice bed. To enhance the iodine absorption capacity of the ice, the ice solution is adjusted to an alkaline pH to promote iodine hydrolysis to non-volatile forms.

The physical characteristics of the Ice Condenser System are discussed in Section [6.7](#). The ice bed fission product removal capability is discussed in this section.

6.5.4.1 Ice Condenser Design Basis (Fission Product Cleanup Function)

The design basis of the ice condenser as an iodine removal system is to use the chemical and physical properties of ice to reduce the fission product iodine concentration in the post LOCA containment atmosphere.

6.5.4.2 Ice Condenser System Design

The function of the post LOCA iodine removal served by the Ice Condenser is accomplished by chemically controlling the alkaline ice to a pH range of 9.0 to 9.5. This is accomplished by adding sodium tetraborate to the Grade A feedwater in the solution of $\text{Na}_2\text{B}_4\text{O}_7 \cdot 10\text{H}_2\text{O}$ with approximately 2000 ppm of boron prior to ice basket loading. During the accident, the melting

ice provides a medium for removal of iodine from the containment atmosphere and fixation in solution.

6.5.4.2.1 Component Description

The component description of the Ice Condenser System is given in Section [6.7](#).

6.5.4.2.2 System Operation

The operation of the Ice Condenser System is described in Section [6.7](#).

6.5.4.3 Ice Condenser System Design Evaluation (Fission Product Cleanup Function)

Experimental and analytical efforts by Westinghouse have proved the Ice Condenser System to be an effective system for removing elemental iodine from the containment atmosphere and thereby reducing the off-site doses following a Loss of Coolant Accident.

The results of the ice condenser experimental program are reported in WCAP-7426, a non-proprietary topical report. The results of these bench scale tests indicate that an ice condenser system containing sodium tetraborate ice could effectively remove elemental iodine from the containment atmosphere.

To apply the results of the bench scale tests to a full size system an analytical model has been developed from the experimental data.

The purpose of this section is to describe the analytical model and present the results of the ice condenser iodine removal effectiveness analysis.

Analytical Model

Following a LOCA a large volume of steam will discharge into the containment lower compartment. Containment pressure and temperature would immediately rise. Initially, the increased pressure in the lower compartment will force steam through the ice condenser sections and later recirculation fans would circulate the iodine-air-steam mixture.

Elemental iodine may be liberated into the containment in gaseous form. A fraction of the iodine in the containment atmosphere will exist as methyl iodine which is not assumed to be removed by the ice condenser. Elemental iodine is removed from the air-steam mixture by the ice condenser, as it is readily soluble in alkaline solution.

The ice in the ice condenser will contain sodium tetraborate normally referred to as alkaline ice by virtue of the alkalinity of the ice melt.

Data obtained from the experimental program as reported in WCAP-7426 is based on both alkaline and acid ice. The ice condenser iodine removal efficiency is based on the alkaline ice tests.

The theoretical analysis for iodine removal by alkaline ice treats the ice condenser as two distinct compartments, an ice section and a rain section. Melt, falling from the ice into the sump comprises the rain section (see [Figure 6-137](#)). Steam condenses from the air-steam mixture in both sections. In the ice section $(1 + \lambda_v/\lambda_f)$ grams of melt mixture are formed per gram of steam condensed, where λ_v is latent heat of vaporization of water and λ_f is latent heat of fusion of water. In the rain section, however, only 1 gram of melt mixture is formed per gram of steam condensed. Melt temperature rises above 32°F as steam condenses in the rain. As time progresses, melting ice, the rain section plays a more significant role in iodine removal.

An equation for iodine removal efficiency is obtained by solving the multicomponent diffusion equations for steam-air-iodine mixtures in both the ice and rain sections.

In the rain section iodine is treated as a trace component with air and steam as the bulk constituents. Iodine from the bulk vapor diffuses through a gaseous boundary layer into the spherical drop as it falls through the rain section.

Condensation of water vapor and absorption of iodine in the ice section are treated in a similar manner. Ice is modeled as a flat plate surrounded by an essentially stagnant air-steam-iodine boundary layer through which steam and iodine diffuse.

The solution of the diffusion equations based on the above assumptions results in the following relationship:

$$\eta_I = Y_s \eta_s$$

Where

η is the iodine removal efficiency $\frac{\text{gm iodine removed}}{\text{gm iodine fed to condenser}}$

Y_s is the mole fraction of steam in the inlet gas stream

η_s is the steam condensation efficiency $\frac{\text{gm steam condensed}}{\text{gm steam fed to condenser}}$

Since the steam condensation efficiency in an ice condenser is nearly 100% the iodine removal efficiency is directly related to the mole fraction of steam in the inlet gas stream.

Application of Ice Condenser Iodine Removal Model

The ice condenser iodine removal model has been applied to the ice condenser containment.

This model assumes that iodine is released from the Reactor Coolant System after blowdown, mixed with steam from boiloff, and swept to the ice condenser by recirculation fans.

The vapor composition of the lower compartment is assumed to be a homogeneous mixture of iodine, steam from core boiloff, and air.

The ice bed iodine removal efficiency, I , has been computed on a time dependent basis and is shown in [Table 6-102](#).

6.5.4.4 Ice Condenser System Tests and Inspection

During initial ice loading, periodic tests will be conducted to verify that the boron concentration and pH of the ice is within acceptable limits. This will be accomplished by measuring the pH and boron concentration of samples of the solution prior to freezing. At routine intervals, samples of the ice will be analyzed to verify that the pH and boron values are still within acceptable limits.

6.5.4.4.1 Ice Condenser System Instrumentation

The ice condenser is a passive system which requires no instrumentation for operation.

6.5.4.5 Ice Condenser Materials

See Section [6.7.18](#).

THIS IS THE LAST PAGE OF THE TEXT SECTION 6.5.

6.6 Inservice Inspection of Class 2 and 3 Components

6.6.1 Components Subject to Examination

Class 2 and 3 components are those components classified as Duke Power Class B and C respectively and are equivalent to Quality Groups B and C respectively of Regulatory Guide 1.26. These components will be examined in accordance with the provisions of the ASME Boiler and Pressure Vessel Code Section XI in effect as specified in 10CFR 50.55 Pressure Vessel Code Section XI in effect as specified in 10CFR 50.55 a(g) to the extent practical. Requests for relief from inservice inspection requirements determined to be impractical will be submitted to the NRC for review in accordance with NRC guidelines for submitting such requests.

6.6.2 Accessibility

The various Class 2 and 3 components have been designed with provisions for access as required by Section XI of the ASME code. Access for manual and/or remote examination has been considered when specifying component design, equipment layout, and support component placement.

6.6.3 Examination Techniques and Procedures

The examination techniques to be used for inservice inspection will include radiographic, ultrasonic, magnetic particle, liquid penetrant, eddy current, and visual examination methods. For all examinations, both remote and manual, specific procedures will be prepared describing the equipment, inspection technique, operator qualifications calibration standards, flaw evaluation, and records. These techniques and procedures will meet the requirements of the Section XI edition in effect as stated in Section [6.6.1](#).

6.6.4 Inspection Schedule

The inservice inspection interval for ASME Class 2 and 3 components will be 10 years. Detailed inspection listings and scheduling will be contained in the Catawba Inservice Inspection Plan.

6.6.5 Examination Categories and Requirements

The examination categories and requirements shall meet Section XI in effect as stated in Section [6.6.1](#) except where specific relief has been requested in accordance with NRC guidelines.

6.6.6 Evaluation of Examination Results

Evaluation of examination results shall be in accordance with the Section XI in effect as stated in Section [6.6.1](#) where these evaluation standards are contained in Section XI. For examination where evaluation standards are not contained in Section XI, evaluation shall be performed in accordance with the original construction code.

6.6.7 System Leakage and Hydrostatic Pressure Test

Pressure testing of Class 2 and 3 systems shall be performed in accordance with the Section XI in effect as stated in Section [6.6.1](#).

6.6.8 Augmented Inservice Inspection to Protect Against Postulated Piping Failures

The augmented inservice inspection program defined in Standard Review Plan Section [6.6](#), paragraph 11.8 will be implemented as follows:

1. If "break exclusion" is claimed, then an augmented inservice program in accordance with Standard Review Plan Section [6.6](#) will be implemented.
2. Where breaks are not assumed to be excluded, breaks will be postulated in accordance with the criteria of Branch Technical Position MEB 3-1, "Postulated Break and Leakage Locations in Fluid System Piping Outside Containment" of Standard Review Plan Section [3.6.2](#), and the plant will be designed to withstand the consequences of these breaks, including the full dynamic effects of the breaks. These lines will receive the normal inservice inspection of Article IWC-2000 of the reference codes as defined in 10CFR 50.55a(g) to the extent practical.
3. Where guard pipes are used on process pipes to mitigate the consequences of a rupture of the process pipe, the guard pipes will be designed for the full dynamic effects of a longitudinal or circumferential break of the process pipe. Inspection ports have been provided where possible, and these lines will receive the normal inservice inspection of Article IWC-2000 of the reference code of (2) above.

The areas subject to examination and the methods of examination are in accordance with the above referenced code. In general, ultrasonic examination will be the technique employed for volumetric examination; however, radiography will be used for the main steam welds which are encased in guard pipe.

[Table 6-103](#) lists those lines requiring augmented inservice inspection. The weld listing and scheduling will be contained in the Catawba Nuclear Station Inservice Inspection Plan. This plan was implemented effective June 29, 1985 for Unit 1 and August 19, 1986 for Unit 2.

THIS IS THE LAST PAGE OF THE TEXT SECTION 6.6.

6.7 Ice Condenser System

[Figure 6-138](#) shows the general layout of the Ice Condenser System.

6.7.1 Floor Structure and Cooling System

6.7.1.1 Design Bases

The ice condenser floor is a concrete structure containing embedded refrigeration system piping.

[Figure 6-139](#) shows the general layout of the floor structure. The functional requirements for both normal and accident conditions can be separated into five groups: wear slab, floor cooling, insulation section, subfloor, and the floor drain. Each group is now described in detail.

Wear Slab and Floor Cooling System

Function

The wear slab is a concrete structure whose function is to provide a cooled surface as well as to provide personnel access support for maintenance and/or inspection. The wear slab also serves to contain the floor cooling piping.

The Floor Cooling System intercepts approximately 90 percent of the heat flowing toward the ice condenser compartments from the lower crane wall and equipment room during normal operation. The Floor Cooling System is designed with defrost capability. During periods of wall panel defrosting it is necessary to heat the floor above 32°F. During an accident the floor cooling is terminated by the Containment isolation valves which are closed automatically. The Refrigeration System interface and cooling function is described in Section [6.7.6.2](#). The cavity below the wear slab is filled with an insulation material to resist the flow of heat into the ice bed during all operating conditions.

Design Criteria and Codes

Refer to Section [6.7.16](#). The following codes are also used in the design:

ANSI B31.5-66 including Addenda B31.5a 1968 Refrigeration Piping.

American Welding Society Structural Welding Code - 1972, AWS Publication D1.1-72.

ANSI Standard Code for Pressure Piping Refrigeration Piping ANSI B31.5 including Addenda B31.5a 1968.

AISC Manual of Steel Construction, Seventh Edition, 1970.

Design Conditions

Thermal Conditions

Initial Cooldown

top of Wear Slab 70°F

bottom of Wear Slab 50°F

Defrost Cycle

top of Wear Slab 33°F

bottom of Wear Slab 70°F

Seismic Loading

Operating Basis Earthquake (OBE)

| | |
|-------------------------------|------|
| Vertical (OBE) | .35g |
| Horizontal - Radial (OBE) | .14g |
| Horizontal - Tangential (OBE) | .38g |

Safe Shutdown Earthquake (SSE)

| | |
|-------------------------------|------|
| Vertical (SSE) | .55g |
| Horizontal - Radial (SSE) | .28g |
| Horizontal - Tangential (SSE) | .75g |

Design Basis Accident (DBA) Loads

| | |
|--|-------------------------|
| Pressure load on floor | 9 psi |
| Floor momentum load (due to deflectors) | 36.4 kips |
| Ice Loading - assume 6 in. solid ice on floor | 4300 lbs/bay |
| Live Loading | 250 lbs/ft ² |
| Dead Loads | |
| 1/4 inch plate | 1410 lbs |
| 1/2 inch pipe | 164 lbs |
| Concrete Wear Slab | 9700 lbs |
| Wall Panel - 121 lbs/in. over back 8 in. of slab | |
| Volume of cavity in floor structure | 7 yds ³ /bay |
| "Foam" concrete density | 40 lbs/ft ³ |

During seismic and/or accident conditions the insulation is designed to support loads transferred by the wear slab.

Structural Subfloor

Refer to [Chapter 3](#).

Floor Drain

Function

The floor drain is a passive structural component during normal operation as its only function is to minimize heat/air inflow to the lower plenum. The section of the floor drain pipe inserted vertically below the wear slab is designed to provide a high thermal resistance to minimize heat gain to the ice condenser. Under accident conditions the floor drains must not fail in a mode which prevents outflow of water.

Design Criteria and Codes

Welding complies with American Welding Society, Structural Welding Code, AWS D1.1-1972, as specified in Section [6.7.18](#).

Design Conditions

Normal Operation

| | |
|---------------------------------|-----------------|
| Design temperature, maximum | 120°F |
| Nominal ΔP across valve | less than 1 psf |

Accident Conditions

| | |
|-------------------------------|-----------------------------|
| ΔP across check valve | 12-14 psi |
| Temperature of pipe and valve | 317°F (The Peak Containment |

Temperature Transient is discussed in Section [6.2.1.1.3.3.](#))

6.7.1.2 System Design

Wear Slab and Floor Cooling System

The wear slab is a 4 inch thick layer of high strength concrete (3000 psi) having an exposed top surface area of 145 ft²/bay. See [Figure 6-140](#) for top surface typical geometry. The concrete has a density of 150 lbs/ft³ and is prepared with air entrainment admixtures to minimize spalling from freeze/thaw cycles. Steel reinforcing is used in the wear slab to assure adequate and uniform strength. A protective coating is applied to the top of the wear slab which provides an additional water barrier for the wear slab. The Floor Cooling System consists of 1/2 inch schedule 80 carbon-steel ASTM A-333 Grade 6 piping which is embedded in the wear slab to each bay in a serpentine fashion (See [Figure 6-140](#)) thereby providing ample cooling of the wear slab surface. The cooling pipes contained in each wear slab rest on a steel plate which extends across the full width of the floor for maximum effectiveness in intercepting heat passing up through the floor. Expansion joints are located at each bay and expansion material is located at the slab perimeter. The Floor Cooling System maximum coolant pressure is approximately 300 psi. The floor coolant flow rate per bay is adjusted by means of needle valves and is monitored by a temperature sensing element located at the downstream end of each of the bay floor piping. Should a leak develop each individual bay piping loop can be isolated by closing two valves. The coolant contained in the piping is a corrosion inhibited glycol/water solution.

For defrosting purposes, electric heating of the glycol is provided. In general, components requiring periodic maintenance such as pumps, heaters and control valves are located in the upper compartment.

The insulation cavity is filled with a low density, closed cell, foam concrete. The nominal density of the foam concrete is 35 lbs/ft³; the compressive strength is 110 psi. The thermal conductivity per inch thickness is nominally 1.0 Btu/hr-F-ft². The insulation cavity for the foam concrete is sealed by a vapor barrier to provide additional assurance that the insulation section resists infusion of water vapor and thus retains a high thermal resistance. The top surface of the foam concrete is covered with a course of grouting which provides seating surface for the floor plate and cooling coil assemblies.

Floor Drain

Special consideration has been given in the design to prevent freezing of the floor drains and to minimize check valve leakage.

The floor drains employ a low thermal conductivity (insulate) section of pipe 12 inches in diameter, inserted vertically below the wear slab to minimize heat gain to the ice bed. The horizontal run is a 12 inch diameter steel pipe embedded in the subfloor which is at a relatively warm temperature. The drain check valve is a 12 inch diameter horizontal valve weld fabricated from stainless steel. The valve is designed to remain closed against the cold air head in the ice

condenser to minimize air outleakage during normal operation. The valve is designed to tolerate a 15 psi back pressure when closed. The check valve is in a warm environment and no freezing will occur.

6.7.1.3 Design Evaluation

Wear Slab

The wear slab, during normal operating conditions, is subject only to its dead weight consisting of concrete, steel reinforcing, steel plates and piping. Six inches of 100 percent density ice is assumed to be uniformly distributed over the entire floor. The dead weight amounts to 11,200 lbs per bay, the equivalent of 0.56 psi. The live load for maintenance purposes is assumed to be 250 lbs.ft². The vertical seismic input is .35 g for OBE and 0.55 for SSE. The dead load plus seismic loads are insignificant because the highest load on the floor is contributed by blowdown pressure during design accident conditions. The blowdown pressure is 9 psi, and added to this value, for design purposes, is a 40 percent design margin, and a dynamic load factor of 1.53. This results in a minimum value for design of 19.28 psi.

The most severe loading condition is the combination of the dead load, the SSE seismic acceleration of .55 g, the 19.28 psi pressure load and 8.1 psi locally near the deflectors due to flow impulse loadings. The wear slab is designed to accommodate the heatup and cooldown cycles and OBE without over-stressing the concrete and coolant piping.

Floor Cooling System

The embedded piping for floor cooling is 1/2 inch schedule 80 pipe. The maximum coolant pressure in the pipe is approximately 300 psi. ANSI B31.5-68 data shows that the pipe can tolerate internal pressures of 4812 psi.

In addition, the piping is pressure tested before it is put in service. The pipe is sized to allow for at least 38 mils of corrosion. Nevertheless, the glycol coolant contains corrosion inhibitors, and as a result pipe corrosion is negligible. The 1/4 inch floor plate is integrated with the concrete through 1/2 inch diameter anchors welded to the plate on 12 inch centers. These anchors prevent thermal loads from concentrating in the piping.

Insulation Section

The insulation section supports wear slab loads. For a conservative analysis the wear slab dead weight + seismic + DBA loads were assumed to be transferred to the foam concrete section. The compressive strength of the foam concrete is sufficient to accept these floor loads.

Floor Drain

Drains are provided at the bottom of the ice condenser compartment to allow the melt/condensate water to flow out of the compartment during a loss-of-coolant accident. These drains are provided with check valves that are designed to seal the ice condenser during normal plant operation to prevent loss of cold air from the ice condenser. These check valves remain closed against the cold air head of the ice condenser and open before the water head reaches a value of 18 inches of water.

For a small pipe break, the water inventory in the ice condenser is produced in proportion to the energy added from the accident. The water collecting on the floor of the condenser compartment then flows out through the drains. For intermediate and large pipe breaks the ice condenser doors are open and water drains through both the doors and the drains.

For a large pipe break, a short time of the order of seconds is required for the water to fall from the ice condenser to the floor of the compartment. Results of fullscale section tests performed at

Waltz Mill show that, for the design blowdown accident, a major fraction of the water drained from the ice condenser, and no increase in Containment pressure was indicated even for the severe case with no drains.

A number of tests were performed with the reference flow proportional-type door installed at the inlet to the ice condenser and a representative hinged door installed at the top of the condenser. Tests were conducted with and without the reference water drain area, equivalent to 15 ft² for the plant, at the bottom of the condenser compartment.

These tests were performed with the maximum reference blowdown rate, with an initial low blowdown rate followed by the reference rate, and with a low blowdown rate followed by the simulated core residual heat rate.

The results of all of these tests show satisfactory condenser performance with the reference type doors, vent, and drain for a wide range of blowdown rates. Also, these tests demonstrate the insensitivity of the final peak pressure to the water drain area. In particular, the results of these full-scale section tests indicate that, even for the reference blowdown rate, and with no drain area provided, the drain water did not exert a significant back pressure on the ice condenser lower doors. This showed that a major fraction of the water had drained from the ice condenser compartment by the end of the initial blowdown. The effect of this test result is that Containment final peak pressure is not affected by drain performance.

Although drains are not necessary for the large break performance, 15 ft² of drain area was provided for small breaks.

For small breaks, water flows through the drains at the same rate that it is produced in the ice condenser. Therefore, the water on the floor of the compartment reaches a steady height which is dependent only on the energy input rate.

To determine that the 15 ft² drain area met these requirements, the water height is calculated for various small break sizes up to a 30,000 gpm break. Above 30,000 gpm the ice condenser doors would be open to provide additional drainage. The maximum height of water required was calculated to be 2.2 ft above the drain check valve. Since this height resulted in a water level which is more than 1 ft below the bottom elevation of the inlet doors, it is concluded that water does not accumulate in the ice condenser for this condition and that a 15 ft² drain gives satisfactory performance.

During normal unit operation, the sole function of the valve is to remain in a closed position, minimizing air leakage across the seat. To avoid unnecessary unseating of the valve seat, a 1/2 inch drain line leading to a 2 inch drain header is connected to the 12 inch line immediately ahead of the valve. Any spillage or defrost water drains off without causing the valve to be opened.

The arrangement of the Drain System for the lower inlet region of the ice compartment is shown in [Figure 6-139](#).

Special consideration has been given in the design to prevent freezing of the check valves and to minimize check valve leakage.

To minimize the potential for valve freezing, a low conductivity (transite) section of pipe is located vertically below the wear slab, while the horizontal run of pipe (steel) is imbedded in a warm concrete wall before it reaches the valve. The valve itself is in the upper region of the lower compartment, where ambient temperature is above the freezing temperature.

The valve is held in a closed position by virtue of its design as an almost vertical flapper with a hinge at the top. The flap is held closed by gravity. In order to reduce valve leakage to an acceptable value, a sealant is applied to the seating surface after installation of the valves.

Tests show that this reduces leakage to practically zero. Maximum allowable leakage rate would be approached as a limit only if all the sealant were to disappear completely from all the valves, which is unlikely. Sealant grease is periodically removed and replaced.

Conclusion

On the basis of the structural analysis performed on the floor structure, it is concluded that the floor is adequate for all anticipated loading conditions. In addition, the floor design is compatible with ice condenser wall panel defrosting. The water resulting from the wall panel defrosting produces no adverse effect on the structural integrity of the floor. The use of concrete with entrained air affords ample resistance to the effects of water. Additionally, the floor structure contains water vapor seals. The seals typically include: a protective surface coating on the wear slab top surface, a vapor barrier between the foam concrete and the structural subfloor, a leveling course of grout on the top surface of the foam concrete, and a steel plate (in the wear slab) with lapping material in the plate to plate joints. As a result the effects of water on the floor and insulation is negligible.

6.7.2 Wall Panels

6.7.2.1 Design Bases

Function

The wall panels are designed to thermally insulate the ice bed, under normal operating conditions, from the heat conducted through the crane wall, the Containment wall and the end walls. In addition, they are designed to provide a circulation path for cold air and a heat transfer surface next to the ice bed so that the ice is maintained at its design temperature range.

The supporting structure of the wall panel also provides for transfer of radial and tangential loads from the lattice frame columns to the crane wall anchor embedments.

Criteria and Codes

The structural parts of the wall panels are designed to meet the requirements given in Section [6.7.16](#).

Design Conditions

The service temperature range is 10°F to 20°F. The Peak Containment temperature following a DBA is 317°F. (The Peak Containment Temperature Transient is discussed in Section [6.2.1.1.3.3](#).)

The design loads are presented in [Table 6-104](#). The loading combinations considered in the design are those given in Section [6.7.16](#). For the SSE plus DBA combination, ten loading cases are considered.

6.7.2.2 System Design

The wall panel design incorporates provisions for installation on the crane wall, Containment wall, and end walls of the ice bed annulus. Containment and end wall panels are similar except for the omission of the lattice frame column attachments.

The crane wall panel design incorporates transverse beam sections which are fabricated from standard structural sections and to which the lattice frame column mounting lugs are attached. These sections are attached to the rear mounting angle assemblies by insulated bolts.

Wall panels are attached to the crane and end walls by studs welded to the anchor embedments and to the Containment by studs welded to the shell. The crane wall panels extend from the bottom of the upper plenum to the lower support structure where they are supported on the inner circumferential beams of the horizontal platform. The Containment wall panels extend from the bottom of the upper plenum to the top of the floor wear slab.

Cooling ducts are incorporated in the design to provide flow from the air handlers in the duct adjacent to the ice bed and return flow in the outer duct of the panel. This provides an even distribution of duct free temperature. Each bottom duct assembly provides a flow path between the inner and outer duct to allow return flow through the outer duct.

The ducts are fabricated as sandwich panels utilizing corrugated sheet sections enclosed in sheet metal enclosures. This type of sandwich construction provides resistance to differential pressure loads and results in minimal overall weight and flow restrictions. Flow sections of wall panels are seal welded to prevent air leakage.

Materials of construction of the wall panels conform to the Design Criteria of Section [6.7.18](#).

Areas between air ducts and walls are insulated and areas between adjacent air ducts are insulated and covered with a lap strip to provide a seal between wall surface and ice bed. Elastomers and sealants are insignificantly affected by exposure to a 5 R/hr gamma radiation field over a period of forty years.

6.7.2.3 Design Evaluation

The wall panels have been analyzed for seismic and Design Basis Accident loading conditions as well as service loads.

Analysis for DBA Pressure Load

The wall panels are bolted to transverse beam sections with a maximum span of about 24 inches. In the analysis, the wall panels were taken as a 24 in. x 36 in. sandwich plate simply supported on all four sides.

It is noted that a DBA pressure of 18.7 psig was used in these analyses. The duct internal pressure was neglected in the analyses because it is negligible in relation to the 18.7 psig (internal design pressure 0.5 psig).

Analysis for Seismic and DBA Transverse Beam Loads

A transverse beam section was investigated for its ability to transmit the imposed Seismic and DBA loads from the lattice frame column attachment to the crane wall. A two dimensional beam analysis utilizing the "STASYS" program was employed. Various loading modes were used with values as shown in [Table 6-104](#) Parts B, C, D and E.

Overall Conclusion

Based on the analyses described in the foregoing, it is concluded that the wall panel assembly meets the design requirements given in Sections [6.7.16](#) and [6.7.18](#).

6.7.3 Lattice Frames and Support Columns

6.7.3.1 Design Bases

Function

The lattice frames and support columns assembly provide the following functions:

Positions the ice baskets in the ice bed and controls the hydraulic diameter.

Provides lateral support for the ice baskets under normal seismic and accident loads.

Allows passage of steam and air through the space around ice baskets.

Allows for basket installation and removal requirements.

Structural Requirements

Refer to Section [6.7.16](#).

Design Criteria

The lattice frames are designed to be compatible with the periodic weighing procedure for the ice baskets.

The structure is designed to position the ice columns in the required array to maintain the performance of the ice condenser. In particular, the flow area around each ice column is maintained within the limits established by the general design criteria.

The lattice frame allows loading of the ice baskets in position, and permits lifting of complete basket columns for removal in sections.

Materials Requirements

Refer to the listing of acceptable materials in Section [6.7.18](#). All accessible steel components are covered by protective coating.

General Thermal and Hydraulic Performance

The lattice frames space the ice basket columns so that the hydraulic diameter around each ice column is maintained for all modes of operation.

Differential thermal expansion between crane wall and lattice frame structure, together with other applicable loads, does not stress the lattice frames or its associated supporting structure beyond the design limits, or adversely affect the spacing between lattice frames.

Forces across the lattice frames in the horizontal and vertical direction due to seismic and blowdown loads do not overstress the lattice frame and supporting structure beyond the design limits.

Interface Requirements

Lattice Frame to Ice Basket Columns

The lattice frame locates and aligns the ice basket array. Sufficient clearance shall be provided to assure ease of ice basket installation but shall limit radial basket motion to a nominal amount. The lattice frame structure is also capable of withstanding design and operating seismic and accident loading.

Lattice Frame to Lattice Frame Column

The lattice frame is attached to the lattice frame columns. The column bases are adjustable so that matching of columns to lower support structure can accommodate the range of manufacturing and installation tolerances.

Lattice Frame Columns to Crane Wall Air Duct Panels

The lattice frame columns are bolted to the wall panel cradles. Lateral seismic loading from ice baskets and lattice frame is transmitted to the crane wall through the lattice frame columns and the wall panel cradles.

Lattice Frame Columns to Lower Support Structure

Lattice frame columns interface with the lower support structures. The columns are designed to allow for accumulation of dimensional tolerances at interfaces.

Lattice Frame Columns to Intermediate Deck

The top end of the lattice frame columns at each bay support the intermediate deck and related supports.

Allowance is made for mounting the Ice Condenser Temperature Sensing System onto the lattice frames.

Design Load

The lattice frames and support columns are designed to withstand dead loads, live loads, seismic loads including impact and accident loads and remain within the allowable limits established in Section [6.7.16](#). Differential thermal expansion loads due to normal and accident conditions are also considered. Structural loads are not transmitted through the lattice frames and columns to the containment structure. [Figure 6-141](#) and [Figure 6-142](#) show the lattice frame loading orientation and distribution.

The lattice frame and column are designed to withstand the following load combinations in both the tangential and radial directions:

Dead Loads + Operating Basis Earthquake

Dead Loads + Safe Shutdown Earthquake

Dead Loads + Design Basis Accident

Dead Loads + Design Basis Accident + Safe Shutdown Earthquake

6.7.3.2 System Design

The lattice frames are structural steel grid work structures located in the ice condenser annulus and fitted between the lattice frame support columns and clearing the wall panel air ducts.

The lattice frames are mounted radially across the ice condenser annulus for the full 300 degrees of annulus circumference at each of eight levels between the lower support structure and the intermediate deck. The first level is located 15'9" ft above the wear slab or ice condenser floor and the next seven levels are vertically spaced at approximately 6 ft intervals. A total of 576 lattice frames are required for the ice condenser assembly. Three lattice frames are required per level in each of the 24 bays and this configuration is repeated for the eight levels.

The lattice frames are mounted to rectangular steel columns which are placed at the crane wall side and at the Containment side of the condenser annulus. The column bases are attached to the lower support structures. Columns at the crane wall are attached along the length of the wall panel cradles and to the lower support structure, while those at the Containment side are free-standing, i.e., the bases are fastened to the lower support structure but there are no connections with the wall panels or the containment vessel wall. This arrangement prevents transmission of loads from ice baskets, lattice frames and columns to the containment vessel. The vertical columns and crane wall support and maintain the lattice frame geometry during normal and accident loading conditions.

The lattice frames are welded steel structures consisting of radial struts supported by welded cross bracing as shown in [Figure 6-143](#). Basically the lattice frame is about 125 in. long, 48 in.

at its widest point, and 7 1/2 in. deep. The entire welded structure weighs about 1200 lbs. Individual free path penetrations are provided for each of twenty-seven ice baskets. The lattice frame struts that form the ice basket restraints are all double fillet welded to the stringers. This assures a consistent weld design and ensure the integrity of the entire structure in operation.

Flexible radial members on the lattice frame are located at the Containment side to accommodate differential thermal expansion in the tangential direction, and to allow for minor column misalignment at installation. The flexible radial members are attached to the vertical support columns.

The lattice frame attachment at the crane wall consists of horizontal ear-like tabs that accommodate the bolting. One tab is slotted in the tangential direction to allow for differential thermal expansion between the concrete crane wall and the steel structures. Lattice frame tabs are fastened to brackets on the vertical support columns. The columns, in turn are bolted to the crane-side wall panel cradles. The wall panel cradles are fastened to the crane wall studs and transmit the lattice frame and ice basket horizontal loads to the crane wall, while the vertical loads are transmitted to the lower support structure.

The cross bracings and radial struts are arranged so that the ice baskets are positioned in the free path penetrations. The free path diameter controls the radial clearance between ice baskets and the lattice frames. The penetrations are spaced to assure the proper hydraulic diameter around each ice basket and to allow free passage of air and steam through the surrounding passages. Small pads on the radial struts control the tangential ice basket clearance.

All of the welding and inspection was done in accordance with the American Welding Standard Procedure, D1.1-72. The welds are inspected visually and then by magnetic particle inspection. The magnetic particle inspection is applied to selectively located welds throughout the structure.

All accessible exposed steel components are covered by a protective coating.

6.7.3.3 Design Evaluation

The lattice frames are analyzed using the ICES-STRUDLE II System of computer programs for frame analysis. STRUDLE is a general program operating as a subsystem of the Integrated Civil Engineering (ICES) program. The lattice frames are treated as three dimensional structures composed of joints, support joints, and structural members connecting the joints. [Figure 6-144](#) illustrates the analytical model generated for the lattice frames. Each structural joint is assigned a circled number, and each structural member an uncircled number.

The lattice frame is treated as a cantilevered structure in the horizontal plane and restrained vertically at the four column connections. The model in [Figure 6-17](#) shows flexible connections at the crane wall and no connection at the Containment wall. Variations in flexibility of the crane wall connections are considered in the analysis to simulate the behavior of the slotted tab connection and the connections to lattice frame columns and air duct wall panels.

The analysis of the loads for the individual maximums of D + OBE, D + SSE and D + DBA is determined. A survey is also conducted for the loading combinations of D + SSE + DBA for each lattice frame level at reference seismic orientation, 45 degrees and 90 degrees from reference to determine the maximum loading condition on the lattice frame. The survey shows that the highest loads occur on the lattice frame at the 33 ft level, and that the combination of D + SSE + DBA, horizontally and vertically produces the maximum stresses.

Maximum stresses are calculated at each structural member at the edge of the fillet weld for all loading conditions.

Fatigue stresses due to OBE loading were calculated and are within the allowable limits defined in Section [6.2.2.6](#).

The vertical support columns and brackets which support the lattice frames are structurally analyzed to determine structural integrity. The worst load combinations of D + OBE, D + SSE, D + SSE + DBA are considered in the analysis. The stress analysis indicates that the stress for all loading conditions is below the allowable limits as defined in Section [6.7.16](#).

The vertical support numbers are also analyzed to determine buckling characteristics. Analysis using classical buckling methods indicates that this phenomena is not a concern.

6.7.4 Ice Baskets

6.7.4.1 Design Bases

Function

The function of the ice baskets is to contain borated ice in approximately 12 inch diameter columns that are approximately 48 feet high. The ice absorbs the thermal energy resulting from LOCA or steam line break in the Containment structure. The baskets are arranged to promote heat transfer from the steam to ice during and following these accidents. The function of the ice baskets is also to provide adequate structural support for the ice and maintain the geometry for heat transfer during or following the worst loading combinations.

Loading Modes

The following loading conditions are considered in the design of the ice baskets; dead weight, seismic loads, blowdown loads, and impact loads between the basket, ice and lattice frames. The baskets withstand these loads and remain within the allowable limits established in Section [6.7.16](#).

Design Consideration

The structural stability and deformation requirements are determined to ensure no loss of function under accident and safe shutdown earthquake loads.

The ice baskets are designed to facilitate maintenance and for a lifetime consistent with that of the unit.

The structure is designed to maintain the ice in the required array to maintain the integrity of performance of the ice condenser. In particular, the hydraulic diameter and heat transfer area are maintained within the limits established by test to be consistent with the containment design pressure.

Any section of the ice basket is capable of supporting the total weight of the ice above that section.

General Thermal and Hydraulic Performance Requirements

The ice baskets are fabricated from perforated sheet metal which has open area to provide sufficient ice heat transfer surface. The adequacy of the design and the performance were confirmed by test.

Interface Requirements

Lattice Frame

The lattice frames at every 6 ft act as horizontal restraints along the length. The design provides a nominal 1/4 in. radial clearance between the ice baskets and the lattice frames when

internal coupling and stiffening rings are used, and 0.123 inch radial clearance when external minimum restriction coupling rings are used. Lattice frame and basket coupling elevations coincide to prevent damage to the basket during impact.

Lower Support Structure

Ice basket bottoms are designed to be supported by and held down by attachments to the lower support structure. The basket supports are designed for structural adequacy under accident and safe shutdown earthquake loads and permit weighing of selected ice baskets.

Basket Alignment

The ice condenser crane aligns with baskets to facilitate basket weighing and/or removal. The baskets are capable of accepting basket lifting and handling tools.

Basket Loading

The ice baskets are capable of being loaded with flakice using the pneumatic ice distribution system or with block ice using equipment located in the upper ice condenser.

External Basket Design

The baskets are designed to minimize any external protrusions which would interfere with lifting, weighing, removal and insertion. Some baskets may have top rings mounted with screws driven from inside the basket. While the ends of these screws will create external protrusions, this is considered acceptable since the basket top is clear of lattice interferences. There will be no interference with basket and ice lifting, weighing, removal, and insertion.

Basket Coupling

Baskets are capable of being coupled together in columns approximately 48 feet long.

Basket Couplings and Stiffening Rings

Couplings or rings are located at 6 ft intervals along the basket at lattice frame elevations. Internal inserts, either attached to the rings or a central cable, are designed to support the ice from falling down to the bottom of the ice column during and after a DBA and/or SSE.

Design and Test Loads

The minimum test and basic design loads are given in [Table 6-105](#) for baskets with internal rings and [Table 6-136](#), [6-137](#) and [6-138](#) for baskets with external rings and the cable suspension system.

6.7.4.2 System Design

The Ice Condenser is an insulated cold storage room in which ice is maintained in an array of vertical cylindrical columns. The columns are formed by perforated baskets with the space between columns forming the flow channels for steam and air. The Ice Condenser is contained in the annulus formed by the Containment vessel wall and the crane wall circumferentially over a 300 degree arc.

The ice columns are composed of four baskets approximately 12 feet long each, 16 baskets approximately 3 feet long each, 24 baskets approximately 2 feet long each, or any combination of 2,3, or 12 foot baskets making up the 48 foot column of ice baskets, filled with flake ice or block ice. Location of the different length baskets is controlled to provide assurance that a coupling or stiffener ring is located at every lattice frame level. The baskets are formed from a 14 gauge (.075) perforated sheet metal, as shown in [Figure 6-145](#). The perforations are 1.0 in. x 1.0 in. holes, spaced on a 1.25 inch center. The radius at the junction of the perforation is

1/16 inch. The ice basket material is made from ASTM-A569 which is a commercial quality, low carbon steel. The basket component parts are corrosion protected by a hot dip galvanized process. The perforated basket assembly has an open area of approximately 64 percent to provide the necessary surface area for heat transfer between the steam/air mixture and the ice to limit the Containment pressure within design limits. The basket heat transfer performance was confirmed by the autoclave test.

Cruciforms are installed in ice baskets at 6 foot intervals. These cruciforms prevent the ice in the basket from displacing axially in the event of loss of ice caused by sublimation of partial melt down due to accident conditions. Cruciforms can be either welded to the internal coupling and stiffener rings or attached to a steel cable (Cruciform Cable Suspension System, [Figure 6-198](#)) that is extended down through the center of the basket.

Interconnection couplings and stiffening rings are located at the bottom and 6 foot levels (12 foot baskets only) respectively of each basket section. Internal coupling and stiffening rings are cylindrical in shape and approximately 3 inches high with a rolled internal lip. The lip provides stiffening to the basket. These couplings are attached to the ice baskets by locking sheet metal screws and basket detents.

External coupling and stiffening rings are cylindrical in shape and approximately 3 inches high with no rolled lip. The actual pieces used for coupling and stiffening rings are the same. These rings are attached to the basket by stainless steel rivets with coupling rings using 24 rivets and stiffening rings using 12 rivets. Refer to [Figure 6-198](#) for a drawing of the external rings and the Cruciform Cable Suspension System.

The baskets are assembled into the lattice frames to form a continuous column of ice approximately 48 ft. high. The bottom wire mesh is designed to allow water to flow out of the basket and has attachments for mechanical connection to the lower support structure to prevent uplift of the ice baskets during SSE and DBA. The lattice frames provide only lateral ice basket support at intervals corresponding to the stiffened ice basket sections. The vertical loads of the ice and ice basket is transmitted by the basket to the lower support structure. The attachment between the ice basket and the lower support structure may be disengaged if required to permit weighing of the baskets. The columns of ice can be lifted and removed in sections, and provision is made for lifting and weighing the whole length of selected columns for surveillance purposes.

Basket Fabrication

The fabrication steps are as follows:

The sheet metal is purchased in the hot-rolled and pickled condition.

The perforator oils and perforates the material and ships to the basket fabricator.

The basket fabricator rolls the perforated metal into a cylindrical shape 12 inches in diameter by 141.57 or 143.25 inches long, for bottom or upper baskets respectively (for 12 foot baskets), 22.19 or 23.87 inches long, for bottom or upper baskets respectively (for 2 foot baskets), or 34.17 or 35.81 inches long, for bottom or upper baskets respectively (for 3 foot baskets), and material is degreased.

The sides of the rolled cylinder are continuously welded using the gas metal arc process.

Following the welding the cylinder is pickled, washed, fluxed, hot dip galvanized.

The couplings and stiffening ring blanks are cut from sheets or coils of hot rolled, pickled and oiled material. These are formed by a rolling process and are 3 inches high with a roll-formed internal lip and are of a diameter to fit inside the perforated basket. The 3 inch high external

coupling and stiffening rings are cut from sheets or coils of stainless steel material, formed by a rolling process without any internal or external lip, and ends welded together at a diameter to fit the outside surface of the perforated basket cylinder.

The cruciforms are die-formed from steel strip.

Following the forming operations, internal stiffeners and couplings with or without cruciforms in place are pickled, washed, fluxed, hot dip galvanized. Replacement cruciforms and external coupling and stiffening rings are made of stainless steel and will not be subjected to this treatment.

The column bottom is fabricated by a procedure similar to item (6) above. The appurtenances are welded in place and the piece is galvanized per item (8) above.

The remaining appurtenances are cut to size, machined, welded, where required followed by galvanizing as above, and plated where required.

The completed couplings, bottoms, appurtenances, stiffening rings and cylinders are next assembled. The internal stiffening rings are inserted inside the cylinder until the side is adjacent to the 2.5 inch unperforated area in the center of the cylinder and attached by a self drilling, self tapping, locking machine screw and four basket detents. External stiffener rings are attached with 12 stainless steel rivets.

For the column bottom, two U-bolts and nuts and washers fasten the mounting bracket assembly to the plate of the basket end. Swivel Bracket Assemblies may be substituted for the U-bolt assemblies.

The bottom is inserted into the cylinder until the cylinder rests against the step of the bottom and is attached mechanically by 12 self drilling, self tapping, locking machine screws.

For the upper baskets, the couplings are inserted in the cylinders approximately 1-1/2 inches and attached with 12 screws as above. External coupling rings are attached with 24 stainless steel rivets, with 12 rivets attaching the ring to each basket.

All welding and inspection is performed in accordance with AWS publication D1.1-72, including latest revisions.

Basket Installation

The completed baskets are placed in the lattice frames from the top deck by first lowering a bottom basket into the lattice frames and locking in place, extending approximately 2 inches above the top lattice frame. The second upper basket is lifted with the crane and gripper fixture and placed on top of the bottom basket inserting the coupling into (over the top for external rings) the top of the bottom basket and attaching with self drilling, self tapping screws (rivets for external coupling rings).

Next the locking or holding fixture is released and the two baskets lowered until the top is approximately 2 inches above the lattice frames as above. The third and fourth baskets are installed in the same manner as the second.

When the full column is assembled and ready to set on the lower support structure, the bolts and mounting bracket are loosened and the column lowered to facilitate alignment of the yoke with the hole in the support structure. After alignment and insertion of the clevis pin, the 4 bolts are tightened. A hitch pin cotter is inserted to retain the clevis pin.

Materials

The listing of acceptable materials for the ice basket are presented in Section [6.7.18](#).

6.7.4.3 Design Evaluation

Basket Evaluation

The perforated metal baskets are evaluated by analyses and tests and found to be within the allowable limits defined in Section [6.7.16](#). Three different methods are used in determining the baskets' adequacy. The first method employs classical strength of materials techniques, the second uses limit analysis, and the third confirmed the basket integrity by tests.

Stress Analysis

This method considers the ice basket as being composed of a number of line (vertical basket element) and stay (circumferential basket element) elements and the collapse of the ice basket may be precipitated by the local yielding and/or buckling of the individual line elements.

When the basket is loaded both axially and laterally as a beam, the line elements are subjected to an axial compression, a lateral shear and a bending load. This combined stress state can possibly lead to local yielding, plastic collapse, line element buckling and ultimately to structural failure. All these modes of possible failures are analyzed and the results are found to be within the allowable criteria. Analysis indicates that the critical line element buckling load is about 77,000 lbs. The maximum vertical load, D + SSE is 3410 lbs. Therefore, the possibility of elastic buckling is remote. For a case with only lateral load, the analysis indicates that a factor of safety of 3.15 exists between the allowable basket load and the maximum lateral load that exists. A summary of stresses are tabulated in [Table 6-106](#). For the various design cases considered, it is seen that the design stress is always below the allowable stress.

Analysis was also made of the case where the ice melts out so that it occupies only one half side of the basket. The eccentricity would be 3 inches but the ice mass would be halved giving a shear stress of 450 psi, for a combined maximum shear stress of 3850 psi, again well below the allowable.

Limit Analysis

Limit analysis is performed on the ice basket in order to determine by analysis the lower bound collapse load when the basket is simultaneously loaded in the axial and lateral directions. The following mode of failures are considered as follows:

Plastic collapse of the compression side

Shear yield of the neutral plane

Plastic yield of the compression side.

Plastic yield of the neutral surface of line elements.

A summary of the combinations of concentric axial load and distributed load that causes basket failure is presented in [Figure 6-146](#). Also superimposed in this figure is the design and test load envelope. It can be seen that this envelope is well below the governing failure mechanism of plastic yielding of the neutral surface of the line elements.

Ice Basket Appurtenance Evaluation

The ice basket connections are analyzed to ensure structural integrity during all design load combinations of dead weight, Operating Basis Earthquake, Safe Shutdown Earthquake and Design Bases Accident. The primary area of concern is the ice basket to lower support structure connection. This area is shown in [Figure 6-145](#). The item, material and minimum yield stress are presented in [Table 6-107](#). The allowable stress limits for D + OBE, D + SSE, and D + SSE + DBA are tabulated in [Table 6-108](#) through [Table 6-110](#) respectively. The loads used in

the analysis of these parts envelop minimum design loads plus load factors necessary for the Catawba analysis.

Clevis Pin

The clevis pin transmits the ice basket loads to the lower support structure through a 1 x 2 inch bar welded to the top of the structure. A minimum clearance of 1/16 inches is provided both vertically and horizontally to provide a pinned connection, thereby eliminating the transfer of any moment to the structure resulting from basket deflection because of horizontal loads.

The stresses on the 1/2 inch diameter pin are tabulated in [Table 6-111](#).

Column Bottom Mounting

The mounting bracket is attached to the basket bottom as shown in [Figure 6-145](#). The design loads are transmitted through the mountings and clevis pin from the ice basket bottom.

The stresses in the mounting bracket, plates and bolt are tabulated in [Table 6-112](#) through [Table 6-114](#), respectively.

Swivel Bracket Assemblies

A design change which allows the replacement of u-bolts and mounting brackets with a lug and two coupling halves (Swivel Brackets) has been implemented. This design consist of a lug which rests on the lower support structure, and two coupling halves which capture the plate spanning the ice basket bottom. The Swivel Bracket Assembly allows the ice basket to be rotated while the clevis is still secured, enabling the baskets to be freed of frost accumulation and weighed in place. Refer to [Figure 6-197](#) for details of the basket bottom modification. All parts are stainless steel for corrosion resistance. The cast pieces are A-747 OR A-352, while the bolting is grade B8.

The swivel bracket assembly increases the gap between the clevis pin and basket bottom, which increases the impact loads during combined SSE and DBA events. The revised basket loadings and swivel bracket stress analysis was evaluated by Reference (19). Refer to [Table 6-134](#) for a stress summary.

Ice Basket End

The column bottom is shown in [Figure 6-145](#). The loads that are transmitted through the clevis pin assembly are distributed to the ice basket through the rigid plate and the cylindrical ice basket end section. Wire mesh is used to contain the ice and to provide drainage for the water. The stress summary for the ice basket end is shown in [Table 6-115](#).

The intermediate ice basket coupling screws and rivets were also analyzed and the results of the analysis are given in [Table 6-116](#) through [Table 6-119](#) and [Table 6-137](#). Results indicate that they are structurally adequate for maximum loading conditions defined in [Section 6.7.16](#).

6.7.5 Crane and Rail Assembly

6.7.5.1 Design Bases

Function

The crane and rail assembly is designed to carry components and tools into, out of, and within the ice condenser area during erection, maintenance, and inspection periods.

The italicized text below is HISTORICAL INFORMATION, NOT REQUIRED TO BE REVISED.

Criteria and Codes

The crane is designed in accordance with the requirements of the Electric Overhead Crane Institute Specification 61. It is designed so that under all loadings it is not derailed.

The rail is designed according to Section [6.7.16](#). These criteria provide assurance that the rail maintains its structural integrity.

Design Conditions

The service temperature range is 15°F to 100°F.

During unit erection, two cranes can be used in the ice condenser region, each carrying up to 6000 pounds. A separation of at least two bays is maintained between their centers. Prior to installation of air handling units, one crane is removed. The heaviest load actually expected after this time is less than 2,500 pounds. The crane remains normally parked (without load) outside the ice condenser while the reactor is at power. The crane and supporting structure are designed to withstand dynamic loading during operating modes specified above.

The design loads for the crane are presented in [Table 6-120](#).

6.7.5.2 System Design

The design of the 3 ton capacity crane is shown in [Figure 6-147](#). The bridge, boom and hoist of the crane are all motor operated. The two speeds of crane travel are approximately 34 and 100 feet per minute. The boom member is capable of rotating 360 degrees in either direction at a speed of approximately 2 revolutions per minute. The electric hoist is mounted on the boom member (cage section) of the crane. The wire rope lifting cable has one part reeved over one sheave mounted on the boom and another part reeved around another sheave mounted on the load block assembly. The cable is dead end fastened on the boom. The hoist provides a total life of approximately 69' 7", at speeds of 7 and 20 feet per minute. The hoist is equipped with an upper limit switch to ensure that the load block will not damage the boom assembly. The hoist automatically switches to low speed approximately 2 feet below the highest point of travel.

The total crane weight is approximately 7200 pounds.

The predominant material of construction is A36 steel. The main structural members are painted to prevent corrosion.

The crane travels on two circular rails that run through the ice condenser area as shown in [Figure 6-147](#). The circular diameters of the rails are 95 and 109 feet. The top flange plate and rail section are continuously welded to the web plate under controlled conditions. The top flange and web plates are A36 steel and the lower rail section is special analysis steel with a hard non-peening rolling surface.

6.7.5.3 Design Evaluation

The crane rails and supporting structures are analyzed as a part of the top deck structure (see Section [6.7.10](#)). It is found that all stresses were maintained within limits prescribed in the design criteria, Section [6.7.16](#), for all design conditions defined in Section [6.7.5.1](#).

6.7.6 Refrigeration System

6.7.6.1 Design Bases

Function

The Refrigeration System cools the Ice Condenser from ambient conditions of the reactor containment and maintains the desired equilibrium temperature in the ice compartment. It also provides the coolant supply for the ice machines during ice loading. The Refrigeration System additionally includes a defrost capability for critical surfaces within the ice compartment.

During a postulated loss-of-coolant accident the Refrigeration System is not required to provide any heat removal function. However, The Refrigeration System components which are physically located within the Containment must be structurally secured (not become missiles) and the component materials must be compatible with the post-LOCA environment.

Design Conditions

Operating Conditions

See individual component sections:

Floor cooling - Section [6.7.1](#)

AHU - Section [6.7.7](#)

Performance Requirements

The mandatory design parameters that relate to refrigeration performance are:

Nominal initial total weight of ice in columns 3,000,000 lbs

Minimum total weight of ice in columns 2,330,856 lbs

Nominal ice condenser cooling air temperature 10°F - 20°F

The design must also provide a sufficiently well insulated ice condenser annulus such that with a complete loss of all refrigeration capacity, sufficient time exists for an orderly reactor shutdown prior to ice melting. A design objective is that the insulation of the cavity is adequate to prevent ice melting for approximately 7 days in the unlikely event of a complete loss of refrigeration capability.

The non-directly safety related design objective parameters are:

Ice Sublimation

Ice sublimation and mass transfer is reduced to the lowest possible limits by maintaining essentially isothermal conditions within the ice bed and by minimizing local temperature gradients. A design objective is to limit the sublimation of the ice bed to less than 2 percent per year by weight. The normal steady state sublimation appearing on the wall panels as frost is calculated to be significantly less than the total design objective. Calculations incorporating both radiative and convective modes of heat transfer result in a sublimation rate of less than 0.5 percent per year to the wall panels.

An appropriate combination of refrigeration capacity and insulation capability is achieved to permit the following:

Maintain the average ice bed temperature in the range of 10° to 20°F under the most adverse non-accident conditions.

Cool the ice condenser down to 15°F in 14 days (initial cooldown prior to ice loading.)

The Ice Condenser is structurally designed to withstand the various extreme loading parameters including DBA + SSE. The ice condenser design and the reactor Containment supporting walls are analyzed for heat transfer through the boundaries of the ice condenser. The configuration and sizing of the cooling components is then determined to achieve the various design requirements.

One of the most important design criteria for the ice condenser is that the insulation shall maintain the ice condenser chamber below 31°F for a significant period of time given that a malfunction or failure of any refrigeration component has occurred. Most system anomalies can be remedied during this period. For any repair which would require more time, a scheduled reactor shutdown can be completed in a safe and orderly fashion. Eliminating the "emergency factor" from the operation of the Refrigeration System places the performance of the refrigeration components in an operational category without mandatory safety related design requirements.

6.7.6.2 System Design

The Refrigeration System serves as a central heat sink for sensible heat and heat of fusion picked up, respectively, in the ice condensers and in the ice machines. A circulating loop of ethylene glycol solution carries the heat from the various heat transfer surfaces to the chiller packages. Cooling of the ice condenser is achieved by a Three Stage System:

First Stage - Refrigerant Loop

Second Stage - Glycol Loop

Third Stage - Air Cooling Loop

First Stage - Refrigerant Loop

Four 50 ton chiller packages and two 25 ton chillers are installed for the station. Each 50 ton chiller package consists of two separate 25 ton compressor units. See [Figure 6-149](#) for refrigerant cycle diagram. Ethylene glycol solution is cooled during its passage through the evaporator, and heat is removed from the chiller unit by cooling water flowing through the condenser. The condenser cooling water is provided from the Recirculated Cooling Water System. The chiller units operate individually to maintain outlet temperature of ethylene glycol at -6.5°F.

Refer to [Table 6-121](#) for chiller package parameters such as operating temperatures, flow rates, pressure drops, rating basis, etc.

Second Stage - Glycol Loop

The second cycle ([Figure 6-150](#)) carries the heat removed from the ice condenser air handling units, the Floor Cooling System and the ice machines (when operating) to the refrigerant cycle evaporator/cooler units. The liquid circulating through this cycle is a corrosion inhibited 50 percent ethylene glycol solution. It is compatible with most common piping materials and standard gasket and packing materials. Piping and valve materials used in this loop are predominantly carbon steel with stainless or alloy trim. Diaphragm valves are provided with ethylene propylene diaphragms. Piping and equipment carrying chilled ethylene glycol solution are covered with low temperature thermal insulation.

Six glycol circulating pumps (6 operating, 3 per unit) are provided to convey the cooled glycol from the ten refrigeration units to the air handling packages (30 per Containment) and to the ice compartment floor cooling coils of both Containments. The heated glycol is returned to the refrigeration units completing the glycol loop. The heat is extracted from the air in its passage through the air handlers and from the floor cooling coils. Two rows of air handlers located along inner and outer walls are served by respective glycol supply and return headers. The return headers are connected to a vented expansion tank located above the upper deck in each unit. Pairs of containment isolation valves are installed on supply and return lines on both sides of Containment penetration. Closure of these valves in response to an ST-signal¹ isolates the ethylene glycol piping inside the containment vessel from the External Refrigeration System. In the event of a LOCA, the glycol heats up from approximately -6.5°F or 0°F to the containment accident temperature and expands harmlessly into the expansion tank. The liquid trapped between a pair of isolation valves is relieved around the inner isolation valve through a bypass line via a small check valve. The bypass line also contains test connections for periodic leak testing of the isolation valves and the check valve.

The Ice Condenser floor is kept cold by chilled glycol solution circulating through pipe coils embedded in the concrete wear slab. (See Section [6.7.1](#) and Figures [6-139](#), [6-140](#), and [6-150](#)). During normal operation, one floor cooling pump feeds a circular header, which distributes the coolant to individual coils located in each bay. A second circular header returns the flow to the AHU supply header.

The glycol solution is maintained at the proper temperature by continuously bleeding solution out of the system and feeding cold solution into it at the same rate. The cold solution is taken from the glycol stream to the air handling units. The bleed flow is sent back into the same line downstream of the feed connection. Feed and bleed flow is maintained by the pump that drives solution through the coils. The operators manually control bleed flow rate based on temperature. A second pump is available for use while the other is being serviced.

Floor temperature is generally maintained between the temperatures of the ice bed and the wall panels. There should, therefore, be essentially no frosting on the floor surface. It is necessary to heat the floor above 32°F any time the wall panels are being defrosted in order to keep the water melting off the wall panels from freezing to the floor. At this time, the floor is heated with warm glycol. After defrosting is completed, the system is restored to its normal cooling status. The defrost cycle is relatively brief and its effect on the ice bed is negligible.

Components requiring periodic maintenance (pumps, heater, control valve) are located in the upper compartment. The cooling coils in the concrete wear slab rest on a steel plate to effectively intercept heat passing up through the floor. The coils are made of heavy steel pipe to minimize the chances of developing a leak by gradual corrosion of pipe material. Should a leak develop, any individual loop can be isolated by closing two valves inside the lower region of the ice condenser.

¹ Containment isolation signal, phase A, derived from Safety Injection or manually.

[Table 6-121](#) has additional detailed parameters for the glycol cycle components.

Third Stage - Air Cooling Loop

The ice condenser compartment is designed to be kept below the freezing point throughout the life of the unit. It is cooled to 15°F prior to ice loading and kept near that temperature indefinitely, barring occurrence of a loss-of-coolant accident, extensive failure of the chilled glycol loop or permissible excursion during ice loading. Ice bed temperature is maintained at the specified level by means of chilled air circulating through the boundary planes of the compartment. Starting in the upper plenum, which constitutes the top boundary, air enters one of 30 air handling packages located in the plenum. The air handler cools the air then blows it down through a series of insulated duct panels lining the inner, outer and end walls of the ice condenser. When the air reaches the lower support structure at the inner wall or end walls or the floor level at the outer wall, it turns back up to the plenum through a parallel path in the wall panels. See [Figure 6-151](#) for a schematic flow diagram of the air cooling cycle.

The air handling units are designed for automatic self-defrost operation. The self-defrost cycle is initiated by a preset timer. The timer programs defrost time and duration for each individual air handler unit. Both the time and duration of the defrost can be adjusted by resetting the timer. When the timer setting is reached, the AHU power operated valve is closed, stopping glycol flow, and a limit switch is activated which de-energizes the fan motor and energizes the defrost heaters of the AHU. The normal self-defrost cycle is terminated by a thermostat when the coil temperature reaches 100°F. The total self defrost cycle is completed in less than 30 minutes. In addition to the coil defrost heaters mounted on the face of the coil, each unit has a drain pan heater and a condensate drain heater. These heaters prevent refreezing of the coil defrost water during the defrost cycle.

The coil defrost heaters have a high limit thermostat that will terminate the defrost heat if a high setpoint of 180°F is exceeded.

Provisions also exist for defrosting the wall panels by circulating heated air through the wall panels. The structural function and capabilities of the air cooling cycle components are discussed in the following sections:

AHU - Section [6.7.7](#)

Wall Panels - Section [6.7.2](#)

Air distribution ducts - Section [6.7.12](#)

[Table 6-121](#) has additional parameters for the air handling units.

6.7.6.3 Design Evaluation

The Refrigeration System is sized to maintain the required ice inventory even under worst case operating conditions. The chiller package total capacity is sufficient to maintain both ice condensers.

| | | |
|----|--|-------|
| 1. | Lower Containment, air temperature | 120°F |
| 2. | Upper Containment, air temperature | 100°F |
| 3. | Equipment room air temperature | 120°F |
| 4. | Exterior Containment wall design air temperature | 110°F |

Items 1 through 3 are specified in the general design criteria for the Ice Condenser. Item 4 is the design dry-bulb temperature in the region of South Carolina where the Catawba units are located for a 50 year hot summer, plus an additional margin of 9°F.

The 1 percent factor is defined such that only 1 percent of the time the dry-bulb temperature during the summer months is above the specified temperature for a 50 year hot summer. Data was obtained from ASHRAE climatic guide for cooling and heating design conditions. For an average summer, the 1 percent design dry-bulb temperature is 96°F and for a 50 year hot summer, is 101°F.

The major thermal boundaries of the ice condenser including the floor, cooled walls with ducts, lower inlet doors, and top deck support beams are analyzed using a Westinghouse developed computerized technique, TAP-A (or TAP-B). A program for Computing Transient or Steady-State Temperature Distributions, WANL-TME-1872, Dec. 1969, Subcontract NP-1.

The TAP-A program is applicable to both "transient and steady-state heat transfer in multi-dimensional systems having arbitrary geometric configurations, boundary conditions, and physical properties. The program can be utilized to consider internal conduction and radiation, free and forced convection, radiation at external surfaces, specified time dependent surface temperatures, and specified time dependent surface heat fluxes."

The solution of the general heat conduction equation is determined with finite difference techniques. The program solves the equation as determined for the particular finite element or nodal model set up, either explicitly or implicitly. All cases studied for the ice condenser are solved implicitly.

The TAP-B program is a variation of TAP-A but includes fluid coupling to the finite element model. The TAP-B variation is used to analyze the cooled wall panels. Since the duct air temperature distribution is included in the model it is possible to evaluate the temperature distribution of the surface of the wall panel facing the ice condenser over the complete length of the duct.

The wall panel heat load comprises about 70 percent of the total heat load, through the thermal boundaries with the inner surface area of the wall panels covering just under 30,000 ft².

The wall panel model for the crane wall is 48 ft long with 8 axial stations each 6 ft in length. The width of the model covers the region from the centerline of the cut region to the centerline of the lap strip region.

There are approximately 1,000 interior and surface nodes for the 48 foot length of the model which consists of 1/2 of a duct section.

Roughly 70 percent of the thermal load through the wall panels flows through the mounting brackets (or about 50 percent of the total thermal load of the ice condenser). The cold boundary temperature of the model was assumed to be 12°F in the ice bed with a 10°F duct entrance temperature.

The basic floor model utilizes TAP-B. The basic floor design is analyzed with fluid coupling. The results of the basic model justifies the design concept. Variations in the basic floor design are checked by hand calculations for overall thermal load. The basic floor model is comprised of approximately 1200 nodes in 5 layers and covers one quarter of a typical floor bay, of which there are 24 bays. The air temperature over the floor is assumed to be 14°F. The temperature of the glycol boundary is calculated for each fluid node. Over 90 percent of the heat entering the floor region is found to be removed by the floor cooling coils. Use is made of the transient capabilities of the program to determine the defrost or warm-up time required when the glycol is heated. The heat transfer through the top surface of the floor is in two directions, both into and

out of the wear slab. The new flow from the top surface to the ice condenser chamber is about 1000 Btu/hr. About 78,000 Btu/hr total is absorbed by the floor glycol coolant using the basic model.

The lower inlet door region while not contributing significantly to the overall thermal load is extremely important when considering sublimation. Various models of portions of the door are postulated to determine effective means of limiting the heat flux through the lower inlet doors.

The total heat load through doors with appropriate insulation is maintained at less than 11,000 Btu/hr to the ice bed. The door assembly is analyzed in two segments, there are 24 complete 2 door assemblies in the ice condenser. The first door model covers the region from the centerline of one door panel to the central seal region. Hand calculations are used to determine the nature of the convection between the two door panels in the central seal region, and in the outer hinge region. The information on the type of convection present is necessary to be gained from positioning flaps or boots around the door perimeter. Flaps are not considered necessary in the door center because the convection is determined to be laminar with air conduction dominating. The central door model contains about 150 internal nodes including insulation. The second region covered by a model is the hinge region. The hinge model is 15 inches deep (about 1/6 of) the door length and included effects of the reinforcement channels along the full width of the door. The extremities further away from the hinge region are only grossly modeled. There are a total of 168 internal nodes in the "hinge" model including a protective boot around the hinge. The hinge model also includes effects of the pillar in the crane wall upon which the door is mounted. The hinge region is of major importance in contributing to the internal thermal load with most of the heat input coming from the massive concrete pillar. It is necessary to protect the hinges with boots to limit the convective heat transfer which is quite effective in reducing the heat flow.

The top deck support beams are similarly modeled using TAP-A. The beams are a major source of thermal load in the plenum are thermal boundaries but only a small fraction of the total thermal load on the air handlers (not including air handler motor heat).

The modeling required for analysis of the components is extensive and detailed. The admittance of each node and connection; involving the determination of the length, volume, and area of each element was conservatively estimated where simplification of the model was required. The models are realistic since sufficient detail was considered and all significant modes of heat transfer were considered. Hand calculations back-up all major assumptions used to arrive at a model.

The summation of the thermal analysis gives a total nominal thermal load of 60.6 tons or 727,600 Btu/hr.

The breakdown is listed below. The values given are considered to be nominal expected loads.

| | x 10 ⁴ .Btu/hr |
|---------------------|---------------------------|
| Wall panels | 27.3 |
| Plenum and Top Deck | 9.3 |
| Leakage 50 cfm | 1.3 |
| Lower inlet doors | 1.1 |
| Floor | 0.2 |
| End walls | 1.17 |

| | |
|--------------------|---------------------------|
| | x 10 ⁴ .Btu/hr |
| Total thermal load | 40.37 |

The calculated heat loads show that a heat gain of 432,000 Btu/hr per containment may be expected from thermal boundaries of the ice condenser. Additionally, each air handling unit fan motor generates less than 6,000 Btu/hr (Subtotal 30 AHU x 6,000 Btu/hr = 180,000 Btu/hr) based on 30 operating air handlers with a design allowance of 1.5 in. of H₂O over the Air Delivery System. The Floor Cooling System, including pump heat, has a heat gain of 90,000 Btu/hr nominal.

Two additional 25 ton chillers were added prior to commercial operation to support maintenance activities and add cooling margin.

The circulating pumps (2 operating) add a total of 100,200 Btu/hr. The piping is estimated to pickup 7,000 Btu/hr. Therefore, a chiller package capacity of about 800,000 Btu/hr per Containment (base load) is required. Since this is a dual unit application and the chiller packages serve both units, the total chiller package capacity was chosen to be three (3) times the base load which is 2,400,000 Btu/hr. Since each chiller package is rated nominally at 600,000 Btu/hr, depending on cooling water temperatures, four chiller packages are installed.

The six circulating pumps (3 pumps/unit) are conservatively sized to deliver the required coolant to each unit. Similarly the air handling units are conservatively sized to handle the worst case cooling load. Thirty air handling packages are installed based on a 10/7 ratio of installed capacity to base load.

The ice bed is sufficiently subcooled and insulated so that even a complete breakdown of the refrigeration system or of all air handlers does not permit the average temperature of the ice bed to rise above the melting point of the borated ice for a period of approximately one week. Anomalous conditions in the ice condenser are indicated by alarm annunciation from expansion tank level switches, the Temperature Monitoring System, or the Door Position Monitoring System. Refer to Section [6.7.15](#) for a discussion of the Ice Condenser Instrumentation System.

If one bay in the floor is not cooled because the glycol flow has to be isolated from that bay the heat load from that bay is about 3,000 Btu/hr. The additional sublimation rate would be under 0.25 percent per year per bay. It would be expected that one bay would not be permitted to go uncooled for extensive length of time. Once an operational sublimation rate is established it would not be unreasonable to assume that possibly 3 isolated - uncooled floor bays could be permitted to be uncooled for about 1 year. If the Floor Cooling System is shut off completely, it should be put back in operation as soon as convenient. An annual sublimation rate of about 5 percent per year will result with no cooling in the floor, which would require ice bed replenishing in 3 years.

6.7.7 Air Handling Units

6.7.7.1 Design Bases

Air Handling Units (AHU)

During normal operation the air handling units cool and circulate the air through the ice condenser wall panels to keep the ice subcooled. Normal structural loads expected are dead weight, seismic, SSE and thermal loads. During an accident the AHU structure is designed to resist the normal structural loads plus SSE + DBA induced loads. Welding, welder qualification,

and weld procedures are in accordance with USASI B31.5 Refrigeration Piping and the ASME Boiler and Pressure Vessel Code, Section IX "Welding Qualification".

AHU Support Structure

Function

The AHU support structure supports the air handling unit package under various design conditions which are detailed below:

Design Criteria and Codes

Refer to Section [6.7.16](#)

Design Conditions

Normal Operation

Deadweight loads due to AHU, structure 2500lbs

Design temperature, min. 15°F

Accident Conditions

Post-accident Temperature 317°F (The Peak Containment Temperature
(no uplift) Transient is discussed in Section [6.2.1.1.3.3.](#))

6.7.7.2 System Design

Air Handling Units

Each AHU is supported from its support structure, transmitting its major loads to top deck cross beams. See the AHU Support Structure Design Criteria for additional details.

The air is drawn by each AHU from the upper plenum, is cooled in the AHU and is discharged into the air distribution header. The gross cooling capacity of each AHU package is 30,000 Btu/hr with the plenum air entering at a nominal 19°F and cooled to 10°F nominal. Each package has a 2,200 cfm nominal air delivery capacity. The entering glycol mixture is at -5°F nominal temperature and discharged at 1.0°F nominal. Electrical power is provided for fan motor and defrost heaters as well as for control circuits.

In order to limit seismically induced loads the AHU and supports are designed to have a natural frequency in excess of 20 Hz. All materials used in the AHU's are compatible with both normal and post LOCA environments.

AHU Support Structure

The support structure supports the air handling unit vertically and tangentially from the cross beam of the top deck structure and is radially hinged from channels attached to the crane or Containment wall. All parts are coated with a paint suitable for use inside Containment. [Figure 6-152](#) shows the design of the structure.

6.7.7.3 Design Evaluation

The pressure drop through the ducts and manifolds was estimated by using loss coefficients determined by using a standard reference (Reference [7](#)) as a guide. The pressure drop through the air handlers was determined by test. The overall system flow rate was established by superimposing the system flow versus P curve over the fan flow versus P curve.

With the flow rate established the capacity of the air handlers was determined. First the air handler capacity was theoretically determined for a set of design conditions approximating operating conditions. Next the air handler units were tested by the manufacturer to the set of specified design conditions. It was determined that the theoretical relationships adequately predicted air handler performance and these techniques were then used to adjust the test values to those of actual operation. The gross operating capacity of one air handler is just under 30,000 Btu/hr by test and calculation.

The air handling unit heat load is adjusted by a factor of 10/7 to insure adequate capacity under operating conditions for fouling, defrosting or isolated instances of one or several unit failures. Maintenance and inspection insures reliable mechanical operation and cooling performance.

An estimate of the number of air handlers required is made to initiate the calculation, the flow pressure and rates drops are then calculated and the fan motor heat and heat transfer rates of the air handler unit predicted. The predicted performance is compared with the required capability and the calculation is reiterated varying the number of AH units until the predicted performance just exceeds the required capability.

The final number of required air handlers was determined to be 30.

A modal frequency analysis was performed for the air handling unit housings and support structure. The results indicate that the design frequency is approximately 20 Hz, so that the fundamental mode is well out of the frequency range of peak amplification on the response spectra. In the process of designing the structure on the basis of stiffness, strength of members subjected to various combinations exceeds specified limits by generous margins.

6.7.8 Lower Inlet Doors

6.7.8.1 Design Bases

Function

The ice condenser inlet doors form the barrier to air flow through the inlet ports of the ice condenser for normal unit operation. They also provide the continuation of thermal insulation around the lower section of the crane wall to minimize heat input that would promote sublimation and mass transfer of ice in the ice condenser compartment. In the event of a loss-of-coolant accident, LOCA, causing a pressure increase in the lower compartment, the doors open, venting air and steam relatively evenly into all sections of the ice condenser.

The door panels are provided with tension spring mechanisms that produce a small closing torque on the door panels as they open. The closing torque (along with the developed ice condenser cold head) is intended to re-close the door panel should it briefly and inadvertently open during normal operation. The zero load position of the spring mechanisms is set such that, with zero differential pressure across the door panels, the gasket holds the door slightly open.

For larger incidents, the doors open fully and flow distribution is controlled by the flow area and pressure drops of inlet ports. The doors are provided with shock absorber assemblies to dissipate the larger door kinetic energies generated during large break incidents.

Design Criteria

Radiation Exposure

Maximum radiation at inlet door is 5 rad/hr gamma during normal operations. No secondary radiation due to neutron exposure.

Structural Requirements

Refer to Section [6.7.16](#)

Loading Modes

The door hinges and crane wall embeddings, etc., must support the dead weight of the door assembly during all conditions of operation. Door hinges shall be designed and fabricated to preclude galling and self welding.

Seismic Loads tend to open the door.

During normal operations the outer surface of the door operates at a temperature approaching that of the lower compartment while the inner surface approaches that of the ice bed. During loss-of-coolant accidents, the outer surface is subjected to higher temperatures on a transient basis. Resultant thermal stresses are considered in the door design.

During large break accidents, the doors are accelerated by pressure gradients then stopped by the Shock Absorber System. During small break accidents, doors open in proportion to the applied pressure with restoring force provided by springs. Upon removal of pressure, door closure results as a result of spring action.

Design Criteria - Accident Conditions

All doors open to allow venting of energy to the ice condenser for any leak rate which results in a divider deck differential pressure in excess of the ice condenser cold head.

The force required to open the doors of the ice condenser is sufficiently low such that the energy from any leakage of steam through the divider barrier can be readily absorbed by the Containment Spray System without exceeding Containment design pressure.

Deleted Per 2010 Update.

The basic performance requirement for lower inlet doors for design basis accident conditions is to open rapidly and fully, to insure proper venting of released energy into the ice condenser. The opening rate of the inlet doors is important to insure minimizing the pressure buildup in the lower compartment due to the rapid release of energy to that compartment. The rate of pressure rise and the magnitude of the peak pressure in any lower compartment region is related to the confinement of that compartment. The time period to reach peak lower compartment pressure due to the design basis accident is approximately 0.05 seconds.

Doors are of simple mechanical design to minimize the possibility of malfunction.

The inertia of the doors is low, consistent with producing a minimal effect on initial pressure.

Design Criteria - Normal Operation

The doors restrict the leakage of air into and out of the ice condenser to the minimum practicable limit. The inlet door leakage has been confirmed by test to be within the 50 cfm total used for the ice condenser design.

The doors restrict local heat input in the ice condenser to the minimum practicable limit. Heat leakage through the doors to the ice bed is a total of 20,000 Btu/hr or less (for 24 pairs of doors).

The doors are instrumented to provide indication of their closed position. Under zero differential pressure conditions all doors remain 3/8 inch open.

Provision for adequate means of inspecting the doors during reactor shutdown.

The doors are designed to withstand earthquake loadings without damage so as not to affect subsequent ice condenser operation for normal and accident conditions. These loads are derived from the seismic analysis of the Containment.

Deleted Per 2010 Update.

Interface Requirements

Crane wall attachment of the door frame is via bolts into embedded anchor plates with a compressible seal. Attachment to the crane wall is critical for the safety function of the doors.

Sufficient clearance is required for doors to open into the ice condenser. Items to be considered in this interface are floor clearance, lower support structure clearance and floor drain operation and sufficient clearance (approximately six inches) to accommodate ice fallout in the event of a seismic disturbance occurring coincident with a loss-of-coolant accident.

Original ice basket qualification testing (Topical Report WCAP-8110, Supplement 9-A), has shown freshly loaded ice is considered fused after five weeks. In the event of an earthquake (OBE or greater) which occurs within five weeks following the completion of ice basket replenishment, plant procedures require a visual inspection of applicable areas of the ice condenser within 24 hours to confirm that opening of the ice condenser lower inlet doors is not impeded by any ice fallout resulting from the seismic disturbance. This alternative method of compliance with the requirements of GDC 2 is credible based upon the reasonable assurance that the ice condenser doors will open following a seismic event during the 5 week period and the low probability of a seismic event occurring coincident with or subsequently followed by a Design Basis Accident.

Door opening and stopping forces are transmitted to the crane wall and lower support structure, respectively.

Design Loads

Pressure loading during LOCA is provided by the Transient Mass Distribution (TMD) code from an analysis of a double-ended hot leg break in the corner formed by the refueling canal, with 100 percent entrainment of water in the flow. For conservatism, TMD results were increased by 40 percent in performing the design analysis for the lower inlet doors.

The lower inlet door design parameters and loads are presented in [Table 6-122](#).

6.7.8.2 System Design

Twenty-four pairs of inlet doors are located on the ice condenser side of ports in the crane wall at an elevation immediately above the ice condenser floor. General details of these doors are shown in [Figure 6-154](#) through [Figure 6-158](#). Each door panel is 92.5 in. high, 42 in. wide and 7.5 in thick. Each pair is hinged vertically on a common frame.

Each door consists of a 0.5 in. thick Fiber Reinforced Polyester (FRP) plate stiffened by six steel ribs, bolted to the plate. The FRP plate is designed to take vertical bending moments resulting from pressures generated from a LOCA and from subsequent stopping forces on the door. The ribs are designed to take horizontal bending moments and reactions, as well as tensile loads resulting from the door angular velocity, and transmit them to the crane wall via the hinges and door frame.

Seven inches of urethane foam are bonded to the back of the FRP plate to provide thermal insulation. The front and back surfaces of the door are protected with 26 gauge stainless steel covers which provide a complete vapor barrier around the insulation. The urethane foam and stainless steel covers do not carry overall door moments and shearing forces.

Three hinge assemblies are provided for each door panel; each assembly is connected to two of the door ribs. Loads from each of the two ribs are transmitted to a single 1.572 inch diameter hinge shaft through brass bushings. These bushings have a spherical outer surface which prevents binding which might otherwise be caused by door rib and hinge bar flexure during accident loading conditions. The hinge shaft is supported by two self-aligning, spherical roller bearings in a cast steel housing. Vertical positioning of the door panel and shaft with respect to the bearing housing are provided by steel caps bolted to the ends of the shaft and brass spacer rings between the door ribs and bearings. Shims are provided between the shaft and caps to obtain final alignment. Each bearing housing is bolted to the door frame by four bolts, threaded into tapped holes in the housing. Again, shims are provided between the housings and door frame to maintain hinge alignment. Hinges are designed and fabricated to prevent galling and self welding.

The door frame is fabricated mainly from steel angle sections; 6 in x 6 in. on the sides and 6 in. x 4 in. on the top and bottom. A 4 in. central I beam divides the frame into sections for each door. At each hinge bracket, extensions and gusset plates, fabricated from steel plate, are welded to the frame to carry loads to the crane wall.

The door panel is sealed to the frame by a compliant rubber seal which attaches to channels welded to the door frame. During normal unit operations these seals are compressed by the cold air head of the ice bed acting on the door panels. As the seals operate at a much warmer temperature than the ice bed, frosting of the seal region is extremely unlikely.

Each door is provided with four springs. One end of each spring is attached to the door panel and the other to a spring housing mounted on the door frame. These springs, along with the developed ice condenser cold head, assure that the doors close in the event they are inadvertently opened during normal unit operations. The springs are adjusted such that, with no load on the doors, the doors are slightly open.

In order to dissipate the large kinetic energies resulting from pressures acting on the doors during a LOCA, each door is provided with a shock absorber assembly as shown in [Figure 6-158](#). The shock absorber element is a sheet metal air box approximately 93 in. high, 46 in. wide, and 29.6 in. thick at its thickest section. The air box is attached to a back plate assembly which is bolted to the ice condenser lower support structure.

Two edges of the sheet metal box are fastened to the ends of back plate by clamping bars and bolts, making them air tight joints. The sheet metal is bent such that it has an impact face and a pre-folded side.

When the lower inlet doors open due to sudden pressure rise, they impact on the impact face of the air box. The impact face moves with the door. Because of a restraining rod within the box, the pre-folded side of the air box collapses inwards. The volume of the air trapped in the air box decreases as the impact face moves towards the back plate, thereby increasing air pressure. Part of the kinetic energy of the door is used up in compressing air. To prevent excessive pressure rise, the air is allowed to escape through the clearance gap between the sheet metal and end plates. A portion of the energy of the doors is also used in buckling of stiffeners.

Material

Door materials are consistent with the listing of acceptable materials as presented in Section [6.7.18](#). All exposed surfaces are made of stainless steel or coated with paint suitable for use inside the Containment. All insulation material is compatible with containment chemistry requirements for normal and accident conditions.

6.7.8.3 Design Evaluation

The lower inlet doors are dynamically analyzed to determine the loads and structural integrity of the door for the design basis load conditions.

Using TMD results as input, the door dynamic analysis is performed using the "D00R" Program. This computer program has been developed to predict door dynamic behavior under accident conditions. This program takes the door geometry and the pressures and calculates flow conditions in the door port. From the flow are derived the forces on the door due to static pressure, dynamic pressure and momentum. These forces, plus a door movement generated force, i.e., air friction, are used to find the moment on the door and from this the hinge loads. Output from the program includes door opening angle, velocity and acceleration as functions of time as well as both radial and tangential hinge reactions.

Analysis Due to LOCA

The net load distributions on the door for both opening and stopping are determined by considering the applied pressures acting on the door and then solving the rigid body equations of motion such that the net forces and moments at the hinge point are zero. In the process, this produces expressions for the inertial forces in the door and a hinge reaction as functions of the applied pressure.

The expressions for net load distribution are integrated to determine door shear and moment as functions of distance from the hinge point. The resultant load, shear and moment distribution curves and the total hinge loads, calculated by the "D00R" Program, provides the inputs for subsequent stress analysis.

Using this input, the door assembly is analyzed as a stiffened plate structure with vertical bending being taken by the FRP outer plate and horizontal bending plus radial tensile loads being resisted by the steel ribs. As inertial forces are directly accounted for in the analysis, no dynamic load factor was applied.

Hinge pin, hinge bracket, and frame stresses are analyzed under hinge reactions considering the effects of tension, shear bending, and torsion as appropriate. For these components, a dynamic load factor of 1.2 was calculated and applied.

Stresses in the door returns springs are calculated considering dynamic effects as well as static ones. Welded and bolted connections are analyzed as part of the overall door, frame and hinge analysis.

All portions of the door and frame show factors of safety greater than one. The general acceptance criterion is that stresses be within the allowable limits of the AISC-69 Structural Code. This provides an additional margin of conservatism over the general ice condenser design criteria for D + DBA which permit stresses up to 1.33 times the AISC limits. For materials and components not covered by the Code, i.e., bearings, non-metallic materials, etc., conservative acceptance criteria are established on the basis of manufacturer's recommendations and/or engineering evaluations.

The effects of door closure were evaluated assuming the pressure is suddenly released from a fully opened door and the door allowed to shut under the effect of the return springs. Stress levels in the door, gasket, and frame are found to be acceptable for this condition. In addition to the above analysis, full scale simulated blowdown tests have been performed on prototype door and shock absorber assemblies. These tests confirm the adequacy of these components at test levels up to 140 percent of maximum loading conditions predicted by the TMD Code.

Analysis of Seismic Loading

Seismic analysis of the doors indicates that stresses are insignificant in comparison with those occurring during a LOCA. Under a SSE the doors could open several inches (actually, the crane wall will move away from the doors). At the termination of the earthquake, the doors immediately close and reseal under the effects of return spring tension and the ice bed cold air head. Thus, any loss of cold air during a OBE or SSE is small and limited to a short period of time.

The dynamic testing of the air box shock absorber is discussed in Reference [12](#).

Surveillance Testing

To verify that the Lower Inlet Doors (LIDs) will function as intended, periodic testing is performed. Section 3.6.13 of Technical Specifications specifies tests and inspections performed to verify the functional capability of the LIDs. Bases for the surveillance tests and inspections are provided in the Bases for Section 3.6.13 of Technical Specifications.

Visual inspections of the LIDs are performed to verify that the doors are not impaired by ice, frost or debris. This provides assurance that the doors are free to open in the event of a Design Basis Accident (DBA). To provide assurance that the doors are not stuck in the closed position, a physical test is performed on the closed LIDs to determine the torque required to pull the doors off of their seals. In addition, a visual assessment of the door's motion through its swing arc (i.e., approximately 40° or up to slight contact with the shock absorber) is performed to ensure the inlet door moves freely and returns the door back toward the closed position, and to monitor the performance of the hinges and spring closure mechanisms to ensure they are being properly maintained.

Deleted Per 2010 Update.

6.7.9 Lower Support Structure

6.7.9.1 Design Bases

The lower support structure is designed to support and hold down the ice baskets in the required array, to provide an adequate flow area into the ice bed for the air and steam mixture in the event of a Design Basis Accident, to direct and distribute the flow of air and steam through the ice bed, and to protect the Containment structure opposite the ice condenser inlet doors from direct jet impingement forces.

The last two functions are accomplished by turning vanes that are designed to turn the flow of the air and steam mixture up through the ice bed in event of a Design Basis Accident. For such an event, the vanes would serve to reduce the drag forces on the lower support structural members, reduce the impingement forces on the Containment across from the lower inlet doors and to distribute the flow more uniformly over the ice bed. In addition to the turning vanes, the lower support structure has a continuous impingement plate around the outer circumference of the lower support structure, designed to reduce the jet impingement forces on the Containment structure across from the lower inlet doors in the event of a Design Basis Accident.

Design Criteria and Codes

The loading combinations, stress limits and material specifications used in the design of the lower support structure are given in Sections [6.7.16](#) and [6.7.18](#).

Design Conditions

The normal operating temperature range is 10°F to 25°F. The normal operational temperature change, including maintenance operations is 10°F to 70°F. The maximum temperature during a

Design Basis Accident is 317°F (The Peak Containment Temperature Transient is discussed in Section [6.2.1.1.3.3.](#))

The loads used for the design of the lower support structure consist of dead weight (gravity), forces as a result of DBA, OBE and SSE seismic loads and loads as a result of thermal changes.

The dead loads include the weight of the crane wall insulated duct panels, the weight of the intermediate deck doors and frames, the weight of the lattice frames and columns, and the weight of the turning vanes. The weight of the ice baskets filled with ice, the slotted jet impingement plate assemblies and the door shock absorber, also act on the lower support structure.

Forces and loadings that occur during LOCA were provided by the Transient Mass Distribution (TMD) Code from analysis of double-ended breaks in an end compartment, with 100 percent entrainment of water in the flow. For conservatism, all forces and loads that are a result of TMD were increased by 40 percent in performing the detail design and analysis for the lower support structure.

The lower support structure seismic design loads were developed using dynamic seismic analysis and the defined seismic response curves for the Catawba Nuclear Station.

Thermal loading conditions, which result from two thermal excursions were specified for the lower support structure. One thermal excursion from 10°F to 70°F, is defined as a normal operating service load, and the other, defined as 70°F to 250°F, is the thermal excursion seen by the lower support structure following a LOCA.

The loading combinations considered in the design are given in Section [6.7.16.](#)

6.7.9.2 System Design

The lower support structure is shown on [Figure 6-159](#) and [Figure 6-160](#). The lower support structure is contained in a 300 degree circular arc of the Containment. The three-pier lower support structure consists of 24 horizontal platform assemblies, 24 upper turning vane assemblies, 24 floor turning vane assemblies, and 24 impingement plate assemblies. The aforementioned assemblies are supported by 25 radial portal frame assemblies with columns at radii of 45 feet 6 inches, 49 feet 11 3/4 inches, and 55 feet 8 1/2 inches. The 25 portal frame assemblies are spaced at approximately 12-1/2 degrees between adjacent portal frames. The total height of the structure is 9 feet 7 7/8 inches, measured from the top surface of the lower support structure to the pin. The design is such that the flow area at the ice basket interface for all 24 bays is at least 1088 square feet.

The horizontal platform consists of an inner and outer platform assembly for each bay. As assembled, the platform includes inner, middle and outer straight circumferential beams which span each portal frame. Nine radial beams formed by bar sections are welded to the inner, middle and outer circumferential beam. There is horizontal cross bracing between the inner and middle circumferential beams and the outer and middle circumferential beams.

The outer horizontal platform assembly consists of nine radial beams welded to the outer circumferential beam and welded to a channel which forms one half of the middle circumferential beam. The inner horizontal assembly is similar to the outer platform assembly. The channels of the inner and outer horizontal platform assemblies are field bolted to form a continuous middle circumferential beam.

For each bay, the platform inner and middle circumferential beams are connected to the portal frames with a shear connection, i.e., no moment is transmitted to the columns. The outer

circumferential beam is connected to the portal column, but the connection is designed to transmit moment about a vertical axis. Every alternate horizontal platform (per bay) is connected to the columns at one side by bolted connections, which are slotted along the axis of the circumferential beams to accommodate circumferential thermal expansion. The adjacent bay is not slotted in the circumferential direction and supplies the tangential shear resistance for the slotted bay.

There are nine radial beams in each portal bay and each radial beam supports nine ice basket columns. Provision is made for attaching, by bolting, each ice basket column to the radial beams.

The inner and outer circumferential beams of the platform assembly have the lattice frame column supports bolted to them. The insulated duct panels on the Containment wall interface, the floor, and the insulated duct panels on the crane wall are supported by the inner circumferential beams of the lower support structure.

Each radial portal frame is comprised of three columns. The primary radial shear resistance is provided by a 2 in. thick plate with attached welded channels forming the inner and middle columns thus forming a steel shear wall. The outer column (radius 55 feet 8 1/2 inches) is attached to the middle column assembly by a 2 in. thick plate. The 2 in. thick plate is pin-connected to the outer column by bars pinned at both ends and welded to the middle column. The column base plates are pin-connected to the ice condenser support floor. To accommodate thermal expansion, the middle pier column pin connections are designed to allow radial expansion, and every other outer column base plate pin connection is designed to allow circumferential expansion. The inner pier columns (near the crane wall) are designed to transmit all three force components. The base plate pin arrangement is shown on [Figure 6-159](#). The lower inlet door shock absorbers are mounted to the 2 in. thick portal frame plate.

Tangential or circumferential rigidity of the lower support structure is provided by a cross bracing system between the outer columns. The cross bracing system is provided in alternate bays, which coincide with the bays in which the circumferential platform beams are not slotted in their axial direction at the column attachment points.

To turn, direct and distribute the flow through the lower inlet doors during a LOCA, each portal bay has five turning vanes that span between the adjacent radial portal frames. The vanes are as indicated on [Figure 6-159](#). The vanes are slotted on one side in each bay to allow circumferential thermal growth.

In addition to the turning vanes, a beam gridwork spans between adjacent outer columns ([Figure 6-159](#)) and acts as a jet impingement shield for the fluid flow not turned by the vanes. The slotted plate assembly is provided in each bay of the lower support structure and is attached to the outer columns with a bolted connection. Similar to the turning vanes, the slotted plate assembly is bolted on one side with slotted holes to allow for circumferential thermal growth.

The material for a lower support structure is ASTM-A588 steel. Bolting materials are ASTM-A320 Grade L7 and nut material is ASTM-194 Grade 7. These materials conform to the Design Criteria (Section [6.7.18](#)). All welding meets the requirements of the American Welding Society Structural Welding Code-1972-AWS Publication D1.1-72.

The material used for the pins in the lower support structure is ASTM-A434 steel, Grade 4340, Class BD. The material is normalized, then quenched and tempered. Chemical properties, physical test data and Charpy-V Notch test values at minus 20°F are required.

6.7.9.3 Design Evaluation

General

The lower support structure was analyzed using a finite element model. The ANSYS structural analysis program was used in the analysis. The seismic responses, in terms of equivalent acceleration and interface forces, in two horizontal directions (radial and tangential) and the vertical direction (z) were developed from a dynamic seismic response analysis performed for a combined lattice frame/ice basket/lower support structure model. The seismic loads, as well as loads due to dead weight, thermal and the forces due to DBA, were applied to the lower support structure as static forces.

[Figure 6-161](#) and [Figure 6-162](#) show the finite element model used to represent the three pier lower support structure. The model is comprised of three dimensional beam elements having six degrees of freedom per node; flat triangular shell elements, each having six degrees of freedom per node such that both membrane and bending action of the plates is considered; and general six degrees-of-freedom lumped masses having a 6 x 6 diagonal mass matrix with three values, M_x , M_y , M_z and three moments of inertia, I_x , I_y , and I_z . No horizontal ice mass is considered since this effect on the seismic response is accounted for in the results of the dynamic analysis of the combined lattice frames/ice baskets/lower support structure model. Rotary inertia terms are not used for the lumped masses.

Structural Representation

General

[Figure 6-161](#) shows an overall view of the one bay finite element model of the structural members. Each of the line members represents three dimensional beam elements. The loads generated from the model are used to design all the connecting joints, to the AISC-69 Code, Section 2.8. A separate finite element model is used to determine the maximum stresses in the beams. The impingement plate which spans the chord between the two outer columns is modeled using equivalent beam elements.

At beam connections where the beam centroidal axes do not intersect, either rigid links or specified offsets, which can be automatically accommodated for ANSYS beam elements, are used to preserve geometric compatibility between the elements. The connections of the horizontal platform to the portal frame are considered to be pin connections except at the outer column line where it is assumed that a moment around a vertical axis can be transmitted.

The impingement plate is attached to the outer columns assuming no moment can be transmitted from the plate to the columns. Similarly, the upper and floor turning vanes are idealized as beam elements which are pin connected to the portal assemblies. The remaining structural connections are considered to be moment connections.

Mass Distribution

Structural Mass

The structural mass of the lower support structure is represented automatically in the ANSYS program through the use of consistent mass matrices associated with each of the structural finite elements. Thus, only the material density is input to account for the structural mass.

Ice Mass

The mass of the ice baskets is represented as lumped masses at node points along each radial beam. The mass is distributed based on the geometric placement of the ice baskets on the radial beams. Only mass in the vertical, Z direction, is assigned to the lumped masses representing the ice baskets, since the horizontal seismic effect of the ice basket mass is

incorporated as loads on the radial beams. The horizontal seismic loads are determined from a dynamic analysis of a combined wall panel/lattice frame/ice basket/lower support structure model.

Displacement Boundary Conditions

Displacement boundary conditions are not specified for the tops of the columns nor for other nodes contained in the column radial plane. However, forces are applied to the columns which account for the adjacent bay loading.

To accommodate the thermally induced loads in the structural members, the base plates of the two middle columns are free to expand in a radial direction. Likewise, to accommodate the circumferential thermal expansion, every other outer column base plate connection is free to expand circumferentially.

Referring to [Figure 6-159](#), the above boundary conditions imply that the outer column bases at odd numbered column lines are restrained against motion in the vertical, radial and circumferential directions, while the outer column bases at even numbered column lines are free to displace circumferentially.

The middle columns are free to move in the radial direction at all column lines and the inside columns (near the crane wall) are restrained for all three translations at all column lines. These boundary conditions minimize the thermally induced stresses and floor loads.

Loading Conditions

Seismic Loads

General

Analysis indicates that the frequency of the lower support structure is sufficiently high relative to the peaks of the response spectra and is one mode dominant in the vertical direction, so that a seismic modal response analysis is not required. Instead, an equivalent static analysis was performed for vertical accelerations based on the assumption of one mode dominance. For horizontal seismic loads, the largest forces in the radial and tangential directions as determined from a dynamic analysis of a combined ice basket/lattice frame/lower support structure model are applied as static concentrated forces to the lower support structure. A schematic of the applied loads is shown in [Figure 6-163](#).

Horizontal Radial Excitation

To account for the seismic loads transmitted from the ice baskets, lattice frames, and lattice columns, a dynamic analysis of the lattice frame and ice basket structures coupled to the lower support structure by means of flexibility coefficients which represent the lower support structure is performed. The loads transmitted to the lower support structure at the interface between the lower support structure and the ice baskets are applied as static concentrated forces. To account for the seismic loads transmitted from adjacent bays, radial forces are applied to the model at the required nodes.

Horizontal Tangential Excitation

The tangential loads transmitted from the lattice frames and ice baskets are determined in the same manner as the radial forces from the dynamic analysis performed.

The total tangential loads applied to the radial beams by the ice baskets are distributed in the same manner as the mass. Since the ice baskets are attached to the top surface of the radial beams, concentrated torques are applied at each of the nodes of the radial beams to account for the distance of approximately six inches from the top of the radial beam to the centroid of the

cross section of the radial beam. The seismic loads from adjacent bays are considered by applying concentrated circumferential forces to the appropriate nodes.

Blowdown Loads

General

The blowdown forces applied to the lower support structure are divided into four classifications:

Vertical Forces

Horizontal Radial Forces

Lower Inlet Door Impact Forces

Horizontal Tangential Forces

The following sections discuss the loads for each of the classifications and the application of the loads to the finite element model of the three pier lower support structure.

Vertical Blowdown Loads

The vertical uplift loads acting on the lower support structure arise from the following phenomena:

Uplift on the ice baskets

Uplift on the radial beams

Uplift on the horizontal platform bracing

Uplift pressure across the intermediate deck

Uplift on lattice frames and lattice columns

Horizontal Radial Blowdown Forces

The horizontal blowdown forces acting on the structure arise from the following phenomena:

Momentum forces on the middle circumferential beam turning vane.

Momentum forces on the upper three turning vanes attached to the middle column.

Momentum forces on the floor turning vane attached to the middle column.

Momentum loading on the slotted impingement plate.

Forces on the outer circumferential beam.

Radial forces on the ice baskets.

The forces are transient in nature. However, only the basic static values with Dynamic Load Factors applied to account for the transient nature of the loading have been applied to the structural model, as concentrated forces on the appropriate nodes. To account for forces from adjacent bays, concentrated loads were applied to the portal frame connection points, as required.

Lower Inlet Door Impact Load

From results of studies and tests performed to determine the forcetime history transmitted through the shock absorber which arrests the inlet door motion, a tangential load was applied to the lower support structure portal frame. The dynamic pulse characteristics of the force are accounted for by recommending a dynamic load factor of 2.0 for the pulse taken to represent the force versus time relationship for the shock absorber.

The door impact load is applied simultaneously in the same direction at both column lines 1 and 2 as a worst case. Thus, the loading considered is anti-symmetric tangential loading on the one bay model and creates an overturning moment about a radial axis through the lower support structure. In the design of the lower support structure, the bolt connections between the columns and the circumferential beams are designed to consider the possible loading from the door impact loads being applied in opposite tangential directions on the door arrestor plates.

Horizontal Ice Basket Forces

The tangential and radial forces acting on the ice baskets due to cross flow are assumed to act on the bottom three feet of ice basket (one-half of the span between the top of the lower support structure and the attachment of the ice baskets to the first lattice frame). The loads are applied to the finite element model as uniformly distributed loads on each of the beam elements comprising a radial beam.

Dynamic Load Factors

General

To account for the dynamic nature of the blowdown forces, dynamic load factors are applied to the DBA forces applied statically to the finite element representation of the lower support structure. The dynamic load factors (DLF) are as follows:

| | |
|--------------------------------|-----------------|
| Vertical Uplift Forces | DLF = 0 or 1.8 |
| Horizontal Radial Forces | DLF = 0 or 1.2 |
| Lower Inlet Door Impact Forces | DLF = 0 or 2.0 |
| Horizontal Tangential Forces | DLF = ± 1.2 |

Transient Analysis of Blowdown Loads

Following a LOCA, the inlet doors open admitting steam flow into the ice condenser chamber. The fluid flow through the lower support structure and upward through the ice bed cause time-dependent forces to be applied to the lower support structure. In general, there are four classifications of transient forces applied to the lower support structure: (A) vertical forces on the radial beams, ice baskets, lattice frames, lattice columns, and intermediate deck; (b) horizontal radial forces acting on the outer columns, the jet impingement plate, the outer circumferential beam, and turning vanes attached to the middle circumferential beam and middle column; (c) tangential forces, applied to the impact plates attached to the portal frames, resulting from arresting the motion of the inlet doors; and (d) tangential forces on the radial beams due to cross flow in the ice condenser compartment.

The dynamic load factors are determined by performing a transient response spectrum analysis for each force-time history, as described below.

Single Degree of Freedom Representation

In general, the transient structural response of multi-degree of freedom system is given by the expression:

$$y_i(t) = \sum_{j=1}^N \Gamma_j \eta_j(t) \psi_{ij} \quad \text{Equation 1}$$

where,

$y_i(t)$ is the structural response to any time (t).

- Ψ_{ij} is the j th mode shape of the structure.
 Γ_j is the participation factor of the j th mode shape for the transient load.
 $\eta_j(t)$ is the generalized coordinate of the j th mode shape at any time (t).

The generalized coordinate η_j of the j th mode is given in terms of the forcing function $f(t)$ by Duhamel's integral, or the convolution integral as:

$$\eta_j(t) = \omega \int_0^t f(\tau) \sin \omega(t - \tau) d\tau \quad \text{Equation 2}$$

Thus, the expression for the generalized coordinate for each mode, j , is the same as the amplification factor, or Dynamic Load Factor (DLF) definition for a single degree of freedom system:

$$\text{DLF}(t) = \omega \int_0^t f(\tau) \sin \omega(t - \tau) d\tau \quad \text{Equation 3}$$

Assuming that $\Gamma_j = 1$ for some $j = k$ and $\Gamma_j \sim 0$ for $j \neq k$, amounts to the assumption that only one mode dominates, in the structural response to the transient. In this case, the structural response becomes:

$$y_i(t) = \eta_k(t) \Psi_{ik} \quad \text{Equation 4}$$

or

$$y_i(t) = \text{DLF}(t) \Psi_{ik} \quad \text{Equation 5}$$

In which case the maximum structural response is given by:

$$y_{i \max} = \text{DLF}_{\max} \Psi_{ik} \quad \text{Equation 6}$$

Assuming that the dominant mode Ψ_{ik} can be approximated by the static deflection shape due to the loads applied to approximated by:

$$y_{i \max} = \text{DLF}_{\max} y_{i \text{ static}} \quad \text{Equation 7}$$

Thus, assuming that the response of the lower support structure to the transient blowdown forces may be represented by Equation 7, the dynamic effects of the transient may be investigated by evaluating the transient response spectra given by:

$$\text{DLF}_{\max}(\omega) = \max \left[\omega \int_0^t f(\tau) \sin \omega(t - \tau) d\tau \right] \quad \text{Equation 8}$$

evaluated for $\omega = \omega_n$ where ω_n is the natural frequency estimated for the lower support structure.

A typical force transient for a hot leg break is shown in [Figure 6-164](#) the resulting dynamic load factor plot is shown in [Figure 6-165](#).

Discussion

The recommended dynamic load factors are the maximum values from the transient response spectra for zero damping and for a frequency greater than 10 Hz (lowest estimated L.S.S. - Floor frequency).

As previously stated, transient response spectra used to determine the DLF are for zero damping, rather than, a damping of between 5 to 10 percent, which is more appropriated for the highly stressed, bolted lower support structure. Damping will reduce the dynamic response as indicated typically in [Figure 6-165](#), which shows the response for horizontal forces for 0, 5, 10 and 20 percent damping. Thus, the DLF recommended are conservative from this standpoint.

In addition to the conservatism used to derive the DLF's used for design, additional conservatism has been incorporated into the design by specifying that the forces scaled by the DLF's be applied to the structure in the worst manner to determine the maximum member forces. Since the maximum DLF for each transient will not occur at the same time, combining the member forces derived for each transient in this manner is conservative. In particular, an RMS combination similar to that used in earthquake analysis could be justified because of the time separation of peak occurrence.

The recommended DLF's have been conservatively derived and applied in the design of the lower support structure. Therefore, the resultant member forces determined for the DBA, using the recommended DLF, result in a conservative prediction of the stresses induced in the structure.

Design Load Case

Because of the magnitude of the DBA forces, the proportions of all members and structural elements of the lower support structure are sized by the load combinations which include DBA forces. The DBA forces are 2 to 5 times larger than other forces that are applied to the lower support structure. The seismic, blowdown, and combined seismic and blowdown loads were considered in the design.

The combined load case is represented below:

DL + TN + EV + ER + ET + AV + AR + AT + LIDI

DL = Gravity

TN = Thermal 70°F to 317°F (The Peak Containment Temperature Transient is discussed in Section [6.2.1.1.3.3](#).)

EV = Safe Shutdown Earthquake Forces in the Vertical Direction

ER = Safe Shutdown Earthquake Forces in the Radial Direction

ET = Safe Shutdown Earthquake Forces in the Tangential Direction

AV = Vertical Forces Due to DBA

AR = Radial Horizontal Forces Due to DBA

AT = Tangential Horizontal Forces Due to DBA

LIDI = Lower Inlet Door Impact

Result of Stress Analysis

Members

The stress in the various structural members for all of the design load cases was found to be below the design criteria as specified in Section [6.7.16](#).

Joints

The member forces at connections from all load cases were used to proportion the connections. In the design of the connection for the load conditions, the recommendations of the AISC - 69 Code Section 2.8 were followed as specified in Section [6.7.16](#).

6.7.10 Top Deck and Doors

The top deck, intermediate deck, Containment shell, crane wall, and end walls form the boundaries of the ice condenser upper plenum. The upper plenum houses the air handling units and the distribution ducts to the wall panels and provides a working space for loading, weighing and maintaining the ice baskets.

6.7.10.1 Design Bases

Function

An array of blanket panels forms a thermal and vapor barrier atop the upper plenum, allowing limited movement of air through vents during unit operation and free outflow of air during DBA.

A grating deck supports the blanket panels and accommodates traffic by inspectors. The top deck structure supports the grating as well as the bridge crane and rail assembly and the air handling units.

The following loading conditions are considered in the design of the top deck: deadweight, seismic loads, blowdown loads, and live loads. The top deck structure withstands these loads and remains within the allowable limits established in Section [6.7.16](#).

Design Considerations

The blanket panels are hinged on top of the crane wall. The major loads are applied directly into the crane wall.

A blanket panel must be flexible, i.e., be capable of deforming out of its plane in response to relatively low forces without disintegrating. Deformation of panels during DBA is permissible, but formation of missiles must be averted.

The deck forms an integral part of ice condenser performance during DBA. Structural loads are a function of air pressure and flow relationships, which in turn are effected by deck characteristics.

The top deck structures are subjected to loads from the air handling units and bridge crane in addition to the deck design loads.

Material Consideration

Refer to Section [6.7.18](#) for steel structures.

Blanket material is fire resistant by its own composition or by means of a suitable cover sheet.

Blanket material is not a significant source of halides in gaseous form, whether by gradual diffusion of inherent ingredients or by radiolysis of component material following a DBA.

Blanket material is not a significant source of leachable halides during exposure to Containment spray following a DBA.

Thermal and Hydraulic Performance Requirements

Heat input to the plenum through the top deck assembly is limited to 13.5 Btu/hr-ft².

Resistance to air flow during DBA is minimized, in terms of both inertia of panels and obstruction by grating. Panels may reclose or remain open following DBA. Vents open on low differential pressure for small flow rates.

A vapor barrier is established on the upper surface of the blanket panels.

Interface Requirements

In the process of opening, adjacent blanket panels interfere with each other. This is acceptable in view of their flexibility.

Sealing strips are installed to connect panel vapor barrier to adjacent panels, to crane wall, to end walls and to containment shell, without transmitting appreciable loads to the containment shell.

The grating rests on, and is attached to, the cross beams between the top deck beams and transmits operating and drag loads to these structures. The structural members received loads from bridge crane and air handling units as well as the deck itself.

Design Loads

Design loads used in the design of the top deck assembly are shown in [Table 6-123](#).

6.7.10.2 System Design

The design of the top deck is shown in [Figure 6-166](#) and [Figure 6-167](#).

The top deck doors consist of radially aligned flexible blanket panels resting on a grating deck and hinged on top of the crane wall.

A blanket pair covers one-half bay, extending from the radial centerline of a bay to the edge of the adjacent top deck beam. It consists of two blanket assemblies, one resting on the grating, the second one resting (mirror image) on the first one, with bands touching.

The parts of a blanket assembly and their respective functions are as follows:

Thermal insulation is provided by a flexible polyurethane foam blanket, 1 inch thick.

Approximately one-half of the centrifugal load is carried by bands of fully hardened stainless steel, 0.005 inch thick.

A stainless steel cover sheet ("skin") serves as a vapor barrier (top surface), protects the blanket against wear and fire (top and bottom surfaces), and provides all of the lateral and about one-half of the centrifugal strength.

Parts 2 and 3 are bonded to the faces of the foam and extended along one edge to form a hinge.

The grating deck performs the structural functions of the top during non-accident conditions. It is supported from pairs of cross beams spanning the top deck beams, and its upper surface is flush with the top of the top deck beams. The bearing bars of the grating run parallel to the centerline of the particular bay. They are 2 inches high, 3/16 inch thick, and spaced on 2 3/8 inch centers. This design satisfied all requirements for open area and upward drag loads during DBA as well as for normal traffic loads. A clearance of no less than 4.0 inches is maintained between the grating and the containment.

The grating is fabricated from carbon steel, ASTM-A36, to A569 and provided with trim banding adjacent to top deck beams. Completed grating sections are galvanized for corrosion protection.

A hinge bar clamps one edge of each blanket assembly to the surface of the crane wall. Anchor bolts transmit the hinge loads into the crane wall.

Static insulation pads are attached to the top of the radial beams.

Flexible seal membranes are attached between vapor barrier (top) surfaces of the blanket panels and against vent base, and walls, and static insulation.

A pressure equalization "curtain" is suspended around the periphery of the top deck. The vent curtain minimizes diffusion of air under steady state conditions while permitting free movement of air in or out during momentary periods of pressure imbalance. A vent curtain dam has been added to prevent excessive moisture intrusion into the upper plenum. The dam does not prevent the rapid equalization of pressure between the ice condenser and upper containment.

Fabrication

Grating Sections are fabricated to specific shapes, complete with trim banding. The finished assemblies are cleaned and hot dip galvanized.

Structurals are cut and welded to suit.

Blanket assemblies are fabricated by an insulation contractor using specified bonding methods.

Hinge bars are machined from rectangular steel bars and painted or galvanized.

Installation

Radial and cross beams are installed.

The grating sections are placed and bolted down.

Static insulation pads and blankets are placed in position all around top deck.

Vent assemblies are installed.

Seals are installed.

Hinge bars are installed. Blankets are clamped. Static insulation is attached.

Top Deck Blanket Doors

The top deck doors were dynamically analyzed to determine the loads and structural integrity of the door for the design basis load conditions.

Using TMD results as input, the door dynamic analysis was performed using a separate computer code named the "D00R" Program. This computer program has been developed to predict door dynamic behavior under accident conditions. This program takes the door geometry and the pressures and calculates flow conditions in the door port. From the flow are derived the forces on the door due to static pressure, dynamic pressure and momentum. These forces, plus a door movement generated force, i.e., air friction, are used to find the moment on the door and from this are derived the hinge loads. Output from the program includes door opening angle, velocity and acceleration as functions of time as well as both radial and tangential hinge reactions.

Analysis Due to LOCA

The net load distributions on the door opening are determined by considering the applied pressures acting on the door and then solving the rigid body equations of motion such that the net forces and moments at the hinge point are zero. In the process, this produces expressions for the inertial forces in the door and the hinge bar reaction as functions of the applied pressure.

The resultant horizontal and vertical hinge loads, calculated by the D00R Program, provides the inputs for subsequent stress analysis.

Using this input, the blanket assembly is analyzed with horizontal and vertical forces being taken by direct stress in the skin and bands. As inertial forces are directly accounted for in the analysis, no dynamic load factor is applied.

The hinge bar and anchor bolt stresses are analyzed under hinge reactions considering the effects of the horizontal and vertical components of the tension band. For these components, no dynamic load factor is applied since the bars are very rigid themselves and are rigidly attached to the crane wall. Stresses in the blanket floor grating due to aerodynamic drag are also calculated. Loads used for stress calculations include 40 percent margin above computed TMD values. Certain aspects of the dynamic performance of a flexible door (e.g. tangential distortion, whipping, bowing) cannot be modeled with sufficient confidence.

A summary of the analysis performed and results are presented in [Table 6-124](#). All portions of the door show factors of safety equal to or greater than one. The general acceptance criterion was that stresses be within the allowable limits of the AISC-69 Structural Code. For materials and components not covered by the Code, i.e., spring temper stainless steel non-metallic materials, floor grating, etc., conservative acceptance criteria are established on the basis of manufacturer's recommendations for ASTM minimum tensile specifications.

Dynamic Test

A full scale test of a blanket pair (one-half bay) is performed for verification of analysis. Observed dynamic characteristics are found to correlate well with computed TMD values, and integrity of blankets is maintained within acceptable limits.

Top Deck Structure

The top deck structure is analyzed using the ANSYS finite element computer program, with three-dimensional beams representing the structural members, three-dimensional lumped masses representing the mass elements, and a stiffness matrix to represent the flexible connections in the system. Geometric compatibility is maintained using three-dimensional rigid elements.

Two bays considered representative of the system were isolated and modeled. Conservatively, four air handling units are assumed to be located in the two-bay region, two next to the crane wall and two next to the Containment wall.

Stresses are calculated for the various combinations of dead load, thermal, seismic and accident conditions. A modal analysis is performed to determine seismic amplification. Blowdown stresses are calculated using a computed dynamic load factor. Maximum stresses produced in major members are all within the limits given in Section [6.7.16](#). The circumferential struts, AHU beams and crane rails have been analyzed and are structurally acceptable.

6.7.11 Intermediate Deck and Doors

6.7.11.1 Design Bases

Function

The intermediate deck forms the ceiling of the ice bed region and the floor of the upper plenum. It serves as a thermal and vapor barrier, which allows limited air movement, through vents, between regions during normal plant operation and free out-flow of air and steam following DBA.

Criteria

Refer to Section [6.7.16](#) for structural design criteria.

Loading Modes

The following loading conditions are considered in the design of the intermediate deck: deadweight, seismic loads, blowdown loads, and loads due to personnel traffic on deck. The intermediate deck structure withstands these loads and remain within the allowable limits established in Section [6.7.16](#).

Design Criteria - Accident Conditions

Resistance to air flow during DBA is minimized, in terms of both inertia of door panels and obstruction by the frames. Panels may reclose or remain open. Panels open on low pressure differential for small flow rates.

At the end of their movement, pairs of doors collide. Distortion at the time is acceptable, provided doors do not become missiles.

The doors are of simple mechanical design to minimize the possibility of malfunction.

Design Criteria - Normal Conditions

Heat conduction through the intermediated deck is limited to 0.6 Btu/F-hr-ft².

The design of the deck permits its use as a walking surface for maintenance of the air handling units and inspection of the ice bed.

The design of the deck provides a vapor barrier between the ice bed and upper plenum area.

The design of the deck provides access to selected ice baskets for weighing and visual inspection.

Interface Requirements

Sealing strips are installed to seal deck frames to wall panels as a continuation of the vapor barrier.

Hinge loads, drag loads, and live loads are transmitted from the deck through support beams to the lattice frame support columns.

Instrumentation cables from the Temperature Monitoring System penetrate the seal area of the deck.

Design Loads

Pressure loading during LOCA is provided by the Transient Mass Distribution (TMD) code from an analysis of double-ended hot leg break in the corner formed by the refueling canal, with 100 percent entrainment of water in the flow.

The intermediate deck design parameters and loads are presented in [Table 6-125](#).

6.7.11.2 System Design

The intermediate deck is shown in [Figure 6-168](#). For ease of manufacture and installation, the deck is separated into 48 subsections. Each subsection covers an area extending over a length of three lattice frames and a width of approximately half of the ice condenser annulus. Two types of subsections are used; the inner subsections have overall dimensions of 11 ft. long by 5 ft. 7 in. wide; and the outer subsections have dimensions of 12 ft. by 4 ft. 7 in. Except for dimensional differences, the designs of inner and outer subsections are identical.

Each subsection consists of four door panels mounted on a steel frame. The door panels are sandwich structures, consisting of 26 gauge galvanized steel sheets bonded to a 2.5 inch thick urethane foam core. Loads developed in the sandwich structures are transmitted to two panel hinge points by a 2.5 in. x 5 in. rectangular steel tube which forms a backbone for the panel. The panel is reinforced and sealed by a peripheral channel and two internal ribs, formed from 18 gauge steel sheet.

Plates, which are welded to the ends of the tubular backbone, are drilled to accommodate 1 in. diameter stainless steel hinge pins. These pins in turn are supported by welded steel support brackets which are bolted, through the door frame, to intermediate deck support beams. Thus, hinge loads are taken directly into the support beams and not into the frame itself.

The door frame is fabricated from steel angle and T-sections. A formed channel on the frame holds a compliant bulb-type rubber seal which is compressed by the door in its closed position. In addition to being clamped in place by the hinge support brackets as described above, additional bolts in the frame angles fasten the corners of the frame to the support beams and connect adjacent members of the inner and outer assemblies to each other.

The intermediate deck support beams are 8 in. wide flange steel members, which radially span the ice condenser annulus. They are bolted to the lattice frame support columns via welded plate bracket assemblies and compliant pads. The latter feature assures that beam and moments are not transmitted to the relatively flexible support columns.

Flexible membranes are installed between the intermediate deck frame and adjacent wall panels to provide a continuous vapor barrier.

Pressure equalization vents are installed at the Containment wall side of the intermediate deck. Vertical flaps minimize diffusion of air under steady state conditions while permitting free movement of air in or out during momentary periods of pressure imbalance.

6.7.11.3 Design Evaluation

The intermediate deck doors are dynamically analyzed to determine the loads and structural integrity of the door for the design basis load conditions.

Using TMD results as input, the door dynamic analysis is performed using a separate computer code named the D00R Program. This computer program has been developed to predict door dynamic behavior under accident conditions. This program takes the door geometry and the pressures and calculates flow conditions in the door port. From the flow are derived the forces on the door due to static pressure, dynamic pressure and momentum. These forces, plus a door movement generated force, i.e., air friction, are used to find the moment on the door and from this are derived the hinge loads. Output from the program includes door opening angle, velocity and acceleration as functions of time as well as both radial and tangential hinge reactions.

Analysis Due to LOCA

The net load distributions on the door during opening are determined by considering the applied pressures acting on the door and then utilizing an analysis similar to that derived for the lower inlet door (Section [6.7.8](#)), to obtain shear, moment, and hinge reactions.

Using this input the door panel is analyzed as a sandwich panel; i.e., the outer steel skins are assumed to carry tensile and compressive membrane loads, while the urethane core carries transverse shear loads between the outer skins. The tubular backbone is analyzed as a beam with biaxial bending and torsion under the combined effects of panel shear loading, panel centrifugal loading and hinge reactions. Hinge pins and support brackets, including bolting, are

analyzed by considering the effects of tension, shear, and bending as appropriate. No dynamic load factor is applied, as inertial forces are directly accounted for in the analysis.

The door frame and attachment bolting are analyzed under loadings created by the differential pressure acting on the frame members. The intermediate deck beams and attachments are analyzed under the effects of loads transmitted to them by the door hinges and frames. For these latter analyses, appropriate dynamic load factors are calculated and applied.

All results indicated positive margins of safety in comparison with the criteria contained in Section [6.7.16](#).

During a LOCA, stopping of the doors is accomplished by impacting adjacent door panels against each other. In the process, a significant portion of the door kinetic energy is absorbed through plastic deformation of the door panels. This is an acceptable mode of behavior as long as the doors do not break up and lose their insulation or otherwise generate missiles. During simulated blowdown tests on full-scale prototype doors at levels of maximum pressures predicted by TMD, the ability of the doors to withstand opening and stopping loads is confirmed. Only local deformation of the panels results and no missiles or insulation are released.

Seismic Analysis

A response spectra nodal analysis is performed on the intermediate deck structure to determine maximum seismic loadings during OBE and SSE. Resultant loadings on the structure are found to be negligible in comparison with LOCA loadings. Further, calculations indicate the doors will not open during either earthquake.

6.7.12 Air Distribution Ducts

6.7.12.1 Design Bases

Function

The air distribution ducts distribute the cold air from all air handling units to the wall panels. (See [Figure 6-169](#) and [Figure 6-170](#).)

The loss of the air distribution function does not affect the safety of the unit as the ice bed is a passive component and can tolerate refrigeration failures.

Design Criteria

The air distribution ducts are permitted to deform during accident conditions, but must not affect any safety related components located nearby.

Design Conditions

Normal Operation

Design temperature normal 10°F - 15°F

ΔP normal

Accident Conditions

Accident temperature maximum 190°F

(without ΔP)

6.7.12.2 System Design

The air distribution ducts are located in the upper plenum. The cuts are made of galvanized sheet steel. The design includes flexible connections separating each duct and each AHU. The flexible connections also serve as vibration breaks.

6.7.12.3 Design Evaluation

The air distribution ducts distribute cold air to the wall panels thereby maintaining the readiness of the ice in the ice bed. The air distribution ducts are not required to function during an accident. They are, therefore, non-safety-related components. Refer to Section [6.7.6](#) for detailed discussions of the Refrigeration System performance during normal operating conditions and of its ability to tolerate refrigeration component failures.

During a LOCA the air distribution ducts are permitted to deform. Any deformation is outward toward the crane and liner wall insulation and therefore presents no problem to nearby safety-related components.

6.7.13 Equipment Access Door

6.7.13.1 Design Bases

Function

The equipment access door permits movement of crane, equipment and personnel into and out of the ice condenser plenum for ice loading and maintenance.

In closed position, the door constitutes a thermal and vapor barrier (normal unit operation) between ice condenser air and upper Containment atmosphere.

The basic functions of the equipment access door are non-safety related. It is important, however, to prevent failure of the door in any manner that may affect safety related components located nearby.

Design Criteria and Codes

The door is designed to comply with structural requirements of Section [6.7.16](#).

Design Conditions

Normal Operation

Design temperature inside 15°F

Design temperature outside 100°F

Accident Conditions

Maximum surface temperature 190°F

(without ΔP)

6.7.13.2 System Design

An equipment access door is provided in each end wall thereby providing ample access to the upper plenum. The equipment access door includes: the insulated door panel, frame and hoist assembly, gasketing, and fasteners. The door frame slides from closed to open position within a fixed frame embedded in the concrete end wall. All exposed surfaces are protected against corrosion by appropriate coating.

Limit switches are provided to monitor movement of each door and to indicate position as a part of the Door Position Monitoring System.

6.7.13.3 Design Evaluation

The equipment access door is a non-safety related component. The door stresses during SSE + DBA loadings are below the allowable levels.

6.7.14 Ice Technology, Ice Performance, and Ice Chemistry

6.7.14.1 Design Bases

The operational principle of the ice condenser is the condensation of steam by means of melting ice. Approximately four pounds of ice per pound of reactor coolant are required to absorb the coolant energy to prevent excessive Containment pressure and temperature buildup. The liquid resulting from the thawing process drains to the Containment sump where it is utilized during the recirculation phase of cooldown by the Emergency Core Cooling System. It is, therefore, necessary that the boron concentration of the recirculated primary coolant not be diminished through the action of the ice condenser. Hence, the ice condenser utilizes borated ice, which upon bulk melting delivers an aqueous solution containing approximately 2000 ppm boron to the Containment sump. The solution used in this case to produce the ice for the condenser is one containing approximately 2,000 ppm borax ($\text{Na}_2\text{B}_4\text{O}_7 \cdot 10\text{H}_2\text{O}$) as boron.

The complete equilibrium freezing of this solution forms a eutectic composition with a melting point of -0.42°C (31.2°F).

On a microscopic scale, the complete equilibrium freezing of a 2,000 ppm aqueous solution of boron as sodium tetraborate, results in a solid consisting of crystals of pure ice (approximately 91 percent of the original water), surrounded by frozen eutectic. Microscopically this eutectic solid consists of individual crystals of pure ice and pure $\text{Na}_2\text{B}_4\text{O}_7 \cdot 10\text{H}_2\text{O}$ (See Reference [8](#)).

6.7.14.2 System Design

The ice for the ice condenser is produced in machines that yield ice in the form of a continuous ribbon, approximately 1/8 inch thick which is deposited in a storage bin via gravity chutes. An additional ice machine has been added at Catawba which produces ice in sheets approximately 1/2 inch thick which have the same properties as the ice formed by the original machines.

The ice is kept at subcooled temperatures by chilled air flowing through the hollow walls and floor of the bin and over the exposed surface of the ice.

Ice is pushed out of the bin by a mechanized rake and carried to an ice chopper via two screw conveyors. The chopper reduces the size of the ice flakes to approximately 2 in. x 2 in. or less. The ice chopper discharges through a metering hopper into a pneumatic conveying valve.

The pneumatic conveying valve feeds ice at a measured rate into a stream of chilled compressed air, which carries the ice through temporarily erected piping to either one of the ice condenser units. The air/ice mixture is fed into a cyclone receiver in the upper ice condenser where it is either loaded into baskets directly or placed into bins for use in fabricating ice blocks while the air is released into the containment vessel. Air is removed during this procedure in order to maintain a stable containment vessel pressure.

The quantity and distribution of ice in the ice condenser must be verified to be maintained consistent with the design basis accident analyses. The operating characteristics of the ice condenser and methods for determining the quantity of ice mass in each ice basket have been considered in technical specifications which ensure the required quantity and distribution of the ice in the ice condenser. The basis for the methodologies used in establishing these technical specification requirements and acceptable methods for statistically verifying compliance with these requirements are described in Reference [21](#) and [22](#).

6.7.14.3 Design Evaluation

As the Ice Condenser is to be available to perform its engineered safety feature function for the life of the unit, ice storage characteristics are an important consideration. Two mechanisms influence the long term storage of the ice, the diffusion of sodium borate crystals through the ice crystals, and the sublimation of the ice.

Diffusion

For a discussion of the first mechanisms, it will be necessary to refer to the phase diagram presented in [Figure 6-171](#). When the temperature of an aqueous sodium tetraborate solution is continuously lowered, freezing begins with the formation of crystals of pure water surrounded by the salt solution. The temperature at which the first ice crystals form (assuming no supercooling) depends on the initial concentration of the solution. For example, a solution of $\text{Na}_2\text{B}_4\text{O}_7 \cdot 10\text{H}_2\text{O}$ containing 2,000 ppm boron begins to freeze at -0.41°C ($+31.27^\circ\text{F}$), under one atmosphere pressure (Point A in [Figure 6-171](#)). If the freezing process is allowed to continue reversibly, i.e., under conditions of the thermodynamic equilibrium, more ice crystallizes and the surrounding solution increases in concentration according to line AB in [Figure 6-171](#). Finally, when the system temperature is -0.42°C ($+31.24^\circ\text{F}$), the remaining liquid freezes to a solid with a boron concentration of 2220 ppm. The composition of this solid is known as the eutectic composition.

If the borated ice is made by the very slow freezing process just described, the pure water crystals first formed become the centers for further crystallization and therefore grow until the liquid reaches the eutectic composition. The total number of these relatively large pure ice crystals is determined by the number of nucleation sites available in the solution during the initial phase of the process. If the freezing rate is made extremely large, i.e., the process is carried out in an irreversible manner, the initial crystals do not have time to grow appreciably before all the water sodium borate has crystallized. Such a path is represented by the line CD in [Figure 6-171](#). The solid obtained by this process is a uniform mixture of very small crystals of two kinds, ice and sodium tetraborate.

When a collection of various sized crystals of a substance are maintained at constant temperature and pressure in contact with a solution saturated with respect to the substance, two processes tend to occur. The larger crystals tend to grow at the expense of the smaller ones, and the crystals of irregular form tend to become of regular form. Both of these phenomena are manifestations of systems tending toward thermodynamic equilibrium where the total free energy of the system (in this case the surface free energy) is at a minimum. The solution referred to above can also be a vapor and in the simplest case can be the pure saturated vapor of the crystalline substance. Note that kinetically the two processes are competitive and that both are subject to diffusional control. Therefore, diffusion of molecules, from one site to an adjacent one of the same crystal would be favored over migration to another larger crystal, in the case where rapid cooling of very dilute solutions causes many crystals to form that are small compared to the separation between them. Such is the case in practice with the ice condenser.

The driving force for diffusion between crystals of sodium borate through the pure ice matrix is a concentration gradient. If a large crystal is tending to grow, it causes depletion of sodium and borate ions in the immediately surrounding ice. If a small crystal tends to give up sodium and borate ions to feed the growth of the larger crystal then there is an increase in the concentrations of sodium borate surrounding the shrinking crystal. Since ice and sodium borate do not form an appreciable solid solution (eutectic mixture of ice and sodium borate crystals), then the concentration of sodium borate around the shrinking crystal cannot be large. For the sake of constructing an upper bound on diffusional effects in the borated ice, assume the maximum concentration to be approximately 10 percent of the eutectic solution concentration (i.e., 220 ppm).

Diffusion of sodium borate across a slab of pure ice can be estimated as follows:

Data for the diffusion of sodium borate in ice are not available, but the self-diffusion coefficients for deuterium, tritium and oxygen in ice have been reported by Franks (Reference 9). At -11°C ($+12^{\circ}\text{F}$) the value for all species is approximately 10^{-11} cm^2/sec . Assuming that the coefficient for sodium and borate ions is of the same order of magnitude, the rate of diffusion of sodium borate through a 1/32 inch slab of pure ice is estimated to be approximately 2×10^{-13} $\text{g}/\text{cm}^2\text{-sec}$. for an initial concentration of 220 ppm boron. If the concentration of boron in the ice phase on one face of the slab remained constant at 220 ppm while diffusion through the pure ice slab took place, it would take over 100 years for an amount of boron in a single piece of condenser ice to diffuse 1/32 in., or halfway through the ice flake.

Since the quick frozen borated ice is of stable uniform composition, then upon bulk melting there should be formed a solution of borax of uniform concentration. If the entire borated ice-mass were to be uniformly warmed above -0.42°C ($+31.24^{\circ}\text{F}$) then melting would begin at the points of contact between water crystals and $\text{Na}_2\text{B}_4\text{O}_7 \cdot 10\text{H}_2\text{O}$ crystals, and the ice-mass would lose structure. This is a phenomenon known as "rotting" and has been observed at times in sea-ice which has been subjected to slow (order of hours or days) temperature excursions to just above the melting point. If the melting process is rapid then the fact that the borated ice-mass is a mixture of crystals and not a homogeneous solid solution does not affect the performance of the ice condenser. Melting in the ice condenser occurs over a time span of the order of seconds, beginning at the contact between the steam and the ice-mass and progressing inwardly.

The above arguments are greatly simplified, but lead to conservative results. It can therefore be concluded from the above arguments that while some local changes undoubtedly occur in the quick-frozen borated ice, a mal-distribution of the solute boron in the ice condenser, of such magnitude as to affect the operation of the condenser as described in the first paragraph, is extremely remote. Furthermore, the microscopically heterogeneous composition of the borated ice-mass does not reflect itself in the ice condenser performance.

Sublimation

The other mechanism that affects the long term storage of the ice is sublimation. Sublimation has several effects inside the ice condenser. The geometry of the ice mass changes where sublimation occurs, and the resulting vapor is deposited on a colder surface at another location inside the ice condenser.

In normal cold storage room application, the cooling coil is exposed to the air in the room, and moisture in the air freezes on the coil. If ice is stored in the room, all of the ice eventually migrates to the coil (which is defrosted periodically, draining the water outside the room) through a sublimation-mass transfer mechanism.

To avoid the mechanism, and maintain a constant mass of ice, the ice condenser is provided with double wall insulation. The annular gap between the insulated walls is provided with a heat sink in the form of a flow of cool, dry air that enters and leaves through the insulated panels.

However, a small amount of heat enters the system through the inlet doors, which are not double insulated, and also through the Double Layer Insulation System. The effect of this heat gain on the ice condenser has been examined analytically.

An analytical model of the sublimation process has been developed to provide an estimate of the expected sublimation rate as well as identify the significant parameters affecting the sublimation rate. The model developed a relationship identifying the fraction of total heat input which sublimates ice (the rest of the heat raises the temperature of the air, which transports the vapor to the cold surface where it freezes). The sublimation fraction depends on the difference in vapor pressure between warmest and coldest air temperatures within the ice condenser. The sublimation fraction decreases as the T decreases and also as the average ice condenser temperature decreases. For an average temperature of 15°F in the ice condenser compartment, the analytical model predicts a sublimation rate of about 1 percent of the ice mass sublimed per year per ton (12,000 Btu/hr) of heat gain to the ice storage compartment. The final heat gain calculations identified a heat gain into the ice storage compartment of 1. to 1.5 tons, most of which enters the compartment through the doors. For the purposes of this report, it is assumed that the reference heat gain for the unit is 1 ton, and therefore, the calculated reference sublimation rate would be 1 percent of the ice weight per year.

Selected baskets are weighed as indicated in the Technical Specifications to verify that the actual sublimation rate has not excessively depleted the ice inventory.

Chemical Additives

Sodium tetraborate is used as a chemical additive to the ice in the plant. The boron is needed for recirculation through the core and the tetraborate is used for iodine removal and containment sump pH control. Boron or sodium tetraborate was also added to the ice used in the long-term storage tests. Chemical analyses were performed before and after certain storage tests to identify any change in boron concentration in the ice. These chemical tests showed that the boron concentration did not significantly change during long-term ice storage. Also, the tests proved that the boron is not transferred with the ice during the sublimation process. It remains as a residue at the original point of sublimation.

Samples of flake ice with sodium tetraborate additive were placed in the cold storage room at Waltz Mill on August 29, 1969, and chemical analyses were made of the ice used in the test samples. The samples were suitably isolated so that sublimation would be minimized or prevented. The tests were terminated on June 19, 1970, approximately 9-1/2 months after initiation, and chemical analyses were again made of several samples taken from different locations in the test section. These analyses indicated that there was essentially no change in the boron concentration from beginning to end of testing, confirming the diffusion theory discussed above.

Testing

General

The ice condenser design consists of columns of ice approximately 48 feet long contained within perforated metal baskets.

In the long term storage of ice, the compression, shear and creep characteristics are important considerations. Several years of testing at the Waltz Mill facility in these areas of interest has indicated that the ice bed maintains its geometry for its design life. While the construction of the

ice baskets has changed since these tests were performed, the data is still applicable as the basic geometric configuration of the baskets has remained the same, and the same type of ice to be used in the unit was incorporated in the final series of tests. These Waltz Mill tests provide background on the testing that has been done to date, and presented in the next section is a discussion of planned tests that will provide additional information to further evaluate the mechanical performance of ice.

A number of mechanical loading test series have been performed at Waltz Mill to determine compaction, shear, or creep rates in the ice bed. The first series of tests initiated in 1966 used the tube ice (hollow cylinders, 1.50 inch o.d. by 0.5 inch i.d. by 2 inch length) produced in a commercial ice machine. The ice used in the above tests was made with no chemical additive, or with boron as a chemical additive to the ice. In some of these tests lead weights were placed on top of the ice samples to simulate the weight of various ice column heights.

The final series of tests initiated in 1969 used flake ice in the same type of baskets to determine the compaction and shear rates of the ice.

As the flake ice represents the basis for the configuration used in the ice condenser, only those test results applicable for this ice form are discussed.

Compaction Tests

[Table 6-126](#) lists and describes the flake ice compaction tests performed, the duration of these tests, and the resulting compaction after one year of testing for these tests. The results of all of the tests showed that the greatest amount of compaction occurred during the first several months of testing. The amount of compaction varied with the equivalent height of the ice column, and depended on the type of ice employed. [Figure 6-172](#) presents the percent compaction versus time for flake ice test D'. Compaction of flake ice occurs much more rapidly than the other forms of ice due to the smaller and random size of the individual pieces of ice. After the initial year of compaction, the rate of compaction reduces significantly. The rate of compaction reduced almost to zero as the ice density approaches some value close to the density of solid ice. Inspection of the compaction tests indicated no evidence of ice being extruded out through the sides of the baskets.

For these tests the compaction measured is for the bottom section of the ice bed only; the ice above this level (simulated by lead blocks) would be compacted to a lesser extent since it is loaded with less weight. Therefore, the test results were corrected for the effect of continuously reducing load from bottom to top of the ice column. When this correction was made, the results of the flake ice tests (D', E') suggest that the amount of compaction of an increment in the ice bed varies linearly with the height of the ice bed above the increment, as shown by [Figure 6-173](#). For flake ice the compaction rate must eventually change, as indicated by the dotted line, as the density of solid ice is approached. Application of this relationship would result in the estimated compaction relationship, shown in [Figure 6-174](#), for total compaction (in the first year) versus unsupported height of the ice bed. Since the baskets provide supports for the ice every 6 feet, the compaction of any 6 foot section of the ice bed would be limited to less than 4 inches. Density enhancement via water addition is expected to reduce compaction.

Shear Tests

In these tests, ice was loaded into the basket on top of a temporary bottom support which was removed within one or two weeks after loading. The initial series of tests employed tube ice in expanded metal baskets with lead weights added to simulate additional weight of ice. All of the tests experienced an initial settlement within the first two months (after the temporary support was removed). Afterwards, the results show very low creep rates, which appear to be

proportional to the weight added. Subsequently it was concluded that each increment of ice in the basket would support its own weight by shear on the adjacent basket walls.

To evaluate this theory with flake ice, additional shear tests (G',H',I') were initiated. In these tests, unsupported ice bed heights of 1 foot, 3 feet and 5 feet were tested, with no lead weights added. In theory the shear rate should be the same, since each foot of ice column had the same shear support.

The results presented in [Table 6-126](#), confirmed that the shear rates for the three ice bed heights were of similar magnitude for a period of about 6 months. The rate measured was about 1 inch per year and was about 10 times the rate measured in the previous tests with tube ice in expanded metal baskets. From this information it is concluded that the shear capability of flake ice on the sides of the wire baskets is small. However, in the unit design the ice is supported by the horizontal supports at the bottom and center of each 12 foot section of ice column, so the stability of the ice bed does not depend on the shear forces existing between the ice and the baskets.

6.7.15 Ice Condenser Instrumentation

6.7.15.1 Design Bases

The ice condenser is a passive device requiring only the maintenance of the ice inventory in the ice bed. As such there are no actuation circuits or equipment which are required for the ice condenser to operate in the event of a LOCA. The instrumentation provided for the ice condenser serves only to monitor the ice bed status. Since the ice bed has a very large thermal capacity, postulated off-normal conditions can be successfully tolerated for a week to two weeks. Therefore, the ice condenser instrumentation provides an early warning of any incipient ice condenser anomalies. In this way the operator can evaluate the anomaly and take the proper remedial action. Depending upon the anomaly, the operator typically may perform a local or system defrost, switch to a backup glycol circulation pump, start a backup chiller package, provide glycol makeup, isolate a glycol leak, or perform a safe and orderly shutdown. Since the ice condenser instrumentation can in no way actuate, nor prevent, a reactor trip or engineered safeguards action, there are no codes which apply to the design of the instrumentation systems. Any instrumentation failures or anomalies, however, are apparent in the control room where ice condenser temperature monitors, door position monitors, coolant liquid level and valve position indications are displayed and alarmed. Ample time is available to investigate and alleviate or eliminate any off-normal condition without seriously degrading the ice inventory. The instrumentation is nevertheless designed for reliable operation which includes sufficient redundancy to insure that the operator can accurately monitor the ice condenser status. There are no special provisions for periodic testing of the instrumentation since normal testing and maintenance can be performed and is sufficient.

6.7.15.2 Design Description

Each equipment package (e.g., air handler, ice machine, chiller package) is provided with controls needed to regulate its normal operation. The ice condenser instrumentation serves to monitor the operation of the equipment packages and the ice bed status by providing to the operator the following control room information:

Ice Bed Temperature Monitoring

Resistance temperature detectors are located in various parts of the Ice Condenser. They serve to verify attainment of a uniform equilibrium temperature in the ice bed and to detect general gradual temperature rise in the cooling system if break-down occurs.

Forty-eight resistance temperature detectors are mounted on ice bed probes which are located throughout the ice bed. These forty-eight resistance temperature detectors tie into a temperature scanner unit located in the incore instrument room. The scanner is a multiplexing unit which consists of two selector units, each unit capable of reading data from 24 RTD's. The scanner unit interfaces with a 48 point recorder, utilizing a potentiometric measuring circuit, located in the control room. The scanning system is fully automatic, advancing successively through the 48 RTD's. Controls located on the recorder permit the operator to select the mode of operation. By varying the selector position the recorder will advance successively printing all 48 points, or scan all points without printing and automatically convert to the print mode if a pre-determined set point is exceeded, or continuously monitor a single point without printing. Should an RTD fail, a point bypass switch enables that point or any number of specified points to be omitted from the normal scanning sequence. The recorder provides three alarm set points to detect a lo, hi, or hi-hi ice bed temperature. A common alarm is provided on the control room annunciator should the ice bed temperature exceed any one of the pre set values.

There are six temperature switches located at various points in the ice condenser bed to serve as back up indication should the scanner unit or recorder fail to operate. The switches are temperature actuated, snap action, with normally open contacts which close at set point. All six switches are wired in parallel so that the action of any one switch will initiate an alarm. Should the ice bed temperature exceed a preset value the action of one or more of the switches will initiate an alarm on the control room annunciator panel, independent of the scanner/recorder alarm.

Refer to [Table 6-127](#) and [Figure 6-175](#) for locations of these detectors. Refer to [Figure 6-176](#) for a monitor system block diagram.

Lower Inlet Door Position Indication

Ninety-six limit switches are mounted on the lower inlet door frames with two limit switches per door panel, forty-eight door panels per containment unit. The position and movement of the switches are such that the doors must be effectively sealed before the switches are actuated. A single annunciator window in the control room gives a common alarm signal when any door is open.

For door monitoring purposes, the Ice Condenser is divided into six zones (Refer to [Figure 6-177](#)). Each zone contains four inlet door assemblies, or a total of eight door panels. Each lower inlet door is provided with two single pole double throw limit switches, herein designated as Switch X and Switch Y.

Within each zone, the normally closed contacts of all the "X" switches are connected in a series to a monitor light ("Door Closed") on the door position display panel in the Incore Instrument Room. (Refer to [Figure 6-179](#)).

Within each zone, the normally open contacts of all the "X" switches are connected in parallel to a monitor light ("Door Open") on the door position display panel. (Refer to [Figure 6-179](#)).

The normally closed contacts of all "Y" switches are not used. The normally open contacts of all "Y" switches in the ice condenser are connected in parallel to the alarm on the annunciator panel ("Ice Cond Lower Inlet Doors Open") in the control room. (Refer to [Figure 6-178](#)).

The door position display panel, located in the incore instrument room, is accessible during normal plant operation in the event an ice condenser door open alarm is annunciated in the control room.

Equipment and Personnel Access Doors

Two Equipment Access Doors located on opposite ends of the ice condenser provide access to the upper ice condenser area. Within each Equipment Access Door is a smaller Equipment Access Personnel Door. With all of these doors closed, and with the Equipment Access Door seals inflated, a "Door Closed" light energizes on the door position display panel in the incore instrument room. If any of these doors opens, or if the Equipment Access Door seals deflate, the "Door Closed" light de-energizes and a "Door Open" light on the same panel energizes. A control room annunciator will also energize with any of these doors open or with the seals deflated.

A separate Personnel Access Door provides access to the lower ice condenser area. With the door closed and latched, a "Door Closed" light energizes on the door position display panel in the incore instrument room, and the Personnel Access Door Seals inflate. If the door is unlatched, the "Door Closed" light de-energizes, a "Door Open" light energizes, the seals deflate, and a separate "Door Open" light located on the door energizes. A control room annunciator will also energize with the door open or unlatched.

Expansion Tank Level

Main Control Board indication and annunciation alarms, and computer point alarms are provided to warn the operator of coolant level excursions in the glycol expansion tank. Two annunciator alarms and indication are displayed corresponding to HI/LO and LO-LO liquid levels and two computer alarms are provided corresponding to HI or LO tank level. A loss of level would indicate a leak somewhere in the system or an erroneous valve operation. High level would result from mal-operation or failure of the Refrigeration System. Three independent tank level sensors are provided for glycol level alarm and indication. One sensor provides the input signal for the LO-LO level annunciation. Another sensor provides the input signal for the HI/LO level annunciation. The third sensor provides the input signal for the HI and LO computer alarms.

Isolation Valves

Two position lights (open and closed) located in the control room are provided for each of the glycol containment isolation valves. Individual annunciator windows in the control room alarm on isolation valve closure.

6.7.15.3 Design Evaluation

The Ice Condenser design provides adequate time for the proper evaluation of any adverse situations such that corrective action can be performed or an orderly unit shutdown can be scheduled and accomplished within the Technical Specification limits. The ice condenser monitoring instrumentation is tested and/or inspected on a periodic basis. In addition, the ice condenser is defrosted on a periodic basis. Since the temperature recorders and alarms are active during the defrost periods, the performance of the monitoring instrumentation can be verified. Sufficient redundancy is provided in the ice condenser instrumentation to assure accurate monitoring of the ice condenser status.

6.7.16 Ice Condenser Structural Design

6.7.16.1 Applicable Codes, Standards, and Specifications

The ice condenser structural design analysis is based on the AISC specification 10 where applicable. Material codes are discussed in Section [6.7.18](#).

6.7.16.2 Loads and Loading Combinations

Dead Load + Operating Basis Earthquake Loads (D + OBE)²

Dead Load + Accident induced loads (D + DBA)

Dead Load + Safe Shutdown Earthquake (D + SSE).

Dead Load + Safe Shutdown Earthquake + Accident induced loads ((D + SSE + DBA).

The loads are defined as follows:

Dead Load (D)

Weight of structural steel and full ice bed at the maximum ice load specified.

Live Load (L)

Live load includes any erection and maintenance loads, and loads during the filling and weighing operation.

Thermal Induced Load

Includes those loads resulting from differential thermal expansion during operation plus any loads induced by the cooling of ice containment structure from an assumed ambient temperature at the time of installation.

Accident Fluid Dynamic and Pressure Loads (DBA)

Accident pressure load includes those loads induced by any pressure differential drag loads across the ice beds, and loads due to change in momentum.

Operating Basis Earthquake (OBE)

The Operating Basis Earthquake loads are those induced loads determined from the response of the ice bed and supporting structure to the OBE defined for the site.

Safe Shutdown Earthquake (SSE)

The Safe Shutdown Earthquake loads are those induced loads determined from the response of the ice bed and supporting structure to the SSE defined for the site.

² Also considered is D + L.

6.7.16.3 Design and Analytical Procedures

Analysis, meeting the criteria presented in Section [6.7.16.4](#) is on the basis of elastic system and component analyses. Limited load analysis may be used as an alternate to the elastic analysis. Limit loads are defined using limit analysis by calculating the lower bound of the collapse load of the structure. Load factors are applied to the defined design basis loads and compared to the limit loads. The load factors determined for design basis load are used to provide margins of safety of the structure against collapse. A load factor of 1.43 is used when considering the mechanical loads due to dead weight and OBE. A load factor of 1.3 is used for either D + SSE or D + DBA. A load factor of 1.18 is used for D + SSE + DBA. The material is assumed to behave in an elastic-perfectly-plastic manner. The minimum specified yield strength is used. Mechanical plus thermal induced load combination and fatigue is analyzed on an elastic basis and satisfy the limits of Section [6.7.16.4](#).

Experimental or Test Verification of Design

In lieu of analysis, experimental verification of design using actual or simulated load conditions may be used.

In testing, account is taken of size effect and dimensional tolerances (similitude relationships) which may exist between the actual component and the test models, to assure that the loads obtained from the test are a conservative representation of the load carrying capability of the actual component under postulated loading. The load factors associated with such verification are: 1.87 for D + OBE, 1.43 for D + DBA or D + SSE, and 1.3 for D + SSE + DBA. If the load factor of 1.87 for D + SSE cannot be met, a load factor of 1.7 is used and these cases are presented to the NRC for their review.

A single test sample is permitted but in such cases test results are derated by 10 percent. Otherwise at least three samples are tested and the design is based on the minimum load carrying capability.

6.7.16.4 Structural Acceptance Criteria

[Table 6-128](#) provides a summary of the allowable limits to be used in the design of the Ice Condenser Components.

For all cases the stress analysis is performed by considering the load combinations producing the largest possible stress values.

When limit analysis is performed on the ice condenser structure, or parts thereof, using the Alternate Analytical Criteria method, Section [6.7.16.3](#) justification is provided to show that the results of the elastic systems analysis are valid.

Stress Criteria

The stress limits for elastic analysis are:

D + OBE

Stress is limited to normal AISC, Part 1 Specification allowables (S). The members and their connections are designed to satisfy the requirements of Part 1, Sections 1.5, 1.7, 1.7, 1.8, 1.9, 1.10, 1.14, 1.16, 1.17, 1.20, 1.21 and 1.22 of the AISC Specification (stress increase in Sections 1.5 and 1.6 is disallowed for these loads). Where the requirements of Section 1.20 are not met, differential thermal expansion stresses are evaluated and the maximum range of the sum of mechanical and thermal induced stresses are limited to three times the appropriate allowable stresses provided in Sections 1.5 and 1.6 of AISC Specification.

D + SSE, D + DBA

Stresses are limited to normal AISC Specifications allowables given in Sections 1.5 and 1.6, increased by 33 percent (1.33 S). No evaluation of thermal induced stresses or fatigue is required. In a few areas, where the stresses exceed 1.33 S but are below 1.5 S, these cases are presented to the NRC for their review.

D + SSE + DBA

Stresses are limited to normal AISC Specification allowables given in Sections 1.5 and 1.6, increased by 65 percent (1.65 S). No evaluation of thermal induced stresses for fatigue is required.

For all cases, direct (membrane) mechanical stresses are not to exceed 0.7 Su, where Su is the ultimate tensile strength of the material.

The summary of the ice condenser allowable limits is given in [Table 6-128](#).

6.7.17 Seismic Analysis

6.7.17.1 Seismic Analysis Methods

The lattice frames, ice baskets, wall panels on the crane wall side, and lower support of the ice condenser structure form a complex structural system. In order to perform a realistic seismic analysis of this structure, it is necessary to consider the gaps between the ice baskets and the lattice frame. It is not feasible to perform a response spectrum model analysis when considering gaps because the structure is non-linear, thus requiring a dynamic time history analysis. Six different non-linear models are used to develop the design loads. Results are documented in Section [6.7.17.2](#).

Linear Seismic Analysis

Each level of lattice frames encompasses an approximate 300 degree horizontal arc and consists of 72 lattice frames. One level of eight levels of lattice frames is modeled so that the structural coupling between individual lattice frames could be evaluated.

The dynamic model used to determine the horizontal response characteristics of one level of lattice frames is shown in [Figure 6-181](#). It is a lumped-mass beam representation. Cantilever beam elements are used to represent the bending and shear stiffness of six interconnected lattice frames as shown in [Figure 6-182](#). For the model shown in [Figure 6-181](#), the mass associated with a set of six lattice frames is lumped at the end of the cantilever beam. The length used for the cantilever beam is representative of the distance to the center of gravity of the ice baskets associated with one lattice frame. The lumped masses are connected by tie members representing the combined coupling stiffness of six lattice frames.

The dynamic response characteristics of one level of lattice frames is obtained by computer program. It was determined that the structural coupling between individual lattice frames is negligible and that the fundamental response of the ice bed-lattice frame is essentially that of the individual lattice frames acting independently. Therefore, a lattice frame can be uncoupled from those in the same level for modeling purposes.

Non-Linear Seismic Analysis

Ice Condenser Seismic Load Study of the Effect of Gaps

A clearance or gap is required at the ice basket supports for installation and maintenance reasons. A schematic view of the ice basket gap is shown in [Figure 6-183](#). The design value for the gap is 1/4 inch radially or 1/2 inch on the diameter for baskets with internal rings and a gap of 0.123 inch radially or 0.246 inch on the diameter for baskets with external rings.

The effect of the gap during a seismic excitation is two-fold. First, impact loads are applied to the ice basket as it bounces within the clearance, which produce higher loads in the ice basket that would exist if there were no gap. Second, the repetitive impacting at the ice basket supports dissipate substantial amounts of energy. Stated differently, there is a higher damping within the structure than would exist if there were no gaps. This effect is illustrated with actual test results in [Figure 6-184](#). Reference [20](#), "Ice Condenser Cable Suspension System for Block Ice Technology-Design Qualification" contains the necessary information to ensure the external rings with their reduced gap are acceptable for use in the ice condenser.

Description of Non-Linear Models

Four non-linear models of lattice frames uncoupled from those in the same level were used to determine the effect of ice basket impact on the ice condenser loads. Two additional models with adjacent lattice frame bays coupled by a phasing link were used to investigate lattice frame phasing. The six models are shown in [Figure 6-185](#) through [Figure 6-190](#) and are described as follows:

Shown in [Figure 6-185](#) is the two-mass model which is composed of two non-linear elements which represent the local impact stiffness existing between the lattice frame and ice basket, and a lattice frame spring between the lattice frame mass and the crane wall. The impacting mass represents twenty-seven ice baskets of six foot length.

Five other models were developed to assess the validity of the two-mass model.

[Figure 6-186](#) shows the three-mass tangential model whose purpose was to assess the effect of phasing between ice baskets in the tangential direction. There are three rows of ice baskets in the tangential direction across each lattice frame. Each lumped mass represents one ice basket. The lattice frame is modeled as truss members spanning each ice basket.

[Figure 6-187](#) shows the nine-mass radial model whose purpose is to assess phasing in the radial direction. Nine rows of ice baskets in the radial direction going out from the crane wall are represented in the model. Each basket has its associated impact elements on each side and the effective properties of the lattice frame spanning each ice basket.

[Figure 6-188](#) shows the 48 ft. beam model which is a non-linear model containing twenty-seven ice baskets modeled as a continuous beam. The local effect of each lattice frame is represented by a pair of impact elements, one on each side of the ice basket. The lattice frame-wall panel stiffness is represented by a stiffness element. The lower support structure is modeled by a stiffness element at the bottom of the ice basket. The purpose of this model is to investigate the influence of the full 48 ft. ice basket column.

[Figure 6-189](#) shows the phasing mass model whose purpose is to evaluate the phasing link loads and crane wall reactions when adjacent bays of lattice frames respond out of phase with each other. The phasing mass model consists of a pair of two-mass models representing adjacent bays of the ice condenser. The lattice frames of the adjacent bays are coupled together with a phasing link. The design value for the phasing link gap is 1/16 inch between adjacent lattice frames.

[Figure 6-190](#) shows the non-linear 300 degree phasing model. The non-linear 300 degree phasing model is similar to the linear model shown in [Figure 6-181](#) except that it incorporates a phasing connector between lattice frames with a phasing gap of 1/16 inch between adjacent lattice frames. The purpose of this model was to demonstrate that the phasing link creates "phasing" within a specified tolerance and to demonstrate that it is still valid to model the basic ice condenser structure using only one lattice frame per level even though a phasing connector is used.

Analytical Procedure and Typical Results

Using typical results obtained from the two-mass dynamic model, the procedure used in the non-linear analysis will now be discussed. First, the input acceleration-time histories are converted to displacement-time histories by double integration. The displacement-time histories as shown in [Figure 6-191](#) were then input to the non-linear dynamic model. Results are shown in [Figure 6-192](#) through [Figure 6-194](#) for the case corresponding to a one-half inch gap between the ice basket and lattice frame, for tangential excitation.

[Figure 6-192](#) shows the output displacement-time history of the ice basket mass superimposed on the input displacement. It shows that the response generally follows the input displacements except for some amplification in the neighborhood of the peaks.

[Figure 6-193](#) shows the impact loads on the ice baskets for this particular case. Note the short duration time of the impact loads.

[Figure 6-194](#) shows the forces induced in the wall panels on the crane wall side as obtained from the two-mass dynamic model.

6.7.17.2 Seismic Load Development

Time History Dynamic Input

Crane wall seismic time histories for the OBE and SSE, in the EW and NS directions, were developed using four synthesized earthquakes. These earthquakes are the same as used to develop the McGuire response spectra. Comparisons between McGuire and Catawba response spectra were made; it was concluded that the Catawba crane wall seismic response will be similar to that of McGuire. These time histories were the actual earthquake records as modified by the building, i.e., as filtered through the building to the points of interest on the crane wall.

The structural response is computed for each earthquake and then averaged by computing the arithmetic mean of the four sets of response values. The seismic design loads are based on the seismic loads obtained by averaging.

Design Load Verification Analyses

Non-linear seismic results obtained using the two-mass dynamic model are shown in [Table 6-129](#) and [Table 6-130](#) for the tangential and radial cases, respectively. The wall panel loads and impact loads are shown for the OBE and SSE north-south and east-west earthquakes with the respective design loads. The lattice frame-wall panel stiffness used to obtain the analysis results shown were 24,000 lb/in for the tangential case and 50,000 lb/in for the radial case. These values are consistent with stiffness obtained from tests.

The analyses made using the two-mass dynamic model used the time histories at the highest point on the crane wall associated with the lattice frames. The highest lattice frame level is used since it has the highest seismic response characteristics.

[Table 6-131](#) gives a summary of SSE load results obtained from the five non-linear dynamic models.

Seismic tangential and radial load distributions along the crane wall were found using the 48 ft. beam model and are presented in [Figure 6-195](#) and [Figure 6-196](#). They represent the portion of the seismic design load used at the various lattice frame locations. All loads obtained from analysis are within the seismic load distribution design "envelope."

Many seismic studies have been performed to understand the dynamic behavior of the ice condenser system. The effect of sublimation on the ice condenser system response has been

studied. Phasing studies have been performed. The findings from these studies have been reported in other submittals, and therefore are not reported here. For a discussion of these studies, see References [11](#) and [18](#).

Seismic Design Loads

Seismic design loads have been developed for the lattice frames, ice baskets, and the wall panels. They are shown in [Table 6-129](#) and [Table 6-130](#). The seismic design load distributions developed using the 48 ft. beam model are shown in [Figure 6-194](#) and [Figure 6-196](#).

In the non-linear analyses performed to develop seismic design loads, a nominal gap size of 1/2 inch on the diameter between the baskets and the lattice frames is enveloped, and a nominal gap size of 1/16 inch exists in the link between adjacent lattice frames, and 3/8 inch in the cradle support arm assemblies are used. A value of 10 percent impact damping was used in the development of the seismic loads, and a 5 percent structural damping value applies.

[Table 6-132](#) gives a summary of parameters used in the seismic analyses. These parameters are based on analyses and test of the Ice Condenser System.

6.7.17.3 Vertical Seismic Response

The combined floor and lower support structure are modeled in the vertical direction. The full weight of the baskets and ice were considered. It was found that the fundamental frequency, the dominant model, of the combined structure in the vertical direction is above 14.7 Hz. There is no amplification of the crane wall in the vertical direction at the elevation of the lower support structure. Therefore, the vertical response spectra have the shape of the ground response spectra and are normalized to two-thirds of the seismic ground acceleration.

6.7.18 Materials

6.7.18.1 Design Criteria

Structural steels for ice condenser components are selected from the various steels listed in the AISC Manual of Steel Construction (Reference [10](#)) or ASTM Specifications. When materials such as steel sheets, stainless steel or non-ferrous metals are required and are not obtainable in the AISC Code, these materials are chosen from ASTM specifications. Proprietary materials such as insulating materials, gaskets and adhesives are listed with the manufacturer's name on the component drawings.

Material certifications for chemical analysis and mechanical properties will be required with testing procedure and acceptance standards meeting the AISC or ASTM requirements.

Because the concept of non-ductile fracture of ferritic steel is not a part of the AISC Code and Westinghouse recognizes its importance in certain ice condenser components where heavy plates and structurals are used such as the Lower Support Structure, Charpy V-Notch (CVN) energy absorption requirements are stipulated as shown in [Table 6-133](#).

These criteria apply to the design of the following ice condenser components:

Lattice frame and columns including attachments and bolts greater than one inch in diameter.

Structural steel supporting structures comprising the lower support structure, door frames and bolts greater than one inch in diameter.

The supports of auxiliary components which are located within the ice condenser cavity but which have no safety function.

Wall panels and cooling duct support studs attached to the crane wall and end walls will be tested as follows:

A hammer bend test on the gun-welded and fillet welded studs will be performed in accordance with AWS D 1.1. This test shall be performed at temperatures of +70°F, +20°F, and -20°F.

A bend test to measure the flexural strength of the studs, at the above temperature will be performed. The studs will be welded to a plate of similar physical and chemical properties by the method and position (flat, vertical, overhead, sloping) in installation. Acceptance will be based on the stud's ability to meet the minimum ultimate strength prior to failure.

The various candidate materials, i.e., steel sheets, structural shapes, plates and bolting used in the Ice Condenser System are selected on the following criteria:

Provide satisfactory service performance under design loading and environment and pressure or construction performance.

Assure adequate fracture toughness characteristics at ice condenser design conditions.

Be readily fabricated, welded, erected.

Be readily coated for corrosion resistance, when required.

The candidate materials are of high quality and shall be made by steelmaking practices to be specified by Westinghouse. Principal candidate materials meeting the above bases are listed below. Other materials for specific applications are selected on a case by case basis.

6.7.18.2 Environmental Effects

The atmosphere in the ice bed environment is at 10°F - 20°F and the absolute humidity is very low. Therefore, corrosion of uncoated carbon steel is negligible.

To ensure that corrosion is minimized while the components of the ice condenser are in storage at the site or in operation in the Containment, components shall be galvanized, painted, or placed in a protective container. Galvanizing shall be in accordance with ASTM, A123, or A386.

Materials such as stainless steels with low corrosion rates shall be used without protective coatings.

Corrosion has been considered in the detailed design of the ice condenser components, and it has been determined that the performance characteristics of the ice condenser materials of construction are not impaired by long term exposure to the ice condenser environment.

Since metal corrosion rates are directly proportional to temperature and humidity, corrosion of ice condenser components at operating temperatures has been considered to be almost non-existent. Data available in the open literature do not reflect the exact temperature range and chemistry conditions that are expected to exist in the ice condenser, but do indicate that corrosion rates decreased with decreasing temperatures for the materials and conditions being considered. Although the data in the literature indicated that corrosion of components is not expected, several preventive measures in the construction of the Ice Condenser System will be used. To inhibit corrosion, the ice baskets will be galvanized. Tests have shown that galvanized material would not be expected to fail due to corrosion during a 40 year exposure to ice condenser refrigerated air environment. Other structural members will either be galvanized or protected by corrosion resistant paints that meet the requirements of ANSI 101.2-1972 (Protective Coatings (Paints) for Light Water Nuclear Reactor Containment Facilities) as a minimum, or will be constructed of stainless steel. Heavy plate and structural fabrications made

from A588 steel may be installed in the blasted and/or bare condition. A tightly adherent scale forms on the surface of this steel when it is exposed to the atmosphere.

Quenched and tempered steel components will not be hot dip galvanized but will be painted or left in the base condition.

With due consideration of the non-corrosive environment, and judicious selection of component materials based upon sound engineering judgment, the structural integrity of the ice condenser components is not jeopardized, and the design criteria for the plant are met.

6.7.18.3 Compliance With 10CFR50, Appendix B

The following sections of this report address themselves to demonstrating compliance with 10CFR50, Appendix B. The Design Process Control Policy defines the criteria that must be considered when establishing design process control procedures. The design process procedures represent how Westinghouse controls its design processes relative to 10CFR50, Appendix B requirements. The subject procedures are supplementary to the flow diagram and cross-reference is obtained through the use of activity numbers.

The products and scope of responsibility at Westinghouse are defined by the shop order description. From this base, the shop order flow diagrams were developed for the purpose of sub-dividing the job into its component activities and thereby creating generic categories of activities that require similar control systems. These categories are:

Interface Control

Interfaces are controlled by specifically identifying the relationship on the flow diagram and also by quantifying the information transmitted across the interface. There must be documentary evidence in the file of the vehicle used to cross the interface.

Document Control - a procedure employing a file log book is carefully maintained and provides control of document issue.

Analysis (includes review and comment, approval responsibilities)

These activities involved in providing or commenting on design information are controlled according to methods outlined in design process procedures. The nature of the product and its relative technical importance determine the level of controls applied.

Verification

These activities fulfill the requirement that design information must be validated by the originator prior to communication to a user. Techniques used vary due to the diverse nature of the products involved.

There is a design process control procedure for each shop order which consists of at least, a flow diagram, a shop order description, and Design Process Procedures.

The Design Process Procedures are related to the flow chart through the use of the activity numbers and the specific control methods.

Quality assurance of material; when required parts or welded fabrications will be inspected by visual, magnetic-particle (MT), liquid penetrant (PT) or ultrasonic (UT) methods according to ASTM Procedures, AWS D1.1, or Westinghouse Process Specifications. The method and extent of inspection will be designated on the component drawings.

6.7.18.4 Materials Specifications

Sheets

Carbon steel sheets are commercial quality (CQ), drawing quality (DQ), or drawing quality-special kilned (DQ-SK). The selection of the quality depends upon the part being formed. When higher strength, structural quality sheets are required, ASTM specification A607 is used.

The ice baskets will be made from perforated sheet material. The wall duct panels will be made from sheet material.

Structural Sections, Plates, and Bar Flats

Structural sections, plates, and bar flats are generally High-Strength, Low-Alloy steels selected for suitable strength, toughness, formability, and weldability.

The high strength, low alloy steels are A441, A588, or A572. These steels are readily oxygen cut and possess good weldability.

Bolting

High strength alloy steel Type A320 L7 bolting for low temperature service, is used for the lower support structure. Stocked bolting made from A325, A449 and ASTM A354 Grade BD (SAE J429 Grade 8) materials will be used for other parts. The above bolts must meet CVN 20 ft-lb at -20°F, for sizes greater than 1 inch in diameter.

Non-metallic Materials

Non-metallic materials such as gaskets, insulation, adhesives and spacers are selected for specific uses. Freedom from detrimental radiation effects is required.

Welding

All structural welding shall be in accordance with the AWS Structural Code for Welding, D1.1. (AWS Code), latest edition. The AWS Code is an overall welding system for the design of welded connections, technique, workmanship, qualification and inspections for buildings, bridges, and tubular structures. The quality of welds for the Ice Condenser System are based on paragraph 9.25 of the AWS Code.

Resistance welding is in accordance with AWS, Recommended Practices for Resistance Welding, C1.1.

Magnetic particle examination is performed on at least 5 percent of the welds in each critical member of the lower support structure. Magnetic particle or liquid penetrant examinations where applicable, are performed on at least 5 percent of the welds in each critical member of the balance of the ice condenser structure. The welds selected for non-destructive test examination are designated on the component drawings or in the Design Specifications. The NDE method and acceptance standards are shown in the AWS Code, Section 6 and Paragraph 9.2.5, Quality of Welds.

6.7.19 Tests and Inspections

The test and inspections are given in the Technical Specifications and [Chapter 14](#).

6.7.20 References

1. Test Plans and Results for the Ice Condenser System, *WCAP-8110*, April 16, 1973.

2. Test Plans and Results for the Ice Condenser System, *WCAP-8110*, Supplement 1, April 30, 1973.
3. Test Plans and Results for the Ice Condenser System, *WCAP-8110*, Supplement 2, June 19, 1973.
4. Test Plans and Results for the Ice Condenser System, *WCAP-8110*, Supplement 3, July 19, 1973.
5. Test Plans and Results for the Ice Condenser System, *WCAP-8110*, Supplement 4, November 15, 1973.
6. Plantema, F. F., *Sandwich Construction*, John Wiley, New York, 1966.
7. Idel'chik, Handbook of Hydraulic Resistance, *AECTR 6630*, NTIS, Springfield, Va.
8. Nies, N. P. and Hulbert, R. W., Journal of Chemical and Engineering Data, Vol. 12, No. 3, pp. 303-313, 1967.
9. Flanks, F., *Water*, V. 1, Plenum (1972), Ch. 4.
10. Specification for the Design, Fabrication and Erection of Structural Steel for Buildings, American Institute of Steel Construction, 1969 Edition.
11. *Donald C. Cook Nuclear Plant, FSAR*, American Electric Power Service Corporation, Docket Numbers 50-315 and 50-316.
12. Ice Condenser System Lower Inlet Door Shock Absorber Test Plans and Results, *WCAP-8336*, May 1974 (Westinghouse NES Proprietary) and *WCAP-8110*, Supplement 5, May, 1974.
13. Final Report-Ice Condenser Full-Scale Tests at the Waltz Mill Facility, *WCAP-8282*, February 1974 (Westinghouse NES Proprietary), and *WCAP-8110*, Supplement 6, May, 1974.
14. Final Report-Ice Condenser Full-Scale Tests at the Waltz Mill Facility, *WCAP-8282*, Addendum 1, May, 1974 (Westinghouse NES Proprietary), and *WCAP-8110*, Supplement 7, May, 1974.
15. Stress and Structural Analysis and Testing of Ice Baskets, *WCAP-8304*, (Westinghouse NES Proprietary), and *WCAP-8110*, Supplement 8, May, 1974.
16. Ice Fallout From Seismic Testing of Fused Ice Basket, *WCAP-8110*, Supplement 9-A, May, 1974.
17. Static Testing of Production Ice Baskets, *WCAP-8110*, Supplement 10, September, 1974.
18. Sequoyah Nuclear Plant Final Safety Analysis Report, Tennessee Valley Authority, Docket Numbers 50-327 and 50-328.
19. Stress Evaluation for Revised Ice Basket Lower Supports, McGuire Nuclear Station Units 1 and 2, Westinghouse Calculation No. MED-PCE-10522, June 1991, revised June 1992, M.F. Hankinson; and letter from T.R. Puryear, Westinghouse Technical Services Manager, regarding applicability to CNS Units 1 and 2. CNM number CNM 1201.17-30 sh20.
20. Ice Condenser Cable Suspension System for Block Ice Technology - Design Qualification, *WCAP-14624*, April, 1996, Duke Number CNM 1201.17-30 sh30.

HISTORICAL INFORMATION IN ITALICS BELOW NOT REQUIRED TO BE REVISED

21. *Application of the Active Ice Mass Management Concept to the Ice Condenser Ice Mass Technical Specification, ICUG-001, Ice Condenser Utility Group, Revision 2, June 2003.*
22. "Mass & Energy Release and Containment Response Methodology," DPC-NE-3004-PA, Rev. 1, Duke Power Co., SER dated February 29, 2000.
23. Deleted Per 2010 Update.
24. ND Suction Pressure Control Setpoint Determination for 1(2)FW96 and 1(2)FW97, CNC-1223.21-00-0020.
25. Documentation of Design Basis for 1(2)FW28 and 1(2)FW56 and Bypass Line, CNC-1223.21-00-0021.

THIS IS LAST PAGE OF THE CHAPTER 6 TEXT PORTION.

THIS IS THE LAST PAGE OF THE TEXT SECTION 6.7.